

Copyright © 1989, by the author(s).  
All rights reserved.

Permission to make digital or hard copies of all or part of this work for personal or classroom use is granted without fee provided that copies are not made or distributed for profit or commercial advantage and that copies bear this notice and the full citation on the first page. To copy otherwise, to republish, to post on servers or to redistribute to lists, requires prior specific permission.

**STEADY-STATE METHODS FOR  
SIMULATING ANALOG CIRCUITS**

by

Kenneth Scott Kundert

Memorandum No. UCB/ERL M89/63

28 April 1989

**STEADY-STATE METHODS FOR  
SIMULATING ANALOG CIRCUITS**

by

Kenneth Scott Kundert

Memorandum No. UCB/ERL M89/63

28 April 1989

**ELECTRONICS RESEARCH LABORATORY**

College of Engineering  
University of California, Berkeley  
94720

TITLE PAGE

**STEADY-STATE METHODS FOR  
SIMULATING ANALOG CIRCUITS**

by

**Kenneth Scott Kundert**

**Memorandum No. UCB/ERL M89/63**

**28 April 1989**

**ELECTRONICS RESEARCH LABORATORY**

College of Engineering  
University of California, Berkeley  
94720

# Abstract

---

Circuit simulation is an important tool for the design and verification of analog and microwave circuits. However, traditional transient analysis methods can result in very long computer run times when the steady-state response is desired of a circuit with long time constants or widely separated frequencies. A number of new approaches to finding the periodic and quasiperiodic steady-state solution to the systems of nonlinear ordinary- and integro-differential equations that describe analog and microwave circuits have been developed and are described in this dissertation. One new approach, the mixed frequency-time method, combines frequency- and time-domain concepts to attack the problem of finding quasiperiodic solutions in the time domain. Another approach involves accelerating harmonic balance, a frequency-domain method, by solving the resulting nonlinear equations with a method that combines nonlinear relaxation (providing speed) and the Newton-Raphson algorithm (providing better convergence properties) into one algorithm that is robust and fast. New programs that incorporate these techniques have been developed and used to simulate a variety of typical analog and microwave circuits. The results from these simulations are provided. These techniques are shown to be much faster than transient analysis when finding the steady-state solution of certain important classes of circuits. In addition, the methods allow some circuits to be simulated that were virtually impossible to simulate before.

# Acknowledgements

---

I wish to express my deepest appreciation to my research advisor, Professor Alberto Sangiovanni-Vincentelli, for his wisdom, guidance, loyalty, and friendship. If not for his encouragement, I would not have gone on for my Ph.D. And if not for his belief, that in CAD research, it is just as important to work at a clear understanding of the theory as it is to work at achieving practical results, I would not have accomplished nearly as much. Finally, I would like to thank Alberto for cultivating my ability to make clear presentations, both oral and written. Unfortunately, in this regard, I am leaving before my education is complete.

Several other professors have contributed graciously their time on my behalf, and I would like to express my gratitude. Professor D. O. Pederson provided useful direction and good advice. I wish to thank him for giving me the benefit of his years of experience and, along with Professors R. Brayton, A. R. Newton, and A. Sangiovanni-Vincentelli, for providing an excellent research environment. I appreciate Professors D. O. Pederson, A. Sangiovanni-Vincentelli, R. Brayton, and B. Parlett for agreeing to serve on my qualifying committee, and Professors A. Sangiovanni-Vincentelli, R. Brayton, B. Parlett and J. White for reviewing this dissertation.

I would like to thank my mentor, Professor Jacob White of MIT. Jacob is an inspiration, a friend, and a machine for turning diet Coke into technical papers. I would also like to thank his wife Barbara, for tolerating patiently the loss of her husband whenever I visit Boston.

Greg Sorkin was a principal contributor to the work on the APFT. He was also my house-mate in Boston for a semester when Alberto took his research group on the road. He was able to make a miserable housing experience with the “Landlord from Hell” quite entertaining.

I wish to acknowledge and express my gratitude to the Network Measurements Division of Hewlett-Packard for their support. In particular, I would like to thank Irv Hawley, Doug Rytting, and Bruce Donecker for their belief in my abilities. In addition, I wish to thank Bruce Donecker, Jeff Meyer, David Sharrit, David Root, and Tom Parker for many valuable discussions and suggestions. I further appreciate Bruce Donecker for allowing me to use Hewlett-Packard’s 85150B Microwave Nonlinear Simulator (MNS) for measuring some of the results presented in Chapter 8. This simulator is a descendant of *Spectre*, and implements several algorithms presented in this dissertation but, due to time constraints, were never implemented in *Spectre*.

Cadence Design Systems has provided generous support while I wrote this dissertation. I appreciate the patience of James Spotto and Jim Solomon.

Many people made contributions to the *Spectre* and *Nitswit* programs. Jacob White wrote *Relax*, which was the starting point for *Nitswit*. Peter Moore wrote the input parser for both programs. Wayne Christopher and Dave Harrison wrote the output processing tools (*Nutmeg* and *Xgraph* respectively). Mireille Brouke wrote the topology checker. Barbara Mills and Nhat Nguyen contributed to the BJT model while Ellen Sentovich contributed to the GaAs MESFET model and Dr. Robert Pucel provided guidance with the microstrip transmission line model. Richard Rudell wrote the memory allocator and the architecture was modeled after SPICE3, written by Tom Quarles.

I am grateful to Prasad Subrahmanyam, Larry Nagel, Vish Visvanathan, and Micheal Fang of AT&T Bell Labs, Jamie Pierce, Peter O'brien, and Steve Greenberg of Digital Equipment Corporation, Dr. Robert Pucell of Ratheon, Steve Hamm of MCC, and Yo-Chien Yuan and Chuck Holmes of EEs of for interesting and useful discussions on the various aspects of circuit simulation in an industrial setting.

An essential aspect of being a graduate student is the interaction that goes on with other graduate students. A considerable amount of innovation occurs during discussions with these bright and talented people. It was my pleasure to exchange ideas with Fabio Romeo, Kartikeya Mayaram, Howard Ko, Don Webber, Giorgio Casinovi, Tom Quarles, Hormoz Yagahutiel, Richard Rudell, Resve Saleh, Pranav Ashur, Nick Weiner, Tammy Huang, Ron Gyurscik, Rick Spickelmier, Beorn Johnson, Cormac Conroy and Mark Reichelt.

Finally, I thank my new wife Mary, for making me laugh when things got to be too much, and my parents, for everything they have done.

Funding for this research was provided by Hewlett-Packard Company and the California MICRO program. Computer resources provided by Digital Equipment Corporation and Hewlett-Packard Company.

# Table of Contents

---

Chapter 1. Introduction .....	1
1. Steady State .....	4
2. Steady-State Methods .....	6
3. Historical Perspective .....	8
3.1. Shooting Methods .....	9
3.2. Harmonic Balance .....	9
3.2.1. Harmonic Balance for Quasiperiodic Signals .....	12
3.3. Switched-Capacitor Filter Simulation .....	15
4. Organization of the Dissertation .....	16
Chapter 2. Motivation .....	21
1. Self-Biasing Amplifiers .....	21
2. Mixers .....	23
3. Narrow-band Amplifiers and Filters .....	24
4. Switched-Capacitor Filters .....	25
5. Traveling-Wave Amplifiers .....	27
6. Measured Devices .....	29
7. Crystal and Cavity Oscillators .....	29
Chapter 3. Background: Signals .....	31
1. Signals .....	31
1.1. Truncation and Discretization .....	33
2. Almost-Periodic Fourier Transform .....	35
2.1. Matrix Formulation .....	36
2.1.1. Previous Work .....	38
2.1.2. Condition Number and Orthonormality .....	38
2.1.3. Condition Number and Time Point Selection .....	40
2.1.4. Condition Number and Aliasing .....	41
2.2. Near-Orthogonal Selection Algorithm .....	44
2.2.1. Time Point Selection .....	44
2.2.2. Constructing the Transform Matrix .....	46
2.2.3. APFT Algorithm Results .....	48
Chapter 4. Background: Systems .....	51
1. Systems .....	51
1.1. State .....	52
2. Problem Formulation .....	53
2.1. Lumped Test Problem .....	54

2.2. Distributed Test Problem .....	54
3. Differential Equations .....	55
3.1. Initial-Value Problems .....	56
3.2. Boundary-Value Problems .....	57
3.2.1. Existence and Uniqueness of Solutions .....	57
3.3. Boundary-Value Problems in Circuit Simulation .....	61
3.3.1. Periodic Boundary Constraint .....	61
3.3.2. Oscillators .....	62
3.4. Numerical Solution of Initial-Value Problems .....	64
3.4.1. Discretization .....	64
4. Numerical Solution of Nonlinear Algebraic Equations .....	65
4.1. Simplified Newton-Raphson Methods .....	67
4.2. Continuation Methods .....	69
4.2.1. Pseudo-Arc Length Continuation .....	72
Chapter 5. Time-Domain Methods .....	78
1. Finite-Difference Methods .....	78
2. Shooting Methods .....	83
2.1. Shooting by Extrapolation .....	84
2.2. Shooting with Newton-Raphson .....	87
2.3. Oscillators .....	94
2.4. Distributed Devices .....	98
2.5. Parallel Shooting .....	100
Chapter 6. The Mixed Frequency-Time Method .....	103
1. Previous Work .....	104
1.1. Quasiperiodicity Via the Periodic Boundary Constraint .....	104
1.2. Quasiperiodicity Via an N-Point Boundary Constraint .....	105
2. The Mixed Frequency-Time Method .....	107
2.1. The Delay Operator .....	110
2.2. The Differential Equation Relation .....	114
2.3. An Example .....	115
2.4. MFT as a Two-Point Quasiperiodic Boundary Constraint .....	117
3. Practical Issues .....	118
3.1. The Quasiperiodic Sampled Waveform .....	118
3.2. Selecting the Clock .....	121
4. Nitswit .....	121
4.1. Equation Formulation .....	122
4.2. Implementation .....	123
4.2.1. Application Examples .....	123
4.2.2. Comparison to Direct Methods .....	127
Chapter 7. Harmonic Balance: Theory .....	131

1. Introduction .....	131
1.1. An Example .....	134
2. Error Mechanisms .....	135
3. Derivation .....	137
4. Harmonic Programming .....	139
4.1. Root Finding as a Nonlinear Least Squares Problem .....	141
4.2. Equation Solution with Performance Optimization .....	145
5. Harmonic Relaxation .....	147
5.1. Splitting .....	148
5.2. Gauss-Jacobi Newton Harmonic Relaxation .....	151
6. Harmonic Newton .....	157
7. Error Estimation .....	159
8. Oscillators .....	163
<b>Chapter 8. Harmonic Balance: Implementation .....</b>	<b>165</b>
1. Accelerating Harmonic Balance .....	166
1.1. Transforms for Quasiperiodic Harmonic Balance .....	167
1.2. Harmonic Balance and the Discrete Fourier Transform .....	168
1.2.1. Choosing the Artificial Frequencies .....	170
2. Harmonic Newton .....	172
2.1. Harmonic Relaxation-Newton .....	179
2.1.1. Adaptively Pruning the Harmonic Jacobian .....	181
2.1.2. Harmonic Jacobian Data Structure .....	183
3. Spectre .....	184
3.1. Comparisons to Transient Analysis .....	185
3.2. Profiles .....	192
3.3. Harmonic Relaxation versus Harmonic Newton .....	194
3.4. APFT versus FFT .....	198
<b>Chapter 9. Comparisons .....</b>	<b>199</b>
1. Finite-Difference Methods .....	199
2. Shooting Methods .....	201
3. Harmonic Balance .....	203
4. Examples .....	205
4.1. Self-Biasing Amplifier .....	205
4.2. Mixers .....	205
4.3. Narrow-band Amplifiers and Filters .....	206
4.4. Switched-Capacitor Filters .....	206
4.5. Traveling-Wave Amplifiers .....	207
4.6. Measured Devices .....	207
4.7. Crystal and Cavity Oscillators .....	207
<b>Chapter 10. Summary .....</b>	<b>208</b>



# Prologue

---

There is nothing wrong with your simulator. Do not attempt to adjust the options. We are controlling the analysis.... We will control the LTE. We will control the time-step. We can crash the simulator, make it dump core. We can change the accuracy to a soft blur, or sharpen it to crystal clarity. For the next simulation interval, sit quietly and we will control all you see. We repeat: There is nothing wrong with your simulator. You are about to participate in a great adventure. You are about to experience the awe and mystery that reaches from *No DC convergence* to ...

*Harmonic convergence.*

# Chapter 1

## Introduction

---

In general, analog and microwave circuit designers rely heavily on circuit simulation programs such as SPICE [nagel75], ASTAP [weeks73], and *Touchstone*<sup>1</sup> to insure the correctness and the performance of their designs. With the cost of prototype GaAs integrated circuits over \$60,000 and the time required to build the prototype over 4 months, it is crucial to have the circuit operate correctly and meet specifications on the first iteration. Circuit simulators are used to “prototype” circuits on a computer rather than in silicon or gallium arsenide. These programs simulate a circuit by constructing a system of differential equations and solving them numerically. With SPICE or ASTAP, the equations are integrated with a time discretization method such as one of the implicit multistep methods, and so circuits with linear and nonlinear components can be simulated. *Touchstone* uses phasors to solve the equations and so only linear circuits can be simulated.

Often when simulating analog and microwave circuits, the steady-state behavior of the circuit is of primary interest. It is easier to characterize and verify certain aspects of system performance in steady state. Examples of quantities that are best measured when a circuit is in steady state include distortion, power, frequency, noise, and transfer characteristics such as gain and impedance. Therefore, any circuit simulator that specializes in

---

<sup>1</sup>*Touchstone* is a registered trademark of EEsof.

analog or microwave circuits should be able to calculate the steady-state response of a circuit efficiently and accurately.

If the underlying circuit is asymptotically stable, then it is possible to use transient analysis simulators such as SPICE or ASTAP to find the steady-state solution by choosing an arbitrary initial condition and integrating the circuit equations until any transient decays. However, this is often impractical because one or more circuit time constants may be considerably longer than the interval of interest, or signals present may be very widely separated in frequency. In either case, the equations need to be numerically integrated over an interval that is long compared to the time-step that is required to follow accurately the high frequency signals present in the solution.

If the underlying circuit is linear, then phasor analysis simulators such as *Touchstone* can be used to find directly and efficiently the steady-state solution. Unfortunately, this restriction eliminates large and important classes of circuits such as mixers and oscillators that are inherently nonlinear.

This dissertation presents several time-domain and frequency-domain methods for computing the periodic and quasiperiodic solution of nonlinear circuit directly. A quasiperiodic solution is one that consists of the sum of sinusoids at the sum and difference frequencies of a finite set of fundamentals and their harmonics. Mixers and switched-capacitor filters are common examples of circuits that exhibits a quasiperiodic steady-state response.

Previously, there was no practical way to compute a quasiperiodic steady-state solution directly in the time domain. The mixed frequency-time method is a new approach that finds these solutions and that has proven to be practical in a large number of situations.

Time domain methods, either transient or steady state, are not well suited for distributed circuits (or integro-differential equations). Time domain evaluation of distributed components requires either the impulse responses as measured from the component terminals or a lumped equivalent model. The impulse response is usually difficult to compute or measure and the lumped equivalent is very difficult to determine from measurement and usually contains many internal nodes.

Harmonic balance is a frequency-domain method for computing the steady-state solution of a circuit. The benefit of this method is that the linear components are evaluated in the frequency domain. Any linear components for which a frequency response is known can be included. Thus, it is very easy to include component measurements directly. It is also relatively easy to develop frequency-domain models for distributed devices, even those that exhibit loss, dispersion, and coupling. Harmonic balance represents the signals present in a circuit using sums of sinusoids. It is a natural consequence that the steady-state solution is computed since a transient is not representable. Harmonic balance tends to be efficient when the solution can be accurately approximated by the sum of just a few sinusoids.

The computational effort required for methods that directly compute the steady-state solution of a circuit is independent of time constants and separation in frequencies. Thus, while for circuits with no slow time constants and no widely separated frequencies, transient methods might be more efficient at calculating the steady-state solution than steady-state methods, for any circuit there is always some value for the time constants or frequencies for which steady-state methods are more efficient. For practical problems, they are often considerably more efficient.

Determining the steady-state solution of ordinary- and integro-differential equations is an important problem in many fields. Analog and microwave circuit simulation is the vehicle used in this dissertation for discussing methods useful for finding steady-state solutions, but the methods are general in nature and useful in other disciplines. Both frequency-domain and time-domain methods for computing the periodic and quasiperiodic solution of systems of nonlinear differential equations are presented. These periodic and quasiperiodic solutions represent steady-state solutions if the system of equations is asymptotically stable about the solution.

## 1. Steady State

This dissertation presents a number of methods for directly computing the steady-state response of nonlinear circuits. Before introducing these methods, we clarify what is meant by steady state. In the most general terms, the *steady-state solution* of a differential equation is the one that is asymptotically approached as the effect of the initial condition dies out. Notice that it is not necessary for the steady-state solution to be unique, but for each steady-state solution there must correspond a region of attraction. Any solution with an initial condition that falls within the region of attraction for a steady-state solution will eventually asymptotically approach that steady-state solution. For example, a circuit such as a flip-flop with more than one stable state has distinct initial conditions that eventually result in different steady-state solutions. However, each steady-state solution is reached regardless of small changes in the initial condition. This is equivalent to saying that if the differential equation is at a steady-state solution and is perturbed slightly and temporarily, it will return to the same solution. Such a solution is referred to as being *asymptotically stable*. Notice that this definition excludes lossless linear integrators and LC oscillators.

There are several different kinds of steady-state behavior that are of interest. The first is *DC steady state*. Here the solution is an equilibrium point of the circuit and is independent of time. Asymptotically stable linear circuits driven by sinusoidal sources eventually exhibit *sinusoidal steady state* solutions, which are characterized as being purely sinusoidal except possibly for some DC offset. *Periodic steady state* is the steady-state response of a nonlinear circuit that consists solely of a DC offset and harmonically related sinusoids. It results either from self oscillations or periodically varying inputs. The period of the solution is usually equal to that of the input, though occasionally the periods of the two will be multiples of some common period. If a nonlinear circuit is driven with several periodic sources at unrelated frequencies, the steady-state response is called *quasiperiodic*. A quasiperiodic steady-state response consist of sinusoids at the sum and difference frequencies of two or more fundamental frequencies and their harmonics. The frequencies of the input signals usually equal that of the fundamentals, though sometimes they are even multiples. There are steady-state responses that do not fit in any of the above classifications. These occur when either the input sources are not quasiperiodic or when the circuit is strange. Examples include chaotic circuits and circuits with noise as the input.

In this dissertation we discuss the computation of periodic and quasiperiodic solutions. There is no guarantee that these solutions represent steady-state solutions because the methods presented are unable to distinguish between stable and unstable solutions. Methods for determining the stability of a solution are available [parker] [hente86].

## 2. Steady-State Methods

One approach to calculating the steady-state response is to integrate the differential equations that describe the circuit from some chosen initial state until any transient behavior dies out; an approach that suffers from several fundamental drawbacks.

First, transients may take a long time to decay and so require an expensive calculation. Second, it can be quite difficult to determine when the transient has died out. If the time constants involved in the transient are large, the circuit can be erroneously declared as being in steady state when in reality is quite far from it. Finally, many analog and microwave circuits, such as mixers, have inputs at two or more independent frequencies. These frequencies are often such that the ratio of the highest to lowest frequency present in the circuit is large. In a transient simulation, the size of the time-step is proportional to the highest frequency and the length of the simulation interval proportional to the lowest. As a result, these circuits often require a vast number of time-points.

One approach to accelerating the calculation of the periodic or quasiperiodic steady-state response is to pose the problem as a two-point boundary-value problem. There is a considerable amount of literature available on the numerical solution of these problems for systems of ordinary differential equations. For example, see [childs79] [fox57] [hall76] [keller68] [keller76] [press86] [stoer80]. The two-point boundary-value problem is fundamentally different from the initial-value problem, and substantially more difficult to solve — however, long initial transients are avoided. The crucial difference between initial-value and two-point boundary-value problems is that in the former case one starts from a known state and progresses forward in time with no constraints placed on the final state. Attention is focused locally; when finding the solution at a particular time-point only the current

time-point and a few previous time-points are of interest. In the latter case, the temporal unidirectionality of the initial-value problem is lost so attention must be focused on the entire solution interval. There is a known relationship between the initial state and the final state, but neither are fully known. Hence, a critical aspect of this case is that it is necessary to devise a numerical algorithm that finds a solution such that the initial and final states satisfy the given requirements, when neither is specified fully in advance.

In general, it is possible to classify the accelerated methods for finding steady-state solutions into three basic categories; shooting methods, finite-difference methods, and expansion methods. Shooting methods treat the problem as an initial-value problem to be evaluated between the boundaries. They try to find an initial state that eliminates any transient behavior and results immediately in steady state. Shooting methods attempt to find such an initial state using an iterative algorithm. The algorithm for a periodically driven circuit begins by guessing the initial conditions and simulating the circuit for one period using these conditions. The response is checked to see if it is periodic and if not, how far is it from being periodic. A new initial guess is then generated that presumably results in a response that is closer to being periodic. The method used to generate the new initial conditions is what differentiates the shooting method variants.

Finite difference methods replace the differential equations with finite-difference equations on a mesh of points that cover the interval of interest. Trial solutions consist of discrete values, one for each point on the mesh, that do not necessarily satisfy the difference equations but do satisfy the boundary conditions. The trial solution at each point is adjusted simultaneously until it also satisfies the difference equations.

Expansion methods start with a collection of linearly independent functions that form a basis to an appropriate function space and then represent the solution as a linear combination of those functions. The basis functions are chosen such that any linear combination always satisfies the boundary conditions. The process of finding a solution is viewed as one of simply finding the coefficients of the basis functions so that the result satisfies the differential equation. Only the expansion method known as harmonic balance has gained any popularity, a method characterized by the use of trigonometric polynomials as basis functions.

### 3. Historical Perspective

There are four different general approaches to solving for the steady-state response of a circuit. The first is to accelerate transient analysis by adapting it to the problem at hand. Examples of this include the methods of Gautschi and Petzold. Gautschi [gautschi61] attacked the problem of systems with lightly damped oscillatory solutions by using a custom integration method that integrates trigonometric polynomials exactly. This method allows time-steps to be used that are on the same order as the period of the oscillation. Petzold [kundert88c,petzold81] attacked the same problem by developing an integration method that follows the envelope of the solution rather than the solution itself.

Approaches for finding the steady-state response of a circuit directly include the shooting methods, the finite-difference method, and harmonic balance. Of these methods, the finite difference method has not attracted much attention from the circuit simulation community.

### 3.1. Shooting Methods

Shooting methods have been used for years by numerical analysts for solving two-point boundary-value problems [keller68,keller76,stoer80]. The first advance in shooting methods in recent years came when first applied to find the steady-state behavior of electrical circuits. Aprille and Trick [aprille72a,aprille72b] used Newton-Raphson to solve the shooting equations and they showed that the Jacobian (or the sensitivity matrix) could be computed efficiently during the transient analysis from quantities that are normally present. This method was also used by several others and has since become the preferred approach [colon73,director76,trick75]. A slightly different approach was taken by Skelboe, who used extrapolation rather than Newton-Raphson to solve the shooting equations [skelboe80] [skelboe82].

In 1981, Ushida and Chua became the first to try to apply shooting methods to finding quasiperiodic solutions [chua81]. They proposed a very interesting and unique algorithm that, unfortunately, turned out to be quite inefficient. The inefficiency resulted from a severely ill-conditioned algorithm; the ill-conditioning could only be eliminated at great computational expense. Although developed independently, some of the flavor of Ushida and Chua's algorithm can be found in the mixed frequency-time method of Kundert, White and Sangiovanni-Vincentelli [kundert88d] [kundert89]. This algorithm avoided the ill-conditioning present in the earlier algorithm and so is considerably more efficient.

### 3.2. Harmonic Balance

Harmonic balance has been around for many decades. It was originally considered an approximate technique for finding analytically the near-sinusoidal solution of a differential equation [cunningham58] (a solution where all components except for one sinusoid is

negligible). Baily formulated harmonic balance as a numerical method in 1969 [baily69]. He described the nonlinearities using polynomials, formulated Kirchoff's laws in terms of the Fourier coefficients, and solved the resulting nonlinear equations with nonlinear programming techniques. In the last 15 years, it has been reformulated into an accurate method for finding numerically the solution of a differential equation driven by sinusoids without having to approximate the nonlinearities with polynomials. The conventional approach begins by partitioning the circuit into linear and nonlinear subcircuits. The linear subcircuit is evaluated in the frequency domain while the nonlinear subcircuit is evaluated in the time-domain. The problem then becomes one of finding the voltage waveforms (or spectra) on the nodes that appear in both subcircuits that result in Kirchoff's current law being satisfied at those nodes. In 1974, Egami showed that it is possible to solve these equations using Newton-Raphson [egami74]. He was quickly followed by Gwarek and Kerr, who solved the equations using nonlinear relaxation [gwarek74] [kerr75], and Nakhla and Vlach who used optimization methods [nakhla76]. Variations of these three approaches have been presented by a large collection of authors [gopal78] [filicori79] [faber80] [mees81] [hicks82b] [hicks82a] [lipparini82] [penalosa83] [rizzoli83] [ushida84] [rizzoli86] [hente86] [schuppert86] [penalosa87a] [penalosa87b] [curtice87] [maas88].

The relaxation methods presented before 1986 were based on simple splitting of the linear and nonlinear portions of the Jacobian [faber80,hicks82b]. At that time, Kundert and Sangiovanni-Vincentelli explored the convergence properties of the various harmonic balance methods and showed that convergence properties of this method were poor [kundert86b]. We proposed an alternative relaxation method called Gauss-Jacobi-Newton harmonic relaxation that has superior convergence properties.

Relaxation methods were found to be quite fast but suffered from convergence problems. Newton-Raphson, on the other hand, is more robust but is slow. In 1985, Kundert and Sangiovanni-Vincentelli [kundert85] [kundert86b] presented a method, referred to here as harmonic relaxation-Newton, that combines most of the advantages of both relaxation and Newton-Raphson. The method smoothly adapts from relaxation to Newton-Raphson at the component level as individual devices are driven harder and their nonlinear character becomes more apparent. In one limit, a purely linear circuit, the method becomes equivalent to Gauss-Jacobi-Newton harmonic relaxation, which converges in one inexpensive iteration. In the other limit, for portions of the circuit behaving very nonlinearly, the method becomes identical to Newton-Raphson. This approach provides the speed of the relaxation methods without the risk.

This work is unique in another way. One assumption common to all previous approaches is that the circuit should be partitioned into two subcircuits. With such an approach, the system of equations that describe the linear subcircuit can be factored into triangular form once and quickly evaluated thereafter. This is desirable when the linear subcircuit is much larger than the nonlinear subcircuit. This is invariably true for hybrid circuits. However, treating the circuit as two separated subcircuits places constraints on the way the nonlinear equations can be factored and so is inefficient for monolithic circuits, where the number of nonlinear devices is large. Kundert and Sangiovanni-Vincentelli were the first to suggest that the circuit should not be partitioned into two subcircuits. Instead, the system of equations for the whole circuit should be carefully factored in a manner that is efficient for both hybrid and monolithic circuits.

A significant departure from conventional harmonic balance was suggested by Steer and Kahn in 1983 [steer83] [rhyne88]. They propose to evaluate the nonlinear devices directly in the frequency domain. It is only possible to do this for selected nonlinearities, such as those described by polynomials (making the method reminiscent of that of Baily). Thus, when analyzing circuits containing nonlinearities described by arbitrary continuous functions, the first step is to model the functions over the anticipated operating range with a polynomial. This approach has the advantage of eliminating any Fourier transforms in the nonlinear device evaluations, however these transforms usually do not require much time, and so the gain in efficiency due to this feature is negligible. The disadvantage of this method is that it is very difficult to approximate accurately strongly nonlinear functions over a wide range with polynomials, thus the method should only be applied to circuits with mild nonlinearities.

### **3.2.1. Harmonic Balance for Quasiperiodic Signals**

Until 1984, harmonic balance was only used to analyze circuits with a periodic response. The reason being is that with the linear devices evaluated in the frequency domain and the nonlinear devices evaluated in the time domain, a transform is needed to convert signals between the two domains. The Fast Fourier Transform (FFT) was used to perform this operation, however the FFT is only applicable to periodic signals, which excludes a very important class of circuits whose steady-state response is not periodic: mixers. The signals present in mixers consist of sinusoids at the sum and difference frequencies of the two or more input frequencies and their harmonics. In general, these input frequencies are not harmonically related, and so the signals found in mixers are not periodic, but rather quasi-periodic.

In 1984, Ushida and Chua showed that a transform for the quasiperiodic signals present in mixers could be developed by starting from the matrix form of the Discrete Fourier Transform (DFT) but that more than the normal number of time-points were needed in the sampled time-domain waveforms [ushida84]. The excess number of samples necessitated the use of least-squares to perform the transformation of signals to and from the time and frequency domains. This approach allowed harmonic balance to be applied to mixers, but was disappointing for two reasons. First, the extra time samples represented a computational burden, the need for which remained unexplained. Second, the normal equation was used to formulate the least-squares problem, which is notoriously ill-conditioned.

Also in 1984, Gilmore and Rosenbaum [gilmore84, gilmore86] presented a completely different transform that exploited sparsity in a spectrum. In theory, it was limited to periodic signals, but in practice, quasiperiodic signals can be approximated arbitrarily closely by periodic signals. This fact is not usually useful when using conventional transforms such as the DFT and the FFT because to approximate quasiperiodic signal accurately with a periodic signal it is usually necessary to use a very low fundamental frequency. Thus the ratio between the highest and lowest frequencies, and hence the number of frequencies needed, is very large. However, the signal at almost all harmonics is zero (i.e., the spectrum is sparse), and so Gilmore and Rosenbaum's transform still remains competitive. The transform samples the waveform using several small sets of equally spaced time-points. The DFT is applied to each set individually. The sets are too small to prevent aliasing in the computed spectra. The aliasing is eliminated by taking an appropriate linear combination of the computed spectra. The spectra are constrained to be periodic in this method because the DFT is used. Though this transform can be much more efficient

than the standard DFT on sparse spectra, the total number of time-points used is normally greater than the theoretical minimum by about 50%.

In 1987, Sorkin, Kundert, and Sangiovanni-Vincentelli [kundert88b, sorkin87] showed that using equally spaced samples in the time domain leads to severe ill-conditioning in the transform that could only be remedied by either using more than the theoretical minimum number of time samples (as in the least squares approach above), or using unequally spaced samples. We presented an algorithm for finding a minimum set of unequally spaced time samples that yields a well-conditioned transform. Using that transform, deemed the Almost-Periodic Fourier Transform (APFT), we developed a very simple and theoretically useful derivation of the harmonic balance algorithm for both the periodic and quasiperiodic cases.

If harmonic balance is applied to a circuit containing algebraic nonlinearities, then it is possible to use the FFT rather than a transform designed for quasiperiodic signals. One such approach based on multidimensional FFTs was proposed by Bava et al [bava82]<sup>2</sup> and later presented by Rizzoli [rizzoli87] and Ushida in 1987 [ushida87]. A slightly more flexible approach was developed independently by Hente and Jansen in 1986 [hente86] and by Kundert and Sangiovanni-Vincentelli in 1987 that uses one-dimensional FFTs. There are two aspects of the second approach that make it very attractive, first is simply that the quasiperiodic algorithm can be made essentially identical to the periodic algorithm. The second reason is very subtle and involves the interaction of aliasing and convergence, but the end result is a considerable reduction in the computation time. While this transform appears to be the most attractive for use in harmonic balance, it seems to have been

---

<sup>2</sup>This claim was made by Filicori and Monaco [filicori88]. I was unable to acquire a copy of the original reference to verify the claim.

completely overlooked by all but its developers.

### 3.3. Switched-Capacitor Filter Simulation

The most common approach to simulating a switched-capacitor (SC) filter is first to break the circuit up into functional blocks such as operational amplifiers and switches. Each functional block is simulated, using a traditional circuit simulator, for some short period. The simulations of the functional blocks are used to construct extremely simple macromodels, which replace the functional blocks in the circuit. The result is a much simplified circuit that can be simulated easily. This simplified circuit is then simulated for the thousands of clock cycles necessary to construct a solution meaningful enough to verify the design.

Ad hoc simulators of this macromodeling sort have commonly been written by frustrated analog designers, but the techniques have also been formalized in programs like *Diana* [de man80] and *Switcap* [fang83]. Although these programs have served designers well, a macromodeling approach is only as good as the macromodel. If a second order effect in a functional block changes overall performance, but this effect is not included in the macromodel, the effect will never be seen in the simulation.

The simulators traditionally intended for use with SC filters, such as *Diana* and *Switcap*, also make the "slow-clock" approximation. After each clock transition, every node in the circuit is assumed to reach its equilibrium point before another transition occurs. This assumption, along with the use of algebraic macromodels, allow the filter to be treated as a discrete-time system with one time-point per clock transition. A set of difference equations is then used to describe the filter.

The slow-clock approach suffers from several serious drawbacks. First, SC filters are being pushed to operate at ever higher frequencies, and the assumption that signals reach

equilibrium between clock transitions is often violated. Also, since signals between clock transitions are not computed, it is possible to miss events that occur in these intervals that might interfere with proper and reliable operation (e.g., clock feed-through spikes causing an operational amplifier to saturate). Lastly, it is not possible to capture the effects of dynamic distortion processes, such as the important effect of the channel conductance on charge redistribution when a transistor switch turns off.

In 1988, Kundert, White, and Sangiovanni-Vincentelli proposed the Mixed Frequency-Time algorithm (MFT) as a method for accelerating detailed simulation when solving for the steady-state solution of switched-capacitor filters. MFT accelerates the detailed simulation of SC filters without resorting to macromodeling or the slow-clock assumption. Thus, it does not suffer from the limitations detailed above. It also does not require a large investment in macromodeling and is suitable for use with automated circuit extractors. Since this approach finds the steady-state solution directly and performs a circuit-level simulation, it is capable of accurately predicting distortion performance, including intermodulation distortion, which is particularly useful for bandpass filters. MFT can be applied to any set of differential or difference equations. Thus, MFT can be applied to the equations resulting from the macromodeling approach, accelerating those methods as well when the steady-state solution is desired.

#### **4. Organization of the Dissertation**

This dissertation presents a number of new algorithms for numerically finding the steady-state response of nonlinear systems of differential equations. The contributions primarily center around harmonic balance and the mixed frequency-time methods. Harmonic balance is a frequency-domain method that has been around for many years while the mixed

frequency-time method uses both frequency- and time-domain concepts and is new. The dissertation presents these methods and the background needed to fully appreciate them in a unified mathematical framework. The presentation blends theory, practice, and results. The theory is given so that the algorithms can be fully understood and their correctness is established. The practical details are given so that the algorithms can be implemented efficiently and accurately. The results are presented to give a feel for what can be expected of these algorithms. Most of the algorithms presented in this dissertation have been implemented and tested in the *Spectre* and *Nitswit* circuit simulators.

Chapter 2 presents several typical circuits for which the steady-state response is of interest but difficult to compute without steady-state methods. These circuits illustrate a few of the common real-world problems to which traditional transient analysis simulators are applied, even though they are overly expensive. This chapter provides motivation for steady-state methods presented in later chapters. The circuits are revisited in Chapter 9 to show the advantages steady-state methods enjoy over transient methods. Also, the various steady-state methods are compared for each of the circuits, and the strengths and weakness of each of the steady-state methods are given in the context of practical applications.

In Chapter 3, rigorous definitions are given for terms associated with signals and a new discrete Fourier transform is presented that is suitable for quasiperiodic signals. The Almost-Periodic Fourier Transform (or APFT) allows both frequency and time data to be spaced nonuniformly. Much of this chapter focuses on presenting the errors that occur in discrete Fourier transforms and methods for reducing the size of those errors. A practical APFT algorithm is given and results from timing and error measurements are provided.

Important background material on differential equations is given in Chapter 4. The chapter begins by defining the concept of the state of a differential equation. Several fundamental properties of differential equations in the context of initial- and boundary-value problems are presented. It is also shown how to formulate the problem of finding a periodic solution as a boundary-value problem. The differential equations that describe analog and microwave circuits are formulated. Next, methods for numerically solving initial-value problems are introduced. These methods convert the problem of solving a nonlinear system of differential equations into one of solving a sequence of nonlinear systems of algebraic equations. The chapter closes by showing how to solve nonlinear algebraic equations using the Newton-Raphson algorithm and what to do if things go wrong.

Chapter 4 shows that the periodic steady state of a differential equation can be found by formulating and solving a particular boundary-value problem. Similarly, Chapter 6 will show that the same is true for the quasiperiodic steady state. Chapter 5 presents the well-known finite-difference and shooting methods as ways of solving boundary-value problems. Both finite-difference and shooting methods are time-domain methods. Along with finite-difference methods, the extrapolation- and Newton-Raphson-based shooting methods are covered.

The important and previously unsolved problem of finding quasiperiodic solutions directly in the time-domain is attacked in Chapter 6. Three approaches are taken, the first involves approximating the problem of finding a quasiperiodic solution with that of finding a periodic solution. This is shown to be inefficient for most problems and in the process it is found that there are many periodic problems that are better to approach as quasiperiodic problems. The second approach is to constrain the solution of a differential equation to be

quasiperiodic by using a particular  $N$ -point boundary constraint. This method is also shown to be inefficient due to some numerical accuracy problems that can only be avoided by integrating the differential equations over a long period of time. The mixed frequency-time (or MFT) method is formulated to avoid the ill-conditioning of the previous method. It combines concepts from both the frequency and time domains and the resulting algorithm is efficient and accurate. This algorithm is explored in some depth and is shown to be simply a way of formulating the quasiperiodic requirement as a two-point boundary-value problem. The implementation of MFT in *Nitswit* is described and results from several different types of circuits are given.

The time-domain steady-state methods are in general a poor fit for microwave circuits because they have trouble handling distributed devices, and microwave circuits usually contain a large number of distributed devices. The traditional choice for microwave circuit simulation has been phasor analysis, a frequency-domain method. Chapter 7 presents harmonic balance, the extension of phasor analysis to nonlinear systems. The harmonic balance equations are formulated and explored. Then discussion focuses on ways to solve these equations. Three different methods are presented, minimization methods based on nonlinear programming, nonlinear relaxation methods, and the Newton-Raphson method. The relaxation methods provide the best speed, but suffer from convergence problems. Newton-Raphson is the most robust approach, but is slow.

Chapter 8 continues the discussion on harmonic balance with an emphasis on practical matters. It is first shown that while in general, harmonic balance requires a quasiperiodic Fourier transform to convert signals to and from the time-domain while evaluating the nonlinear devices, certain fundamental assumptions in the harmonic balance formulation

allow the use of a simpler periodic Fourier transform. This observation allows periodic and quasiperiodic problems to be treated similarly, which makes implementing the algorithm easier, and provides certain efficiencies. Next, a method of solving the harmonic balance equations is derived that inherits the best qualities of the nonlinear relaxation and Newton-Raphson methods. The method is able to adapt to the circuit on a per nonlinearity and per iteration basis. Thus, the method looks as much like the relaxation method to provide the best speed, but for selected devices as determined on each iteration, the method will behave more like Newton-Raphson to avoid convergence problems. These ideas were implemented in *Spectre*, and results are provided to show their effectiveness.

Finally, Chapter 9 compares the various methods for finding steady-state solutions in both a general setting, and with regard to their performance on typical circuits. Chapter 10 summarizes and concludes the dissertation. Appendix A lists standard nomenclature used throughout the dissertation.

# Chapter 2

## Motivation

---

Transient analysis is, by far, the most commonly used method for simulating nonlinear circuits. There are, however, large classes of analog and microwave circuits for which transient analysis is either inappropriate or inefficient. As a motivation for the chapters that follow, this section presents examples from many classes of circuits for which standard performance criteria are difficult to measure using transient analysis. The circuits were selected because they represent an important class of circuits and because they exhibit a common characteristic that make the application of most traditional methods difficult but that can be dealt with by using one or more of the techniques, or foreseeable extensions of the techniques, presented in this dissertation. These circuits are revisited in Chapter 9 at the end of the dissertation where it explained how the these techniques would be applied.

### 1. Self-Biasing Amplifiers

Self-biasing amplifiers are AC-coupled JFET or GaAsFET amplifiers that use a deceptively simple biasing network to reduce the gain of an amplifier when very large signals are applied. Consider the self-biasing amplifier shown in Figure 2.1. When a small input signal is applied, the DC level measured at the gate would be  $v_{bias}$ . However, when large signals are applied, the gate junction diode of the FET will conduct on the positive peaks of the input signal, which results in a DC current flowing into the gate. No DC current

can flow through a capacitor, and so the DC voltage on the gate must fall so that  $R_{bias}$  will provide an average DC current equal to that flowing into the gate. When the DC bias level of the gate falls, so does the gain of the amplifier.

When trying to find the steady-state response of a self-biasing amplifier, the transient that results from the bias circuitry reacting to the large input signal applied suddenly at start-up results in the transient analysis approach being very expensive. There are two factors that aggravate the problem. First, the time constant of the bias circuitry is always chosen to be much longer than the period of the lowest input frequency. Thus, when simulating a wide bandwidth amplifier at its highest input frequencies, the time required for the bias network to settle could be on the order of thousands of cycles of the input, making a transient analysis very expensive. Second, the time required by the bias circuitry to settle is virtually impossible to predict by the user and is often so slow that it is even very difficult to detect when steady-state has been reached. This requires a conservative user to simulate the circuit over a much longer time interval than is probably necessary. The only alternative is to trust a suspect answer with no way of checking its accuracy except to

---

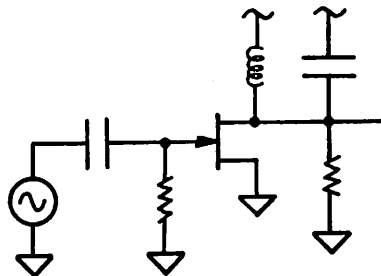


Figure 2.1 : A self-biasing amplifier.

---

resimulate the circuit over a longer time interval to see if the answer changes.

## 2. Mixers

A mixer is a nonlinear circuit that is very commonly used in communications to translate a signal from one frequency to another. A mixer has two inputs, one (RF) is the signal to be translated, and the other (LO) is the translating frequency. The output predominantly contains two signals, the RF translated to the sum and difference frequencies of the RF and LO signals. Usually only the signal at one frequency is desired, and so the mixer is followed by a filter. A simple double-balanced mixer is shown in Figure 2.2.

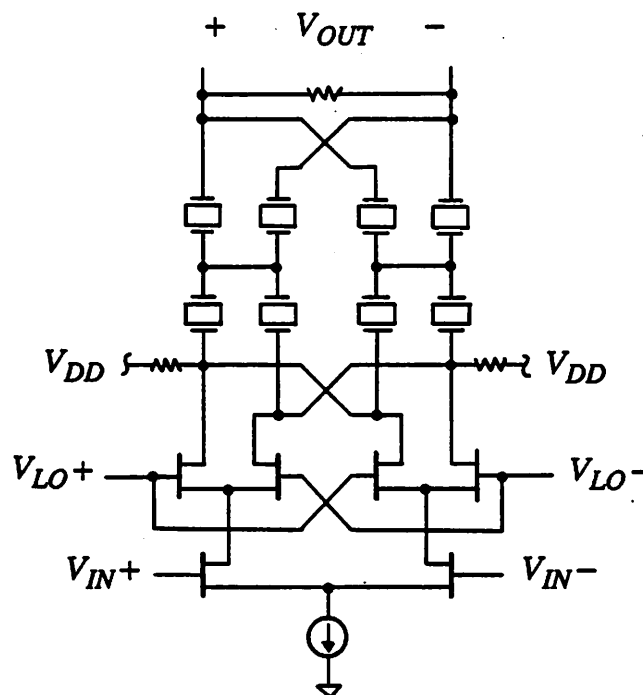


Figure 2.2 : GaAs double balanced mixer.

---

Mixers are very difficult to simulate for two reasons. First, the frequencies of the signals present can be very widely separated. Second, the settling time of the output filter can be very much longer than the period of the lowest frequency present in the mixer. Consider the down conversion mixer in the HP8505 network analyzer [dalichow76]. The mixer has an input RF frequency that ranges from 500kHz to 1.3GHz and an LO frequency that is always offset from the RF by 100kHz. The desired output frequency is 100kHz, and the output is fed directly into a high-Q low-pass filter to assure that this is the only signal present at the output. Simulating this circuit is extremely difficult because the ratio of the input to output frequency can be as high as 13,000 to 1, and because the output filter has a long settling time. Transient simulation of this circuit requires a sampling rate well over 1.3GHz and a simulation interval of at least 100 $\mu$ s — a minimum of  $10^6$  time-points are needed. It is difficult to present meaningful results in the presence of such a large amount of data, particularly with the vastly different time scales involved. Normally, this problem is avoided by converting the solution into the frequency domain, but the many unequally spaced time-points generated by the simulator along with the nonperiodic signals make this a difficult task.

### 3. Narrow-band Amplifiers and Filters

Finding the periodic steady-state response of a narrow-band amplifier and/or filter can be expensive using transient analysis simply because the settling time of the amplifier is usually long in comparison to the period of its center frequency. It can be *extremely* expensive, however, to find the distortion performance of such an amplifier using transient analysis. The method used to measure the distortion of a wide-band amplifier is to apply a pure sinusoid to the input, and determine by how much the output deviates from being a

pure sinusoid in steady state. The distortion products in the output signal will fall at frequencies that are integer multiples of the input frequency. If this same technique were applied to measure the distortion of a narrow-band amplifier, the distortion products would be attenuated because they are outside the bandwidth of the amplifier, and the calculated amount of distortion would be much too low.

Distortion is measured in narrow-band amplifiers by applying two pure sinusoids that have frequencies well within the bandwidth of the amplifier (call these frequencies  $f_1$  and  $f_2$ ). The harmonics of these two frequencies will be outside the bandwidth of the amplifier, however there will be distortion products that fall at the frequencies  $2f_1 - f_2$  and  $f_1 - 2f_2$ . These frequencies should also be well within the bandwidth of the amplifier and so can be used to measure accurately the distortion produced by the amplifier.

Performing such a measurement using transient analysis would require a simulation time interval greater than the period of the difference frequency,  $f_1 - f_2$ .  $f_1$  and  $f_2$  are always chosen such that the difference frequency is well within the passband, so measuring distortion with transient analysis is always considerably more expensive than measuring settling time.

#### 4. Switched-Capacitor Filters

Switched-capacitor filters are simply active RC filters where the resistors have been replaced with a switch and a capacitor. The switch and capacitor are configured as shown in Figure 2.3. The switch alternates between its two positions at the clock frequency, and during each cycle transfers  $C(V_a - V_b)$  coulombs of charge from terminals a to b. Thus, if the clock rate is much higher than the highest frequency present in  $V_a(t)$  and  $V_b(t)$ , then the average current transferred equals  $Cf_c(V_a - V_b)$ , where  $f_c$  is the frequency of the

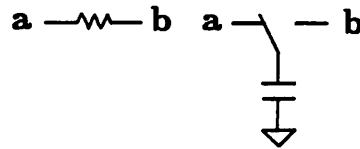


Figure 2.3 : A resistor and its switched-capacitor equivalent.

---

clock. For low frequency signals, the switch and capacitor act like a resistor with resistance  $R = Cf_c$ .

That the clock frequency must be considerably higher than the frequency of the signals being filtered make the transient analysis of switched-capacitor filters particularly expensive. The problem is aggravated because switched-capacitor filters are large circuits. Designers have avoided the expense of detailed simulation of these circuits by replacing the op amps in the active filters with algebraic macromodels and the MOSFET switches with ideal switches. For the actual simulation, they formulate and solve the charge equations once per clock transition.

This approach allows the design of a switched-capacitor filter to be verified from a high-level point of view (i.e., the circuit topology, clocking scheme, and capacitor values are all verified), but error mechanisms due to switch and op-amp dynamics are ignored completely. These effects are quite important and can only be explored using detailed circuit simulation. For example, consider the effect of a power dissipation specification on filter distortion. Circuit designers usually fix the clock rate of the filter based on external specifications and then reduce the bias current in the op-amps as much as possible. As bias current is reduced, so is the speed of the op-amps. The designers must be careful not

to reduce the bias current so low as to interfere with the op-amps ability to handle the required clock frequency. When the op-amp/switch system is not able to settle during a clock cycle, distortion increases dramatically. The macromodel/charge redistribution approach to simulating switched-capacitor filters is useless when trying to predict the lowest possible op-amp bias current because of the necessary assumption that all signals reach their equilibrium values before each clock transition.

## 5. Traveling-Wave Amplifiers

A traveling-wave or distributed amplifier is a circuit that is very important at microwave frequencies. An example amplifier is shown in Figure 2.4 where the small rectangles represent microstrip transmission lines. Traveling-wave amplifiers (TWAs) are representative of most microwave circuits in that they contain a large number of distributed components. These components are difficult to simulate numerically with transient analysis for two reasons. First, formulating the model equations for nonideal distributed components such as lossy or dispersive transmission lines in a manner compatible with numerical integration algorithms is very difficult. Second, evaluation of such models, even for ideal

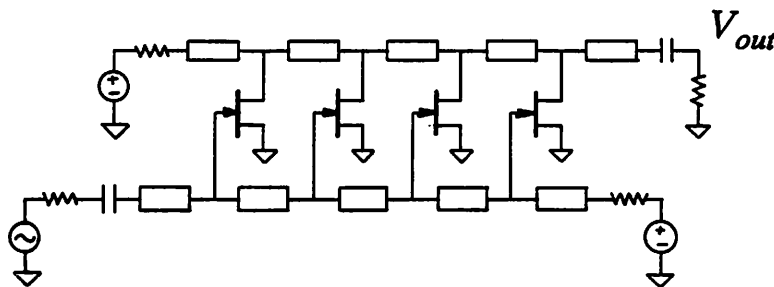


Figure 2.4 : A four-segment GaAs traveling-wave amplifier.

---

transmission lines, can prove to be extraordinarily expensive. This results from an ugly interaction between the nature of transmission lines and the break-point algorithm found in all transient simulators.

A break-point is a point in time when a signal could have an abrupt discontinuity in its first derivative. Break-points occur at each corner of square and triangle waves, and at time 0 for steps, ramps, and sine waves, which are zero for all negative time. It has been found that transient analysis on digital circuits runs moderately faster and is much less likely to miss small but important details in the solution if a time-point is placed at each break-point. If there are no transmission lines in a circuit, the number of break-points is usually quite small because all break-points are assumed to result directly from input signals. Signals other than inputs are ignored when looking for break-points because the finite bandwidth of most circuits will smooth any discontinuities. However, ideal transmission lines have delay and infinite bandwidth. As a result, transmission lines increase the number of break-points. If a mismatched and resistively terminated transmission line is excited by a signal with a discontinuity at time  $t = 0$ , then that signal will propagate down the line and reflect off the terminations, resulting in signals at the ends of the line with discontinuities at times  $\tau, 2\tau, 3\tau, 4\tau, \dots$ , where  $\tau$  is the electrical length of the line. If  $\tau$  is short compared to the simulation interval, then a considerable number of break-points are generated. The situation becomes much worse when several transmission lines with differing lengths are present in the circuit. Break-points generated by one line could enter another line and generate many others. For example, with two lines of length  $\tau_1$  and  $\tau_2$ , break-points could occur at any time  $t = j\tau_1 + k\tau_2$ , where  $j$  and  $k$  are nonnegative integers. With several short lines, the number of break-points could explode in a combinatorial fashion. When the number of break-points explodes, so does the number of time-

points, and so the transient analysis becomes expensive. This situation occurred in the circuit shown in Figure 2.4. This circuit contained transmission lines with 60ps, 186ps, and 250ps electrical length, was driven with a 100MHz sine wave, and was simulated for 2 periods. SPICE2 required over 17 hours and 16 Mbytes to simulate this circuit on a VAX780.

## 6. Measured Devices

It often happens at microwave frequencies that the distributed devices are complex or unusual enough that there are no adequate models available. In these cases, designers rely on measured data to describe their devices to the simulator. For various reasons, network analyzers, which operate in the frequency domain, are used to characterize linear circuits and devices at microwave frequencies. They do so by using S-parameters. Microwave designers routinely employ measured S-parameters in their simulations, however they have always simulated linear circuits in the frequency domain using phasor analysis. These linear frequency-domain simulators are not capable of simulating nonlinear circuits. Transient simulators, which do handle nonlinear circuits, are inherently incompatible with the frequency-domain S-parameter measurements and the measurements must be translated into a form compatible with the integration method. How to do this efficiently is an open research question.

## 7. Crystal and Cavity Oscillators

Crystal and cavity oscillators use very high-Q resonators to achieve very high stability and low noise. The Q of the best resonators can be as high as 1,000,000, leading to a Q in well designed oscillators of up to 100,000. A Q of 100,000 implies that the time constant of the turn-on transient for an oscillator with such a Q is roughly 100,000 cycles of the

oscillation frequency in length. Clearly, transient simulation of such circuit to steady-state is very painful, however steady state is required in order to determine important characteristics, such as the output power and frequency of the oscillator. Designers try to reduce the time required to simulate these circuits by carefully choosing the initial state of the resonator to eliminate any transients. However, in this example, it would be necessary to simulate the oscillator for 1000 cycles simply to notice a 1% difference in the signal envelope. Designers usually do not have the patience to find the initial state that results immediately in steady-state when to do so requires the trial-and-error selection of initial states and where each guess requires simulating the oscillator for over 1000 cycles. Thus, designers usually settle for approximate hand calculations when determining the steady-state characteristics of their oscillators.

# Chapter 3

## Background: Signals

---

This chapter defines important terminology and nomenclature that apply to signals and transforms. For a complete list of nomenclature, see Appendix A. It also introduces the Almost-Periodic Fourier Transform (APFT), a new variation on the Discrete Fourier Transform (DFT) that is suitable for use on the nonperiodic signals found in circuits in steady state with two or more nonharmonically related periodic input signals.

### 1. Signals

A *signal* is a function that maps either  $\mathbb{R}$  (the reals) or  $\mathbb{Z}$  (the integers) into  $\mathbb{R}$  or  $\mathbb{C}$  (the space of real pairs)<sup>1</sup>. The domain and range of the map are physical quantities; the domain is typically time or frequency, and the range is typically voltage or current. A signal whose domain is time is called a *waveform*; one whose domain is frequency is called a *spectrum*. All waveforms are assumed  $\mathbb{R}$ -valued whereas all spectra are assumed  $\mathbb{C}$ -valued.

---

<sup>1</sup>Throughout this dissertation, the trigonometric Fourier series is used rather than the exponential to avoid problems with complex numbers and nonanalytic functions when deriving the harmonic Newton algorithm. Thus, a signal at one frequency in a spectrum is described using the coefficients of sine and cosine. The pair of these are said to reside in  $\mathbb{C} = \mathbb{R}^2$  rather than  $\mathbb{C}$ . Hence, we are using  $\mathbb{C}$  rather than  $\mathbb{C}$  as the scalar field to construct the vector space for spectra. The correspondence between  $\mathbb{C}$  and  $\mathbb{C}$  is established by the invertible function  $\psi: \mathbb{C} \rightarrow \mathbb{C}$  that maps  $a + jb$  to  $[a, b]^T$ .

A waveform  $x$  is *periodic* with *period*  $T$  if  $x(t) = x(t+T)$  for all  $t$ .  $P(T; E)$  denotes the space of all periodic functions<sup>2</sup> with period  $T$  on the domain  $E$  that can be uniformly approximated by the sum of at most a countable number of  $T$ -periodic sinusoids. Thus,  $P(T; \mathbb{R})$  consists of waveforms of the form

$$x(t) = \sum_{k=0}^{\infty} (X^C(k)\cos\omega_k t + X^S(k)\sin\omega_k t), \quad (3.1)$$

where  $X^C(k), X^S(k) \in \mathbb{R}$ ,  $\omega_k = 2\pi k/T$ , and

$$\sum_{k=0}^{\infty} [(X^C(k))^2 + (X^S(k))^2] < \infty. \quad (3.2)$$

A waveform is *almost periodic* if it can be uniformly approximated by the sum of at most a countable number of sinusoids [hale80] [corduneanu68] [besicovitch32] [bohr47] (here there is no assumed relationship between the frequencies of the sinusoids). We use  $AP(\Lambda; E)$  to denote the space of all almost-periodic waveforms on domain  $E$  over the set of frequencies  $\Lambda$ . Thus,  $AP(\Lambda; \mathbb{R})$  consists of waveforms of the form

$$x(t) = \sum_{\omega_k \in \Lambda} (X^C(k)\cos\omega_k t + X^S(k)\sin\omega_k t), \quad (3.3)$$

where  $\Lambda = \{\omega_0, \omega_1, \omega_2, \dots\}$  and (3.2) is satisfied. If  $\Lambda$  is finite with  $K$  elements, it is denoted  $\Lambda_K$ . An evenly sampled almost-periodic signal is denoted  $AP(\Lambda; Z(T, \theta))$  where  $Z$  is the set of sample times  $Z(T, \theta) = \{t : t = sT + \theta, s \in \mathbb{Z}\}$ . Thus  $x \in AP(\Lambda; Z(T, \theta))$  implies

$$x(s) = \sum_{\omega_k \in \Lambda} (X^C(k)\cos\omega_k(sT + \theta) + X^S(k)\sin\omega_k(sT + \theta)),$$

If there is a set of  $d$  frequencies  $\{\lambda_1, \lambda_2, \dots, \lambda_d\}$  and  $\Lambda$  is such that

$$\Lambda = \{\omega \mid \omega = k_1\lambda_1 + k_2\lambda_2 + \dots + k_d\lambda_d; k_1, k_2, \dots, k_d \in \mathbb{Z}\} \quad (3.4)$$

---

<sup>2</sup>In function space, nobody can hear you scream [anobile79].

then  $\Lambda$  is a *module*<sup>3</sup> of dimension  $d$  and the frequencies  $\{\lambda_1, \lambda_2, \dots, \lambda_d\}$  are referred to as the *fundamental frequencies* and form a basis (called the fundamental basis) for  $\Lambda$ . For each  $\omega \in \Lambda$  to correspond uniquely to a sequence of harmonic indices  $\{k_j\}$ , the sequence of fundamental frequencies  $\{\lambda_j\}$  must be linearly independent over the rationals (that is  $\sum_{j=1}^d k_j \lambda_j = 0$  implies  $k_1 = k_2 = \dots = k_d = 0$ ). If  $\Lambda$  is a module, then  $AP(\Lambda; E)$  is also denoted  $QP(\lambda_1, \lambda_2, \dots, \lambda_d; E)$ . Waveforms belonging to such a set are referred to as  $d$ -fundamental *quasiperiodic* or simply *d-quasiperiodic*. Note that  $P(T; \mathbb{R}) = QP(\lambda_1; \mathbb{R})$  if  $\lambda_1 = 2\pi/T$ , and  $P(T; \mathbb{R}) \subset QP(\lambda_1, \lambda_2, \dots, \lambda_d; \mathbb{R})$  if for some  $j$ ,  $\lambda_j = 2\pi/T$ .

The pair  $X(k) = [X^C(k) \ X^S(k)]^T \in \mathbb{C}$  is the *Fourier coefficient* of the *Fourier exponent*  $\omega_k$  and  $X = [X(0), X(1), X(2), \dots]^T$  is called the frequency-domain representation, or *spectrum*, of  $x$ . Conversely,  $x$  is the time-domain representation, or *waveform*, of  $X$ . If all the frequencies  $\omega_k \in \Lambda$  are distinct, (i.e.,  $\omega_i \neq \omega_j$  for all  $i \neq j$ ) then there exists a linear invertible operator,  $\mathbb{F}$ , referred to as the *Fourier transform*, that maps  $x$  to  $X$ . This is a more general definition of the Fourier transform than is in common usage in that the transform applies to almost-periodic as well as to periodic signals. The Fourier transform is a homeomorphism, which allows us to talk of  $x$  and  $X$  as two different representations of the same signal whenever  $X = \mathbb{F}x$ .

## 1.1. Truncation and Discretization

In order for operations involving quasiperiodic signals to be computationally tractable, it is necessary to truncate the frequencies to a finite set. When stimulating a circuit at  $d$  fundamental frequencies, the circuit responds in steady state (if such a solution exists) at

---

<sup>3</sup>Roughly, a module is a set with an identity that is closed under vector addition and scalar multiplication. In this module, the vectors are real numbers, the scalars are integers and the identity is zero.

frequencies equal to the sum and difference of the fundamental frequencies and their harmonics. There are two popular methods for truncating the set of frequencies, the box and diamond truncations. With the box truncation, only the first  $H$  harmonics of each fundamental are considered:

$$\Lambda_K = \{ \omega \mid \omega = k_1 \lambda_1 + k_2 \lambda_2 + \cdots + k_d \lambda_d; \quad (3.5)$$

$$|k_j| = 0, 1, \dots, H; \text{ for } 1 \leq j \leq d; \text{ first nonzero } k_j \text{ positive} \}$$

where  $K = \frac{1}{2}((2H + 1)^d + 1)$ . The first nonzero  $k_j$  must be positive to eliminate frequencies from  $\Lambda_K$  that are negatives of each other. When there are two fundamentals ( $d = 2$ ), this truncation results in a square grid of frequency indices as illustrated in Figure 3.1a.

The diamond truncation limits the absolute sum of the indices  $k_j$  to be less than or equal to  $H$ :

$$\Lambda_K = \{ \omega \mid \omega = k_1 \lambda_1 + k_2 \lambda_2 + \cdots + k_d \lambda_d; \quad (3.6)$$

$$k_j \in \mathbb{Z}; \quad \sum_{j=1}^d |k_j| \leq H; \text{ first nonzero } k_j \text{ positive} \}$$

where  $K = \frac{2^{d-1} H^d}{d!}$ . For  $d = 2$ ,  $K = H^2 + H + 1$ . When there are two fundamentals, this

truncation produces a ‘‘diamond’’ grid as shown in Figure 3.1b. Other truncation schemes are certainly possible. The truncation scheme directly affects the efficiency and accuracy of the simulation, and should be chosen to fit the particular problem being solved.

Now that only a finite set of frequencies  $\Lambda_K$  is being used, the requirement that the fundamental frequencies be linearly independent over the rationals may be relaxed as long as each  $\omega_k \in \Lambda_K$  still corresponds uniquely to a valid sequence of harmonic indices  $\{k_j\}$ .

Once  $\Lambda$  has been truncated to some finite subset  $\Lambda_K$ , it is possible to discretize the waveforms, or represent them as sequences of finite length. Assuming that  $\omega_0 = 0 \in \Lambda_K$

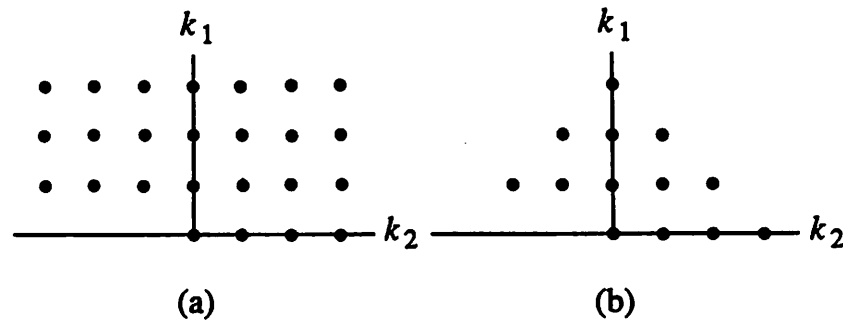


**Figure 3.1** : Two different ways of truncating the set of frequencies to be finite. The box (a) and diamond (b) truncations.

---

and  $x \in AP(\Lambda_K; \mathbb{R})$ , then  $x$  is uniquely specified by almost any set of  $S = 2K - 1$  samples, that is, a set  $\{x(t_i) \mid i = 1, 2, \dots, S; t_i \neq t_j\}$ . This done, the Fourier transform becomes a finite-dimensional operator that depends both on  $\Lambda_K$  and the  $S$  time-points used to sample the waveform. Once the fundamental frequencies and the truncation scheme are specified,  $\Lambda_K$  is fixed, but we are free to choose the time-points as we see fit with the one constraint that  $\mathbb{F}$  be invertible.

## 2. Almost-Periodic Fourier Transform

This section presents a numeric Fourier transform that is an extension over the standard Discrete Fourier Transform (DFT) in the sense that the restriction of harmonically related frequencies is removed. This more general transform is referred to as the Almost-Periodic Fourier Transform (APFT).

## 2.1. Matrix Formulation

To make the transform computationally tractable, it is necessary to consider only a finite number of frequencies. Denote the finite set of frequencies as  $\Lambda_K = \{\omega_0, \omega_1, \omega_2, \dots, \omega_{K-1}\}$  and assume all frequencies are distinct ( $\omega_j \neq \omega_k$  when  $j \neq k$ ) and that  $\omega_0 = 0$ . By considering only a finite number of frequencies, it is possible to sample a waveform at a finite number of time-points and calculate its Fourier coefficients. Since the spaces involved are now finite dimensional, the first representation theorem of linear algebra shows that the Fourier transform  $\mathbb{F}$  and its inverse  $\mathbb{F}^{-1}$  can be viewed as matrices acting on the vectors of samples and coefficients, respectively. That is,

$$\sum_{\omega_k \in \Lambda_K} (X^C(k)\cos\omega_k t + X^S(k)\sin\omega_k t) = x(t)$$

can be sampled at  $S$  time-points, resulting in the set of  $S$  equations and  $2K - 1$  unknowns

$$\Gamma^{-1} \begin{bmatrix} X(0) \\ X^C(k) \\ X^S(k) \\ \vdots \\ X^C(K-1) \\ X^S(K-1) \end{bmatrix} = \begin{bmatrix} x(t_1) \\ x(t_2) \\ x(t_3) \\ \vdots \\ x(t_S) \end{bmatrix} \quad (3.7 \text{ a})$$

where

$$\Gamma^{-1} = \begin{bmatrix} 1 & \cos\omega_1 t_1 & \sin\omega_1 t_1 & \cdots & \cos\omega_{K-1} t_1 & \sin\omega_{K-1} t_1 \\ 1 & \cos\omega_1 t_2 & \sin\omega_1 t_2 & \cdots & \cos\omega_{K-1} t_2 & \sin\omega_{K-1} t_2 \\ 1 & \cos\omega_1 t_3 & \sin\omega_1 t_3 & \cdots & \cos\omega_{K-1} t_3 & \sin\omega_{K-1} t_3 \\ \vdots & \vdots & \vdots & & \vdots & \vdots \\ 1 & \cos\omega_1 t_S & \sin\omega_1 t_S & \cdots & \cos\omega_{K-1} t_S & \sin\omega_{K-1} t_S \end{bmatrix} \quad (3.7 \text{ b})$$

If the frequencies  $\omega_k$  are distinct, and if  $S = 2K - 1$ , this system is invertible for almost all choices of time-points, and can be compactly written as  $\Gamma^{-1}X = x$ . Inverting  $\Gamma^{-1}$  gives  $\Gamma x = X$ .  $\Gamma$  and  $\Gamma^{-1}$  are a discrete Fourier transform pair.

Given a finite set  $\Lambda_K$  of distinct frequencies, and a set of time-points, we say that  $\Gamma$  and  $\Gamma^{-1}$  are one implementation of the almost-periodic Fourier transform for  $AP(\Lambda_K; \mathbb{R})$ . Once  $\Gamma$  and  $\Gamma^{-1}$  are known, performing either the forward (using  $\Gamma$ ) or inverse (using  $\Gamma^{-1}$ ) transform requires just a matrix multiply, or  $(2K - 1)^2$  operations; this is the same number of operations required by the DFT.

The DFT is a special case of (3.7) with  $\omega_k = k\omega$  ( $k = 0, 1, 2, \dots, K-1$ ) and  $t_s = sT/S$  ( $s = 1, 2, \dots, S$ ), i.e. when the frequencies are all multiples of a single fundamental and the time-points are chosen equally spaced within the period. The DFT and its inverse, the IDFT, have the desirable property of being well conditioned, which is to say that very little error is generated when transforming between  $x$  and  $X$ . From the matrix viewpoint, the high accuracy of the DFT corresponds to the fact that the rows of  $\Gamma^{-1}$  are orthogonal. (More is said about this later.) Unfortunately, the DFT and the IDFT are defined only for periodic signals.

For almost-periodic signals, if the time-points are not chosen carefully,  $\Gamma^{-1}$  can be ill-conditioned. In particular, choosing time-points to be equally spaced often is a bad strategy when signals are not periodic. Unlike the periodic case, it is in general impossible to choose a set of time-points over which the sampled sinusoids at frequencies in  $\Lambda_K$  are orthogonal. In fact, it is common for evenly sampled sinusoids at two or more frequencies to be nearly linearly dependent, which causes the ill-conditioning problems encountered in practice. This ill-conditioning can greatly magnify aliasing. Thus, it is important to choose a set of time-points that results in well-conditioned transform matrices. This topic is considered further in the remainder of this chapter.

### 2.1.1. Previous Work

Ushida and Chua [ushida84] use equally spaced time-points, but avoid the ill-conditioning problem by using extra time-points. In doing so, the matrix  $\Gamma^{-1}$  becomes a tall rectangular matrix. To make the system square again, both sides of (3.7) are multiplied by  $(\Gamma^{-1})^T$ , which results in

$$(\Gamma^{-1})^T \Gamma^{-1} X = (\Gamma^{-1})^T x.$$

Thus (3.7) is converted into a least squares problem that is solved in the traditional manner using the normal equation. Unfortunately, the normal equation is notoriously ill-conditioned and so a new ill-conditioning problem may be introduced.

Gilmore [gilmore86] samples the waveform using several small sets of equally spaced time-points. The DFT is applied to each set individually. The sets are too small to prevent aliasing in the computed spectra. The aliasing is eliminated by taking an appropriate linear combination of the computed spectra. Since the DFT is used, the method is constrained to periodic signals, though it can be much more efficient than the standard DFT on sparse spectra. The total number of time-points used is normally greater than the theoretical minimum by about 50%. The numerical stability of this approach is unknown.

### 2.1.2. Condition Number and Orthonormality

It is now necessary to discuss the conditioning of a system of equations, a concept alluded to earlier. Formally, the condition number of a matrix  $A$  is defined as  $\kappa(A) = \|A\| \|A^{-1}\|$  [golub83]. The condition number of a matrix is important because it is a measure of how much errors can be amplified during the course of solving a matrix equation. For example, consider solving  $Ax = b$  for  $x$  when both  $A$  and  $b$  are contaminated with error. Write the contaminated system as

$$(A + \delta A)(x + \delta x) = b + \delta b.$$

If  $\|\delta A\|$  and  $\|\delta b\|$  are small, then  $\|\delta x\|$  can be bounded [golub83] with

$$\frac{\|\delta x\|}{\|x\|} \leq \kappa(A) \left[ \frac{\|\delta A\|}{\|A\|} + \frac{\|\delta b\|}{\|b\|} \right] + \text{higher order terms}$$

The problem of ill-conditioning in (3.7) can be visualized by considering each equation as defining a hyperplane in the Euclidean space  $\mathbb{R}^{2K-1}$ . Let  $\rho_s \in \mathbb{R}^{2K-1}$  be such that  $\rho_s^T$  is the  $s^{\text{th}}$  row in  $\Gamma^{-1}$ ; then the  $s^{\text{th}}$  hyperplane is defined as the set of all points  $X$  such that  $\rho_s^T X = x(t_s)$ . Thus,  $\rho_s$  is a vector orthogonal to the hyperplane. The solution to (3.7) is the intersection of all the hyperplanes. If the system is degenerate because two or more planes are coincident, then the intersection is not a single point and the system of equations has an infinite number of solutions. If there are no coincident hyperplanes, but two or more of the planes are nearly parallel, then a unique solution exists; however, high-precision arithmetic is needed to find it accurately.

A matrix is degenerate if and only if there is a linear dependence among its row vectors, and it is natural to suppose that a matrix has a small (good) condition number if its rows are nearly orthonormal (and thus “far” from being linearly dependent). We now prove this to be true.

Consider an invertible  $N \times N$  matrix  $A$ . Suppose that the rows  $a_n$  of  $A$ , regarded as vectors, are nearly orthonormal. In particular, suppose that each vector has unit Euclidean length and that the orthogonal component of each vector  $a_n$  with respect to the space  $S_n$  spanned by the others is at least  $\alpha \leq 1$  (it would be exactly 1 if the vectors were precisely orthonormal).

When forming the product  $A^{-1}A = \mathbf{1}$ , each row of  $A^{-1}$  can be thought of as the coefficients of a linear combination of the rows of  $A$ . This linear combination yields a

row in the identity matrix — a vector of length 1. Suppose that the  $n^{\text{th}}$  element in a row of  $A^{-1}$  has absolute value  $r > 1/\alpha$ . Then the component of the resulting linear combination that is in the direction orthogonal to  $S_n$  is determined solely by  $ra_n$ , and will have magnitude greater than  $r\alpha > 1$ . Since the linear combination is a vector of unit length, this is a contradiction. Therefore, no element of any row of  $A^{-1}$ , and thus no element of  $A^{-1}$ , has absolute value greater than  $1/\alpha$ .

Since  $A \in \mathbb{R}^{N \times N}$ , it follows that  $\|A^{-1}\|_{\infty}$  (the  $l_{\infty}$  norm of  $A^{-1}$ ) is no more than  $N/\alpha$ . And since, by assumption, the Euclidean norm of the rows of  $A$  equals one,  $\|A\|_{\infty} \leq N$  (employing the equivalence of the  $l_2$  and  $l_{\infty}$  norms in  $\mathbb{R}^N$ ), and therefore,  $\kappa(A) \leq N^2/\alpha$ . In short, the near-orthonormality of a matrix places an upper bound on its condition number.

Note that multiplying a matrix by a scalar  $\beta$  does not affect its condition number, since the norms of the matrix and its inverse are respectively multiplied by  $\beta$  and  $1/\beta$ . Thus, if all rows of a matrix have equal Euclidean length (not necessarily one) and, when scaled to one, satisfy the orthonormality property, the matrix is still well-conditioned. If the rows of a matrix are nearly orthonormal after they have been scaled to unit length, we say that they are (or the original matrix is) nearly orthogonal.

### 2.1.3. Condition Number and Time Point Selection

Given a finite set of frequencies  $\Lambda_K$ , any set of  $S = 2K - 1$  time-points yields a  $\Gamma^{-1}$  whose row vectors (consisting of a single 1 and a set of sine-cosine pairs) have Euclidean norms  $\sqrt{K}$ . Thus, if we could find a set of time-points so that these rows were nearly orthogonal, it would follow from the discussion above that  $\Gamma^{-1}$ , and therefore  $\Gamma$  would be well conditioned.

However the relation between the time-points and the orthogonality of the resultant row vectors is clearly rather involved; finding a set of times which define nearly-orthogonal row vectors seems to be quite difficult. One approach is to write down *a priori* a set of orthogonal vectors and then look for time-points that generate vectors close to these pre-specified ones; this is equivalent to defining the approximate phases of each sine wave and looking for a time where every wave is in the appropriate phase. This in turn can be thought of as a set of approximate equalities modulo  $2\pi$ , but it is far from clear under what circumstances a solution exists or how to go about finding it.

Another approach is to choose time-points equally spaced within a time interval larger than the period corresponding to the smallest nonzero frequency in  $\Lambda_K$ . As we discuss later however, experience shows that this method of time-point selection is unsatisfactory.

#### 2.1.4. Condition Number and Aliasing

As mentioned previously, the condition number provides a measure of how much the error is amplified during a calculation. Roundoff is one source of error in the transform, but there is another that is normally much larger — the error due to truncating  $\Lambda$  to  $\Lambda_K$ . This error consists of two pieces. The Fourier coefficients of the frequencies omitted from  $\Lambda$  are presumably small but may not be exactly zero. Neglecting these frequencies is referred to as truncation error. While neglected in the transforms  $\Gamma$  and  $\Gamma^{-1}$ , these frequencies still exist in the vector of samples  $x$ . They masquerade as frequencies in  $\Lambda_K$  and result in further error that is referred to as aliasing. Because of these errors, the computation of  $X$  will be in error.

Fortunately, this error can be bounded. Suppose that the overlooked sinusoids contribute an error  $\delta x$  to the observed sample vector  $x + \delta x$ . From this we calculate the Fourier coefficients  $X + \delta X$  using

$$X + \delta X = \Gamma(x + \delta x).$$

By construction we know that  $X = \Gamma x$ . Thus,  $\delta X = \Gamma \delta x$ , and  $\|\delta X\| \leq \|\Gamma\| \|\delta x\|$ . By definition,  $\kappa = \|\Gamma\| \|\Gamma^{-1}\|$ . It is easily shown that  $K \leq \|\Gamma^{-1}\|_{\infty} < \sqrt{2}K$ , so  $\|\Gamma\|_{\infty} \leq \kappa_{\infty}/K$  and

$$\|\delta X\|_{\infty} \leq \frac{\kappa_{\infty}}{K} \|\delta x\|_{\infty}. \quad (3.8)$$

That is,  $\kappa_{\infty}/K$  is the upper bound on how much the error due to coefficients of truncated frequencies is amplified in the process of transforming a waveform to the frequency domain. In practice, error amplification factors often approach this bound, so it is very important to select a set of time-points such that  $\kappa$  is small.

The condition number gives a bound on the error that results from aliasing, but it gives little insight and can be pessimistic. Perhaps a better approach to exploring the errors in the APFT is to view the transform as a collection of  $K$  filters, each of which is responsible for computing one Fourier coefficient<sup>4</sup>. These filters take as input a sequence of  $S$  samples and output one coefficient. Such filters are referred to as Finite Impulse Response (FIR) filters [rabiner78] [rabiner75]. Consider the particular filter that computes the coefficient  $X(j)$  from  $\{x_s\}_{s=0}^{S-1}$ . If  $x_s = X^C(k)\cos\omega_k t_s + X^S(k)\sin\omega_k t_s$ ,  $s = 0, 1, \dots, S-1$ , then  $X_j$  must equal zero if  $j \neq k$  and must equal  $[X^C(k), X^S(k)]$  if  $j = k$ . In other words, the filter must have zeros in its transfer response at each frequency  $\omega_k \neq \omega_j$  when  $\omega_k \in \Lambda_K$ , and unity gain when  $\omega_k = \omega_j$ . These constraints are satisfied by

---

<sup>4</sup>Edward Ngoya of Limoges University in France was the first to suggest this interesting and useful interpolation of the APFT.

design. However, the question remains, what is the response of the filter when driven at a frequency  $\omega \notin \Lambda_K$ ? In particular, what is the response when  $\omega \notin \Lambda_K$  but  $\omega \in \Lambda$ ? It is guaranteed by (3.8) that if  $x_s = \cos(\omega t_s + \theta)$  then  $\max_{\omega} |X| \leq \frac{\kappa_{\infty}}{K}$ .

The frequency response of a typical Fourier coefficient filter is shown in Figure 3.2. For this filter,  $\omega_0, \omega_1, \dots, \omega_5 \in \Lambda_K$ ,  $\omega_6, \omega_7, \dots, \omega_9 \notin \Lambda_K$ , and  $\omega_0, \omega_1, \dots, \omega_9 \in \Lambda$ . The actual error due to aliasing is proportional to the response of the filter at frequencies in  $\Lambda$  but not in  $\Lambda_K$ . The condition number bound  $\frac{\kappa_{\infty}}{K}$  may (or may not) be a pessimistic estimation of this error. So far there has been no attempt to choose time-points to minimize the filter response at frequencies in  $\Lambda$  but not in  $\Lambda_K$ . Choosing time-points in this manner would minimize the actual aliasing rather than the bound on the maximum aliasing.

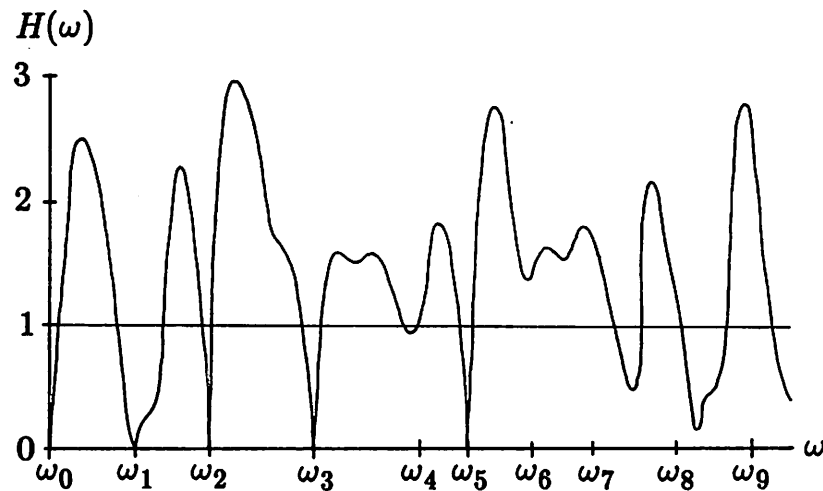


Figure 3.2 : Response of a typical APFT coefficient filter.

---

## 2.2. Near-Orthogonal Selection Algorithm

### 2.2.1. Time Point Selection

Our time-point selection algorithm, referred to as *near-orthogonal selection*, was conceived using some of the ideas discussed above.

First, we thought that if selecting evenly-spaced time-points was likely to yield row vectors particularly close to being linearly dependent, we might be better off selecting time-points randomly from a time interval larger than the period corresponding to the smallest nonzero frequency in  $\Lambda_K$ . (We chose an interval equal to three times this period.) Such a choice is particularly attractive given the complexity of the relationship between the time-points and the orthogonality of the row vectors; making any more intelligent choice of time-points seem quite difficult.

Second, we realized that in essence the problem in recovering  $X$  from  $x$  is that the linear system may be close to being underdetermined, in a numerical sense. So adding additional equations should increase the accuracy of the calculation of  $X$ . In fact, if more than  $S$  time-points are chosen,  $\Gamma^{-1}$  becomes a tall rectangular matrix, and its pseudo-inverse  $\Gamma$  is a wide rectangular matrix satisfying  $X = \Gamma x$ .

Oversampling with twice as many randomly-selected time-points as theoretically necessary proves to be successful: it yields a very well conditioned system. However, when using the transform in the context of harmonic balance, all the nonlinear devices must be evaluated at each time-point. This is an expensive operation because of the complexity of the nonlinear device models. Thus, oversampling is a costly remedy. It is clear, however, that the rows of the tall  $\Gamma^{-1}$  matrix span the space well (in a numerical sense). Perhaps some carefully chosen subset of these rows might also suffice.

The near-orthogonal selection algorithm takes just this approach; from a  $\Gamma^{-1}$  whose dimension is  $M$  rows by  $S$  columns, where  $S = 2K - 1$  and  $M > S$ , it selects a set of just  $S$  rows, thus requiring no extra time samples. In other words, from a pool of more row candidates than necessary (we chose  $M = 2S$ , which seems to give good results practice) and their corresponding time-points, a ‘‘good’’ minimal set is selected during the initialization of the algorithm. When actually performing the transform, only the minimal set of time-points is used. With harmonic balance, all nonlinear devices are evaluated at each time-point. That only the minimum number of time-points is used, and not 1.5 to 2 times the minimum as required by the other methods, is one of the significant advantages of the APFT algorithm.

The near-orthogonal selection algorithm is a variation of the Gram-Schmidt orthogonalization procedure [dahlquist74]. Its input is the matrix formed by randomly choosing twice as many time-points as necessary and forming the corresponding row vectors,  $\rho_s$ . Initially, these vectors all have the same Euclidean length (i.e.,  $l_2$  norm). One of these vectors, say  $\rho_1$ , is chosen arbitrarily. Any component in the direction of  $\rho_1$  is removed from the remaining vectors using

$$\rho_s \leftarrow \rho_s - \frac{\rho_1^T \rho_s}{\rho_1^T \rho_1} \rho_1 \quad s = 2, \dots, M. \quad (3.9)$$

The vectors that remain are now orthogonal to  $\rho_1$ . Since the vectors initially had the same length, the largest remaining vector was originally most orthogonal to  $\rho_1$ . It is chosen to play the role of  $\rho_1$  for the next iteration of the algorithm. This process repeats until the required  $S$  vectors have been chosen. The time-points that correspond to these vectors are the time-points used to form  $\Gamma^{-1}$ . This algorithm is detailed below.

### APFT Near-Orthogonal Selection Algorithm

*Given:*

$\Lambda_K = \{0, \omega_1, \omega_2, \dots, \omega_{K-1}\}$ , the set of frequencies.

*Task:*

To find a set of  $S = 2K - 1$  time-points that results in a well-conditioned  $\Gamma^{-1}$ .

*Algorithm:*

```

 $\omega_{\min} \leftarrow \min(\{|\omega_k| : 1 \leq k < K\})$ 
for ( $s \leftarrow 1, \dots, M$ )
{
  random() returns numbers uniformly distributed between 0 and 1.
   $t_s \leftarrow \frac{6\pi}{\omega_{\min}} \text{random}()$ 
   $\rho_s^{(1)} \leftarrow [1 \ \cos\omega_1 t_s \ \sin\omega_1 t_s \ \dots \ \cos\omega_{K-1} t_s \ \sin\omega_{K-1} t_s]^T$ 
}
for ( $r \leftarrow 1, \dots, S$ )
{
  argmax() returns the index of the largest member of a set.
   $k = \text{argmax}(\{\|\rho_s^{(r)}\| : r \leq s \leq M\})$ 
  swap( $\rho_r^{(1)}, \rho_k^{(1)}$ )
  swap( $\rho_r^{(r)}, \rho_k^{(r)}$ )
  swap( $t_r, t_k$ )
  for ( $s \leftarrow r, \dots, M$ )
    
$$\rho_s^{(r+1)} \leftarrow \rho_s^{(r)} - \frac{\rho_r^{(r)T} \rho_s^{(r)}}{\rho_r^{(r)T} \rho_r^{(r)}} \rho_r^{(r)}$$

}

```

*Results:*

The set  $\{t_s : 1 \leq s \leq S\}$  contains the desired time-points.

Once the time-points are selected,  $\Gamma^{-1}$  is constructed with the rows  $\rho_s^{(1)}$  for  $s = 1, \dots, S$ . It is easy to verify that the time-points are well-chosen either by calculating the condition number  $\kappa = \|\Gamma\| \|\Gamma^{-1}\|$ .

### 2.2.2. Constructing the Transform Matrix

There is another problem that up to now we have ignored. The arguments to the sine and cosine functions in (3.7) are potentially very large, which results in excessive roundoff error. For example, assume  $\lambda_1 = 2\pi 10^9$  and  $\lambda_2 = 2\pi(10^9 + \sqrt{2})$ . Then  $\omega_{\min} = 2\pi\sqrt{2}$  and so the time-points fall between 0 and  $3/\sqrt{2}$  seconds. Thus,  $\omega_i t_s$  can be as large as  $10^{11}$ ,

causing two problems. First, on most computer systems, the trigonometry routines are not designed to handle such large arguments and often return meaningless results. This problem is easily avoided by subtracting from the argument as many multiples of  $2\pi$  as possible without making it negative. The second problem is more troublesome. The approximately  $10^{10}$  multiples of  $2\pi$  in the argument have no effect on the result except to reduce its accuracy by about 10 digits. Since the  $\omega_l t_s$  product must be formed (and so truncated to a finite number of digits by the computer) before the multiples of  $2\pi$  can be removed, the digits are lost and cannot be reclaimed. While this error cannot be eliminated, it can be controlled by assuming  $\Lambda_K$  is a truncated module (note that up to now we have placed no restrictions on the frequencies in  $\Lambda_K$  except that they be distinct and that  $\omega_0 = 0$ ). From (3.6), the product  $\omega_l t_s$  can be written

$$\omega_l t_s = \sum_{j=1}^d k_j \lambda_j t_s.$$

Let

$$\psi_{js} = \text{fract} \left[ \frac{\lambda_j t_s}{2\pi} \right] \quad 1 \leq j \leq d; \quad 1 \leq s \leq S \quad (3.10)$$

and

$$\phi_{ls} = 2\pi \sum_{j=1}^d k_j \psi_{js}. \quad (3.11)$$

Now  $\phi_{ls} = \omega_l t_s - 2\pi m$ , where  $m$  is some integer and  $|\phi_{ls}| \leq 2\pi \sum_{j=1}^d |k_j|$ . Since the  $k_j$  are small integers,  $\phi_{ls}$  is an appropriate argument to trigonometry routines on all computers. Because the product  $t_s \lambda_j / 2\pi$  is formed before the `fract()` operator (which removes any integer portion and leaves only the fractional part) is applied, it is the dominant source of roundoff error. By using (3.10) and (3.11), the roundoff error can be viewed as result-

ing from roundoff error in the  $\lambda_j$  and  $t_s$ . Since the  $t_s$  are chosen randomly, their roundoff errors are of no concern. It will be shown in Chapter 8 that when used with harmonic balance, even errors in  $\lambda_j$  are of no concern.

### 2.2.3. APFT Algorithm Results

The APFT near-orthogonal selection algorithm requires on the order of  $M^2S$  operations, where  $M$  is the number of time-point candidates used, and  $S = 2K - 1$ , where  $K$  is the number of Fourier coefficients. Since we have used  $M = 2S$ , the asymptotic complexity of the algorithm is the same order as that of the matrix inversion needed to compute  $\Gamma$ .

We note that while the initialization of the APFT (that is the time-point selection, formation of  $\Gamma^{-1}$ , and the inversion of  $\Gamma^{-1}$  to find  $\Gamma$ ) requires on the order of  $S^3$  operations, the actual forward and inverse transform requires  $S^2$  operations, the same as the DFT. Thus, the expensive part of the APFT is performed only once per set of frequencies; after this initial overhead has been paid, the APFT is as efficient as the DFT.

To show the numerical stability of our method, we compare the condition number of  $\Gamma^{-1}$  when time-points are 1) evenly spaced, 2) randomly spaced, and 3) determined by the near-orthogonal selection algorithm. The condition number  $\kappa$  is roughly proportional to the errors in computing the inverse. Bear in mind that even the DFT, which is theoretically the best conditioned algorithm for the simpler periodic case, has a condition number  $\kappa \approx N$ , so the best we can hope for is linear growth of the condition number with the number of Fourier coefficients. Observe that, as shown by the results given in Figure 3.3, the condition number from near-orthogonal selection is experimentally observed to grow linearly with  $K$ . That of random selection appears to grow quadratically, and that of evenly spaced grows exponentially.

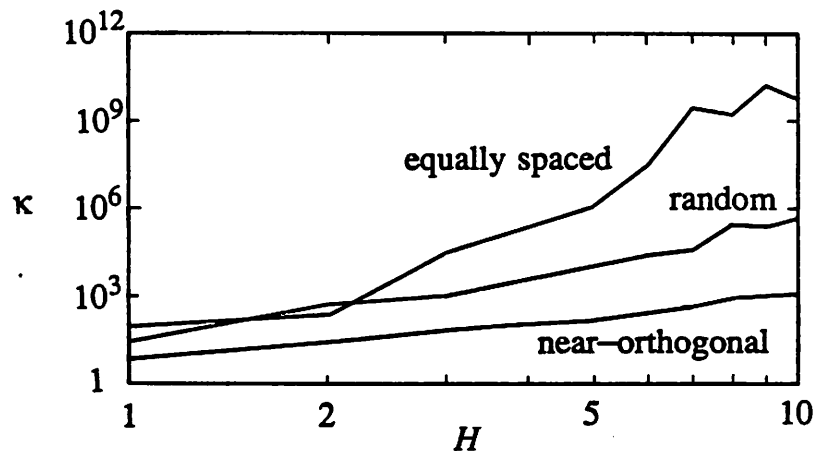


**Figure 3.3** : Condition number of  $\Gamma^{-1}$  versus order  $H$  for the two fundamental APFT with truncation performed using (3.6) and time-points chosen evenly spaced, randomly, and using the near-orthogonal selection algorithm.

The example chosen for comparison was with two fundamentals  $\lambda_1 = 2\pi 10^9$  and  $\lambda_2 = 2\pi(10^9 + \sqrt{2})$ . Thus, the fundamentals differ by only 1 part in  $10^9$ ; also, because the fundamentals are incommensurable, the signal is not periodic. Truncation was performed using (3.6). Comparisons of the condition numbers are shown in Figure 3.3 with the order  $H$  varying between 1 and 10. To smooth the wide variation seen in the results for the case of randomly selected time-points, each condition number plotted is the geometric mean of 10 trials. Similarly, because different intervals give widely varying results for evenly-spaced points, those condition numbers are geometrically averaged over 10 intervals ranging from 1.5 to 4.5 times  $2\pi/\omega_{\min}$ . Results obtained from near-orthogonal selection are so consistent that no averaging was needed, as evidenced by the smoothness of that curve. Graphing the condition number clearly shows that both randomly chosen and evenly spaced samples have accuracy problems when the number of frequencies is large. Near-

orthogonal selection from  $2S$  randomly selected time-points always results in a reasonable condition number. Table 3.1 gives a summary of information on the APFT with the near-orthogonal selection algorithm. Execution times were measured using the C programming language on a VAX 8650 running ULTRIX 2.0.

APFT Summary					
$H$	$K$	$S$	$\kappa$	$t_{init}$	$t_{transform}$
1	3	5	6	17 ms	0
2	7	13	24	67 ms	0.3 ms
3	13	25	64	280 ms	1.7 ms
4	21	41	113	1.1 s	3.6 ms
5	31	61	143	3.3 s	8.5 ms
6	43	85	270	8.6 s	17 ms
7	57	113	420	20 s	30 ms
8	73	145	790	41 s	49 ms
9	91	181	950	79 s	77 ms
10	111	221	1200	142 s	116 ms

**Table 3.1** : Error estimates and execution times for the APFT algorithm using double precision arithmetic on a VAX 8650 with  $\lambda_1 = 10^9$ ,  $\lambda_2 = 10^9 + \sqrt{2}$ , and truncation performed using (3.6).  $H$  is the number of harmonics of each fundamental.  $K$  is the total number of frequencies and  $S$  is the number of time samples.  $\kappa$  is the condition number of  $\Gamma^{-1}$  and  $\varepsilon = \|\Gamma^{-1}\Gamma - 1\|$ .  $t_{init}$  is the time required to choose the time-points and form and invert  $\Gamma^{-1}$ .  $t_{transform}$  is the time required to multiply either  $\Gamma^{-1}$  or  $\Gamma$  by a vector.

Recall that coefficients of frequencies not in  $\Lambda_K$  can be amplified by up to  $\kappa/K$ . For order  $H = 10$ , this amplification factor equals approximately  $10^8$  for evenly spaced points, 2000 for randomly spaced points, and 10 for points chosen using near-orthogonal selection. Thus, even if the coefficients of neglected frequencies are small, for evenly and randomly spaced points, the error  $\delta X$  due to truncation may be so large as to dominate over the desired coefficients  $X$ .

# Chapter 4

## Background: Systems

---

This chapter defines important terminology and nomenclature regarding systems of differential equations. For a complete list of nomenclature, see Appendix A. It also introduces the circuit simulation problem and presents the basic algorithms and techniques used to solve numerically the systems of nonlinear ordinary differential equations that result from this problem.

### 1. Systems

A collection of devices is called a *system* if the devices are arranged to operate on input signals (the *stimulus*) to produce output signals (the *response*). For a given solution of a system's describing equations, the system is considered to be in *steady state* if the solution is *asymptotically stable*. By this it is meant that any solution near the steady-state solution asymptotically approaches it as time increases [hirsch70]. This dissertation considers only systems in periodic and quasiperiodic steady state.

A system is *autonomous* if both it and its stimulus are time invariant, otherwise it is *forced*. An oscillator is an example of an autonomous system while an amplifier, a filter, and a mixer are all examples of forced systems. An *algebraic* or *memoryless* device or system is one whose response is only a function of the present value of its stimulus, not past or future values. Traditionally, a lumped device is one whose physical dimensions are

much smaller than the wavelengths of the signals present in the circuit. In this dissertation, a device is considered *lumped* if it is accurately modeled with an algebraic function of a finite number of network variables (voltage, current, charge, flux). Any device that is not lumped is *distributed*. A lumped system contains only lumped devices.

### 1.1. State

A set of data qualifies to be called the *state* of a system if it satisfies the following two conditions [desoer69].

1. For any time, say  $t_1$ , the state at  $t_1$  and the stimulus specified from  $t_1$  on, determine uniquely the state at any time  $t > t_1$ .
2. The combination of the state and the stimulus at any time  $t$  determine uniquely the value at time  $t$  of any significant quantity of the system. If the system is an electrical circuit, the significant quantities are usually considered the network variables ( $v$ ,  $i$ ,  $q$ ,  $\phi$ ).

In general the state is not unique. There may be many collections of network variables that qualify as the state.

For lumped systems, the state is a finite set of numbers, usually arranged as a vector. The components of this *state vector* are referred to as *state variables*. The state of a distributed device is described using one or more functions rather than a finite set of numbers. For example, consider an ideal transmission line. At some time  $t_1$ , one must know the voltage and current waveforms along the entire length of the line as well as the stimulus from  $t_1$  on in order to predict accurately, say, the future voltages at the ends of the line.

A system can be described with an equation of the form

$$f(x, t) = 0 \quad (4.1)$$

where  $x(t)$  is a vector of network variables. If it is possible to reformulate this equation into the form

$$\dot{y}(t) = g(y(t), t) \quad (4.2)$$

where the  $y(t)$  is a vector of state variables and if there is a one-to-one correspondence between every solution  $y$  of (4.2) and every solution  $x$  of (4.1), then (4.2) is a *state equation in normal form* for the system described by (4.1). A solution  $x$  of (4.1) is called a *trajectory* and the corresponding  $y$  is the *state trajectory*.

Define  $\phi$  to be the function that maps the state  $y_0$  at  $t_0$  into the solution to 4.2. That is,

$$y(t) = \phi(y_0, t_0, t). \quad (4.3)$$

This function is referred to as the *state-transition function*. It has the characteristic that if  $y(t_1) = \phi(y(t_0), t_0, t_1)$  and  $t_1 = t_0$ , then  $y(t_1) = y(t_0)$ .

## 2. Problem Formulation

In the interest of keeping notation simple we consider only nonlinear time-invariant circuits consisting of independent current sources and voltage controlled resistors and capacitors. These restrictions are mostly cosmetic, they allow the use of simple nodal analysis to formulate the circuit equations. All the results in this chapter can be applied to circuits containing inductors, voltage sources, and current-controlled components if a more general equation formulation method such as modified nodal analysis is used [sangiovanni81]. Initially we also only consider nonautonomous (or forced) circuits. That is, circuits with at least one periodic input source. Within these constraints, two test problems are defined,

one appropriate only for lumped devices, and one that allows linear distributed devices.

## 2.1. Lumped Test Problem

Let  $N$  be the number of nodes in a lumped circuit (excluding the reference node, ground). Consider two cases. For the periodic case, assume the input waveforms and the solution  $\hat{v}$  belong to  $P^N(T; \mathbb{R})$ . For the quasiperiodic case with  $d$  fundamental frequencies  $\lambda_1, \lambda_2, \dots, \lambda_d$ , assume both the input and the solution waveforms are members of  $QP^N(\lambda_1, \lambda_2, \dots, \lambda_d; \mathbb{R})$ . Further assume that for both cases the solution is isolated and asymptotically stable and that all device constitutive equations are differentiable when written as a function of voltage. Now the circuit can be described by

$$f(v, t) = i(v(t)) + \dot{q}(v(t)) + u(t) = \mathbf{0} \quad (4.4)$$

where  $v$  is the vector of node voltage waveforms;  $u$  is the vector of source current waveforms;  $i, q: \mathbb{R}^N \rightarrow \mathbb{R}^N$  are differentiable functions representing respectively the sum of the currents entering the nodes from *all* conductors, and the sum of the charge entering the nodes from *all* capacitors;  $f$  is the function that maps the node voltage waveforms into the sum of the currents entering each node;  $t \in \mathbb{R}$  is time; and  $\mathbf{0} \in \mathbb{R}^N$  is the zero vector.

## 2.2. Distributed Test Problem

Again consider two cases, the periodic case (as above) and the quasiperiodic case where the input and solution waveforms belong to  $QP^N(\lambda_1, \lambda_2, \dots, \lambda_d; \mathbb{R})$ . Assume all other conditions for (4.4) hold except that the circuit may contain voltage controlled linear distributed devices. This circuit can be described by

$$f(v, t) = i(v(t)) + \dot{q}(v(t)) + \int_{-\infty}^t y(t-\tau)v(\tau)d\tau + u(t) = \mathbf{0} \quad (4.5)$$

where  $f$  is the function that maps the node voltage waveforms into the sum of the currents

entering each node;  $u \in QP^N(\lambda_1, \lambda_2, \dots, \lambda_d; \mathbb{R})$  is the vector of source current waveforms;  $i, q: \mathbb{R}^N \rightarrow \mathbb{R}^N$  are differentiable functions representing, respectively, the sum of the currents entering the nodes from the *nonlinear* conductors, and the sum of the charge entering the nodes from the *nonlinear* capacitors;  $y$  is the matrix-valued impulse response of the circuit with *all* the nonlinear devices removed<sup>1</sup>,  $t \in \mathbb{R}$  is time; and  $\mathbf{0} \in \mathbb{R}^N$  is the zero vector.

Notice that in this test case,  $y$  represents all linear components and  $i$  and  $q$  represent only nonlinear components. This differs from the lumped test case where  $i$  represents all resistors (both linear and nonlinear) and  $q$  represents all capacitors.

### 3. Differential Equations

In general, differential equations have an infinite number of solutions and it is necessary to place constraints on the solutions until only one remains. If the constraints are all placed at the same point in time, the combination of the differential equation and the constraint equation is called an *initial-value problem* because the constraints are normally placed at the beginning of the interval of interest and the differential equation integrated with  $t$  increasing. It is also possible to put the constraints at the end of the interval of interest. Such a problem is referred to as a *final-value problem* and is treated identically to the initial-value problem except the differential equation is integrated with  $t$  decreasing. It is also possible to place the constraint at a point inside the interval of interest and break the problem into two independent problems, an initial- and a final-value problem.

It is not necessary to place all  $N$  constraints at the same point in time. A differential equation combined with an algebraic equation that constrains the solution at more than one

---

<sup>1</sup>To remove a nonlinear device, simply replace its constitutive equation  $y = f(x)$  with  $y = 0$ .

distinct points in time is referred to as a *boundary-value problem*.

### 3.1. Initial-Value Problems

Consider the equation

$$\dot{x}(t) = f(x(t), t) \quad (4.6)$$

where  $x(t) \in \mathbb{R}^N$  is the state vector, and  $t$  is time. It is enough to specify the value of  $x$  at some point in time (ex.,  $x(0) = x_0$ ) and require that  $f$  be sufficiently smooth to assure that (4.6) has a unique solution.

**Theorem 4.1:** *Let the function  $f(x, t)$  be continuous in  $t$  over the finite interval  $[0, T]$  for all  $x$  and Lipschitz continuous in  $x$ , uniformly in  $t$ . That is,*

$$\|f(x, t) - f(y, t)\| \leq K \|x - y\|$$

*for all  $x, y \in \mathbb{R}^N$  and  $t \in [0, T]$ .  $K$  is known as the Lipschitz constant. Then the initial-value problem*

$$\dot{x}(t) = f(x(t), t), \quad x(0) = x_0$$

*has a unique solution  $x = x(t, x_0)$  over the interval  $0 \leq t \leq T$ . Furthermore, the solution is Lipschitz continuous in  $x_0$ , uniformly in  $t$  and satisfies*

$$\|x(t, x_0) - x(t, y_0)\| \leq e^{Kt} \|x_0 - y_0\|$$

*for all  $t \in [0, T]$  and  $x_0, y_0 \in \mathbb{R}^N$ .*

□

The proof of this theorem is given in Stoer and Bulirsch [stoer80].

It is useful to know when a solution to the initial-value problem defined by (4.4) and an initial state  $v(0) = v_0$  exists and is unique. Theorem 4.1 cannot be used directly because (4.4) is in the wrong form. However, it can be manipulated into the correct form by using the chain rule.

$$i(v(t)) + \frac{dq(v(t))}{dv(t)} \frac{dv(t)}{dt} + u(t) = 0$$

$$i(v(t)) + C(v(t))\dot{v}(t) + u(t) = 0$$

where  $C(t) = \frac{dq(v(t))}{dv(t)}$ ,  $C$  being a time varying capacitance matrix. Assume  $C(v(t))$  is nonsingular for all  $v(t)$ .

$$\dot{v}(t) = -C^{-1}(v(t))(i(v(t)) + u(t))$$

Thus from Theorem 4.1, the solution to the initial-value problem defined by (4.4) and the initial state  $v(0) = v_0$  exists and is unique if  $i$  is Lipschitz continuous and if  $u$  is bounded and  $C^{-1}(v(\cdot))$  is uniformly bounded with respect to  $v$  [hale80].

## 3.2. Boundary-Value Problems

The problem of finding a solution to a system of ordinary differential equations is a boundary-value problem if that solution is required to satisfy subsidiary conditions at two or more distinct points in time. For example, finding the solution to

$$\dot{x}(t) = f(x(t), t)$$

over the interval  $[0, T]$  is a two-point boundary-value problem if the solution is required to satisfy

$$g(x(0), x(T)) = 0.$$

Boundary-value problems are interesting when solving for steady-state solutions because the problem of finding the periodic or quasiperiodic solution to a differential equation can be posed as a boundary-value problem.

### 3.2.1. Existence and Uniqueness of Solutions

From Theorem 4.1, the initial-value problem

$$\dot{x}(t) = f(x(t), t), \quad x(0) = x_0$$

is assured of having a unique solution if  $f$  is continuous in  $t$  and Lipschitz continuous in  $x$  uniformly in  $t$ . However, from the second part of this same theorem, it is clear that these same conditions are insufficient to assure that the two-point boundary-value problem even has a solution. For example, let  $y_0$  be the initial state of the initial-value problem

$$\dot{y}(t) = f(y(t), t), \quad y(0) = y_0$$

Using the solution to this initial-value problem, and given the differential equation

$$\dot{x}(t) = f(x(t), t) \tag{4.7 a}$$

construct the boundary constraint

$$x(T) - (e^{KT} + 1)x(0) = y(T) - (e^{KT} + 1)y(0) \tag{4.7 b}$$

where  $K$  is the Lipschitz constant for  $f$ . This boundary-value problem has no solution because the final state

$$x(T) = y(T) - (e^{KT} + 1)(y(0) - x(0))$$

is unreachable from any initial state  $x(0)$ , which is shown by writing (4.7 b) as

$$x(T) - y(T) = -(e^{KT} + 1)(y(0) - x(0))$$

Then,

$$\|x(T) - y(T)\| = (e^{KT} + 1)\|y(0) - x(0)\|$$

$$\|x(T) - y(T)\| > e^{KT}\|y(0) - x(0)\|,$$

which violates the second part of Theorem 4.1.

The existence and uniqueness theory for boundary-value problems is considerably more complicated and less thoroughly developed than for initial-value problems. If the solution is linearly constrained at only two points, which is the usual case, then some reasonably concise and powerful statements can be made. Consider a system of  $N$  first order differential equations

$$\dot{x}(t) = f(x(t), t) \quad (4.8 \text{ a})$$

subject to the most general linear two-point boundary conditions

$$Ax(0) + Bx(T) = c, \quad (4.8 \text{ b})$$

where  $x(t) \in \mathbb{R}^N$ ,  $f : \mathbb{R}^{N+1} \rightarrow \mathbb{R}^N$ ,  $A, B \in \mathbb{R}^{N \times N}$ , and  $c \in \mathbb{R}^N$ .

The study of the existence and uniqueness of solutions to the boundary-value problem (4.8) reduces to the study of the roots of a system of nonlinear equations by posing (4.8 a) as an initial-value problem. Consider

$$\dot{x}(t) = f(x(t), t) \quad (4.9 \text{ a})$$

$$x(0) = x_0 \quad (4.9 \text{ b})$$

and recall that the state-transition function  $\phi(x_0, t_0, t_1)$  is the solution to this initial-value problem at time  $t_1$  starting from the state  $x_0$  at time  $t_0$ .

The solution to the boundary-value problem (4.8) is the solution to the initial-value problem (4.9) where the  $x_0$  is chosen to satisfy the implicit nonlinear equation

$$Ax_0 + B\phi(x_0, 0, T) - c = 0. \quad (4.10)$$

In other words, if  $x_0$  is a root of (4.10), then  $x(t) = \phi(x_0, 0, t)$  solves (4.8).

**Theorem 4.2 :** *Let the function  $f(x, t)$  be continuous in  $t$  over the interval  $[0, T]$  for all  $x$  and Lipschitz continuous in  $x$ , uniformly in  $t$ . Then the boundary-value problem (4.8) has as many solution as there are distinct roots  $x_0^{(j)}$  of Equation (4.10). These solutions are*

$$x^{(j)}(t) = \phi(x_0^{(j)}, 0, t),$$

*the solutions of the initial-value problem (4.9) with initial state  $x(0) = x_0^{(j)}$ .*

□

This theorem was developed by Keller and the proof is given in [keller68].

Reducing the problem of solving the boundary-value problem (4.8) to that of finding the roots of a system of nonlinear equations is interesting because it is the idea behind shooting methods. Shooting methods, presented in detail in Chapter 5, are the most commonly used methods for finding the solutions to boundary-value problems.

Theorem 4.2 is only mildly interesting when exploring the existence and uniqueness of solution to boundary-value problems because it is generally quite difficult to prove the existence of roots to a system of nonlinear equations. Keller used the contraction mapping theorem (Theorem 7.1) to show the existence of roots to (4.10) under certain conditions [keller68].

**Theorem 4.3 :** *Let the function  $f(x, t)$  for  $0 \leq t \leq T$  and  $\|x\|$  bounded satisfy*

- (a)  $f(x, t)$  continuous;
- (b)  $\frac{\partial f_m(x, t)}{\partial x_n}$  continuous,  $m, n = 1, 2, \dots, N$ ;
- (c)  $\|J_f(x, t)\|_\infty \leq k(t)$  where  $J_f(x, t) = \frac{\partial f(x, t)}{\partial x}$ .

Furthermore, let the scalar function  $k$  and the matrices  $A$  and  $B$  satisfy

- (d)  $A + B$  nonsingular;

- (e)  $\int_0^T k(t) dt \leq \ln(1 + \lambda \alpha)$

for some  $\lambda$  in  $0 < \lambda < 1$ , where

$$\alpha = \|(A + B)^{-1}B\|_\infty.$$

Then the boundary-value problem (4.8) has a unique solution for each  $c$ .

□

This theorem gives a sufficient but not a necessary condition for existence (and by Theorem 4.1, conditions for uniqueness) of a solution to a boundary-value problem. Thus, solutions may exist for boundary-value problems that do not satisfy these conditions. Keller, Stoer and Bulirsch present further theorems on the existence of solutions to boundary-value problems [keller68] [stoer80].

### 3.3. Boundary-Value Problems in Circuit Simulation

One approach to finding the steady-state solution of a circuit is to restrict the solution to be either periodic or quasiperiodic by using an appropriate boundary constraint. Thus, the problem of finding the steady state is converted into a boundary-value problem, to which the standard approaches, such as shooting methods and finite-difference methods, can be applied. In the following section, boundary constraints are formulated for periodic solutions. Boundary conditions for quasiperiodic solutions are presented in Chapter 6.

#### 3.3.1. Periodic Boundary Constraint

A function  $x$  is periodic with period  $T$  if  $x(t) = x(t + T)$  for all  $t$ . This is a difficult condition to apply in practice because it must be verified over all  $t$ . However, if  $x$  is the solution of a differential equation that satisfies the smoothness conditions of Theorem 4.1, then by uniqueness, if  $x(t) = x(t + T)$  for some  $t$ , it is true for all  $t$ .

**Theorem 4.4 :** *Consider the initial-value problem*

$$i(v(t)) + \dot{q}(v(t)) + u(t) = 0 \quad (4.11 a)$$

$$v(0) = v_0, \quad (4.11 b)$$

where  $u(t)$  is  $T$ -periodic. If for all  $v_0$  there exists a unique solution, and if there exists a solution  $v$  that satisfies

$$v(t) = v(t + T) \quad (4.11 c)$$

for some  $t$ , then  $v$  is  $T$ -periodic.

This follows directly from the fact that  $u(t+T) = u(t)$  and the uniqueness assumption of the solution to the differential equation. Thus, to find the periodic steady-state solution of the lumped test problem, it is enough that the solution satisfy the two-point boundary constraint  $v(t) = v(t + T)$  for *some*  $t$  and that (4.4) has a unique solution when formulated as an initial-value problem.

By Theorem 4.2, finding the periodic solution of a differential equation using the periodic boundary constraint (4.11 c) is equivalent to solving for the root of

$$\phi(v(0), 0, T) - v(0) = 0 \quad (4.12)$$

where  $\phi$  is the state-transition function of the differential equation. This equation takes the form of (4.10) with  $A = -\mathbf{1}_N$ ,  $B = \mathbf{1}_N$ ,  $c = \mathbf{0}$ , and  $x = v$ , where  $\mathbf{1}_N$  is the  $N \times N$  identity matrix.

### 3.3.2. Oscillators

A circuit is said to be autonomous if all its components and inputs do not vary with time. That is, the relationship between voltage and current for a resistor, voltage and charge for a capacitor, and flux and current for an inductor is time invariant and independent sources are constant valued. Oscillators are autonomous circuits that have nonconstant periodic solutions. The problem of finding the steady-state solution of an oscillator can be posed as a boundary-value problem with a free boundary. It is possible to adapt each of the methods that will be presented for two-point boundary-value problems to the oscillator problem.

Oscillators present two problems not previously faced. The first, as pointed out above, is that the period of the oscillation is unknown and must be determined. The second is that the time origin is arbitrary and thus if one solution exists, then an infinite continuum of solutions exists. In other words, if  $v$  is a solution, then so is any time shifted version of  $v$  (there is no input signal to fix the phase). The problem is that most of the methods presented use Newton-Raphson, which fails if the solution is not isolated. It is necessary to modify either Newton-Raphson to handle nonisolated solutions or the problem formulation to eliminate the nonisolated solutions.

There are two degenerate cases that cause any Newton-Raphson based method to fail when applied to the oscillator problem. Surprisingly enough, linear problems are one such case. In linear oscillators, the amplitude of the oscillation is not unique: if the circuit supports an undamped oscillation then the oscillation may be of any amplitude. Thus, not only is there a continuum of solutions parameterized on  $t$ , but also a continuum parameterized on the amplitude of the oscillation. A similar situation arises when a solution is a constant waveform. For this case, the additional continuum is parameterized in the period  $T$ .

In general, one needs to worry about quasiperiodic solution to autonomous problems. Examples include driven oscillators where  $\lambda_1, \dots, \lambda_j$  is determined by autonomous oscillations and  $\lambda_{j+1}, \dots, \lambda_d$  are determined from input sources; and coupled oscillators, where  $\lambda_1, \dots, \lambda_d$  are all autonomous oscillations. The methods developed for periodic autonomous oscillators are easily extended to handle these situations.

### 3.4. Numerical Solution of Initial-Value Problems

Lumped circuits are modeled using a system of nonlinear differential equations. Before the system can be solved it is necessary to specify the boundary conditions. Traditionally, circuit simulators treat only initial-value problems, so the initial state (here, the node voltages) are specified at  $t = 0$  and the equations are integrated forward in time. Equation (4.4) can be written as an initial-value problem if the steady-state constraint on  $v$  is lifted and an initial state is specified.

$$i(v(t)) + \dot{q}(v(t)) + u(t) = 0 \quad v(0) = v_0 \quad (4.13)$$

It is not possible to solve numerically systems of nonlinear differential equations directly. Instead, it is common to solve a discretized approximation to the differential equation.

#### 3.4.1. Discretization

Discretization approximates a system of differential equations with a system of difference equations. In other words, the time interval of interest  $[0, T]$  is divided into a finite number of possibly nonuniform subintervals with a monotonically increasing sequence of time-points  $\{t_0, t_1, \dots, t_S\}$  where  $t_0 = 0$  and  $t_S = T$ . The subintervals are called time-steps and denoted by  $h_s = t_s - t_{s-1}$ . At  $t_s$  the solution of the discretized system  $v_s$  is an approximation to  $v(t_s)$ , the solution of the original differential equation (4.13). At each time-point, an algebraic system of equations must be solved, thus discretization converts a differential equation into a sequence of algebraic equations that can be solved numerically.

To discretize a system of differential equations it is necessary to have a discrete approximation to  $\dot{q}$ . A set of approximations commonly used in circuit simulation are the backward difference formulae [chua75] [gear71], which are defined by

$$\dot{q}_{s+1} = \frac{1}{bh_{s+1}} \sum_{r=1}^p a_r q_{s-r} a_{-1} = -1 \quad (4.14)$$

The simplest of the backward difference formulae are the one-step methods

$$\text{Explicit Euler: } \dot{q}_s = \frac{q_{s+1} - q_s}{h_s} \quad (4.15)$$

$$\text{Implicit Euler: } \dot{q}_{s+1} = \frac{q_{s+1} - q_s}{h_{s+1}} \quad (4.16)$$

Of these two methods, implicit Euler has the desirable property of being stiffly stable, which means that it is well behaved even if the differential equations being solved have widely separated time constants. This is not true for explicit Euler [white86] [gear71].

It is natural to apply backward difference formulae to initial-value problems because, when computing the solution at  $t_s$ , it is only necessary to know the solution at previous values of time. The integration is conveniently carried out by starting at  $t_0$  and progressing forward in time toward  $t_s$ .

#### 4. Numerical Solution of Nonlinear Algebraic Equations

The algebraic equations generated by discretization are nonlinear and so are not solvable explicitly. Linearization is the process of converting an implicit nonlinear equation into a sequence of implicit linear equations. The sequence of linear equations is constructed such that, if an accumulation point exists, its solution is the solution of the nonlinear problem. Usually, the Newton-Raphson algorithm, or one of its variants, is used to construct the sequence of linear problems. For example, consider the implicit nonlinear system of equations

$$f(\hat{x}) = 0$$

where  $\hat{x} \in \mathbb{R}^N$  and  $f : \mathbb{R}^N \rightarrow \mathbb{R}^N$ . The Newton-Raphson algorithm needs an initial guess  $x^{(0)}$  of the solution  $\hat{x}$  to start. It then linearizes  $f(x)$  about  $x^{(0)}$  by using the Taylor

expansion while neglecting the higher order terms.

$$f(x^{(1)}) = f(x^{(0)}) + \frac{df(x^{(0)})}{dx}(x^{(1)} - x^{(0)}) + O((x^{(1)} - x^{(0)})^2)$$

where  $\frac{df(x)}{dx}$  is the Frechet derivative of  $f$  with respect to  $x$  [ortega70]. The Jacobian

$J_f(x)$  is a representation of the Frechet derivative, and if it exists it takes the form

$$\frac{df(x)}{dx} = J_f(x) = \left[ \frac{\partial f_m(x)}{\partial x_n} \right], \quad m, n = 1, 2, \dots, N.$$

$O(\cdot)$  is a function that represents the higher order terms and is such that  $\lim_{\alpha \rightarrow 0} \frac{\|O(\alpha)\|}{\alpha}$  is

bounded. Let

$$f_L^{(0)}(x^{(1)}) = f(x^{(0)}) + J_f(x^{(0)})(x^{(1)} - x^{(0)})$$

where  $f_L^{(0)}(x)$  is the linearized approximation to  $f(x)$ . (It is the hyperplane that is tangent to  $f(x)$  at  $x^{(0)}$ .) An improved approximation to  $\hat{x}$  is now found by solving for the root of the linearized approximation to  $f(x)$ . That is, finding the value of  $x$ , denoted by  $x^{(1)}$ , that satisfies  $f_L^{(0)}(x) = 0$ .

$$x^{(1)} = x^{(0)} - J_f^{-1}(x^{(0)})f(x^{(0)})$$

If  $f_L^{(0)}$  is a good approximation to  $f$  near  $\hat{x}$ , then  $x^{(1)}$  will be closer to  $\hat{x}$  than was  $x^{(0)}$ .

This procedure is repeated by replacing the initial guess  $x^{(0)}$  with  $x^{(1)}$ . The iteration, as shown in Figure 4.1, is repeated until some convergence criteria is satisfied.

$$x^{(j+1)} = x^{(j)} - J_f^{-1}(x^{(j)})f(x^{(j)}) \quad (4.17)$$

The sequence generated by (4.17) converges to  $\hat{x}$  if  $f$  is continuously differentiable,  $J_f(\hat{x})$  is nonsingular, and  $x^{(0)}$  is sufficiently close to  $\hat{x}$  [dahlquist74]. Furthermore, if  $J_f(x)$  is Lipschitz continuous, the asymptotic rate of convergence will be at least quadratic. More explicitly, let  $\varepsilon^{(j)} = \|x^{(j)} - \hat{x}\|$  be the error of the  $j^{\text{th}}$  iterate. If there exist constants  $p$  and  $\alpha \neq 0$  such that

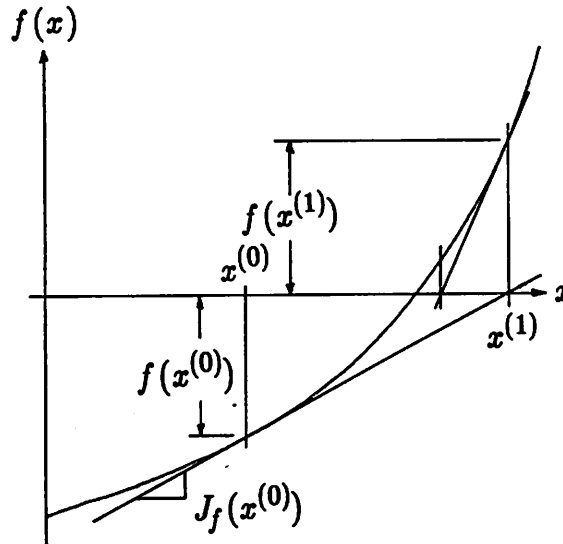


Figure 4.1 : Newton-Raphson illustrated.

$$\lim_{j \rightarrow \infty} \frac{\varepsilon^{(j+1)}}{(\varepsilon^{(j)})^p} = \alpha,$$

then  $p$  is called the rate (or order) of convergence. For Newton-Raphson, when  $J_f(x)$  is Lipschitz,  $p \geq 2$ . In general, there is no way to assure that the initial guess  $x^{(0)}$  is sufficiently close to the solution  $\hat{x}$ , so convergence can be elusive.

#### 4.1. Simplified Newton-Raphson Methods

Newton-Raphson requires that the Jacobian be constructed and factored on each iteration; an expensive series of operations that, under certain circumstances, can be avoided. Several simplified Newton-Raphson methods have been developed over the years that reduce this expense. We are interested here the one in which the Jacobian is formed and factored only for the first iterate.

$$x^{(j+1)} = x^{(j)} - J_f^{-1}(x^{(0)})f(x^{(j)}) \quad (4.18)$$

If the function  $f$  is near-linear then the changes in the Jacobian from iteration to iteration are small and the first Jacobian closely approximates the true Jacobian on subsequent steps. In this case, this new method converges to the correct solution. The Jacobian is only used to generate new iterates, and is not used when confirming convergence, so errors resulting from approximations in the Jacobian only affect the rate and region of convergence, not the accuracy of the final solution. This simplified Newton-Raphson method can often be considerably faster than standard Newton-Raphson with large near linear systems of equations, even though it usually requires a greater number of iterations, because each iteration is less expensive. However, the region of convergence is often smaller than with standard Newton-Raphson.

To increase the region of convergence over the above simplified Newton-Raphson method, reevaluate the Jacobian every  $k$  iterations rather than use the original Jacobian until convergence. This method, referred to as Samanskii's method, may be considered a  $k$  step method, where each iterate is composed of one Newton-Raphson step and  $k - 1$  simplified Newton-Raphson steps. Traub and Samanskii [ortega70] showed that sequence consisting of every  $k^{\text{th}}$  iterate converges with order  $k + 1$ . Thus, if  $k = 2$ , that is, if the Jacobian is updated on every other iterate, then cubic convergence is achieved. As expected, this rate of convergence is inferior to that of conventional Newton-Raphson, where the sequence of consisting of every other iterate converges quarticly.

The advantages of the simplified Newton-Raphson iterates is combined with the large region of convergence of conventional Newton-Raphson by monitoring  $\{\|f(x^{(j)})\|\}$  and using simplified Newton-Raphson iterates as long as a sufficient reduction in this norm is achieved. If a simplified iteration results in an insufficient reduction, the iterate and the old

Jacobian should be discarded and a full Newton-Raphson step taken.

## 4.2. Continuation Methods

In order to assure that Newton-Raphson converges, it is necessary to supply an initial guess that is sufficiently close to the solution. Since, in general, the solution is not known in advance, it is often difficult to supply such a guess. *Continuation methods* provide a way for obtaining starting points that are sufficiently close to assure convergence.

Usually, the problem depends in a natural way on some parameter  $p$ , such that when the parameter is set equal to some specific value, say 1, the particular system for which the solution is desired results, while for  $p = 0$  the system has a known solution  $x_0$ . Thus,

$$f(x,p) = 0 \quad (4.19)$$

where  $f(x,1) = f(x)$  and where  $f(x_0,0) = 0$ . Assume that in (4.19),  $x$  can be written as a function of  $p$ , i.e.,  $f(x(p),p) = 0$ . Then the solution  $x(p)$  can be found for an increasing sequence of values of  $p$ ,  $0 = p_0 < p_1 < p_2 < \dots < p_s = 1$ . If  $x(p)$  is a continuous function of  $p$ , then it is always possible to choose  $p_s$  close enough to  $p_{s-1}$  so that if  $x(p_{s-1})$  is used as a starting point, it is sufficiently close to  $x(p_s)$  to assure convergence.

The fundamental idea in continuation methods is to generate a finite sequence of problems, the solution to the first of which is known, and such that the solutions of each problem is close enough to the solution of the next to be within the region of convergence for Newton-Raphson on the next. The step size  $p_s - p_{s-1}$  should be adjusted on each step to minimize the total number of Newton iterations rather than the number of steps.

Linear extrapolation is normally used with continuation methods to reduce the number of steps required. After the first step, a simple form of linear extrapolation can be used based on the solution at the previous two steps.

$$x^{(0)}(p_s) = x^{(0)}(p_{s-1}) + \frac{p_s - p_{s-1}}{p_{s-1} - p_{s-2}} [x(p_{s-1}) - x(p_{s-2})]$$

A more sophisticated linear extrapolation is performed by using the derivative  $\partial x / \partial p$ .

$$x^{(0)}(p_s) = x^{(0)}(p_{s-1}) + (p_s - p_{s-1}) \frac{\partial x(p_{s-1})}{\partial p_{s-1}}$$

where

$$\frac{\partial x(p_{s-1})}{\partial p_{s-1}} = - \left[ \frac{\partial f(x(p_{s-1}), p_{s-1})}{\partial x(p_{s-1})} \right]^{-1} \frac{\partial f(x(p_{s-1}), p_{s-1})}{\partial p_{s-1}},$$

which can be derived by using the implicit function theorem [rudin76]. This approach is usually preferred if the derivatives are readily available.

When computing the DC operating point of a circuit, it is very common to use as a continuation parameter the fraction of the DC source voltages and currents applied to the circuit. In almost all circuits simulators, all devices except sources pass no current when all terminal potentials are zero. Thus, when all sources are turned off, circuits are guaranteed to have a solution with zero potential at every node and zero current through every branch. From this known solution, the source levels can be slowly increased, while solving the circuit at each step, until the desired source levels are attained. Continuation implemented in this manner is generally referred to as *source stepping*.

Continuation can fail if  $x(p)$  is not a continuous function on the interval  $[0,1]$ . By the implicit function theorem, if  $\frac{\partial f(x(p), p)}{\partial x(p)}$  exists and is continuous over a neighborhood of  $(x_0, p_0)$  and is nonsingular at  $(x_0, p_0)$ , then there exists a neighborhood of  $(x_0, p_0)$  for which  $x$  is a continuous function of  $p$  and  $f(x(p), p) = 0$ . Thus, continuation methods will be successful if  $\frac{\partial f(x(p), p)}{\partial x(p)}$  is continuously differentiable and is nonsingular at  $x(p)$  for all  $p \in [0,1]$ . It is not always possible to assure this in practice.

Consider the circuit in Figure 4.2. The supply potential versus supply current is plotted in Figure 4.3. Supply potential is not a function of input current because there is not a unique potential for each current. Indeed, source stepping would fail on this circuit when the supply reached  $p_0 = 1.6\text{mA}$  because the potential would have to jump discontinuously from 11V to 28V. At this point, which is called a *limit point*, the Jacobian  $J_f(x(p)) = \frac{\partial f(x(p), p)}{\partial x(p)}$  is singular.

Continuation methods fail at limit points for two reasons. First, the Jacobian  $J_f(x(p))$  is singular at limit points, which causes Newton-Raphson to fail. If this were the only problem, limit points would not be a serious difficulty because singularities are isolated points and it would be possible to step beyond them. However, this is prevented by the second reason. Monotonically increasing the parameter  $p$  results in a discontinuous jump in the solution at a limit point.

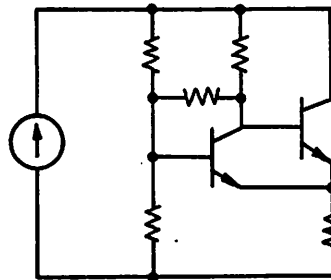


Figure 4.2 : A circuit that causes trouble for simple source-stepping algorithms.

---

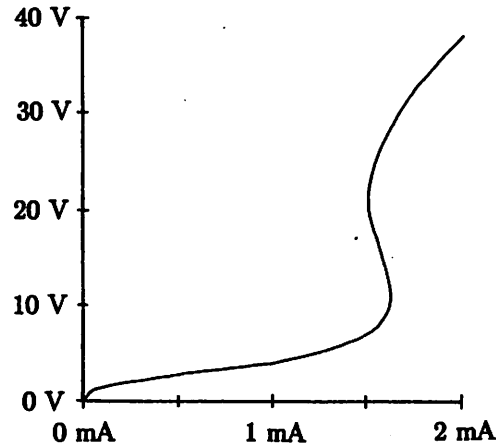


Figure 4.3 : Supply potential versus supply current for the circuit in Figure 4.2.

#### 4.2.1. Pseudo-Arc Length Continuation

One solution to the limit point problem is to use a *path following* or *arc-length* continuation method. These methods treat the manifold of solutions in  $\mathbb{R}^N \times [0,1]$  of (4.19) as a path that must be followed from  $(x_0,0)$  to  $(\hat{x},1)$  by, at each step, solving for a pair  $(x,p)$  that solves (4.19) and makes some progress along the path. The independent parameter becomes arc length or the distance traveled along the path. Rather than specifying  $p$  a priori, it is considered a function of the arc-length parameter  $\alpha$ . The arc length  $\alpha$  is specified and  $p$  is found as a function of  $\alpha$ . In this way,  $p$  is allowed to increase or decrease as needed to provide adequate progress along the path at each step.

The derivation of the pseudo-arc length continuation algorithm [bolstad86] begins by defining  $\xi \in \mathbb{R}^N \times [0,1]$  as  $\xi = [x,p]^T$  and  $c = \{\xi : f(\xi) = 0\}$ . Thus,  $c$  is the curve or manifold of all solutions to (4.19). For simplicity, assume that there is only one curve, that it is connected, and that it passes through  $(s_0,0)$  and  $(\hat{x},0)$ . This curve is

parameterized using the arc length  $\alpha$  from some arbitrary point. Rewriting (4.19) to show the explicit dependence of  $x$  and  $p$  on the arc-length parameter  $\alpha$ ,

$$f(x(\alpha), p(\alpha)) = 0 \quad (4.20)$$

To simplify notation, the dependence of  $\xi$ ,  $x$ , and  $p$  on  $\alpha$  will be implied rather than denoted explicitly.

The first step is, given the solution at the current step, predict the value of the solution at the next step. Do this by extrapolating along the tangent to the path. Let  $\xi_0$  the current solution and  $u(\alpha_0)$  be the unit vector tangent to  $c$  at  $\xi_0 = \xi(\alpha_0)$ . Then  $u = [u_x, u_p]^T$  is such that

$$\left[ \frac{df(\xi)}{d\xi} \right]^T u = \left[ \frac{df(x,p)}{dx} \right] u_x + \frac{df(x,p)}{dp} u_p = 0 \quad (4.21a)$$

and

$$\|u_x\|_2^2 + u_p^2 = 1, \quad (4.21b)$$

where  $\|u_x\|_2$  is the Euclidean norm of  $u_x$ . The first equation states that  $u$  is tangent to the curve and the second that  $u$  has unit length. The quantities  $u_x$  and  $u_p$  can be computed by dividing both sides of (4.21a) by  $u_p$ .

$$\frac{df(x,p)}{dx} \frac{u_x}{u_p} + \frac{df(x,p)}{dp} = 0$$

Let  $\phi = u_x/u_p$ , and find  $\phi$  by solving

$$\frac{df(x,p)}{dx} \phi = - \frac{df(x,p)}{dp} \quad (4.22)$$

Then,  $u_x$  and  $u_p$  are computed from

$$u_p = \frac{1}{\sqrt{1 + \|\phi\|_2^2}} \quad (4.23)$$

$$u_x = u_p \phi \quad (4.24)$$

Given  $\xi_0$  and  $u(\alpha_0)$ , a prediction of the new solution  $\xi_1 = \xi(\alpha_1)$  is computed from

$$x_1^{predict} = x_0 + u_x(\alpha_0)\delta\alpha \quad (4.25a)$$

$$p_1^{predict} = p_0 + u_p(\alpha_0)\delta\alpha \quad (4.25b)$$

where  $x_1^{predict}$  and  $p_1^{predict}$  are the predicted values of  $x_1$  and  $p_1$  and  $\delta\alpha = \alpha_1 - \alpha_0$ .

The next step is to formulate the dependence of both  $x$  and  $p$  on the arc length. It is not important that the distance between  $\xi_0$  and  $\xi_1$  along the curve be exactly  $\delta\alpha$  because  $\xi_1$  is only one step along the path to our true goal  $\xi_S$ , and  $\xi_1$  itself is of no value. Since the distance  $\xi_0$  and  $\xi_1$  need only be roughly equal  $\delta\alpha$ , a computationally simpler *pseudo-arc-length* constraint is employed [bolstad86]. The pseudo-arc-length algorithm requires the new solution to satisfy the equations

$$f(\xi_1) = 0 \quad (4.26a)$$

$$g(\xi, \alpha_1) = \langle u(\alpha_0), \xi_1 - \xi_0 \rangle - (\alpha_1 - \alpha_0) = 0 \quad (4.26b)$$

where  $\langle \cdot, \cdot \rangle$  represents the inner product. Equations (4.26b) forces the new solution  $\xi_1$  to lie on a hyperplane perpendicular to the tangent vector  $u(\alpha_0)$ . The hyperplane intersects the tangent at a distance  $|\delta\alpha|$  from  $\xi(\alpha_0)$  as shown in Figure 4.4.<sup>2</sup> Applying Newton-Raphson to find the solution of (4.26) gives

$$\begin{bmatrix} \frac{df(\xi_1^{(j)})}{dx_1} & \frac{df(\xi_1^{(j)})}{dp_1} \\ \frac{dg(\xi_1^{(j)}, \alpha_1)}{dx_1} & \frac{dg(\xi_1^{(j)}, \alpha_1)}{dp_1} \end{bmatrix}^T \begin{bmatrix} x_1^{(j+1)} - x_1^{(j)} \\ p_1^{(j+1)} - p_1^{(j)} \end{bmatrix} = - \begin{bmatrix} f(\xi_1^{(j)}) \\ g(\xi_1^{(j)}, \alpha_1) \end{bmatrix} \quad (4.27)$$

At simple limit points the Jacobian in (4.27) is nonsingular [keller77], and so Newton-Raphson applied to the augmented system (4.26) is well-defined and quadratic convergence is possible.

<sup>2</sup>Another choice for the pseudo-arc-length constraint is:  $g = \|\xi(\alpha_1) - \xi(\alpha_0)\|_2^2 - |\alpha_1 - \alpha_0| = 0$ . This forces the solution to lie on a sphere of radius  $\delta\alpha$  centered about  $\xi(\alpha_0)$ .

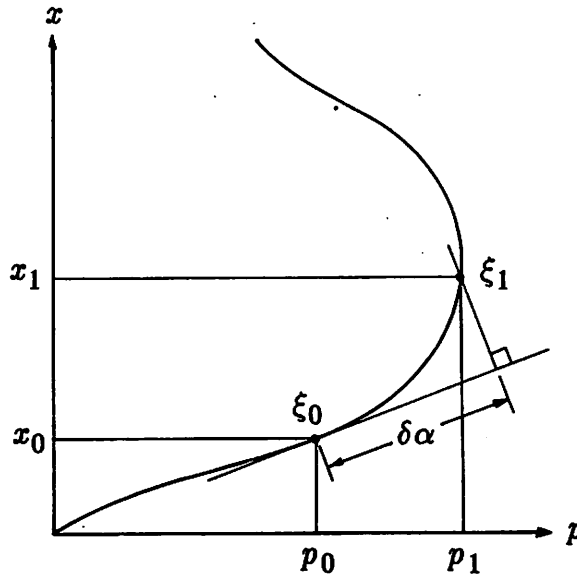


Figure 4.4 : Illustration of the pseudo-arc-length constraint.

If Gaussian elimination is used to solve (4.27), it is best to use pivoting to ensure numeric stability, especially near limit points. However, it is sometimes difficult to exploit the pattern of sparsity in the augmented system (this is true when the equations are generated by harmonic balance because  $df/dx$  is a block matrix while  $dg/dp$  is a scalar). Without pivoting, the algorithm has trouble moving over limit points because  $df/dx$  is singular at these points. In this situation, block Gaussian elimination without pivoting is used along with deflation techniques to avoid numerical instability [chan82]. The equations are now simplified further using block Gaussian elimination.

$$\begin{aligned} & \begin{bmatrix} \frac{df(\xi_1^{(j)})}{dx_1} & \frac{df(\xi_1^{(j)})}{dp_1} \\ 0 & \frac{dg(\xi_1^{(j)}, \alpha_1)}{dp_1} - \frac{dg(\xi_1^{(j)}, \alpha_1)}{dx_1} \left[ \frac{df(\xi_1^{(j)})}{dx_1} \right]^{-1} \frac{df(\xi_1^{(j)})}{dp_1} \end{bmatrix} \begin{bmatrix} x_1^{(j+1)} - x_1^{(j)} \\ p_1^{(j+1)} - p_1^{(j)} \end{bmatrix} \\ & = - \begin{bmatrix} f(\xi_1^{(j)}) \\ g(\xi_1^{(j)}, \alpha_1) - \frac{dg(\xi_1^{(j)}, \alpha_1)}{dx_1} \left[ \frac{df(\xi_1^{(j)})}{dx_1} \right]^{-1} \frac{df(\xi_1^{(j)})}{dp_1} \end{bmatrix}. \end{aligned}$$

Let

$$\frac{df(\xi_1)}{dx_1} y = \frac{df(\xi_1)}{dp_1} \quad (4.28)$$

so that

$$y = \left[ \frac{df(\xi_1)}{dx_1} \right]^{-1} \frac{df(\xi_1)}{dp_1}.$$

And let

$$\frac{df(\xi_1)}{dx_1} z = f(\xi_1) \quad (4.29)$$

so that

$$z = \left[ \frac{df(\xi_1)}{dx_1} \right]^{-1} f(\xi_1).$$

Then finally

$$\delta p^{(j)} = \frac{\frac{dg(\xi_1^{(j)}, \alpha_1)}{dx_1^T} z - g(\xi_1^{(j)}, \alpha_1)}{\frac{dg(\xi_1^{(j)}, \alpha_1)}{dp_1} - \frac{dg(\xi_1^{(j)}, \alpha_1)}{dx_1^T} y} \quad (4.30)$$

and

$$\delta x^{(j)} = - \left[ \frac{df(\xi_1^{(j)})}{dx_1} \right]^{-1} \left[ \frac{df(\xi_1^{(j)})}{dp_1} \delta p + f(\xi_1^{(j)}) \right]$$

$$\delta x^{(j)} = -\gamma \delta p^{(j)} - z. \quad (4.31)$$

The pseudo-arc-length continuation algorithm can be implemented using equations (4.22), (4.23), (4.24), (4.25), (4.26), (4.28), (4.29), (4.30), and (4.31). This algorithm is repeated at each new  $\alpha_s$ ,  $s = 1, 2, \dots, S$ .

The pseudo-arc length continuation method works if numerical pivoting is used when convergence is prevented by simple limit points (or rank one deficiencies in the original Jacobian) along the path. This is generally not the case when convergence problems occur during DC analysis, but is quite common when using harmonic balance on conditionally stable circuits.

# Chapter 5

## Time-Domain Methods

---

A very important approach to finding the steady-state response of a system of differential equations is to formulate a boundary-value problem whose solution is the desired steady-state response. Methods for formulating boundary-value problems for periodic solutions was discussed in Chapter 4 and methods for quasiperiodic solutions will be covered in Chapter 6. This chapter presents two important ways of solving these boundary-value problems.

### 1. Finite-Difference Methods

Like most approaches to solving differential equations numerically, the finite-difference methods approximate the original system with a set of difference equations. Unlike finite-difference methods for transient analysis methods, finite-difference methods for boundary-value problems attempt to find the solution at every time-point simultaneously. To find a  $T$ -periodic solution using a finite-difference method, a mesh  $t_0 < t_1 < t_2 < \dots < t_S$  is chosen where  $t_0 = 0$  and  $t_S = T$ . A finite sequence  $\{v_s\}$  is computed as an approximation to  $v(t)$  on the mesh, where  $v_s \approx v(t_s)$ . The difference equations are formed by using a discrete-time approximation to the time derivative and the convolution integral. For example, consider the slightly modified version of (4.5)

$$f(v, t) = i(v) + \dot{q}(v) + \int_{-\infty}^t y(t-\tau)v(\tau)d\tau + u(t) = 0. \quad (5.1)$$

All symbols have their previous definitions except that  $i$  is a function representing the sum of the current entering the nodes from *all* conductors,  $q$  represents the sum of the charge entering the nodes from *all* capacitors; and  $y$  is the matrix-valued impulse response of the circuits with all *lumped* elements removed.

There are a large number of possible discrete approximations to  $\dot{q}$  that can be used [gear71]. Implicit Euler [white86], the simplest approximation that is suitable for circuit simulation, employs linear interpolation between mesh points and is given by

$$\dot{q}_s = \frac{1}{h_s}(q_s - q_{s-1}) \quad (5.2)$$

where  $h_s = t_s - t_{s-1}$  is the time-step. A discrete approximation to the convolution integral would be given by

$$w_s = \sum_{r=0}^s y_{s-r} v_r \quad (5.3)$$

where  $w_s$  represents the current entering the nodes from distributed devices at time  $t_s$  and  $y_s$  is the discrete approximation to the impulse response  $y$ . Computation of  $y$  is done by evaluating a phasor representation of the distributed device,  $Y(j\omega)$ , over a range of frequencies. The data is then windowed [harris78] and inverse transformed [djordjevic86, schutt-aine88]. Computation of  $w_s$  is done by applying first an interpolation function to the solution between the mesh points and then employing an integration method such as Simpson's rule [stoer80].

Discretizing (5.1) using the approximations of (5.2) and (5.3) yields

$$i(v_s) + \frac{1}{h_s}(q(v_s) - q(v_{s-1})) + \sum_{r=0}^s y_{s-r} v_r + u_s = 0 \quad (5.4)$$

where  $s = 1, \dots, S$ . As  $v$  is  $T$ -periodic,  $v_0 = v_S$ , which results in the following system of nonlinear algebraic equations

$$\begin{aligned} i(v_1) + \frac{q(v_1) - q(v_S)}{h_1} + \sum_{r=0}^S y_{1-r} v_r + u_1 &= 0 \\ i(v_2) + \frac{q(v_2) - q(v_1)}{h_2} + \sum_{r=0}^S y_{2-r} v_r + u_2 &= 0 \\ \vdots & \\ i(v_S) + \frac{q(v_S) - q(v_{S-1})}{h_S} + \sum_{r=0}^S y_{S-r} v_r + u_S &= 0. \end{aligned}$$

The system is solved using the Newton-Raphson algorithm.

The finite-difference methods are elegant and simple. When applied to two-point boundary-value problems with linear boundary constraints, such as the periodicity constraint, they have the characteristic that each iterate generated by the Newton-Raphson algorithm satisfies the boundary condition, though it may not satisfy the difference equation. This contrasts with shooting methods, for which each iterate satisfies the difference equation but not the boundary conditions.

Finite-difference methods can generate large systems of equations, especially if either the number of unknown waveforms or the number of time-points is large. The systems are sparse, and hence, not overly expensive to solve. The sparsity is increased further if there are no distributed devices present in the circuit. In this case the equations take on an interesting structure. To see this, consider implicit Euler applied to the lumped test problem (4.4).

$$f(v, t) = \dot{q}(v(t)) + i(v(t)) + u(t) = 0 \quad (5.5)$$

to generate



[ortega70] to reduce execution time further. The possible efficiency gain for Samanskii's method is considerable if a high order integration method is used (and so the bandwidth of the Jacobian is large and therefore expensive to factor) or if the Jacobian is expensive to construct.

Finite-difference methods are well known in the mathematics community, but have not received much attention from the circuit simulation community. Because of the large number of equations and unknowns, finite-difference methods require a large amount of memory, which often constrains the size of the circuit that can be simulated. Finite-difference methods also tend to have more Newton-Raphson convergence problems than the other popular method for solving boundary-value problems, shooting methods (presented next). The difference results from the shooting method ability to hide nonlinear behavior from the Newton-Raphson algorithm in some common situations.

One feature of the finite-difference methods is not shared by the shooting methods. Once a solution has been found by a finite-difference method, the resulting Jacobian represents a linearization of the circuit over the simulation interval. Thus, if finite-difference methods are used to find a periodic steady-state solution, the Jacobian is the linearization of the circuit about its periodically time-varying operating point. Just as the Jacobian that results from a DC analysis is a linearization of the circuit about its quiescent operating point that is used in small signal calculations such as the AC and noise analyses, the finite-difference method Jacobian can be used in small signal applications as well [sugawara]. Since it represents a time-varying linear circuit, it exhibits frequency conversion.

## 2. Shooting Methods

In general, shooting methods for solving boundary-value problems can be thought of as iterative methods applied to solving the nonlinear algebraic system generated by replacing the differential equation relation with the state-transition function. For example, consider the two-point boundary-value problem with linear constraints,

$$\dot{v}(t) = f(v(t), t) \quad (5.8)$$

subject to

$$Av(0) + Bv(T) = c,$$

By Theorem 4.2, solving this boundary-value problem is equivalent to solving the nonlinear algebraic problem

$$Av(0) + B\phi(v(0), 0, T) - c = 0. \quad (5.9)$$

for  $v(0)$ , where  $\phi$  is the state-transition function for (5.8). As (5.9) is a nonlinear algebraic problem, a variety of standard methods, like fixed-point iteration or Newton-Raphson, can be used to compute  $v(0)$ . The form of (5.9) is more general than required. For simplicity, assume  $A = -D$ ,  $B = 1$ , and  $c = 0$ . With these assumptions

$$\phi(v(0), 0, T) - Dv(0) = 0 \quad (5.10)$$

becomes our generic two-point boundary-value problem. Further assume that  $D$  is non-singular. As shown in Chapter 4, the periodic solution of a differential equation can be found by solving (4.12), or

$$\phi(v(0), 0, T) - v(0) = 0. \quad (5.11)$$

This problem is mapped into (5.10) by setting  $D = I_N$ , the  $N \times N$  identity matrix.

When looking for a periodic solution to the differential equation for the lumped test problem, it is possible to cast the obvious approach of integrating (4.4) until the transient decays to an acceptably small level, as a shooting method. A simple fixed-point iteration

to solve (5.11) is

$$v^{(k+1)}(0) = \phi(v^{(k)}(0), 0, T), \quad (5.12)$$

which is equivalent to integrating the original differential equation from  $v(0) = v_0$  until all transients decay.

There are two well known ways to accelerate the convergence of this iteration to the desired solution, extrapolation methods and Newton methods. In extrapolation methods, several fixed-point iterations, as in (5.12), are computed and progress towards steady state is monitored. The sequence constructed from the fixed-point iterates is used to accelerate the march towards steady state. Use of the extrapolation shooting methods in circuit simulation was championed by Skelboe [skelboe80].

The Newton methods apply the Newton-Raphson algorithm to (5.11), which involves computing the derivative of the final state with respect to changes in the initial state. The combination of Newton-Raphson and the shooting method was first used to find the periodic steady-state response of circuits by Aprille and Trick [aprille72b] [aprille72a].

Both of these approaches apply as well to the generic two-point boundary-value problem (5.10) as to the periodic problem.

## 2.1. Shooting by Extrapolation

Formulate (5.10) as a fixed-point iteration and construct a sequence  $\{v_s\}$  by letting  $v_0 = v(0)$  and using

$$v_{s+1} = D^{-1}\phi(v_s, 0, T). \quad (5.13)$$

Convergence of this sequence can be accelerated by extrapolation. Though several extrapolation techniques can be used [skelboe80], the one based on minimum polynomials is presented here. It is normally the most efficient because it requires the fewest periods to

perform an extrapolation.

The extrapolation is made by assuming that the sequence  $\{v_s\}$  is generated by a linear finite dimensional system of the form

$$v_{s+1} = Av_s + b \quad (5.14)$$

where  $A \in \mathbb{R}^{N \times N}$  and  $b \in \mathbb{R}^N$ . By just observing  $\{v_s\}$  and without explicitly calculating  $A$  and  $b$ , the fixed-point  $v^*$  of this linear model can be found. If  $\phi(\cdot, 0, T)$  is linear, then (5.14) models  $\phi(\cdot, 0, T)$  exactly,  $v^* = \hat{v}$ , and the solution is found in one iteration. However if  $\phi(\cdot, 0, T)$  is nonlinear, then more than one iteration is usually needed. Expand  $\phi(\cdot, 0, T)$  about its fixed-point  $\hat{v}$ :

$$\begin{aligned} \phi(\hat{v} + \delta v, 0, T) &= \phi(\hat{v}, 0, T) + J_\phi(\hat{v}, 0, T)\delta v + O(\delta v^2) \\ &= \phi(\hat{v}, 0, T) - J_\phi(\hat{v}, 0, T)\hat{v} + J_\phi(\hat{v}, 0, T)(\hat{v} + \delta v) + O(\delta v^2). \end{aligned}$$

Let  $b = \phi(\hat{v}, 0, T) - J_\phi(\hat{v}, 0, T)\hat{v}$  and  $A = J_\phi(\hat{v}, 0, T)$ , then

$$\phi(\hat{v} + \delta v, 0, T) = b + A(\hat{v} + \delta v) + O(\delta v^2)$$

If  $\delta v$  is large, then  $O(\delta v^2)$  is large and the extrapolated value  $v^*$  is different from  $\hat{v}$ . Presumably though,  $v^*$  is closer to  $\hat{v}$  than was the initial guess  $v_0$  and the extrapolation process can be repeated until it converges to  $\hat{v}$ . Convergence is achieved if  $v_0$  is close enough to  $\hat{v}$  and if  $J_\phi(\hat{v}, 0, T)$  is nonsingular, and it is quadratic if  $\phi(\cdot, 0, T)$  is sufficiently smooth [skelboe82].

Now the extrapolation algorithm is presented. Consider the sequence  $\{\delta v_s\}$  generated by (5.14) where  $\delta v_s = v_s - v^*$ . It is easy to show that  $\delta v_s = A \delta v_{s-1}$ . For this sequence to converge, the spectral radius of  $A$  must be less than one, but if  $A$  has any eigenvalues with magnitude close to one, then convergence will be slow. The eigenvalues with magnitude close to one correspond to large time constants in the circuit. Assume that there are  $p$

such eigenvalues, then the  $\delta v_s$  vectors will line up along the  $p$  eigenvectors associated with the slow eigenvalues asymptotically as  $s$  increases. It is possible to solve for  $v^*$  by solving a  $p$  order system. In particular, if the  $\delta v_s$  vectors line up along  $p$  eigenvectors, then there exists a set of  $p + 1$  nonzero coefficients  $\{c_s\}$   $s = 0, 1, \dots, p$  such that

$$\sum_{s=0}^p c_s \delta v_s = 0. \quad (5.15)$$

If the coefficients  $c_s$  are found, then it is possible to compute the fixed-point  $v^*$  for (5.14) from (5.15) and the fact that  $\delta v_s = v_s - v^*$ .

$$v^* = \frac{\sum_{s=0}^p c_s v_s}{\sum_{s=0}^p c_s} \quad (5.16)$$

In order to find the coefficients  $c_s$ , define  $\Delta v_s = v_{s+1} - v_s$  and recall that  $v_{s+1} = Av_s + b$  and  $v^* = Av^* + b$ . Then

$$\begin{aligned} \sum_{s=0}^p c_s \Delta v_s &= \sum_{s=0}^p c_s (Av_s + b - v_s), \\ \sum_{s=0}^p c_s \Delta v_s &= \sum_{s=0}^p c_s (Av_s + v^* - Av^* - v_s), \\ \sum_{s=0}^p c_s \Delta v_s &= \sum_{s=0}^p c_s (A - 1)(v_s - v^*), \\ \sum_{s=0}^p c_s \Delta v_s &= (A - 1) \sum_{s=0}^p c_s (v_s - v^*) = 0. \\ \sum_{s=0}^p c_s \Delta v_s &= 0. \end{aligned} \quad (5.17)$$

Thus, the same set of coefficients  $\{c_s\}$  can be used with both  $\{\delta v_s\}$  and  $\{\Delta v_s\}$  to form linear combinations that sum to zero. This allows (5.17) to be used to determine the coefficients and (5.16) to be used to find  $v^*$ . To solve (5.17) for the coefficients  $\{c_s\}$ , let  $V = [\Delta v_0, \Delta v_1, \dots, \Delta v_{p-1}]$ ,  $c = [c_0, c_1, \dots, c_{p-1}]^T$  and  $c_p = -1$ . Then (5.17) becomes

$$Vc = \Delta v_p. \quad (5.18)$$

If  $p < N$ , the problem is overdetermined and so cannot be solved using LU factorization. Even if  $p = N$ , one of more time constants may be short compared to the shooting interval, and so the corresponding eigenvalues will be small, resulting in  $V$  being ill-conditioned and making LU factorization risky. Thus (5.18) is treated as a least squares problem and is solved using QR factorization [dahlquist74]. In other words, the coefficient vector  $c$  is chosen by the QR algorithm to minimize  $\epsilon$ , where

$$\epsilon = \|Vc - \Delta v_p\|_2^2 \quad (5.19)$$

Since  $A$  and its eigenvalues are unknown, there is no way to compute  $p$  explicitly. Instead, its value is estimated by monitoring  $\epsilon$  as the number of periods in the computed response is increased. The value of  $p$  is taken as the smaller of either  $N$  or the number of periods used for the computation of  $c$  when  $\epsilon$  drops below some small threshold. Once  $p$  has been determined, the extrapolation should be performed using (5.16) and (5.18).

The calculation of  $v^*$  represents one iterate of the extrapolation process. The iteration is continued until the sequence of  $v^*$ 's converges. Each iterate requires simulating the circuit for at least  $p$  iterations. The value of  $p$  is roughly equal to the number of independent slowly decaying states in the circuit, so if there are few, the extrapolation version of the shooting method should be efficient. In order to eliminate any effect of the short lived time constants, it is a good idea to discard the first period of the circuit response waveform in each extrapolation iterate.

## 2.2. Shooting with Newton-Raphson

When applying Newton-Raphson directly to (5.11), not only is it necessary to compute the response of the circuit over one period, the sensitivity of the final state with respect to

changes in the initial state  $v_0$  must also be computed. The sensitivity is used to determine how to correct the initial state once the difference between the achieved and the desired final state is found. Perhaps conceptually the easiest way to determine the sensitivity of the final state to the initial state is to use finite differences. In this case, the circuit equations are solved  $N$  times; each time perturbing slightly a different entry in the  $v_0$  vector. The approach taken when using Newton method is similar except that the circuit is linearized about the  $v_0$  solution trajectory and the resulting linear time-varying system is solved for its zero-input response with  $N$  different initial conditions. The  $N$  initial conditions are normally taken to be the  $N$  unit vectors that span  $\mathbb{R}^N$  [aprille72b].

Applying Newton-Raphson to

$$\phi(\hat{v}_0, 0, T) - D\hat{v}_0 = \mathbf{0} \quad (5.20)$$

results in the iteration

$$v_0^{(j+1)} = v_0^{(j)} - [J_{\phi}(v_0^{(j)}, 0, T) - D]^{-1}[\phi(v_0^{(j)}, 0, T) - v_0^{(j)}] \quad (5.21)$$

where  $j$  is the iteration number and

$$[J_{\phi}(v_0, 0, T) - D] = \frac{d}{dv_0}(\phi(v_0, 0, T) - Dv_0) = \frac{dv_s}{dv_0} - D. \quad (5.22)$$

There are two important pieces to the computation of the Newton iteration given in (5.21): factoring the matrix  $[J_{\phi}(v_0, 0, T) - D]$ , which is a full matrix in general, and evaluating the state-transition function  $\phi(v_0, 0, T)$  and its Frechet derivative  $J_{\phi}(v_0, 0, T)$ . The state-transition function is computed by integrating (4.4) numerically over the shooting interval. The derivative of the state-transition function, referred to as the sensitivity matrix, is computed simultaneously because there are several quantities that are common to both computations, as explained below.

At this point it is important to realize that we are not solving the original circuit equation (4.4), but rather a discretized approximation. This distinction is important to achieving quadratic convergence in the Newton-Raphson iteration [skelboe82]. The notation needed to perform the derivation for the general backward difference discretization is complex enough to obscure the basic concepts behind the derivation, so for simplicity and clarity, (4.4) is discretized using implicit Euler (4.16), though any discretization formula could have been used instead.

$$f(v_s) = \frac{1}{h_s} \left[ q(v_s) - q(v_{s-1}) \right] + i(v_s) + u_s = 0 \quad (5.23)$$

where  $s = 1, 2, \dots, S$ ,  $h_s$  is the time-step,  $t_0 = 0$ ,  $t_s = h_s + t_{s-1}$ , and  $t_S = T$ .

$\phi(\cdot, 0, T)$  is found by evaluating (5.23) recursively, at each step solving the implicit set of nonlinear equations using Newton-Raphson.

$$J_f(v_s^{(j-1)})[v_s^{(j)} - v_s^{(j-1)}] = -f(v_s^{(j-1)})$$

$$\left[ \frac{1}{h_s} \frac{dq(v_s^{(j-1)})}{dv_s} + \frac{di(v_s^{(j-1)})}{dv_s} \right] v_s^{(j)} - v_s^{(j-1)} = -\frac{1}{h_s} \left[ q(v_s^{(j-1)}) - q(v_{s-1}) \right] - i(v_s^{(j-1)}) - u_s$$

Let  $di(v)/dv = g(v)$  and  $dq(v)/dv = c(v)$ .

$$\left[ \frac{c(v_s^{(j-1)})}{h_s} + g(v_s^{(j-1)}) \right] [v_s^{(j)} - v_s^{(j-1)}] = -\frac{1}{h_s} \left[ q(v_s^{(j-1)}) - q(v_{s-1}) \right] - i(v_s^{(j-1)}) - u_s \quad (5.24)$$

The sensitivity  $\frac{dv_s}{dv_0}$  is taken to be the final value of the  $\frac{dv_s}{dv_0}$  trajectory, which is found by

differentiating both sides of (5.23) with respect to  $v_0$ .

$$\frac{1}{h_s} \frac{d}{dv_0} \left[ q(v_s) - q(v_{s-1}) \right] + \frac{d}{dv_0} i(v_s) = 0 \quad (5.25)$$

Applying the chain rule

$$\frac{1}{h_s} \left[ \frac{dq(v_s)}{dv_s} \frac{dv_s}{dv_0} - \frac{dq(v_{s-1})}{dv_{s-1}} \frac{dv_{s-1}}{dv_0} \right] + \frac{di(v_s)}{dv_s} \frac{dv_s}{dv_0} = 0.$$

Let  $di(v)/dv = g(v)$  and  $dq(v)/dv = c(v)$ .

$$\left[ \frac{c(v_s)}{h_s} + g(v_s) \right] \frac{dv_s}{dv_0} - \frac{c(v_{s-1})}{h_s} \frac{dv_{s-1}}{dv_0} = 0$$

$$\frac{dv_s}{dv_0} = J_f^{-1}(v_s) \frac{c(v_{s-1})}{h_s} \frac{dv_{s-1}}{dv_0} \quad (5.26)$$

where  $J_f(v_s) = \frac{c(v_s)}{h_s} + g(v_s)$ .

The Jacobian  $J_\phi(v_0, 0, T) = \frac{dv_s}{dv_0}$  is computed by repeated application of (5.26) starting from the initial condition  $\frac{dv_0}{dv_0} = 1_N$ . Note that for each time-step the derivatives  $J_f(v_s)$  and  $c(v_{s-1})$  have been previously computed in (5.24) during the application of Newton-Raphson's method to (5.23). In fact,  $J_f(v_s)$  is available in LU factored form. However,  $dv_{s-1}/dv_0$  is a full  $N \times N$  matrix that must be multiplied by both  $C(v_{s-1})/h_s$  and  $J_f^{-1}(v_s)$  (this last multiplication is done with  $N$  sparse forward and backward substitutions) at every time-step. Thus, (5.26) represents a burdensome calculation that prevents Newton-Raphson-based shooting methods from being applied to large circuits.

The size of  $J_\phi(v_0, 0, T)$  can be reduced somewhat by eliminating entries in  $v$  from consideration that result from algebraic constraints or from quickly decaying states. This approach has also been found to aid convergence [kakizaki85].

Since (5.20) is being solved using Newton-Raphson, it is necessary to assure that  $\phi(v_0, 0, T)$  is continuously differentiable with respect to  $v_0$ . Sufficient conditions for this to be true before time has been discretized are that  $i$ ,  $q$  and  $u$  satisfy the conditions imposed in Section 1.3 to assure that a unique solution to (4.13) exists for every initial

state, as well as the additional conditions that  $i$  and  $q$  are continuously differentiable with respect to  $v$  [hale80]. These conditions are also sufficient to assure that  $\phi(v_0, 0, T)$  is continuously differentiable with respect to  $v_0$  when time has been discretized with a fixed discretization mesh. However,  $\phi(v_0, 0, T)$  is not guaranteed to vary smoothly with changes in the mesh. Indeed, insertion or deletion of points is inherently a discontinuous operation that is likely to introduce convergence problems if a coarse mesh is used unless care is taken. It is possible to avoid this problem by simply using the same mesh on each iteration, however this may result in unacceptable constraints on the time-step-selection algorithm and therefore either excessive truncation error<sup>1</sup> or an excessively fine mesh. To avoid these problems, a mesh is chosen to achieve the desired accuracy and used on successive iterations for as long as that accuracy can be maintained. Once it is no longer maintainable, the Newton iteration is restarted with a new mesh and using the final iterate from the previous mesh as the starting point. It may happen that when far from the solution, the mesh will be changed often, perhaps on each iteration. Once near the solution, however, the mesh should stabilize and allow the Newton iteration to converge.

Like any Newton-Raphson-based method, the shooting method will converge if the function (5.20) varies smoothly in the neighborhood of the solution and if the initial guess is given sufficiently close to the solution. Thus, an important part of the shooting method is the selection of a good initial guess for the solution. A reasonable start is to set the time-varying input sources to their average value and use the resulting DC operating point for  $v_0^{(0)}$ . An improvement on this procedure is to linearize the circuit about the DC operating point, convert the input source waveforms into the frequency domain using the discrete

---

<sup>1</sup>Truncation error is the error generated in discretizing a differential equation [gear71]. The truncation error is normally reduced by reducing the size of the time-steps.

Fourier transform, and perform a phasor analysis [desoer69] to find the periodic steady-state response of the linearized circuit. From this response, determine  $v_0^{(0)}$  (this only requires the inverse discrete Fourier transform to be evaluated at  $t = 0$ ), and use this initial guess to start the shooting method. The initial guess can be further improved by integrating the circuit for several periods before applying the shooting method to allow any rapid time constants to decay. When generating the initial guess the truncation error criteria can be relaxed and larger time-steps taken to reduce the computational cost.

It is still possible for the shooting method to have convergence problems. As always with Newton-Raphson, damping can sometimes be used to improve convergence. A damping factor  $\alpha$  is introduced into (5.21) so that

$$v_0^{(j+1)} = v_0^{(j)} + [\alpha J_{\phi}(v_0^{(j)}, 0, T) - D]^{-1}[v_0^{(j)} - \phi(v_0^{(j)}, 0, T)] \quad (5.27)$$

where  $0 \leq \alpha \leq 1$ . With  $\alpha = 1$ , (5.27) reverts to undamped Newton-Raphson; if  $\alpha = 0$  then (5.27) becomes the fixed-point iteration  $v_0^{(j+1)} = \phi(v_0^{(j)}, 0, T)$ . The damping parameter should be automatically controlled on each iteration with  $\alpha$  close to zero when  $\phi(\cdot, 0, T)$  is strongly nonlinear over the size of a step  $v_0^{(j+1)} - v_0^{(j)}$ , and with  $\alpha$  close to one when  $\phi(\cdot, 0, T)$  is almost linear over the step. To achieve quadratic convergence,  $\alpha$  must go to one as the solution is approached. See [grosz82] [kakizaki85] for specific algorithms to control  $\alpha$ . Note that, for this damped shooting method to work, it is necessary for  $v_0^{(j)}$  to be within the region of attraction for an asymptotically-stable limit cycle of period  $T$ , otherwise the fixed-point iteration that results when  $\alpha = 0$  will not converge.

A very important characteristic of shooting methods is that they converge quickly and reliably if the state-transition function over the shooting interval is near linear. It is quite often the case (usually by design) that  $\phi(\cdot, 0, T)$  is linear even when the overall circuit

behavior is not. For example, consider a simple one-stage switched-capacitor filter. Assume  $v_0 = 0$  and  $C_{in}$  is connected to the input source at  $t = 0^+$ , the switches are thrown connecting  $C_{in}$  in parallel with  $C_f$ . After everything settles,  $v_0 = (V_{in} C_{in}) / (C_{in} + C_f)$ . Before the end of the clock cycle the switches are returned to their original positions. If the shooting interval is taken to be one clock cycle, then  $\phi(v_0, 0, T) = v_0 + (V_{in} C_{in}) / (C_{in} + C_f)$ . The state-transition function over the shooting interval is linear, even though the circuit might behave quite nonlinearly during certain portions of the clock cycle (ex. slew rate limiting). Shooting methods hide this nonlinear behavior from the outer loop, and so few iterations at this level are required. The nonlinear behavior is not a problem for the numerical integration used to evaluate  $\phi(\cdot, 0, T)$  because numerical integration is a natural continuation method where time is the continuation parameter.

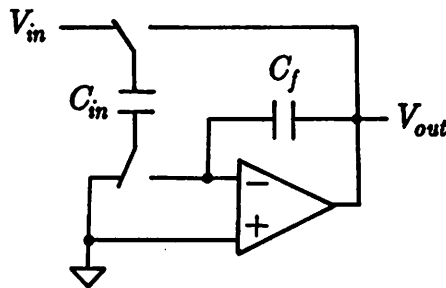


Figure 5.1 : A simple one-pole switched-capacitor filter.

---

### 2.3. Oscillators

It is possible to handle oscillators with extrapolation-based shooting methods [skelboe80], however there is no natural way to find  $T$ . It is necessary to look for the maxima or threshold crossings on the solution waveforms and estimate  $T$ . Other than the methods that need be employed to find  $T$ , extension of extrapolation to the oscillator problem is straight-forward and well-behaved.

When applying Newton-Raphson-based shooting methods to autonomous oscillators,  $T$  is added to the list of unknowns to be determined and an extra equation is added that addresses the problem of having a continuum of solutions. The added equation is constructed either to eliminate almost all solutions (with those that remain being isolated from each other) or to modify Newton-Raphson so that it is capable of handling the continuum. One way to restrict the set of solutions such that each is isolated is to force  $v(0)$  to lie on a hyperplane that has been carefully selected so that it intersects the solution trajectory. The resulting system of equations for a periodic oscillation is

$$\phi(\hat{v}(0), 0, T) - \hat{v}(0) = 0 \quad (5.28)$$

$$\xi^T \hat{v}(0) = \alpha$$

where  $\xi$  is a constant vector that is normal to the hyperplane and  $\alpha$  is a scalar. Unfortunately,  $\xi$  and  $\alpha$  cannot be chosen arbitrarily, they must satisfy

$$\max_t \xi^T \hat{v}(t) > \alpha$$

$$\min_t \xi^T \hat{v}(t) < \alpha$$

$$\xi^T \frac{d\hat{v}(0)}{dt} \neq 0.$$

As shown in Figure 5.2, the first two constraints assure that the hyperplane intersects the solution orbit. The last constraint is necessary to prevent the Jacobian from being singular,

which results if the hyperplane is tangent to the solution trajectory at  $\hat{v}(0)$ . Initially,  $\xi$  and  $\alpha$  are selected after integrating the circuit equations for a few cycles, as are the initial Newton guess of  $T$  and  $v(0)$ . It may be necessary to update  $\alpha$  as the iteration progresses.

Newton-Raphson can be modified [mees81] to handle nonisolated solutions by constraining the Newton-step direction to be perpendicular to the trajectory, as shown in Figure 5.3. Thus if  $\Delta v^{(j+1)}(0) = v^{(j+1)}(0) - v^{(j)}(0)$ , then the equation  $\dot{v}(0)^T \Delta v(0) = 0$  is added to the Newton update iteration for  $\phi(v(0), 0, T) - v(0) = \mathbf{0}$  where both  $v(0)$  and  $T$  are considered unknown.

$$\begin{bmatrix} J_{\phi}(v^{(j)}(0), 0, T^{(j)}) - \mathbf{1} & \frac{\partial \phi(v^{(j)}(0), 0, T^{(j)})}{\partial T} \\ \dot{v}^{(j)}(0)^T & 0 \end{bmatrix} \begin{bmatrix} \Delta v^{(j+1)}(0) \\ \Delta T^{(j+1)} \end{bmatrix} = \begin{bmatrix} v^{(j)}(0) - \phi(v^{(j)}(0), 0, T^{(j)}) \\ \mathbf{0} \end{bmatrix}$$

where

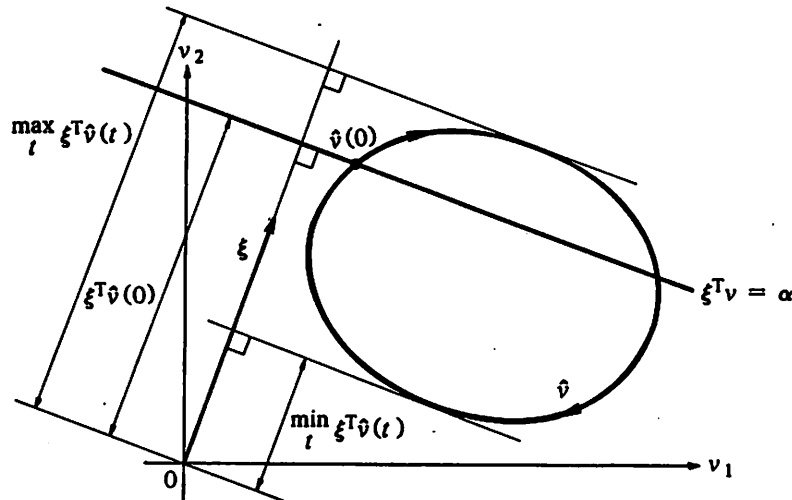


**Figure 5.2 :** Orbit and hyperplane of Eqn. (5.28). Shows in two dimensions how  $v(0)$  is selected by intersecting a hyperplane with the solution trajectory.

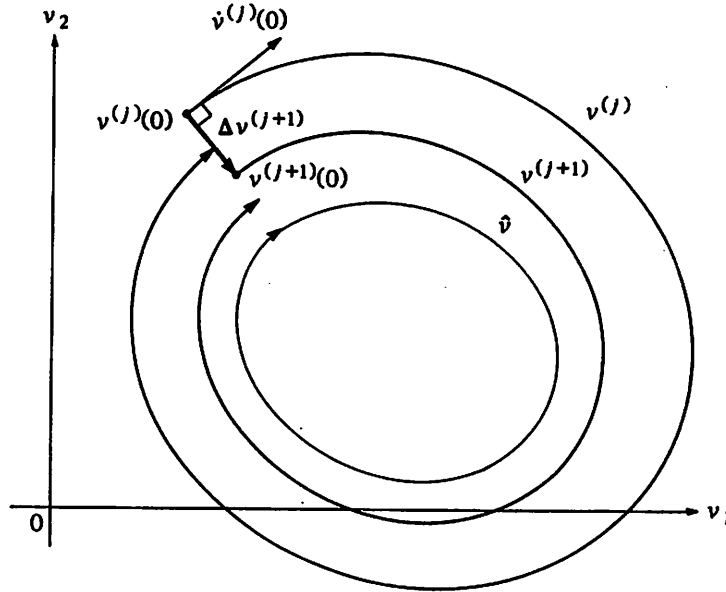


**Figure 5.3 :** Two steps of the shooting method on a two dimensional oscillator problem with  $\Delta v^{(j+1)}$  constrained to be perpendicular to  $\dot{v}^{(j)}(0)$ .

$$J_{\phi}(v(0), 0, T) = \frac{\partial \phi(v(0), 0, T)}{\partial v(0)} \in \mathbb{R}^{N \times N}$$

$$\frac{\partial \phi(v(0), 0, T)}{\partial T} \in \mathbb{R}^N$$

$$\Delta T^{(j+1)} = T^{(j+1)} - T^{(j)}.$$

This approach does not require the selection of parameters such as  $\xi$  and  $\alpha$ , but a standard Newton-Raphson package cannot be used because the added equation is in terms of  $\Delta v(0)$  rather than  $v(0)$ . Small errors in  $\dot{v}^{(j)}(0)$  do not affect the accuracy of the solution, and so it can be calculated using the approximation  $\dot{v}(0) \approx (v(t_1) - v(t_0))/h_1$ . The computation of  $\partial \phi(v(0), 0, T)/\partial T$  is more difficult. As before, the derivative must be derived from the discretized circuit equations. Equation (4.4) is discretized using implicit Euler and  $\partial \phi(v(0), 0, T)/\partial T = \partial v_s/\partial T$  is computed by taking the final value of the  $\partial v_s/\partial T$  trajectory.

To compute  $\partial v_s / \partial T$ , it is necessary to specify how  $t_s$ ,  $s = 0, 1, \dots, S$  vary with  $T$ . Let  $t_s = \alpha_s T$  where  $0 = \alpha_0 < \alpha_1 < \dots < \alpha_S = 1$ . From (5.23)

$$\frac{1}{h_s} \left[ q(v_s) - q(v_{s-1}) \right] + i(v_s) + u_s = 0 \quad s = 1, 2, \dots, S$$

where  $v_s = v(\alpha_s T)$  and  $u_s = u(\alpha_s T)$ . Differentiating with respect to  $T$  leads to

$$\frac{-1}{h_s T} \left[ q(v_s) - q(v_{s-1}) \right] + \frac{1}{h_s} \left[ \frac{\partial q(v_s)}{\partial T} - \frac{\partial q(v_{s-1})}{\partial T} \right] + \frac{\partial i(v_s)}{\partial T} + \frac{\partial u_s}{\partial T} = 0.$$

Applying the chain rule and recalling that  $u$  is constant gives

$$\begin{aligned} \frac{-1}{h_s T} \left[ q(v_s) - q(v_{s-1}) \right] + \frac{1}{h_s} \left[ \frac{\partial q(v_s)}{\partial v_s} \frac{\partial v_s}{\partial T} - \frac{\partial q(v_{s-1})}{\partial v_{s-1}} \frac{\partial v_{s-1}}{\partial T} \right] \\ + \frac{\partial i(v_s)}{\partial v_s} \frac{\partial v_s}{\partial T} = 0. \end{aligned}$$

Again let  $g = \partial i / \partial v$  and  $c = \partial q / \partial v$ .

$$\begin{aligned} \left[ g(v_s) + \frac{c(v_s)}{h_s} \right] \frac{\partial v_s}{\partial T} = c(v_{s-1}) \frac{\partial v_{s-1}}{\partial T} + \frac{1}{h_s T} \left[ q(v_s) - q(v_{s-1}) \right] \\ \frac{\partial v_s}{\partial T} = J_f^{-1}(x_s) \left[ c(v_{s-1}) \frac{\partial v_{s-1}}{\partial T} + \frac{1}{h_s T} \left[ q(v_s) - q(v_{s-1}) \right] \right] \end{aligned} \quad (5.30)$$

This difference equation is solved starting with the initial state  $\frac{\partial v_0}{\partial T} = 0$ .

It is important to realize that Newton-Raphson has been applied to the set of finite-difference equations that approximate the original set of differential equations, and not directly to the differential equations. In computing the derivatives of  $v_s$  needed by Newton-Raphson, it is therefore necessary to use the finite-difference equations. It is also important to notice that the time-points are independent variables that affect the value of  $v_s$ . If the time-points are not fixed, they must be included in the list of independent variables being solved for by the Newton iteration. This has been done in a manner that is at

least tractable by allowing  $T$  to be independent and insisting that  $t_s = \alpha_s T$ ,  $s = 0, 1, \dots, S$ . However, this approach constrains severely the time-steps and may result in excessive truncation error. If the truncation error becomes intolerable, a new mesh is chosen with both  $S$  and the  $\alpha_s$ 's changing in such a way that the error specification is satisfied. In doing so, the finite difference equations are changed and Newton-Raphson should be restarted. However the last iterate from the previous mesh may be used as an initial guess for the iteration on the new mesh. Initially, the mesh may need to be changed often, but once near the solution the mesh should stabilize and allow the Newton iteration to converge.

It is possible to change the way in which  $\partial v_s / \partial T$  is computed, which may result in some gain in efficiency. One way is to fix the time-steps  $t_0, t_1, \dots, t_{S-1}$ , and only allow  $t_S = T$  to vary. This greatly simplifies (5.30) but requires that the mesh be updated more often. Another approach is to use the approximation  $\partial v_s / \partial T \approx \dot{v}(T)$ . Thus, in an interesting twist, the original continuous time solution is used as an approximation to the discrete-time solution. When using this approach, it is necessary to use a fine enough mesh for the approximation to be accurate.

## 2.4. Distributed Devices

When applying finite-difference method to circuits with distributed devices, the approach taken was to use the impulse response to describe a distributed device and discretize the impulse response in time. In doing so, only the signals on the terminals of the distributed device were important, making it easy to characterize the device from measurements made at the terminals. The tradeoff was the signals on the terminals were needed for all past time. This tradeoff was acceptable when computing the steady-state solution with finite-

difference methods because the solution is calculated for all time. However, with shooting methods the solution is not known for any time preceding the shooting interval. Thus, characterizing a distributed device with its impulse response is inappropriate and it is necessary instead to discretize the distributed device in space rather than in time. With shooting methods the initial state of the distributed device along its entire discretized length must be determined. One problem with distributed devices in shooting methods is that measurements made from the terminals are difficult to convert into a space-discretized model for the device.

Commonly, the distributed devices present in high frequency circuits can only be represented accurately by lumped models with a large number of nodes, primarily because these devices have very high delay-bandwidth products. For example, consider an ideal transmission line. A model for the ideal line is a series inductor / shunt capacitor ladder network. The values of inductance ( $L$ ) and capacitance ( $C$ ) per section would be chosen to provide the correct characteristic impedance and to make the bandwidth of the model (roughly equals  $1/2\pi\sqrt{LC}$ ) larger than the frequencies expected in the circuit. The number of sections ( $n$ ) is chosen to give the model the correct amount of delay ( $td \approx n\sqrt{LC}$ ). For lines with considerable delay at the highest frequency of interest, a large number of sections are required. The computational complexity of both extrapolation- and Newton-Raphson-based shooting methods increases rapidly with the number of state variables. As a result, shooting methods are generally impractical for circuits containing more than one or two distributed devices.

## 2.5. Parallel Shooting

Shooting methods can have convergence and overflow problems when applied to circuits with unstable modes. For each iteration, only the initial state is specified, therefore any unstable modes may cause the trajectory to grow exponentially and leave the vicinity of the desired solution. The likelihood of this occurring decreases if the shooting interval  $T$  is reduced. Parallel, or multiple, shooting methods [keller68] [keller76] [stoer80] effectively reduce the shooting interval by dividing it into several subintervals. For example, if the shooting interval is divided into two equally sized subintervals, shooting is performed twice per iteration, once for each subinterval. Thus, the problem is restructured into another two-point boundary-value problem with twice as many unknowns (two sets of initial conditions, one set per subinterval) but with the shooting interval halved.

Consider dividing the interval  $[0, T]$  for the lumped periodic test problem (4.4) into  $K$  subintervals defined by the mesh  $\{\tau_0, \tau_1, \tau_2, \dots, \tau_K\}$  where  $\tau_0 = 0$ ,  $\tau_K = T$  and  $\tau_k < \tau_{k+1}$ . Let  $v_k = v(\tau_k)$  and define  $\phi_k(v_k) = v_{k+1}$ . Since  $v$  is  $T$ -periodic,  $v_0 = v_K$ , and by forcing  $v$  to be continuous at each  $\tau_k$

$$\begin{aligned}
 \phi_0(v_0) - v_1 &= 0 \\
 \phi_1(v_1) - v_2 &= 0 \\
 \vdots & \quad \vdots \quad \vdots \\
 \phi_{K-1}(v_{K-1}) - v_0 &= 0.
 \end{aligned}
 \tag{5.31}$$

This is a system of nonlinear algebraic equations that is solved using Newton-Raphson.

$$\begin{bmatrix} J_{\phi_0}(v_0^{(j)}) & -I & & & \\ & J_{\phi_1}(v_1^{(j)}) & \ddots & & \\ & & \ddots & -I & \\ -I & & & J_{\phi_{K-1}}(v_{K-1}^{(j)}) & \end{bmatrix} \begin{bmatrix} v_0^{(j+1)} - v_0^{(j)} \\ v_1^{(j+1)} - v_1^{(j)} \\ \vdots \\ v_{K-1}^{(j+1)} - v_{K-1}^{(j)} \end{bmatrix} = \begin{bmatrix} v_1^{(j)} - \phi_0(v_0^{(j)}) \\ v_2^{(j)} - \phi_1(v_1^{(j)}) \\ \vdots \\ v_0^{(j)} - \phi_{K-1}(v_{K-1}^{(j)}) \end{bmatrix} \quad (5.32)$$

By taking this iteration to convergence the value of the solution waveform is found at each of the points of the mesh. Both  $\phi_k(v_k)$  and  $J_{\phi_k}(v_k)$  are evaluated by integrating the circuit equations as in the previous subsection.

The computational complexity of the parallel shooting method is higher than the standard shooting method because the Jacobian in (5.32) has much larger dimension than the one in (5.21). The Jacobian is treated as a sparse block matrix and is efficiently factored by simply avoiding operations on zero blocks and possibly by applying the Sherman, Morrison, Woodbury formula [householder75] to convert it into a banded matrix. Besides the disadvantage of increased computational complexity, parallel shooting methods are also more difficult to program and require considerably more memory. These disadvantages, however, are offset by two advantages. First, the parallel shooting methods are more suitable for implementation on parallel processing computers; a feature that should grow in importance in the future. A second minor advantage is that parallel shooting methods have better convergence properties on unstable circuits. In particular, the region of convergence is larger for the parallel shooting methods and increases in size as the number of subintervals increases [keller76].

In the parallel shooting method, the circuit equations must be integrated over each subinterval individually. Thus each subinterval is further subdivided to perform the numerical integration of the differential equations. As the number of shooting subintervals

increases, the number of subdivisions per interval decreases. This causes a problem if it has been deemed desirable to use a high-order integration method. At each step a high-order integration method needs the history of the solution over several past time-steps. This history cannot extend beyond a shooting interval boundary. Thus it is necessary to build up to higher order integration methods by taking several steps of a low order method at the beginning of each interval. When an interval contains only a few time-points, high order methods lose their advantage because of the large percentage of time-steps taken with the low order methods.

## Chapter 6

# The Mixed Frequency-Time Method

---

In this chapter a boundary constraint is developed that restricts the set of solutions of a differential equation to those that are quasiperiodic. A first attempt is made by using the periodic boundary constraint (4.11 c), but it is shown to be computationally too expensive. In the process it is discovered that there are periodic problems that are better handled with a quasiperiodic boundary constraint. Another approach was suggested by Ushida and Chua [chua81]. They construct an  $N$ -point quasiperiodic boundary constraint by, assuming that the quasiperiodic signals are accurately approximated by a Fourier series with just  $K$  frequencies  $\Lambda_K = \{0, \omega_1, \dots, \omega_{K-1}\}$ , sampling the waveforms at  $M > 2K - 1$  points  $\tau = \{t_1, t_2, \dots, t_M\}$ , and insisting that the resulting sampled waveform is quasiperiodic (i.e., it belongs to  $AP(\Lambda_K, \tau)$ ). This method trades off accuracy for efficiency, but the tradeoff is such that the method is impractical for almost all problems. A generalization of this approach, referred to as the mixed frequency-time method (MFT), avoids both the efficiency and accuracy problems of the previous methods and is discussed in much greater

depth.

## 1. Previous Work

### 1.1. Quasiperiodicity Via the Periodic Boundary Constraint

The periodic boundary constraint (4.11 c) can be used to find approximately quasiperiodic solutions to differential equations because an almost periodic function  $x$  always has the property that given some  $\varepsilon > 0$  there always exists a  $T \in \mathbb{R}$  such that

$$\|x(t+T) - x(t)\| < \varepsilon \quad \text{for all } t \in \mathbb{R}. \quad (6.1)$$

$T$  is referred to as an  $\varepsilon$ -almost period of  $x$ . The collection of all  $\varepsilon$ -almost periods make up the  $\varepsilon$ -translation set of  $x$  [hale80].

Given  $\varepsilon$ , it is very difficult to find an  $\varepsilon$ -almost period, however it is possible to find an almost period  $T$  for which  $\max_t \|x(t+T) - x(t)\|$  is small, but not necessarily smaller than some  $\varepsilon$  specified in advance. One approach to finding such an almost period for  $x \in \mathcal{QP}(\lambda_1, \lambda_2, \dots, \lambda_d; \mathbb{R})$  is to choose a frequency  $\nu$  such that for each  $j \in \{1, 2, \dots, d\}$  there exists a  $k_j$  with  $k_j \nu \approx \lambda_j$ . The almost period is then  $2\pi/\nu$ . For example, consider  $x(t) = \cos(t) + \cos(\pi t)$ . This is 2-fundamental quasiperiodic with  $\lambda_1 = 1$  and  $\lambda_2 = \pi$ . A reasonably good rational approximation to  $\pi$  is  $355/113$ . So choose  $\nu = 1/113$ . Then  $113\nu = \lambda_1$  and  $355\nu = \lambda_2 + \delta$  where  $|\delta| < 3 \times 10^{-7}$ . Choosing  $T = 2\pi\nu = 226\pi$  results in  $|x(t+T) - x(t)| < 0.0002$  for all  $t$ .

While it is always possible to find an almost period  $T$  that satisfies (6.1) with some  $\varepsilon$  sufficiently small, the resulting boundary-value problem is usually extraordinarily expensive to solve. For the example, the boundary constraint involves 355 periods of the largest fundamental. Since all methods that solve boundary-value problems require the differential

equation to be integrated over the interval inclosed by the boundaries, using (6.1) as a quasiperiodic boundary constraint is usually prohibitively expensive. This problem also occurs when trying to find the periodic solution of a differential equation. Consider the example again, but this time let  $\lambda_2 = 355/113$  from the beginning. The solution is now periodic, but the boundary constraint still involves 355 periods of fundamental  $\lambda_2$ . In this situation, it is best to use a method specifically developed for quasiperiodic problems, such as the mixed frequency-time method presented later in this chapter.

## 1.2. Quasiperiodicity Via an N-Point Boundary Constraint

Consider the lumped quasiperiodic test problem (4.4). Recall that  $v \in QP(\lambda_1, \lambda_2, \dots, \lambda_d; \mathbb{R})$  and so

$$v(t) = V_0 + \sum_{k_1=1}^{\infty} \cdots \sum_{k_d=1}^{\infty} \left[ V^C(k_1, \dots, k_d) \cos(sT(k_1\lambda_1 + \cdots + k_d\lambda_d)) + V^S(k_1, \dots, k_d) \sin(sT(k_1\lambda_1 + \cdots + k_d\lambda_d)) \right].$$

Assume that this series can be truncated to  $K$  frequencies without introducing significant error, and that the resulting set of frequencies is  $\Lambda_K = \{0, \omega_1, \dots, \omega_d\}$ . If  $S = 2K - 1$  distinct time-points are chosen and  $v$  is sampled at these points, then the  $S$  coefficients of the truncated Fourier series can be determined using the APFT. Once the coefficients are known, the series can be evaluated for the solution to the differential equation for any time  $t$ . If the assumption of only  $K$  frequencies being significant is correct, and if the signal being sampled is quasiperiodic, then the solution as computed by integrating the differential equation and the Fourier series should agree for all time. Thus, the quasiperiodic boundary constraint is formed by selecting another time-point (one that differs from those chosen previously) and insisting that the solution to the differential equation agree with the Fourier

series.

For the lumped test problem (4.4)

$$i(v(t)) + \dot{q}(v(t)) + u(t) = 0. \quad (6.2)$$

Sample the solution at  $S + 1$  time-points  $\{t_1, t_2, \dots, t_{S+1}\}$ . Using  $\Lambda_K$  and all but the last time-point, form the inverse APFT matrix  $\Gamma^{-1}$  (3.7) and solve for the Fourier coefficients

$$\Gamma^{-1} \begin{bmatrix} V_0 \\ V_1^C \\ V_1^S \\ \vdots \\ V_{K-1}^C \\ V_{K-1}^S \end{bmatrix} = \begin{bmatrix} v(t_1) \\ v(t_2) \\ v(t_3) \\ \vdots \\ v(t_S) \end{bmatrix}$$

Evaluate the Fourier series at  $t_{S+1}$

$$\rho(t_{S+1}) \begin{bmatrix} V_0 \\ V_1^C \\ V_1^S \\ \vdots \\ V_{K-1}^C \\ V_{K-1}^S \end{bmatrix} = v(t_{S+1})$$

where  $\rho(t_{S+1}) = [1 \cos(\omega_1 t_{S+1}) \sin(\omega_1 t_{S+1}) \cdots \cos(\omega_{K-1} t_{S+1}) \sin(\omega_{K-1} t_{S+1})]$ . Thus the quasiperiodic boundary constraint on (6.2) is written in short form as

$$\rho(t_{S+1}) \Gamma \begin{bmatrix} v(t_1) \\ v(t_2) \\ v(t_3) \\ \vdots \\ v(t_S) \end{bmatrix} - v(t_{S+1}) = 0 \quad (6.3)$$

For the calculation of  $\Gamma$  from  $\Gamma^{-1}$  to be well conditioned, the time-points should be distributed over at least one period of the smallest frequency in  $\Lambda_K$  (see Chapter 3). This

implies that the differential equation must be integrated for at least one period of the smallest frequency. As an example of how inefficient this can become, consider  $v(t) = \sum_{k_1} \sum_{k_2} (\cos(k_1 \lambda_1 t) + \cos(k_2 \lambda_2 t))$  and truncate the number of frequencies by limiting  $|k_1|, |k_2| \leq 3$ . If  $\lambda_1 = 1$  and  $\lambda_2 = \pi$ , as in the previous example, then  $\omega_{\min} = \pi - 3 \approx 0.1415$  and  $\omega_{\max} = 3\pi$ . The ratio of  $\omega_{\max}$  to  $\omega_{\min}$  is 67, and so the differential equation must be evaluated for at least 67 periods of the highest frequency. This involves solving the differential equation over a much shorter interval than the that required when using the periodic boundary constraint, as we show in the next section, it is possible to reduce this interval further.

## 2. The Mixed Frequency-Time Method

Devising a boundary constraint that restricts the set of possible solutions for a differential equation to those that are quasiperiodic involves blending together both time-domain and frequency-domain concepts. A practical approach for doing this is the Mixed Frequency-Time (or MFT) method [kundert88d, kundert89]. This method can be formulated as a two-point boundary constraint, but to do so obscures the fundamental ideas behind the method. The method is presented in the most natural manner first, and then it is shown that MFT converts a differential equation into a boundary-value problem.

The mixed frequency-time method begins with the assumption that all waveforms present are  $d$ -quasiperiodic and that the frequency of each of the  $d$  fundamentals is known. One fundamental, often the highest in frequency, is chosen to be the clock. The waveforms are then sampled at the beginning of each clock cycle as shown in Figure 6.1 where the beginning of the cycle is chosen arbitrarily, but must be consistent on each cycle. The resulting sampled waveforms are  $(d-1)$ -quasiperiodic, as stated in the

following theorem.

**Theorem 6.1 (Quasiperiodic Sampling Theorem):** Let  $x \in QP(\lambda_1, \lambda_2, \dots, \lambda_d; \mathbb{R})$  and  $T = 2\pi/\lambda_d$  be the clock period. Let  $x_s = x(sT + \theta)$  where  $s \in \mathbb{Z}$  and  $\theta \in \mathbb{R}$  be the clock phase. Then  $\{x_s\} \in QP(\lambda_1, \lambda_2, \dots, \lambda_{d-1}; Z(T, \theta))$  where  $Z$  is the set of sample times  $Z(T, \theta) = \{t : t = rT + \theta, r \in \mathbb{Z}\}$ .

**Proof :**

$$x(t) = \sum_{k_1=-\infty}^{\infty} \sum_{k_2=-\infty}^{\infty} \cdots \sum_{k_d=-\infty}^{\infty} X(k_1, k_2, \dots, k_d) e^{j(k_1\lambda_1 + k_2\lambda_2 + \cdots + k_d\lambda_d)t}$$

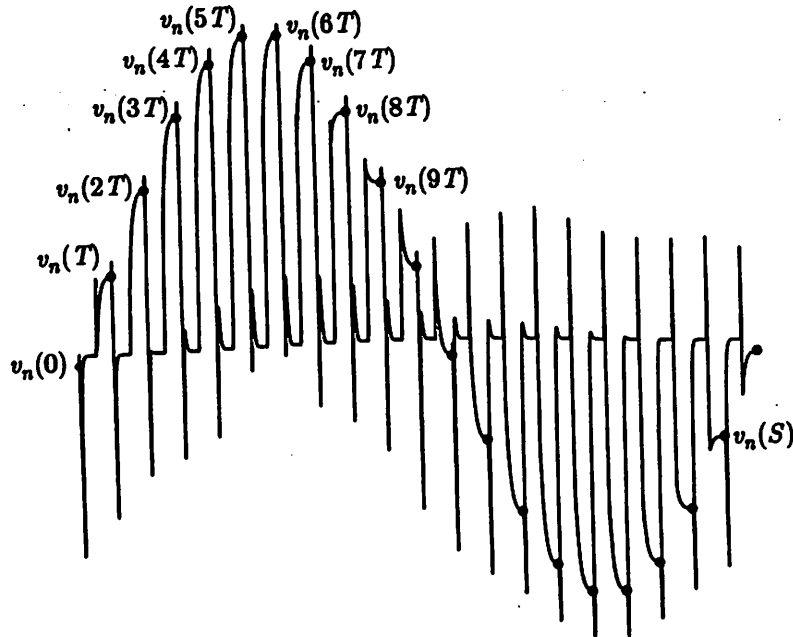


**Figure 6.1 :** The response of a switching filter circuit to a periodic function, with the initial points of each cycle denoted.

$$x_s = x(2\pi s/\lambda_d + \theta)$$

$$x_s = \sum_{k_1=-\infty}^{\infty} \cdots \sum_{k_d=-\infty}^{\infty} X(k_1, k_2, \dots, k_d) e^{j(k_1\lambda_1 + \cdots + k_d\lambda_d)(2\pi s/\lambda_d + \theta)}$$

$$\text{Let } \psi = (k_1\lambda_1 + k_2\lambda_2 + \cdots + k_{d-1}\lambda_{d-1})\theta$$

$$x_s = \sum_{k_1=-\infty}^{\infty} \cdots \sum_{k_d=-\infty}^{\infty} X(k_1, k_2, \dots, k_d) e^{j2\pi s \left[ \frac{k_1\lambda_1}{\lambda_d} + \cdots + \frac{k_{d-1}\lambda_{d-1}}{\lambda_d} + k_d \right] + jk_d\lambda_d\theta + j\psi}$$

$$x_s = \sum_{k_1=-\infty}^{\infty} \cdots \sum_{k_d=-\infty}^{\infty} X(k_1, k_2, \dots, k_d) e^{j2\pi s \left[ \frac{k_1\lambda_1}{\lambda_d} + \cdots + \frac{k_{d-1}\lambda_{d-1}}{\lambda_d} \right]} e^{jk_d(2\pi s + \lambda_d\theta)} e^{j\psi}$$

Recall that  $e^{j2\pi s k_d} = 1$  for all  $s$  and  $k_d$  and so  $e^{jk_d(2\pi s + \lambda_d\theta)} = e^{jk_d\lambda_d\theta}$ .

$$x_s = \sum_{k_1=-\infty}^{\infty} \cdots \sum_{k_d=-\infty}^{\infty} X(k_1, k_2, \dots, k_d) e^{j2\pi s \left[ \frac{k_1\lambda_1}{\lambda_d} + \cdots + \frac{k_{d-1}\lambda_{d-1}}{\lambda_d} \right]} e^{jk_d\lambda_d\theta} e^{j\psi}$$

$$\text{Let } Y(k_1, k_2, \dots, k_{d-1}) = \sum_{k_d=-\infty}^{\infty} X(k_1, k_2, \dots, k_d) e^{jk_d\lambda_d\theta}$$

$$x_s = \sum_{k_1=-\infty}^{\infty} \cdots \sum_{k_{d-1}=-\infty}^{\infty} Y(k_1, k_2, \dots, k_{d-1}) e^{j2\pi s \left[ \frac{k_1\lambda_1}{\lambda_d} + \cdots + \frac{k_{d-1}\lambda_{d-1}}{\lambda_d} \right]} e^{j\psi}$$

□

The MFT method uses the quasiperiodic sampling theorem to insure that the waveforms are  $d$ -quasiperiodic by sampling them at the clock frequency and insisting that the sampled waveforms be  $(d-1)$ -quasiperiodic. This is an easier condition to work with because the quasiperiodic constraint is placed on a discrete waveform with a rather long time between samples as opposed to a continuous waveform. To make this task tractable, it is necessary to assume that the Fourier series of the sampled waveform has only a finite number of nonzero terms. It is always possible to approach this ideal arbitrarily closely because any signal present in a physical system must have finite bandwidth. However, for the MFT method to be practical, there must be only a small number of nonzero terms in the

Fourier series.

Based on Theorem 6.1, the sampled signals can be represented by a Fourier series with  $d-1$  fundamentals. Assume that only  $J$  terms in this Fourier series are nonzero, then knowing the value of  $J$  samples allows the Fourier series of the sampled waveforms to be computed. Once the coefficients of the Fourier series are known, the value of any sample could be computed. In particular, given the value of  $J$  samples, it is possible to compute what must be the value of the immediately following  $J$  samples for the assumption of a finite Fourier series to hold. In other words, the finite Fourier series assumption yields a relationship between any  $J$  non-adjacent points on the sampled waveforms and their immediate successors, which is referred to as the delay operator. Another such relationship exists through the differential equations that describe the circuit. For each of the  $J$  samples, the equations are integrated over an interval of one clock cycle, each time using a different one of the  $J$  samples as an initial state. Thus, using the differential equations, it is also possible to start with  $J$  points on the sampled waveform and compute the immediately following points, as illustrated in Figure 6.2. MFT uses these two relationships to compute the quasiperiodic response of a circuit by finding the value of the  $J$  prespecified non-adjacent samples for which these two relationships agree. If the two relationships agree and if the assumption of only  $J$  nonzero terms in the Fourier series holds, then the entire waveform is a  $d$ -quasiperiodic solution to the differential equations.

## 2.1. The Delay Operator

Consider the sequence of points generated by sampling the quasiperiodic response of the lumped test problem (4.4), and denote the sequence  $\{v(sT) : s \in \mathbb{Z}\}$  where  $T = 2\pi/\lambda_d$  and  $\lambda_d$  is considered the clock. From the quasiperiodic sampling theorem the Fourier series for

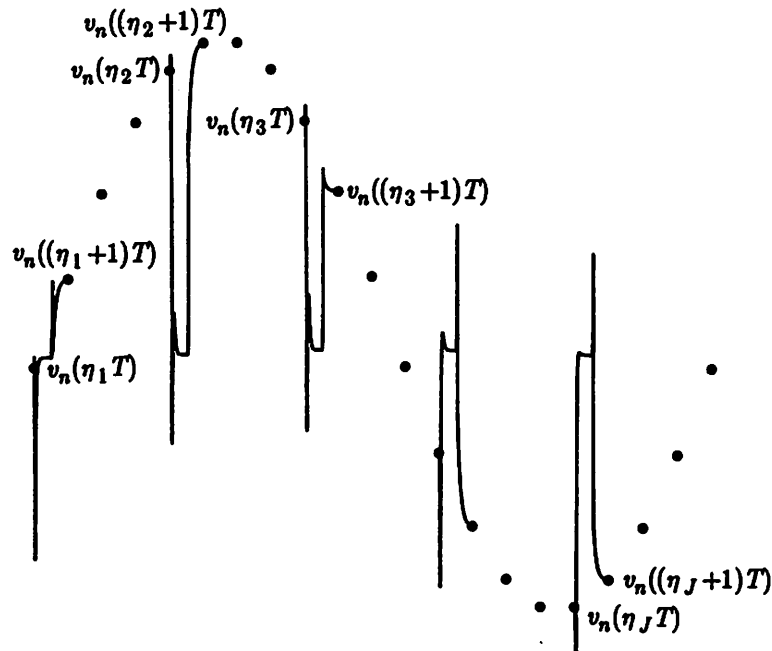


**Figure 6.2 :** The discrete waveform that is constructed by sampling the response of a circuit at the initial point of each clock cycle. Also shown are the  $J$  cycles that are calculated in detail.

this sequence is given by

$$v(sT) = V_0 + \sum_{k_1=1}^{\infty} \cdots \sum_{k_{d-1}=1}^{\infty} \left[ V^C(k_1, \dots, k_{d-1}) \cos(sT(k_1\lambda_1 + \cdots + k_{d-1}\lambda_{d-1})) + V^S(k_1, \dots, k_{d-1}) \sin(sT(k_1\lambda_1 + \cdots + k_{d-1}\lambda_{d-1})) \right]$$

where the clock phase  $\theta$  has been dropped to simplify the notation. Assume the sequence can be accurately approximated by the truncated Fourier series that results from considering only the first  $H$  harmonics of each fundamental (this is the box truncation of Chapter 3). The set of frequencies is given by

$$\Lambda_K = \{\omega : \omega = k_1\lambda_1 + \cdots + k_d\lambda_d;$$

$$|k_j| = 0, 1, \dots, H \text{ for } 1 \leq j \leq d; \text{ first nonzero } k_j \text{ positive}\}.$$

There are  $K$  nonzero frequencies in this series and  $J = 2K + 1$  unknown coefficients.

Assuming all frequencies are distinct, there is a linear relation between any collection of  $J$  initial points and any other collection of  $J$  initial points. However, as mentioned above,

we are most interested in the linear operator that maps a collection  $v(\eta_1 T), \dots, v(\eta_J T)$  into  $v((\eta_1+1)T), \dots, v((\eta_J+1)T)$  where  $T$  is the clock period and  $\{\eta_1, \dots, \eta_J\} \subset \mathbb{Z}$ .

This linear operator is referred to as the delay matrix.

Deriving the delay matrix is a two stage process. First, the  $J$  points,  $v(\eta_1 T), \dots, v(\eta_J T)$  are used to calculate the Fourier coefficients. Then the Fourier series (using these coefficients) is evaluated at the  $J$  times,  $(\eta_1+1)T, \dots, (\eta_J+1)T$ . The Fourier coefficients are then eliminated to yield the desired direct relation. To compute the Fourier coefficients, write the truncated Fourier series as a system of  $J$  linear equations in  $J$  unknowns using the APFT,

$$\Gamma_0^{-1} \begin{bmatrix} V_n(0) \\ V_n^C(1) \\ V_n^S(1) \\ \vdots \\ V_n^C(K) \\ V_n^S(K) \end{bmatrix} = \begin{bmatrix} v_n(\eta_1 T) \\ v_n(\eta_2 T) \\ v_n(\eta_3 T) \\ \vdots \\ v_n(\eta_J T) \end{bmatrix}. \quad (6.4)$$

where  $\Gamma_0^{-1} \in \mathbb{R}^{J \times J}$  is given by

$$\Gamma_0^{-1} = \begin{bmatrix} 1 & \cos\omega_1\eta_1 T & \sin\omega_1\eta_1 T & \cdots & \cos\omega_K\eta_1 T & \sin\omega_K\eta_1 T \\ 1 & \cos\omega_1\eta_2 T & \sin\omega_1\eta_2 T & \cdots & \cos\omega_K\eta_2 T & \sin\omega_K\eta_2 T \\ 1 & \cos\omega_1\eta_3 T & \sin\omega_1\eta_3 T & \cdots & \cos\omega_K\eta_3 T & \sin\omega_K\eta_3 T \\ \vdots & \vdots & \vdots & & \vdots & \vdots \\ 1 & \cos\omega_1\eta_J T & \sin\omega_1\eta_J T & \cdots & \cos\omega_K\eta_J T & \sin\omega_K\eta_J T \end{bmatrix}$$

where  $\omega_k \in \Lambda_K$ . The matrix  $\Gamma_0^{-1}$  maps the Fourier coefficients to a sequence and is referred to as the inverse almost-periodic Fourier transform. Its inverse, if it exists, is the forward almost-periodic Fourier transform and is denoted by  $\Gamma_0$ . We can also write

$$\Gamma_T^{-1} \begin{bmatrix} V_n(0) \\ V_n^C(1) \\ V_n^S(1) \\ \vdots \\ V_n^C(K) \\ V_n^S(K) \end{bmatrix} = \begin{bmatrix} v_n((\eta_1+1)T) \\ v_n((\eta_2+1)T) \\ v_n((\eta_3+1)T) \\ \vdots \\ v_n((\eta_J+1)T) \end{bmatrix} \quad (6.5)$$

where  $\Gamma_T^{-1} \in \mathbb{R}^{J \times J}$  is given by

$$\Gamma_T^{-1} = \begin{bmatrix} 1 & \cos\omega_1(\eta_1+1)T & \sin\omega_1(\eta_1+1)T & \cdots & \cos\omega_K(\eta_1+1)T & \sin\omega_K(\eta_1+1)T \\ 1 & \cos\omega_1(\eta_2+1)T & \sin\omega_1(\eta_2+1)T & \cdots & \cos\omega_K(\eta_2+1)T & \sin\omega_K(\eta_2+1)T \\ 1 & \cos\omega_1(\eta_3+1)T & \sin\omega_1(\eta_3+1)T & \cdots & \cos\omega_K(\eta_3+1)T & \sin\omega_K(\eta_3+1)T \\ \vdots & \vdots & \vdots & \ddots & \vdots & \vdots \\ 1 & \cos\omega_1(\eta_J+1)T & \sin\omega_1(\eta_J+1)T & \cdots & \cos\omega_K(\eta_J+1)T & \sin\omega_K(\eta_J+1)T \end{bmatrix}.$$

Given a sequence, a delayed version is computed by applying  $\Gamma_0$  to the sequence to compute the Fourier coefficients, and then multiplying the vector of coefficients by  $\Gamma_T^{-1}$ .

$$\begin{bmatrix} v_n((\eta_1+1)T) \\ v_n((\eta_2+1)T) \\ \vdots \\ v_n((\eta_J+1)T) \end{bmatrix} = \Gamma_T^{-1} \Gamma_0 \begin{bmatrix} v_n(\eta_1 T) \\ v_n(\eta_2 T) \\ \vdots \\ v_n(\eta_J T) \end{bmatrix} \quad (6.6)$$

Thus, the delay matrix,  $D(T) \in \mathbb{R}^{J \times J}$ , is defined as

$$D(T) = \Gamma_T^{-1} \Gamma_0. \quad (6.7)$$

As the delay matrix is a function only of  $\{\omega_1, \omega_2, \dots, \omega_K\}$ ,  $\{\eta_1, \eta_2, \dots, \eta_J\}$ , and  $T$ , it is computed once and used for every node.

## 2.2. The Differential Equation Relation

If the node voltages are known at some time  $t_0$ , it is possible to solve the equation describing the lumped test problem (4.4) and compute the node voltages at some later time  $t_1$ .

The relationship between  $v(t_0)$  and  $v(t_1)$  is expressed using the state-transition function

$$v(t_1) = \phi(v(t_0), t_0, t_1) \quad (6.8)$$

where  $\phi$  can be expanded as

$$\phi(v(t_0), t_0, t_1) = \begin{bmatrix} \phi_1(v(t_0), t_0, t_1) \\ \phi_2(v(t_0), t_0, t_1) \\ \vdots \\ \phi_N(v(t_0), t_0, t_1) \end{bmatrix} \quad (6.9)$$

where  $\phi_n: \mathbb{R}^{N \times 1 \times 1} \rightarrow \mathbb{R}$  for all circuit nodes  $n = 1, 2, \dots, N$ .

Now reconsider the  $J$  initial points at some circuit node  $n$ ,  $v_n(\eta_1 T), \dots, v_n(\eta_J T)$ .

For each  $j = 1, 2, \dots, J$  and each  $n = 1, 2, \dots, N$  write

$$v_n((\eta_j + 1)T) = \phi_n(v(\eta_j T), \eta_j T, (\eta_j + 1)T) \quad (6.10)$$

where  $T$  is the clock period. Note that  $v_n((\eta_j + 1)T)$  is the initial point of the cycle immediately following the cycle beginning at  $\eta_j T$ . Also, the node voltages at  $\eta_j T$  are related to the node voltages at  $(\eta_j + 1)T$  by the delay matrix,  $D(T)$ . That is,

$$D(T) \begin{bmatrix} v_n(\eta_1 T) \\ v_n(\eta_2 T) \\ \vdots \\ v_n(\eta_J T) \end{bmatrix} = \begin{bmatrix} v_n((\eta_1 + 1)T) \\ v_n((\eta_2 + 1)T) \\ \vdots \\ v_n((\eta_J + 1)T) \end{bmatrix} \quad (6.11)$$

It is possible to use (6.10) to eliminate the  $v_n((\eta_j + 1)T)$  terms from (6.11), which yields

$$D(T) \begin{bmatrix} v_n(\eta_1 T) \\ v_n(\eta_2 T) \\ \vdots \\ v_n(\eta_J T) \end{bmatrix} = \begin{bmatrix} \phi_1(v(\eta_1 T), \eta_1 T, (\eta_1 + 1)T) \\ \phi_2(v(\eta_2 T), \eta_2 T, (\eta_2 + 1)T) \\ \vdots \\ \phi_N(v(\eta_J T), \eta_J T, (\eta_J + 1)T) \end{bmatrix} \quad (6.12)$$

for each node  $n = 1, 2, \dots, N$ .

Solving the  $N$  simultaneous equations (6.12) results in knowing  $v(\eta_j T)$  for  $j = \eta_1, \eta_2, \dots, \eta_J$ . From these numbers, the Fourier coefficients  $V(0), V(1), \dots, V(K)$  can be computed. Once the Fourier coefficients are known, it is possible to compute  $v(jT)$  for any integer  $j$ . The value of  $v(t)$  for any  $t$  is found by integrating (4.4) using the nearest preceding  $v(jT)$  as a starting point.

### 2.3. An Example

Consider the simple switched-capacitor RC one-pole filter shown in Figure 6.3. It is easy to show that

$$\phi_1(v(\eta_j T), \eta_j T, (\eta_j + 1)T) = \frac{C_1 v_{in}(\eta_j T) + C_2 v(\eta_j T)}{C_1 + C_2}.$$

Since the circuit is linear, it is only necessary to consider DC and the fundamental in the solution, and so only three samples are needed. Assume the fundamental is 1 Hz and the clock is 6 Hz, and choose the samples to be taken at  $t = \{0, 1/3, 2/3\}$ . Then

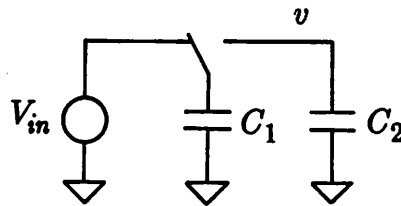


Figure 6.3 : A simple switched-capacitor RC filter.

---

$$\Gamma_0^{-1} = \begin{bmatrix} 1 & \cos(0) & \sin(0) \\ 1 & \cos(\frac{2\pi}{3}) & \sin(\frac{2\pi}{3}) \\ 1 & \cos(\frac{4\pi}{3}) & \sin(\frac{4\pi}{3}) \end{bmatrix} = \begin{bmatrix} 1 & 1 & 0 \\ 1 & -\frac{1}{2} & \frac{\sqrt{3}}{2} \\ 1 & -\frac{1}{2} & -\frac{\sqrt{3}}{2} \end{bmatrix},$$

$$\Gamma_0 = \begin{bmatrix} \frac{1}{3} & \frac{1}{3} & \frac{1}{3} \\ \frac{2}{3} & -\frac{1}{3} & -\frac{1}{3} \\ 0 & \frac{1}{\sqrt{3}} & -\frac{1}{\sqrt{3}} \end{bmatrix},$$

$$\Gamma_T^{-1} = \begin{bmatrix} 1 & \cos(\frac{\pi}{3}) & \sin(\frac{\pi}{3}) \\ 1 & \cos(\pi) & \sin(\pi) \\ 1 & \cos(\frac{5\pi}{3}) & \sin(\frac{5\pi}{3}) \end{bmatrix} = \begin{bmatrix} 1 & \frac{1}{2} & \frac{\sqrt{3}}{2} \\ 1 & -1 & 0 \\ 1 & \frac{1}{2} & -\frac{\sqrt{3}}{2} \end{bmatrix},$$

and

$$D(T) = \Gamma_T^{-1}\Gamma_0 = \frac{1}{3} \begin{bmatrix} 2 & 2 & -1 \\ -1 & 2 & 2 \\ 2 & -1 & 2 \end{bmatrix}.$$

Substituting into (6.12),

$$\frac{1}{3} \begin{bmatrix} 2 & 2 & -1 \\ -1 & 2 & 2 \\ 2 & -1 & 2 \end{bmatrix} \begin{bmatrix} v(0) \\ v(\frac{1}{3}) \\ v(\frac{2}{3}) \end{bmatrix} = \frac{1}{C_1 + C_2} \begin{bmatrix} C_1 v_{in}(0) + C_2 v(0) \\ C_1 v_{in}(\frac{1}{3}) + C_2 v(\frac{1}{3}) \\ C_1 v_{in}(\frac{2}{3}) + C_2 v(\frac{2}{3}) \end{bmatrix}.$$

By giving values for  $C_1$ ,  $C_2$ , and  $v_{in}(sT)$  for  $s = 0, 2, 4$ , this linear equation is solved for

$[v(0) \ v(\frac{1}{3}) \ v(\frac{2}{3})]^T$ . The Fourier coefficients are computed with

$$\begin{bmatrix} V(0) & V^C(1) & V^S(1) \end{bmatrix} = \Gamma_0 \begin{bmatrix} v(0) \\ v(\frac{1}{3}) \\ v(\frac{2}{3}) \end{bmatrix}.$$

## 2.4. MFT as a Two-Point Quasiperiodic Boundary Constraint

To show that the MFT formulation is interpretable as a two-point boundary-value problem, the time for each of the  $J$  intervals is written as a function of a new independent variable  $\tau$  that ranges over the interval  $[0, 1]$ . The boundaries for the two-point boundary-value problem are taken to be  $\tau = 0$  and  $\tau = 1$ . For interval  $j$ ,  $t_j = (\eta_j + \tau)T$  and let

$$V(\tau) = [v((\eta_1 + \tau)T), v((\eta_2 + \tau)T), \dots, v((\eta_J + \tau)T)]^T$$

and so  $V(\tau) \in \mathbb{R}^{NJ}$ . Consider the set of differential equations that describe the circuit over one cycle to be independent from the set that describe the circuit in any other cycle and combine the  $J$  independent sets into one composite set of differential equations for which  $V$  is the state variable. Denote  $\Phi$  as the state-transition function for the enlarged set of equations. The differential equation relation becomes

$$V(1) = \Phi(V(0), 0, 1) = \begin{bmatrix} \phi(v(\eta_1 T), \eta_1 T, (\eta_1 + 1)T) \\ \phi(v(\eta_2 T), \eta_2 T, (\eta_2 + 1)T) \\ \vdots \\ \phi(v(\eta_J T), \eta_J T, (\eta_J + 1)T) \end{bmatrix}. \quad (6.13)$$

The delay equation is written

$$V(1) = D_N(T)V(0). \quad (6.14)$$

$D_N(T) \in \mathbb{R}^{NJ \times NJ}$  is given by

$$D_N(T) = \begin{bmatrix} d_{11} \mathbf{1}_N & \cdots & d_{1J} \mathbf{1}_N \\ d_{J1} \mathbf{1}_N & \cdots & d_{JJ} \mathbf{1}_N \end{bmatrix} \quad (6.15)$$

where  $d_{ij} \in \mathbb{R}$  is the  $ij^{\text{th}}$  element of the delay matrix  $D(T)$  and  $\mathbf{1}_N \in \mathbb{R}^N$  is the identity matrix. Equation (6.14) is a two-point boundary constraint on (6.13). The solution of these two simultaneous equations is a collection of values that fall on a quasiperiodic solution for the lumped test problem at the prespecified points. These two equations can be combined into one by eliminating  $V(1)$ .

$$\Phi(V(0), 0, 1) - D_N(T)V(0) = 0 \quad (6.16)$$

This equation is equivalent to (4.10) with  $A = -D_N(T)$ ,  $B = \mathbf{1}_{NJ}$ ,  $c = \mathbf{0}$ ,  $\phi = \Phi$ , and  $x = V$ .

### 3. Practical Issues

MFT poses the problem of finding a quasiperiodic solution to the lumped test problem (4.4) as a boundary-value problem by using (6.13) and (6.14). These equations can be solved by using either finite-difference methods or shooting methods (Chapter 5). In either case, the number of unknowns, and hence the time required to compute the solution, is likely to be large. For a circuit with  $N$  nodes, the number of unknowns is  $NJ$ , where  $J$  is the number of samples required by MFT. Recall that MFT uses the quasiperiodic sampling theorem to convert the problem of finding a continuous time  $d$ -quasiperiodic solution to the problem of finding a discrete-time  $(d-1)$ -quasiperiodic solution.  $J$  is the number of unknown terms in the Fourier series of the discrete-time  $(d-1)$ -quasiperiodic signal. To reduce the time required to compute the solution, both the structure of the MFT must be exploited during the computations required by the shooting method and  $J$ , the number of terms in the Fourier series, must be minimized.

#### 3.1. The Quasiperiodic Sampled Waveform

The number of unknowns in MFT is proportional to the number of significant terms in the Fourier series of the  $(d-1)$ -quasiperiodic sampled waveform. There are two degrees of freedom that can be exploited to reduce the number of significant terms in this series. First, any one of the  $d$  fundamental frequencies can be chosen as the clock. This is discussed further in the next section. Second, the phase of the clock signal at which the samples are taken ( $\theta$  in the quasiperiodic sampling theorem) is as yet unspecified. It can be

advantageous to choose this phase judiciously when the clock signal is causing the circuit to switch. For example, consider the circuit shown in Figure 6.4. The voltage at the output and summing nodes is sampled with  $\theta = 0$  and  $\theta = 0.25T$ . The spectra of the sampled waveforms are shown in Figure 6.5. This shows that the number of significant terms in the Fourier series of the sampled signal is much higher when  $\theta = 0.25T$ . This behavior

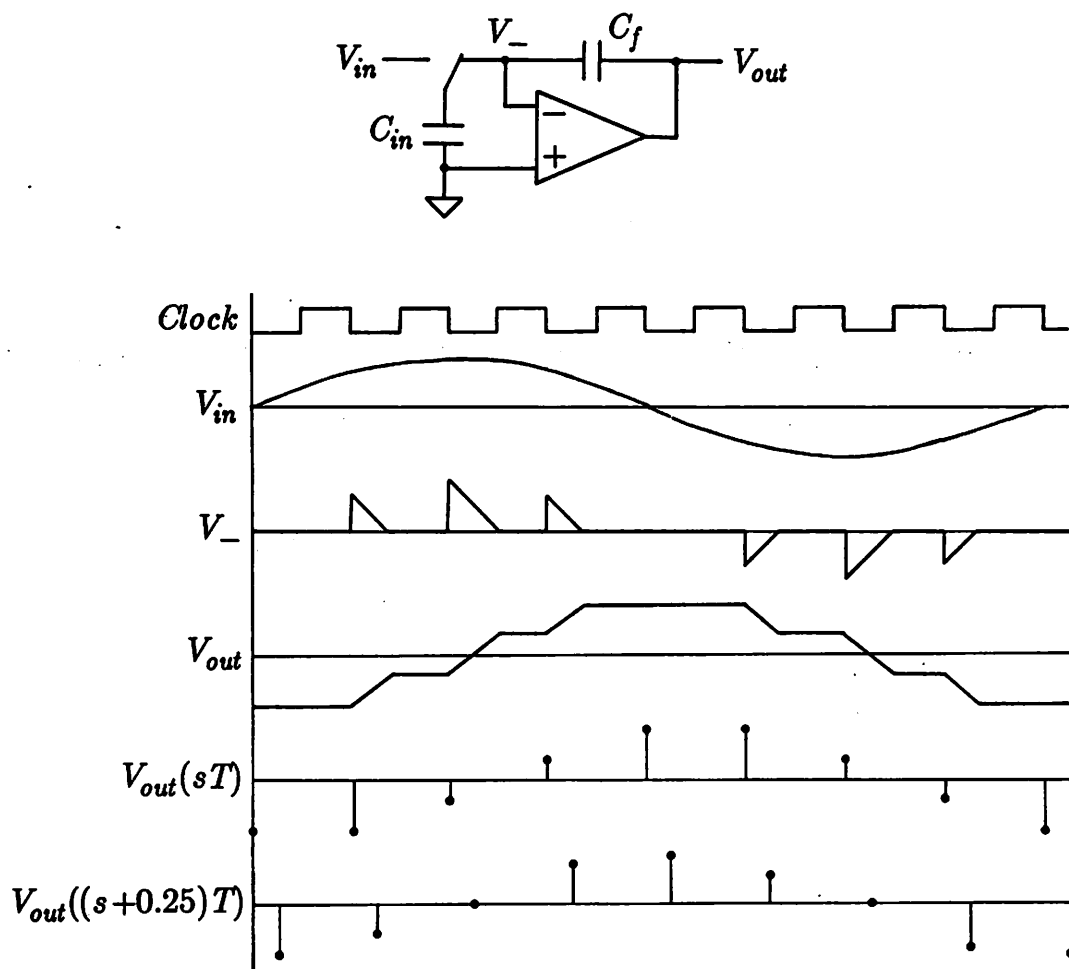
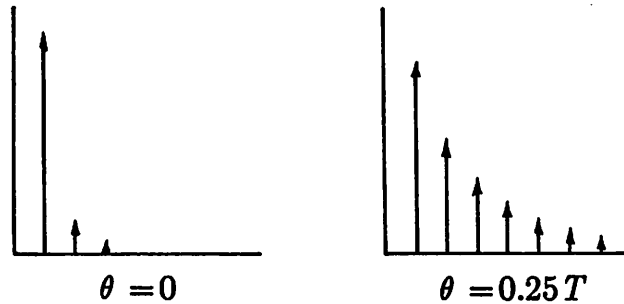


Figure 6.4 : A switched capacitor integrator and its steady-state response to a sinusoidal input.



**Figure 6.5 :** Spectra for the sampled waveforms from 6.4.

---

results because at  $\theta = 0$  there is a delay of  $T$  seconds between when the switch last changed state and when the waveforms are sampled. Conventional design practice dictates that any transients should have decayed to negligible levels during this interval. At this time, feedback in the circuit is acting to minimize distortion. Conversely, when  $\theta = 0.25T$  the samples are being taken at a time when the op amp is undergoing slew rate limiting, an effect that results from nonlinearities in the input stage.

It is very common for analog switching circuits to respond very nonlinearly to the clock signal but respond (by design) nearly linearly to other input signals. Choosing the proper clock phase to sample the waveforms judiciously serves to reduce computation time in two important ways. First, it can greatly reduce the number of Fourier series terms needed to represent the sampled signal accurately. Second, choosing  $\theta$  to reduce  $J$ , also serves to make  $\Phi$  in (6.13) more linear and so reduces the number of iterations required by the shooting method (Chapter 5).

### 3.2. Selecting the Clock

In the MFT the circuit equations are integrated for a total of  $J$  clock cycles. The number of time-points required in one clock period is proportional to  $T\lambda_d$ , where  $\lambda_d$  is the largest of the fundamental frequencies and  $T$  is the clock period. Thus, the total number of time-points required is proportional to  $JT\lambda_d$  where  $\lambda_d$  is fixed. This forms the basis used to choose which fundamental frequency should be the clock: the clock is chosen to be the fundamental that minimizes the  $JT$  product. Clearly, the  $T$  term is minimized by selecting the largest fundamental to be the clock. However, if the largest fundamentals are close in frequency, it is sometimes desirable to use other fundamentals as the clock because a smaller  $J$  can be used. For example, in a circuit that exhibits a  $d$ -quasiperiodic solution with  $\lambda_{d-1}$  close to, but less than,  $\lambda_d$ , it would be preferable to choose  $\lambda_{d-1}$  as the clock if either the input sources had considerably larger signal levels at frequencies  $\lambda_{d-1}$  and its harmonics than at other frequencies, or if the state-transition function of the circuit for one period of the fundamental  $\lambda_{d-1}$  is considerably more linear than for one period of the other fundamentals. If both situations are present, then  $J$  can be smaller if  $\lambda_{d-1}$  is chosen as the clock over  $\lambda_d$ .

## 4. Nitswit

*Nitswit* is a circuit simulator developed during the course of this research that implements the MFT method and solves for quasiperiodic steady-state solutions [kundert88d] [kundert89]. The name results from *Nitswit* being a detailed (nit) level circuit simulator for analog switching (swit) circuits. *Nitswit* is the first circuit simulator capable of finding quasiperiodic steady-state solutions directly in the time domain. It uses the MFT method to formulate the problem of finding a quasiperiodic steady-state solution as a boundary-value

problem and Newton-Raphson-based shooting methods to solve the boundary-value problem. *Nitswit* exploits the property of shooting methods that allows them to easily handle a circuit with a near-linear state-transition function over the shooting interval even when the circuit is behaving very nonlinearly during the interval. This allows *Nitswit* to handle analog switching circuits such as switching mixers and switched-capacitor filters. Even the difficult task of computing the intermodulation distortion of narrow-band switched-capacitor filters is performed efficiently with *Nitswit*. It is designed to simulate these circuits without the approximations of the discrete-time methods of Fang [fang83] and Rabaey [de man80] (such as the slow-clock and macromodeling approximations).

#### 4.1. Equation Formulation

*Nitswit* applies shooting methods to solve the mixed frequency-time formulation equations (6.13) and (6.14), rewritten slightly here as

$$F \begin{bmatrix} v(\eta_1 T) \\ v(\eta_2 T) \\ \vdots \\ v(\eta_J T) \end{bmatrix} = D_N(T) \begin{bmatrix} v(\eta_1 T) \\ v(\eta_2 T) \\ \vdots \\ v(\eta_J T) \end{bmatrix} - \begin{bmatrix} \phi(v(\eta_1 T), \eta_1 T, (\eta_1 + 1)T) \\ \phi(v(\eta_2 T), \eta_2 T, (\eta_2 + 1)T) \\ \vdots \\ \phi(v(\eta_J T), \eta_J T, (\eta_J + 1)T) \end{bmatrix} = \mathbf{0} \quad (6.19)$$

where  $F : \mathbb{R}^{NJ} \rightarrow \mathbb{R}^{NJ}$ , and  $D_N(T)$  is given by

$$D_N(T) = \begin{bmatrix} d_{11} \mathbf{1}_N & \cdots & d_{1J} \mathbf{1}_N \\ d_{J1} \mathbf{1}_N & \cdots & d_{JJ} \mathbf{1}_N \end{bmatrix} \quad (6.20)$$

where  $d_{ij} \in \mathbb{R}$  is the  $ij^{\text{th}}$  element of the delay matrix  $D(T)$  and  $\mathbf{1}_N \in \mathbb{R}^N$  is the identity matrix. This equation is solved with Newton-Raphson based shooting methods as shown in Chapter 5.

## 4.2. Implementation

Both the classical direct methods and the mixed frequency-time methods have been implemented in the simulation program *Nitswit*, which is written in the computer language "C." *Nitswit* takes as input a file with a SPICE-like description of the circuit, that is, a list of elements (MOS transistors, resistors, capacitors, etc) with their node connections, and a list of options to select among methods. If the mixed frequency-time method is used, a switching clock period and an input frequency, along with a number of harmonics, must be specified. The program produces as output waveforms as in Figure 6.1 for direct methods, and waveforms as in Figure 6.2 and Fourier coefficients for the sampled waveforms with the mixed frequency-time algorithm.

### 4.2.1. Application Examples

*Nitswit* is particularly efficient when simulating switched-capacitor filters. One reason is that switched-capacitor filters are usually followed by a sampler, and so only the initial point of each cycle is needed. Also, the circuits are generally designed to exhibit little distortion, so if driven by a sinusoid, only a few harmonics of the sequence of initial points are significant and only a few full clock cycles need to be computed. Finally, the state-transition function for a switched-capacitor filter over a clock cycle is nearly affine (linear plus a constant), and therefore Newton-Raphson applied to (6.19) converges in just a few iterations.

To demonstrate the effectiveness and versatility of the algorithms used in *Nitswit*, we consider analyzing the distortion of a switched-capacitor circuit. Figure 6.6 shows a high-speed fully-differential switched-capacitor sample-and-hold amplifier [lewis87]. This circuit precedes an analog-to-digital converter and has all three characteristics mentioned

above. An important performance specification for this circuit is distortion. Its distortion is measured by applying a sinewave to the input and a periodic clock to the sample/hold input. The output signal is then sampled at the end of each hold interval and a Fourier series is constructed from the sampled signal. If the sample-and-hold is ideal, there will be energy only at the frequency of the input sinusoid. Any energy at other frequencies is considered distortion. The sampling of the output at the end of the hold interval is needed to eliminate settling effects that result at transitions of the sample/hold signal that are ignored by the analog-to-digital converter that follows. Conventional circuit simulators limit the input frequency to be near the sample/hold clock rate and do not sample the output signal at the end of the hold interval before computing its Fourier series.

Figure 6.7 shows the operational amplifier used in the sample-and-hold of Figure 6.6. The combined circuit contains 65 nodes. The distortion of this circuit was measured with *Nitswit* versus the amplitude of the input signal (Figure 6.8) and versus the sample/hold

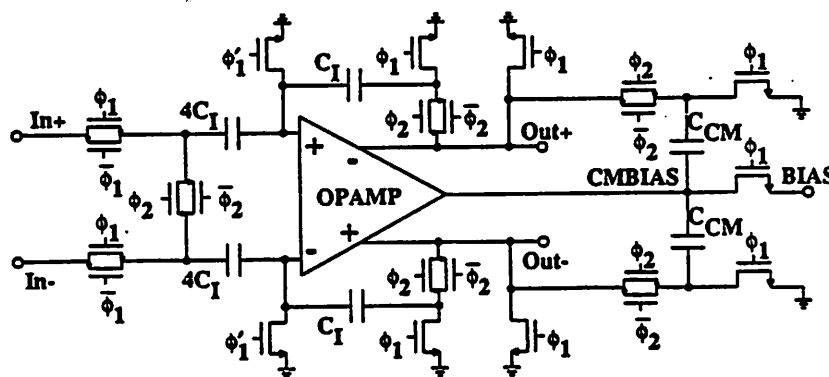


Figure 6.6 : A full-differential switched-capacitor sample-and-hold amplifier [lewis87].

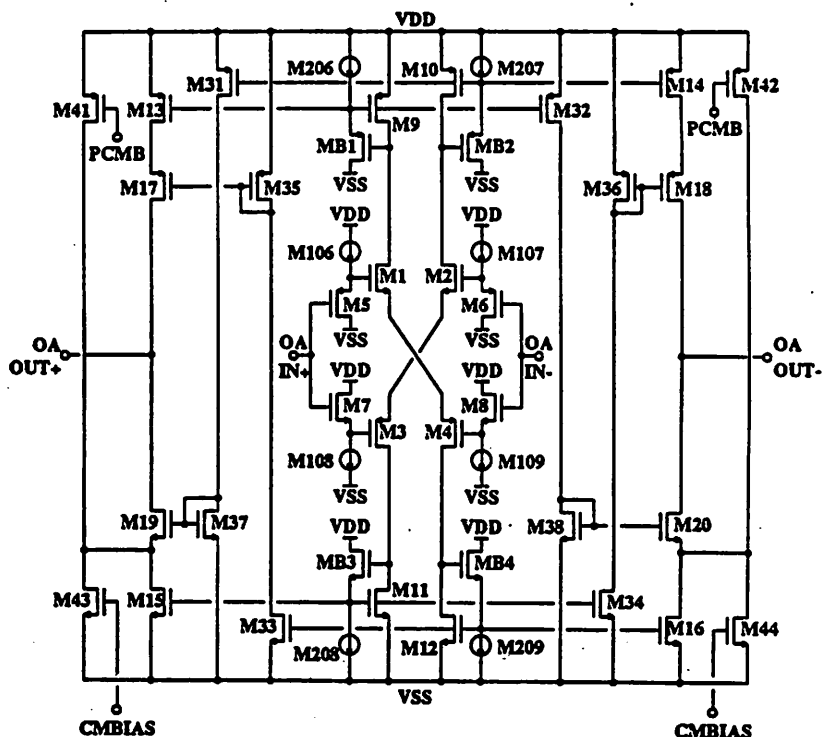
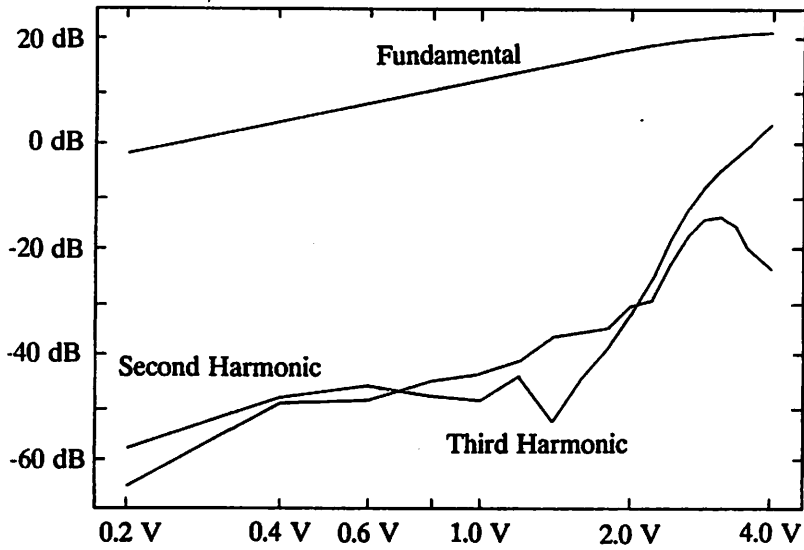


Figure 6.7 : The operational amplifier used in the sample-and-hold amplifier of Figure 6.6 [lewis87].

clock frequency (Figure 6.9). Of particular interest to the designer is the distortion versus clock rate. This is a quantity that cannot be determined except with a circuit-level simulator such as *Nitswit* or by measuring the actual circuit.

These simulation were performed with a SPICE level 1 MOS model with a simplified version of the charge conserving model of Yang, Epler, and Chatterjee [yang83]. This model was chosen simply because it was easy to implement. However, it is generally considered to be too inaccurate to be suitable for analog circuits. Since the mixed frequency-time algorithm has extra overhead (primarily, the time required to construct the sensitivity



**Figure 6.8 :** Distortion of the sample-and-hold amplifier as a function of input signal amplitude. The input signal frequency is 500 kHz and the sample/hold clock rate was 10 MHz.

---

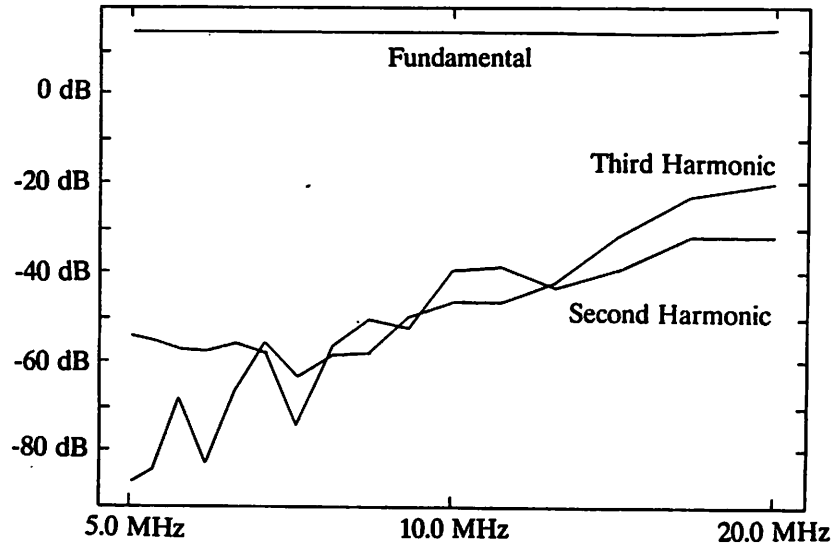


**Figure 6.9** : Distortion of the sample-and-hold amplifier as a function of sample/hold clock frequency. The amplitude of the input signal is 1.25 V differential and its frequency is 500 kHz.

matrix) that dominates over the time required for model evaluation, it is expected that the algorithm should do better with respect to direct methods when a more accurate (and therefore a more complicated) model is used.

The Fourier series for the sampled signal was truncated after three harmonics. For the case where the input was a 2 V differential 500 kHz sine wave and the sample/hold clock rate was 10 MHz, this gave results that were identical to direct methods to within the truncation error of the integration method.

#### 4.2.2. Comparison to Direct Methods

The program *Nitswit* contains two algorithms capable of finding the steady-state response of a circuit. The first is simply a transient analysis that continues until a steady-state is

achieved. The second, of course, is the mixed frequency-time algorithm. Coding both algorithms into the same simulator provides a fair evaluation of the mixed frequency-time approach.

Figure 6.10 shows the time required to simulate the sample-and-hold of Figure 6.6 to steady-state as a function of the input signal frequency for both direct methods and for the mixed-frequency algorithm. The amplitude of the input signal is 1.25 V differential and its frequency is 500 kHz. The sample/hold clock is fixed at 5 MHz and three harmonics of the sampled signal are computed. This figure shows that the time required for the mixed frequency-time algorithm is roughly independent of the frequency of the input signal whereas the time required for direct method is proportional to the ratio of the clock frequency to the input frequency. This circuit provides the freedom of choosing the input frequency close to the clock frequency, allowing transient analysis to be efficient. Many circuits do not provide this freedom.

Results for four circuits are given in Table 6.1. The first, *sclpf*, is an RC one-pole SC filter. The second, *scop*, is a one-pole active CMOS low pass filter. The circuit, *mixer*, is a double-balanced switching mixer with a 1.001 MHz RF input signal and a 1 MHz LO signal. This circuit shows that *Nitswit* is not limited to switched-capacitor circuits. The last circuit, *frog*, is a five pole Chebyshev active CMOS leap frog filter with 0.1 dB ripple. This circuit is driven with a 1 MHz clock, has a 20 kHz bandwidth, and is being driven with a 1 kHz test signal to measure its distortion.

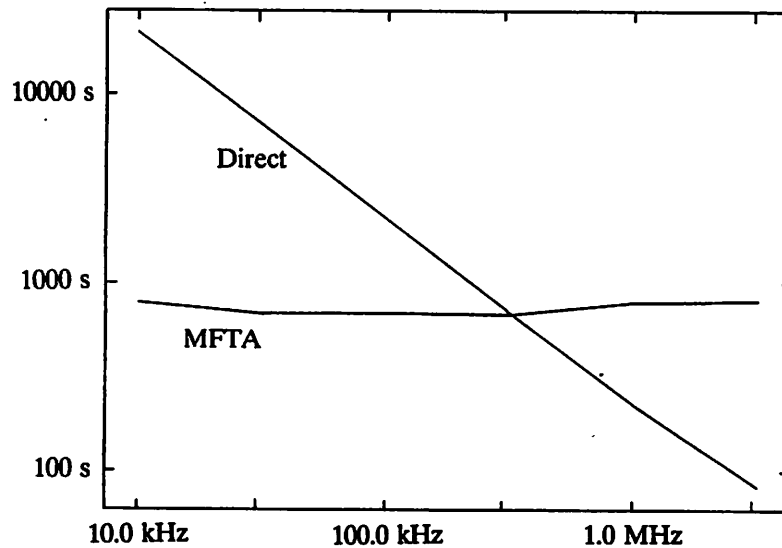


Figure 6.10 : Time required for simulation of sample-and-hold amplifier to steady state versus input frequency using direct methods and the mixed frequency-time algorithm. These time were measured on an HP9000/370 with a floating point accelerator.

circuit		direct	mixed frequency-time			ratio	
name	nodes	cycles/ period	time (sec)	harmonics	Newton iterations	time (sec)	direct/ MFT
<i>sc1pf</i>	2	33	24.5	3	3	4.3	5.7
<i>scop</i>	13	100	522	3	6	90	5.8
<i>mixer</i>	34	1000	7132	3	4	161	44.3
<i>frog</i>	77	1000	12,987	3	6	1228	10.6

Table 6.1 : *Nitswit* results from a VAX 8650 running ULTRIX 2.0.

Examination of the results above indicate as much as an order of magnitude speed increase over traditional methods, but this is not as much as one would expect. Much of the CPU time for large circuits, such as *frog*, is spent calculating the dense sensitivity matrix and factoring the Jacobian. It does turn out however, that almost all the entries of the sensitivity matrix are near zero, and this suggests significant speed improvements can

be achieved by ignoring those terms.



The following text is extremely faint and largely illegible. It appears to be a multi-paragraph discussion, possibly related to the graph above. Some words are difficult to discern but seem to include terms like 'linear', 'fit', 'error', and 'variance'. The text is too light to transcribe accurately.

# Chapter 7

## Harmonic Balance: Theory

---

### 1. Introduction

Harmonic balance differs from traditional transient analysis in two fundamental ways. These differences allow harmonic balance to compute periodic and almost-periodic solutions directly and in certain circumstances give the method significant advantages in terms of accuracy and efficiency. Transient analysis, which uses standard numeric integration, constructs a solution as a collection of time samples with an implied interpolating function. Typically the interpolating function is a low order polynomial. However, polynomials fit sinusoids poorly, and so many points are needed to approximate sinusoidal solutions accurately.

The first difference between harmonic balance and transient analysis is that harmonic balance uses a linear combination of sinusoids to build the solution. Thus, it approximates naturally the periodic and almost-periodic signals found in a steady-state response. If the steady-state response consists of just a few dominant sinusoids, which is common, then harmonic balance needs only a small data set to represent the response accurately. The advantage of using sinusoids to approximate an almost-periodic steady-state response becomes particularly important when the response contains dominant sinusoids at widely separated frequencies.

Harmonic balance also differs from traditional time-domain methods in that time domain simulators represent waveforms as a collection of samples whereas harmonic balance represents them using the coefficients of the sinusoids. (Just as in traditional time-domain methods where it is presumed that a polynomial is used to interpolate between samples, we can use samples to represent the combination of sinusoids, with the understanding that a sum-of-sinusoids interpolation is to be done between samples.) Representing signals with the coefficients is a practical matter, the solution calculated will be the same with either representation, but using coefficients makes it easier to model and evaluate the linear components. Working with the coefficients and exploiting superposition makes it possible to calculate symbolically the response from linear dynamic operations such as time integration, differentiation, convolution, and delay. Because linear devices respond at the same frequency as the stimulus, it is only necessary to determine the magnitude and phase of the response. Using phasor analysis [desoer69], this is easily done for lumped components such as resistors, capacitors and inductors; while it is not trivial for the more esoteric distributed devices like transmission lines with dispersion, it is generally much easier to find their response using phasor analysis than to try to determine their response to sampled waveforms in the time domain. The use of phasors to evaluate the linear devices is perhaps the most useful feature of harmonic balance.

The major difficulty with the harmonic balance approach is determining the response of the nonlinear devices. There is no known way to compute the coefficients of the response directly from the coefficients of the stimulus for an arbitrary nonlinearity, though it is possible if the nonlinearity is described by a polynomial or a power series [steer83] [rhyne88]. It is not necessary to consider only these special cases, nor to accept the error of using them to approximate arbitrary nonlinearities. Instead, we convert the coefficient

representation of the stimulus into a sampled data representation; this is a conversion from the frequency domain to the time domain and is accomplished with the inverse Fourier transform. With this representation the nonlinear devices are easily evaluated. The results are converted back into coefficient form using the forward Fourier transform.

Because the coefficients of the steady-state response are an algebraic function of the coefficients of the stimulus, the dynamic aspect of the problem is eliminated. Thus, the nonlinear integro-differential equations that describe a circuit are converted by harmonic balance into a system of algebraic nonlinear equations whose solution is the steady-state response of the circuit. These equations are solved iteratively.

Harmonic balance was given its name because it was viewed as a method for balancing of currents between the linear and nonlinear subcircuits. Furthermore, harmonic balance is usually considered a mixed-domain method, because the nonlinear devices are evaluated in the time domain while the linear devices are evaluated in the frequency domain. However, evaluating the nonlinear devices in the time domain is not a fundamental part of the algorithm, but rather a convenience that does not affect the essential character of the algorithm. It is the formulation of the circuit equations in the frequency domain that give harmonic balance its essential characteristics. Thus, harmonic balance can be summarized as just being the method where KCL is formulated in the frequency domain.

This chapter starts with a brief example, which is used to illustrate the harmonic balance method and some of its error mechanisms. The harmonic balance equations are then derived for the distributed test problem. The resulting system of nonlinear equations is solved using nonlinear programming methods, nonlinear relaxation, and the Newton-Raphson algorithm. Finally, the magnitude of the errors present in harmonic balance are

estimated and techniques to extend harmonic balance to autonomous circuits are discussed.

### 1.1. An Example

As an example of how harmonic balance can be used to find the solution to a nonlinear differential equation, consider Duffing's equation, which can be used to describe a nonlinear LC circuit.

$$\ddot{x} + \lambda^2 x + \mu x^3 = A_1 \cos(\omega_o t). \quad (7.1)$$

The "amount of nonlinearity" in the equation is controlled by  $\mu$ , and  $\lambda$  is the resonant frequency of the circuit when  $\mu = 0$ . The periodic steady-state solution to this equation has the form  $x = \sum_{k=0}^{\infty} a_k \cos(k\omega_o t)$  where  $a_k = 0$  for  $k = 0, 2, 4, \dots$ . To make the problem tractable, only  $a_1$  and  $a_3$  will be assumed to be nonzero. Substitute the assumed solution  $\hat{x}(t) = a_1 \cos(\omega_o t) + a_3 \cos(3\omega_o t)$  into (7.1).

$$\frac{1}{4}\mu a_3^3 \cos(9\omega_o t) + \frac{3}{4}\mu a_1 a_3^2 \cos(7\omega_o t) + \frac{3}{4}\mu(a_1^2 a_3 + a_1 a_3^2) \cos(5\omega_o t) + \quad (7.2)$$

$$[\frac{1}{4}\mu(3a_3^3 + 6a_1^2 a_3 + a_1^3) + (\lambda^2 - 9\omega_o^2)a_3] \cos(3\omega_o t) +$$

$$[\frac{1}{4}\mu(3a_1^2 a_3 + 6a_1 a_3^2 + 3a_1^3) + (\lambda^2 - \omega_o^2)a_1] \cos(\omega_o t) = A_1 \cos(\omega_o t)$$

Using the orthogonality of sinusoids at different frequencies, rewrite (7.2) as a system of five equations, one for each harmonic generated by the assumed solution.

$$\cos(\omega_o t): \quad \frac{1}{4}\mu(3a_1^2 a_3 + 6a_1 a_3^2 + 3a_1^3) + (\lambda^2 - \omega_o^2)a_1 = A_1 \quad (7.3a)$$

$$\cos(3\omega_o t): \quad \frac{1}{4}\mu(3a_3^3 + 6a_1^2 a_3 + a_1^3) + (\lambda^2 - 9\omega_o^2)a_3 = 0 \quad (7.3b)$$

$$\cos(5\omega_o t): \quad \frac{3}{4}\mu(a_1^2 a_3 + a_1 a_3^2) = 0 \quad (7.3c)$$

$$\cos(7\omega_o t): \quad \frac{3}{4}\mu a_1 a_3^2 = 0 \quad (7.3d)$$

$$\cos(9\omega_o t): \quad \frac{1}{4}\mu a_3^3 = 0 \quad (7.3e)$$

Since there are only two unknowns, it is not possible to satisfy all five equations exactly.

This problem results from including only a finite number of harmonics in the assumed

solution when really an infinite number exists. Traditionally, the coefficients of the sinusoids in the solution are computed by solving the equations at the harmonics present in the solution. Thus  $a_1$  and  $a_3$  are found by solving (7.3a) and (7.3b) simultaneously. In effect, the exact solution is found for (7.1) with a perturbed right-hand side.

$$\ddot{x} + \lambda^2 \dot{x} + \mu \dot{x}^3 = A_1 \cos(\omega_o t) + A_5 \cos(5\omega_o t) + A_7 \cos(7\omega_o t) + A_9 \cos(9\omega_o t) \quad (7.4)$$

$$\text{where } A_5 = -3/4\mu(a_1^2 a_3 + a_1 a_3^2)$$

$$A_7 = -3/4\mu a_1 a_3^2$$

$$A_9 = -1/4\mu a_3^3$$

Notice that no mention has been made about how to solve the system of algebraic equations generated in the last step of the method of harmonic balance. Several different approaches have been used, the most notable being optimization [nakhla76] [gopal78] [filicori79], nonlinear relaxation [hicks82b], and Newton-Raphson [egami74] [ushida84]. All these methods have quite different characteristics, but all have been referred to only as harmonic balance, which has led to a certain amount of confusion. To eliminate any confusion, in this dissertation, the three approaches are referred to as harmonic programming, harmonic relaxation, and harmonic Newton.

## 2. Error Mechanisms

There are three sources of error that are of interest in harmonic balance. The first two result from truncating the harmonics considered to some finite number, and the third results from not completely converging the iteration used to solve the nonlinear system of algebraic equations. If Newton-Raphson is used, then the third source of error can be driven to an arbitrarily small level in relatively few iterations because of the method's quadratic convergence property. So this source of error will be ignored for now.

As shown in (7.4), harmonics that are not in the assumed solution end up perturbing the right-hand-side of the algebraic equations. Recall that (7.3a) and (7.3b) were solved exactly for  $a_1$  and  $a_3$  and (7.3c), (7.3d) and (7.3e) were left unsatisfied; thus (7.1) was also unsatisfied. Let  $\varepsilon$  be the amount by which (7.1) is not satisfied

$$\varepsilon(\hat{x}, t) = \ddot{\hat{x}} + \lambda^2 \hat{x} + \mu \hat{x}^3 - A_1 \cos(\omega_o t)$$

where

$$\hat{x}(t) = \hat{a}_1 \cos(\omega_o t) + \hat{a}_3 \cos(3\omega_o t)$$

From (7.4) it is clear that

$$\varepsilon(\hat{x}, t) = A_5 \cos(5\omega_o t) + A_7 \cos(7\omega_o t) + A_9 \cos(9\omega_o t)$$

Note that the residual  $\varepsilon$  is orthogonal to the form of the assumed solution  $\alpha_1 \cos(\omega_o t) + \alpha_3 \cos(3\omega_o t)$ . This is the defining characteristic of Galerkin methods and is a property of harmonic balance when only a finite number of harmonics are considered. This property is lost if the nonlinear devices are evaluated in the time domain and the transform used exhibits aliasing.

An iterative method is used to solve the nonlinear algebraic system of equations generated by harmonic balance. Equation (7.3) is an example of such a system; it can be represented as

$$F(\hat{X}) = 0$$

where  $F: \mathbb{R}^2 \rightarrow \mathbb{R}^5$  and  $\hat{X} = [\hat{a}_1 \ \hat{a}_3]^T$ . In practice, this system is evaluated at  $X = [\alpha_1 \ \alpha_3]^T$  by computing  $x(t) = \alpha_1 \cos(\omega_o t) + \alpha_3 \cos(3\omega_o t)$  at several time-points  $t_1, t_2, \dots, t_S$ ; evaluating  $f(t) = \ddot{x} + \lambda^2 x + \mu x^3 - A_1 \cos(\omega_o t)$  at these time-points; and converting  $f(t)$  into the frequency domain using the discrete Fourier transform (DFT). In this example,  $f(t)$  is band-limited, so its Fourier coefficients can be calculated exactly. Only the coefficients of the first two harmonics of  $f$  are of interest, the remaining ones are

discarded. However, since there are 9 harmonics present, the Nyquist sampling theorem states that  $f$  must be evaluated at more than 18 time-points to determine the coefficients for the first two harmonics accurately. Originally, when it was decided to compute only two harmonics, it was assumed that the coefficients at the remaining harmonics are small. So for efficiency, when calculating the Fourier series of  $f$ , the remaining harmonics are assumed to be negligible, and  $f$  is evaluated at only enough points to calculate the coefficients of the first two harmonics. Since the remaining harmonics are not zero, they will alias down onto the two, resulting in further error.

### 3. Derivation

Recall that the statement of Kirchoff's current law for the distributed test problem (4.5) is

$$f(v, t) = i(v(t)) + \dot{q}(v(t)) + \int_{-\infty}^t y(t - \tau)v(\tau)d\tau + u(t) = 0$$

When applying harmonic balance to this problem, both  $v$  and  $f(v)$  are transformed into the frequency domain. Since  $v$  is almost periodic (by assumption), both  $i(v)$  and  $q(v)$  are almost periodic; therefore all three waveforms can be written in terms of their Fourier coefficients:  $\mathbb{F}v = V$ ,  $\mathbb{F}i(v) = \mathbb{F}i(\mathbb{F}^{-1}V) = I(V)$  and  $\mathbb{F}q(v) = \mathbb{F}q(\mathbb{F}^{-1}V) = Q(V)$ , where  $\mathbb{F}$  represents the Fourier transform operator. Since  $v$ ,  $i(v)$  and  $q(v)$  are vectors of waveforms — one waveform for each node in the circuit —  $V$ ,  $I(V)$  and  $Q(V)$  are vectors of spectra. The Fourier coefficients of the convolution integral are computed by exploiting its linearity. Assume  $y$  satisfies

$$\int_{-\infty}^{\infty} y(t)^T y(t) dt < \infty,$$

and  $y(t) = 0$  for all  $t < 0$ ; that is, assume  $y$  is causal and has finite energy (or equivalently, that the circuit with all nonlinear devices removed is causal and

asymptotically stable); then

$$\mathbb{F} \int_{-\infty}^t y(t - \tau)v(\tau)d\tau = YV$$

where

$$Y = [Y_{mn}] \quad m, n = 1, 2, \dots, N$$

$$Y_{mn} = [Y_{mn}(k, l)] \quad k, l \in \mathbb{Z}$$

where  $m, n$  are the node indices;  $k, l$  are the frequency indices, and

$$Y_{mn}(k, l) = \begin{cases} \begin{bmatrix} \operatorname{Re}\{Y_{mn}(j\omega_k)\} & \operatorname{Im}\{Y_{mn}(j\omega_k)\} \\ -\operatorname{Im}\{Y_{mn}(j\omega_k)\} & \operatorname{Re}\{Y_{mn}(j\omega_k)\} \end{bmatrix} & \text{if } k = l \\ \mathbf{0} & \text{if } k \neq l \end{cases}$$

where  $Y$  is the Laplace transform of  $y$  [desoer69] and  $j = \sqrt{-1}$ .

Now (4.5) can be rewritten in the frequency domain as

$$F(V) = I(V) + \Omega Q(V) + YV + U = \mathbf{0} \quad (7.5)$$

where  $U = \mathbb{F}u$  contains the Fourier coefficients for the source currents over all nodes and frequencies, and

$$\Omega = [\Omega_{mn}] \quad m, n = 1, 2, \dots, N$$

$$\Omega_{mn} = \begin{cases} [\Omega_{mn}(k, l)] & \text{if } m = n \\ \mathbf{0} & \text{if } m \neq n \end{cases}$$

$$\Omega_{mn}(k, l) = \begin{cases} \begin{bmatrix} 0 & \omega_k \\ -\omega_k & 0 \end{bmatrix} & \text{if } k = l \\ \mathbf{0} & \text{if } k \neq l \end{cases}$$

That  $\mathbb{F}\dot{q}(v) = \Omega Q(V)$  follows from the differentiation rule of the Fourier series. Equation (7.5) is simply the restatement of Kirchoff's current law in the frequency domain.

It is important to realize that the frequency-domain functions for the nonlinear devices ( $I$  and  $Q$ ) are evaluated by transforming the node voltage spectrum  $V$  into the time

domain, calculating the response waveforms  $i$  and  $q$ , and then transforming these waveforms back into the frequency domain. To assure that the nonlinear device response waveforms are almost periodic, we require that the nonlinear devices be algebraic. If not (that is, if the device has memory), then the response waveform has a transient component, is not almost periodic, and cannot be accurately transformed into the frequency domain. The restriction that nonlinear devices be algebraic clearly allows nonlinear resistors. Fortunately, it also allows nonlinear capacitors and inductors (actually, any lumped nonlinear component) because their constitutive relations are algebraic when written in terms of the proper variables;  $v$  and  $i$  for resistors,  $v$  and  $q$  for capacitors, and  $i$  and  $\phi$  for inductors [chua80]. The conversion between  $i$  and  $q$  ( $i = dq/dt$ ) and  $v$  and  $\phi$  ( $v = d\phi/dt$ ) is done in the frequency domain where it is an algebraic operation and does not disturb the steady-state nature of the solution. Nonlinear distributed devices, however, are not algebraic, and the trick of evaluating their response in the time domain and transforming it into the frequency domain cannot be used. Instead, it is necessary to remain in the frequency domain and model the nonlinear device using a Volterra series representation or develop an approximate lumped model for the device. Conventional transient analysis is also not able to handle nonlinear distributed devices, a mixed device / circuit simulator such as CODECS [mayaram88] or MEDUSA [engl82] is needed. Fortunately, the transmission lines used in high-frequency analog and microwave design are all linear, even those that are dispersive or lossy. We will not consider nonlinear distributed devices further.

#### 4. Harmonic Programming

It is possible to apply nonlinear programming techniques to solve (7.5). To do so use  $\varepsilon(V) = \frac{1}{2}F^T(V)F(V)$  as the cost function where  $\varepsilon(V) \in \mathbb{R}$ . An optimizer is used to find

the value of  $V$  that globally minimizes  $\epsilon(V)$ . If a  $\hat{V}$  is found such that  $\epsilon(\hat{V}) = 0$ , then  $\hat{V}$  satisfies (7.5).

Applying nonlinear programming to solve the harmonic balance equations is expensive because there is a very large number of unknowns to be found and because nonlinear programming techniques are expensive for large problems. If a circuit with 20 nodes is simulated at 8 harmonics, then 300 variables need to be optimized. If there are many nodes in the circuit that have only linear devices attached, then it is possible to shrink the number of variables to be optimized by considering the collection of all linear devices as a single multiterminal subcircuit. The nodes with no nonlinear devices attached become internal nodes to the subcircuit and so need not be considered as optimization variables. Figure 7.1 shows a convenient way of visualizing the analysis once the linear devices have been placed in a subcircuit. Here, the substitution theorem has been used to replace the nonlinear devices with sources. The resulting circuit is linear, however, the voltage spectra for the voltage sources that are used to replace the nonlinear devices are unknown. These spectra are generated by the optimization package. Nakhla and Vlach [nakhla76] have taken this idea one step further by considering the collection of nonlinear devices as a subcircuit as well. Neither of these two approaches help when MMIC's are simulated however because each node in a monolithic circuit tends to have linear devices as well as nonlinear resistors and capacitors tied to them.

Using an optimizer to solve the harmonic balance equations is inefficient. To do so requires that a difficult problem, that of solving  $F(V) = 0$  for  $V$ , is converted into an even harder problem, that of solving  $\frac{dF^T(V)F(V)}{dV} = 0$ . That information is lost in the conversion aggravates the situation. All information about each of the individual contributors to  $\epsilon$

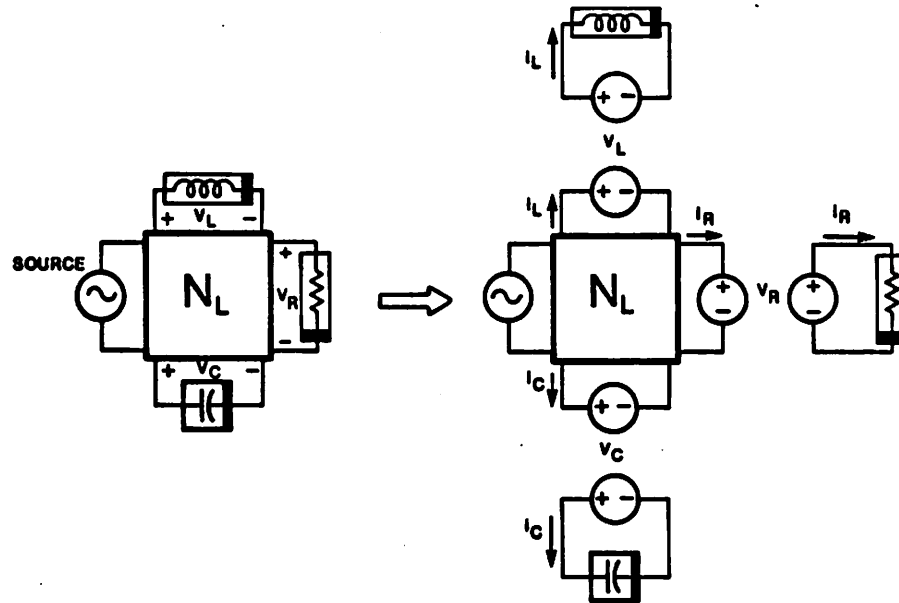


Figure 7.1 : Circuit interpretation of harmonic programming.

is lost when  $F^T(V)F(V)$  is formed to calculate  $\epsilon(V)$ . It is also difficult to exploit the structure of the harmonic balance / node admittance equations. For these reasons, the approaches presented later are preferred over harmonic programming.

The next section presents how to solve the harmonic balance equations with optimization techniques and the reasons why this is not the preferred approach. The situation where it is desired to do performance optimization while solving the harmonic balance equations is also discussed.

#### 4.1. Root Finding as a Nonlinear Least Squares Problem

To use optimization methods to solve (7.5), it is necessary to develop an appropriate cost function that has minima at the same values of  $V$  for which  $F$  has roots. The most com-

monly used cost function results from formulating the problem as a nonlinear least-squares problem,

$$\varepsilon(V) = \frac{1}{2}F^T(V)F(V). \quad (7.6)$$

This cost function has two important characteristics. First, each root of  $F$  corresponds to a global minimum of  $\varepsilon$ , and at these points,  $\varepsilon(V) = 0$ . Second, at each  $V$  that is a local minima of  $\varepsilon$  but is not a root of  $F$ , the Jacobian<sup>1</sup> of  $F$  (that is  $J_F(V) = dF(V)/dV$ ) is singular. We seek  $\hat{V}$ , a global minimizer of  $\varepsilon$ . A necessary condition for  $\hat{V}$  to be a minimizer of  $\varepsilon$  is that the gradient<sup>2</sup> of  $\varepsilon$  at  $\hat{V}$  be zero, i.e.,

$$\nabla\varepsilon(\hat{V}) = 0. \quad (7.7)$$

This problem can be solved by using a wealth of techniques such as steepest descent, conjugate gradient, and Newton's method. The steepest descent algorithm has the advantage of having a region of convergence that is usually much larger than the other methods, however it has only a linear rate of convergence and often converges so slowly as to be impractical. The conjugate gradient algorithm has a superlinear rate of convergence, but for large problems it usually requires a large number of iterations. Each iteration is inexpensive, and so this might be a suitable algorithm for solving the harmonic balance equations. Newton's method uses Newton-Raphson<sup>3</sup> to find the roots of (7.7). Thus with Newton's method we are again faced with using Newton-Raphson method to find the root of a nonlinear equation. However, solving (7.7) with Newton-Raphson is more difficult than solving (7.5) because the equation involves the first derivative of the original function

---

<sup>1</sup>A Jacobian is the first derivative of a vector-valued function with respect to its vector-valued argument.

<sup>2</sup>A gradient is the first derivative of a scalar-valued function with respect to its vector-valued argument.

<sup>3</sup>There can be considerable confusion when discussing optimization methods and root-finding methods simultaneously because both the root-finding method and the optimization method that results from applying Newton-Raphson to find the roots of the gradient are referred to as Newton's method. In this dissertation, the root-finding procedure is referred to as Newton-Raphson and the optimization method as Newton's method.

$F$ , so applying Newton-Raphson requires knowing the second derivatives of  $F$ . In fact, the Newton-Raphson iteration used to solve (7.7) is

$$\nabla^2 \epsilon(V^{(k)})[V^{(k+1)} - V^{(k)}] = -\nabla \epsilon(V^{(k)}), \quad (7.8)$$

where  $\nabla^2 \epsilon$  is the Hessian<sup>4</sup> of  $\epsilon$ .

From (7.6), it is easy to show that

$$\nabla \epsilon(V) = J_F^T(V)F(V) \quad (7.9)$$

and

$$\nabla^2 \epsilon(V) = \frac{dJ_F(F)}{dV}F(V) + J_F^T(V)J_F(V). \quad (7.10)$$

Clearly, the Hessian is denser than is the Jacobian and is therefore considerably more expensive to LU factor. Using (7.9) and (7.10), we can rewrite (7.8) as

$$\left[ \frac{dJ_F(V)}{dV}F(V) + J_F^T(V)J_F(V) \right] [V^{(k+1)} - V^{(k)}] = -J_F^T(V)F(V) \quad (7.11)$$

Traditionally, computing the Hessian is avoided by using quasi-Newton methods [gill81], which build up an approximation to the Hessian by starting with an identity matrix and performing rank-one updates computed from changes in the gradient at each step. Quasi-Newton methods require more iterations because they use an approximate Hessian, and so more gradient evaluations, but avoid computing the Hessian directly. This approach is interesting because it is possible to form the Cholesky<sup>5</sup> factors of the approximate Hessian and perform the rank-one updates on these factors directly. Thus each iteration is considerably less expensive than evaluating (7.11) directly, but a greater number of iterations are needed. If compared against solving (7.5) directly with Newton-Raphson, quasi-Newton

---

<sup>4</sup>A Hessian is the second derivative of a scalar-valued function with respect to its vector-valued argument.

<sup>5</sup>It is possible to write a symmetric positive-definite matrix (such as the Hessian) as a product or a lower triangular matrix and its transpose. These triangular matrices are the Cholesky factors of the original matrix [strang80]

methods are at a disadvantage because the Hessian is denser than the Jacobian and because the Hessian can become ill-conditioned when  $F(V)$  is small, as will be explained below.

It is possible to avoid computing the second derivative terms in the Hessian by exploiting the fact that we are solving for a root of  $F$ . When  $V$  is near the solution  $\hat{V}$ , then  $F(V)$  should be small, and so the second derivative term  $[dJ_F(V)/dV F(V)]$  in (7.11) can be dropped. Thus (7.11) becomes

$$J_F^T(V)J_F(V)[V^{(k+1)} - V^{(k)}] = -J_F^T(V)F(V), \quad (7.12)$$

which is referred to as the Gauss-Newton algorithm. Note that (7.12) is now in the form of the normal equation for a linear least-squares problem. This equation is ill-conditioned because the condition number of  $J_F^T(V)J_F(V)$  is the square of  $J_F(V)$ . Thus, finding the roots of  $F(V)$  using (7.12) is not only computationally more expensive (because  $J_F^T(V)J_F(V)$  is denser than  $J_F(V)$ ), but it is also possibly numerically unstable.

By assuming that  $J_F(V)$  is square and nonsingular, it is possible to cancel  $J_F^T(V)$  from both sides of (7.12), resulting in the following iteration,

$$J_F(V)[V^{(k+1)} - V^{(k)}] = -F(V). \quad (7.13)$$

This iteration is identical to that which results when Newton-Raphson is applied to (7.5). However, by assuming that  $J_F(V)$  is nonsingular, any possibility of finding a minimum of  $\epsilon$  that is not a root of  $F$  has been eliminated. (Recall that minima occur where either  $F$  is zero or where  $J_F$  is singular.) Thus, (7.13) is not an optimization method, but rather a root finding method. Indeed, (7.13) is identical to the Newton-Raphson iteration, and so it can have no hidden powers not shared by Newton-Raphson. In fact, the steps that lead up to (7.13) are just a rather round-about derivation of the harmonic Newton algorithm that is presented later.

The ill-conditioning demonstrated in Gauss-Newton is an inherent consequence of forming the cost function by squaring  $F$ . Any optimization algorithm that begins with (7.6) will suffer from greater numeric instability than results from simply finding the root of  $F$  using Newton-Raphson. In addition, most of the sparsity and the structure of the Jacobian is missing from the Hessian. Methods that use the Hessian must labor under this disadvantage. Optimization methods that do not use the Hessian, such as the conjugate gradient algorithm, require a much greater number of iterations, precisely because they do not use the Hessian. Since these iterations are relatively inexpensive, these methods may be useful for solving the harmonic balance equations, but this has yet to be shown.

## 4.2. Equation Solution with Performance Optimization

An interesting question remains; if it is necessary to both optimize circuit performance and solve the harmonic balance equations, should these two operations be combined into one optimization process? This idea was first suggested by Lipparini, et al [lipparini82]. They proposed to augment the cost function to be minimized with a contribution related to circuit performance, here denoted  $E$ . The list of design parameters is denoted  $p$ . The problem statement becomes

$$\min_{V, p} [F^T(V, p)F(V, p) + E^2(V, p)] \quad (7.14)$$

with the added constraint that  $E = 0$  when all specifications are met and  $E > 0$  otherwise.

This approach appears attractive because simple unconstrained optimization methods are used.

Unfortunately, a serious problem exists: (7.14) is not an appropriate statement of the problem. The correct problem statement is

$$\min_p E^2(V, p) \quad \text{subject to} \quad F(V, p) = 0 \quad (7.15)$$

By using (7.14), we allow the optimizer trade off satisfying Kirchoff's current law to improve circuit performance. The flaw, of course, is that if Kirchoff's current law is not satisfied, the solution calculated is not feasible and therefore the actual circuit performance is not being measured.

It is possible to solve (7.15) directly using a variety of methods, including the method of Lagrange multipliers, exact penalty function methods, and Lagrangian methods [bertsekas82] [luenberger84]. Lipparini's approach should not be used unless something is done to assure that Kirchoff's current law is satisfied. One possibility is to weight Kirchoff's current law so that it is given preference over the performance goals. This weight can be increased as necessary to assure that Kirchoff's current law is sufficiently satisfied. Such an approach is known as a penalty function approach, which is known to be inefficient when the penalty function (here the weighted Kirchoff's current law) is large.

Assuming something can be done to assure that Kirchoff's current law is satisfied, then there are several other important considerations. To treat (7.14) as a nonlinear least squares problem it is necessary to augment the list of equations with the performance cost function to be minimized and augment the list of variables with the optimizable parameters.

Let

$$X = \begin{bmatrix} V \\ p \end{bmatrix} \quad G(X) = \begin{bmatrix} F(X) \\ E(X) \end{bmatrix}. \quad (7.16)$$

The cost function to be minimized becomes

$$G^T(X)G(X). \quad (7.17)$$

Augmenting the lists of equations and variables presents several problems. First, the new equations in  $G$  create new rows and columns in the Jacobian  $J_G$  that do not have the same

structure as in  $J_F$ , making exploitation of the sparsity of the Jacobian more difficult. Second, there is usually more than one design parameter in  $p$ . Thus,  $J_G$  is not square. When applying Newton-Raphson to a system with more variables than equations, it is necessary to solve for the new iterate either by forming the normal equation, which effectively increases the number of equations until equal to the number of unknowns, or to solve the iteration equation with a method that is suitable for under-determined systems, such as QR factorization. The normal equation approach is written as

$$J_G^T(X^{(k)})J_G(X^{(k)})[X^{(k+1)} - X^{(k)}] = -J_G^T(X^{(k)})G(X^{(k)}) \quad (7.18)$$

As mentioned before, this equation is ill-conditioned and not nearly as sparse as when Newton-Raphson is applied directly to (7.5). QR factorization would be applied to

$$J_G(X^{(k)})[X^{(k+1)} - X^{(k)}] = -G(X^{(k)}). \quad (7.19)$$

However, it is not possible to exploit sparsity in any significant way using QR factorization, and so this approach is impractical for large  $J_G(X)$ .

## 5. Harmonic Relaxation

Relaxation methods are another approach that can be used to solve the algebraic set of equations that result from the application of harmonic balance. These methods are attractive when the nonlinear behavior of the circuit is very mild. Two different ways of applying relaxation methods are presented, the first uses a form of nonlinear relaxation called *splitting* that is similar to the approach taken by Gwarek or Kerr [gwarek74] [kerr75] [hicks82b] [faber80]. The second combines relaxation and Newton-Raphson; it has much better convergence properties than the first approach [kundert86b] [ushida87].

## 5.1. Splitting

Splitting is a relaxation technique that was originally developed to solve linear systems of equations and was generalized to handle nonlinear systems [ortega70]. As an introduction, consider the linear system

$$Ax = b \quad (7.20)$$

and consider the splitting of  $A$  into the sum

$$A = B - C$$

where  $B$  is nonsingular and the system  $Bx = d$  is easy to solve. Then a fixed-point iteration that can be applied to find the solution of (7.20) is

$$x^{(j+1)} = B^{-1}(Cx^{(j)} + b)$$

where the superscript on  $x$  is the iteration count. This iteration will converge if all the eigenvalues of  $B^{-1}C$  are smaller in magnitude than one.

The splitting method can be used with harmonic balance by rewriting equation (7.5) as

$$YV^{(j+1)} = -I(V^{(j)}) - \Omega Q(V^{(j)}) - U \quad (7.21)$$

$Y$  is assumed to be nonsingular, which implies that when all nonlinear devices are removed, there can be no floating nodes. Since linear devices are incapable of translating frequencies, the node admittance matrix for the linear portion of the circuit ( $Y$ ) is block diagonal (we are assuming here that the harmonic number is the major index and the node number is the minor index). Thus once the right-hand side of (7.21) has been evaluated, the task of finding  $V^{(j+1)}$  can be broken into solving  $K$  decoupled linear  $N \times N$  systems of equations, one for each harmonic.

To explore the convergence properties of the iteration defined by (7.21), the following well-known theorem [ortega70] [rudin76] [vidyasagar78] from classical analysis is needed.

**Theorem 7.1 (Contraction Mapping Theorem):** *Let  $C$  be a closed subset of  $\mathbb{C}^M$ . If  $f$  is a map from  $C$  into  $C$  and if there exists  $\gamma < 1$  such that*

$$\|f(x) - f(y)\| \leq \gamma \|x - y\|$$

*for all  $x, y \in C$ , then  $f$  is called a contraction map on  $C$ . Furthermore there exists a unique  $\hat{x}$  (called a fixed point of  $f$ ) such that  $f(\hat{x}) = \hat{x}$  and given any  $x^{(0)} \in C$ , the sequence  $\{x^{(j)}\}$  defined by  $x^{(j+1)} = f(x^{(j)})$  converges to  $\hat{x}$ .*

□

If  $C = \mathbb{C}^{KN}$ , then the theorem gives sufficient conditions for the global convergence of (7.21), however it is difficult to apply, so a theorem giving sufficient conditions for local convergence is presented. But first a lemma is needed.

**Lemma:** *Suppose  $f$  maps a convex open set  $E$  contained in  $\mathbb{C}^M$  into  $\mathbb{C}^M$ ,  $f$  is differentiable in  $E$ , and there is a real number  $c$  such that  $J_f(x)$ , the Jacobian of  $f$  at  $x$ , satisfies*

$$\|J_f(x)\| \leq c \quad \text{for every } x \in E$$

*Then  $\|f(x) - f(y)\| \leq c \|x - y\|$  for all  $x, y \in E$ .*

□

The lemma is a straight-forward extension of a theorem given by Rudin [rudin76] for  $\mathbb{R}^N$ .

**Theorem 7.2:** *Let  $E$  be an open subset of  $\mathbb{C}^M$ . Suppose  $f: E \rightarrow \mathbb{C}^M$  is continuously differentiable on  $E$  and can be written in the form*

$$f(x) = Ax - g(x)$$

where  $A \in \mathbb{C}^{M \times M}$  is nonsingular. If there exists  $\hat{x} \in E$  such that  $f(\hat{x}) = 0$  and if  $\|A^{-1}J_g(\hat{x})\| < 1$  then there exists some  $\delta > 0$  such that for all  $x^{(0)}$  in the closed ball  $B_\delta(\hat{x}) \subset E$  the sequence  $\{x^{(j)}\}$  defined by  $x^{j+1} = A^{-1}g(x^{(j)})$  converges to  $\hat{x}$ .

**Proof:** Define  $\phi(x) = A^{-1}g(x)$  and assume there exists some  $\gamma \in [0,1)$  such that  $\|A^{-1}J_g(\hat{x})\| < \gamma$ . Since  $f$ , and hence  $g$ , is continuously differentiable, there exists  $\delta > 0$  such that for all  $x \in B_\delta(\hat{x})$ ,  $\|A^{-1}J_g(x)\| \leq \gamma$ . Note that the derivative of  $\phi(x)$  is  $J_\phi(x) = A^{-1}J_g(x)$ . From the lemma,

$$\|\phi(x) - \phi(y)\| \leq \gamma \|x - y\| \quad (7.22)$$

for all  $x, y$  in the interior of  $B_\delta(\hat{x})$ , and since  $\phi$  is continuous, (7.22) must hold for all of  $B_\delta(\hat{x})$ , not just the interior. By the contraction mapping theorem,  $\phi$  has a unique fixed-point in  $B_\delta(\hat{x})$ , which must be  $\hat{x}$  because it is a fixed-point for  $\phi$ . Also,  $\{x^{(j)}\} \rightarrow \hat{x}$  if  $x^{(0)} \in B_\delta(\hat{x})$

□

If the conclusion of Theorem 7.2 is applied to (7.21), then to assure local convergence we need

$$\|Y^{-1}[J_I(\hat{V}) + j\Omega J_Q(\hat{V})]\| < 1 \quad (7.23)$$

where  $\hat{V}$  is the solution of (7.21). There is no reason to believe this condition will be met in practice. As an example of when it would not be met, consider a very simple circuit with only one node and analyzed at DC only. Then  $Y \in \mathbb{R}$  and  $I, Q : \mathbb{R} \rightarrow \mathbb{R}$ . Let  $Y = 1$ ,  $I(V) = 2V$ , and  $Q(V) = 0$ . Then  $Y^{-1}J_I = 2$  and so the convergence criterion is not satisfied. Indeed, for this circuit convergence will not be achieved for any  $V^{(0)} \neq \hat{V}$ . This example shows that relaxation using the splitting method given by (7.21) has poor convergence properties. In particular, even if the starting value of  $V^{(0)}$  is arbitrarily close to the

final solution, and regardless of how mild the nonlinearities are behaving, convergence is not assured. In fact, convergence can easily be lost if the largest conductance exhibited by any of the nonlinear devices is larger than the smallest conductance to ground present in the circuit when the nonlinear devices are removed.

## 5.2. Gauss-Jacobi Newton Harmonic Relaxation

The second relaxation approach to solving the algebraic harmonic balance equation (7.5) is to use the block Gauss-Jacobi method with a one step Newton-Raphson inner loop [ortega70]. [newton83] known as the block Gauss-Jacobi-Newton method. To apply this method, rewrite (7.5) as

$$F(V, k) = I(V, k) + jk\omega_o Q(V, k) + Y(k, k)V(k) + U(k) = 0 \quad (7.24)$$

where  $k$  is the frequency index and  $k = 0, 1, \dots, K-1$ . The block Gauss-Jacobi algorithm, when applied to (7.24), has the following form:

### *Nonlinear Block Gauss-Jacobi Algorithm*

```

repeat
{
    j ← j + 1;
    forall (k ∈ {0, 1, ..., K-1})
        solve F(V(j)(0), ..., V(j+1)(k), ..., V(j)(K-1), k) for V(j+1)(k)
} until (||V(j+1) - V(j)|| < ε)

```

The equation inside the forall loop is solved using Newton-Raphson for  $V^{(j+1)}(k)$ . Note that in this equation only  $V(k)$  is a variable,  $V(l)$   $l \neq k$  are constant and taken from the previous iteration. Since Newton-Raphson (with quadratic convergence) is being performed inside an outer relaxation loop (with linear convergence), it is not necessary to fully converge the Newton iteration. In fact, it is only necessary to take one step of the “inner” Newton iteration and doing so does not affect the asymptotic rate of convergence of the overall method [ortega70] [newton83].

Block Gauss-Jacobi-Newton is similar to the splitting method, except that each equation in (7.24) is first linearized with one step of Newton-Raphson rather than by just removing the nonlinearities. Applying the Gauss-Jacobi-Newton method to (7.24) results in

$$\frac{\partial F(V^{(j)}, k)}{\partial V(k)} \left[ V^{(j+1)}(k) - V^{(j)}(k) \right] = -F(V^{(j)}, k)$$

where  $k = 0, 1, \dots, K-1$  and

$$\frac{\partial F(V, k)}{\partial V(k)} = \frac{\partial I(V, k)}{\partial V(k)} + j\omega_k \frac{\partial Q(V, k)}{\partial V(k)} + Y(k, k)$$

To continue the derivation, it is necessary to select a set of time-points and then use the APFT (3.7) to develop a concrete representation  $\Gamma$  of the Fourier transform  $\mathbb{F}$ . Only the derivation of  $\frac{\partial I(V, k)}{\partial V(k)}$  is presented, the derivation of  $\frac{\partial Q(V, k)}{\partial V(k)}$  is identical.

$$I_m(V) = \Gamma i_m(v)$$

where  $m$  is the node index. Let  $\rho(k) \in \mathbb{C} \times \mathbb{R}^S$  be the two rows of  $\Gamma$  that compute the sine and cosine terms of the  $k^{\text{th}}$  harmonic of the Fourier series. That is

$$I_m(V, k) = \rho(k)^T i_m(v).$$

Differentiating both sides of  $I_m(k)$  with respect to  $V_n(k)$ ,

$$\frac{dI_m(V, k)}{dV_n(k)} = \rho(k)^T \frac{di_m(v)}{dV_n(k)}.$$

Employing the chain rule gives

$$\frac{dI_m(V, k)}{dV_n(k)} = \rho(k)^T \frac{di_m(v)}{dv_n} \frac{dv_n}{dV_n(k)}.$$

Since  $i(v)$  is algebraic,  $\frac{di_m(v)}{dv_n} = \left[ \frac{di_m(v(t_r))}{dv_n v(t_s)} \right]_{r,s \in \{1, 2, \dots, S\}} \in \mathbb{R}^{S \times S}$  is a diagonal

matrix. Let  $\gamma(k) \in \mathbb{R}^S \times \mathbb{C}$  be the two columns of  $\Gamma^{-1}$  that operate on the sine and cosine terms of the  $k^{\text{th}}$  harmonic of the Fourier series to compute their contribution to the

waveform. Then  $\Gamma^{-1}V_n = v_n$  implies  $\sum_{k=0}^{K-1} \gamma(k)V_n(k) = v_n$ . Thus,

$$\frac{dI(V, k)}{dV_n(k)} = \rho(k)^T \frac{di_m(v)}{dv_n} \gamma(k).$$

The block Gauss-Jacobi-Newton iteration is well-defined only if each of the equations in (7.24) has a unique solution at each step. In addition, convergence can be assured at least in the region local to the solution  $\hat{V}$ , if certain conditions are met by the Jacobian  $J_F(V)$  at the solution. In particular, if  $F$  is continuously differentiable on an open set  $E \subset \mathbb{C}^{KN}$  containing  $\hat{V}$ , and if  $J_F(V) = D(V) + R(V)$  where  $D$  is a nonsingular block diagonal matrix with  $D(V, k, k) = \frac{\partial F(V, k)}{\partial V(k)}$ , then from Theorem 7.2, there exists a closed ball  $B_\delta(\hat{V}) \subset E$  such that for all  $V^{(0)} \in B_\delta(\hat{V})$  the block Gauss-Jacobi iteration is well defined and will converge to  $\hat{V}$  if  $\|D^{-1}(\hat{V})R(\hat{V})\| < 1$ . Notice that  $D(V, k, k)$  is the Jacobian of the circuit at the  $k^{\text{th}}$  harmonic. In other words, it is the node admittance matrix of the circuit at the  $k^{\text{th}}$  harmonic where the circuit has been linearized about the solution.  $R$  represents coupling between signals at different harmonics that results from nonlinearities in the circuit. If the circuit is linear then  $R = 0$  and convergence is assured. The more strongly nonlinear the circuit behaves, the more coupling exists between different harmonics and the larger the terms in  $R$  become. Thus, convergence becomes less likely. So block Gauss-Jacobi-Newton is guaranteed to converge if  $F(V)$  is "sufficiently linear" and if  $V^{(0)}$  is sufficiently close to the solution  $\hat{V}$ .

This method can be generalized by allowing the block bandwidth of  $D$  to be increased. Doing so is the basis of the harmonic relaxation-Newton method presented in Chapter 8.

To illustrate how the two relaxation methods work, consider the network shown in Figure 7.2a. In the splitting method, on each iteration the voltages on the nonlinear devices are fixed at the values of the previous iteration, which fixes the current passed by these devices. So in Equation (7.21) the nonlinear currents are moved to the right-hand side with the constants, and in Figure 7.2 they are replaced with current sources, using the substitution theorem. This “linearizes” the circuit, so the node voltages can be found with Gaussian elimination. These new node voltages are then applied to the nonlinear devices, and their new current is calculated and applied to the linearized circuit, requiring it to be re-evaluated on the next iteration. The linearized circuit never changes, so only forward and backward substitution is needed for reevaluation.

With block Gauss-Jacobi-Newton the circuit is linearized by dividing the nonlinear devices into two parts. One is the best linear approximation to the nonlinear device considering the signal present on the device. The other is the nonlinear residual that when combined with the linear part gives the original nonlinear device. This division is illustrated in Figure 7.3.

By viewing Figures 7.2 and 7.3, it becomes clear why Gauss-Jacobi-Newton has better convergence properties than the splitting method; it has a better model of the nonlinear device in the linear subcircuit, so less correction is needed on each iteration. Indeed, if the nonlinear devices behave linearly, then clearly Gauss-Jacobi-Newton converges in one step while the splitting will require many, and may not even converge.

The Gauss-Jacobi-Newton method has the nice feature that it uses very little memory. The circuit is analyzed at only one frequency at a time, so space is needed for only one sparse  $N \times N$  node admittance matrix and that space is reused for each frequency. (This

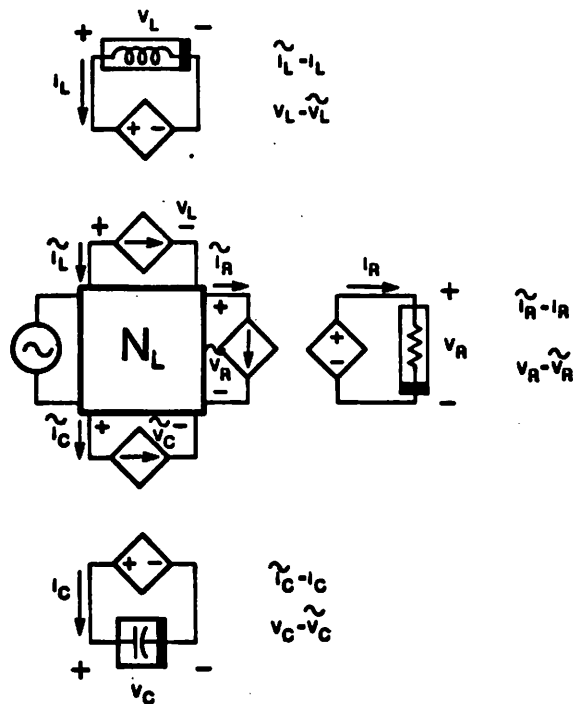


**Figure 7.2 :** Circuit interpretation of the splitting method form of harmonic relaxation.

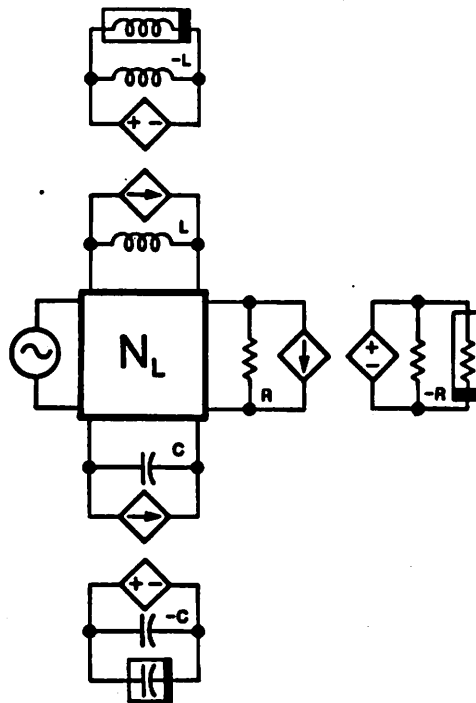


**Figure 7.3 :** Circuit interpretation of the block Gauss-Jacobi-Newton form of harmonic relaxation.

contrasts with the harmonic Newton method presented next. It analyzes the circuit at all frequencies simultaneously, and so it needs a great deal more memory.) The Gauss-Jacobi-Newton method is also quite fast if the circuit is behaving linearly. However it does have severe convergence problems when circuits behave nonlinearly. Harmonic Newton, which can be seen as a logical extension of Gauss-Jacobi-Newton, is much more robust, but also can require much more time on near linear circuits. For this reason, the harmonic relaxation-Newton method, as presented later, modifies harmonic Newton on near linear problems to become much more like Gauss-Jacobi-Newton, resulting in a composite method that can be both fast and robust.

## 6. Harmonic Newton

As shown earlier, the circuit equation

$$f(v, t) = i(v(t)) + \dot{q}(v(t)) + \int_{-\infty}^t y(t-\tau)v(\tau)d\tau + u(t) = 0 \quad (7.25)$$

can be written in the frequency domain as

$$F(V) = I(V) + \Omega Q(V) + YV + U = 0. \quad (7.26)$$

One approach to evaluating the nonlinear devices in (7.26) is to convert the node voltage spectrum  $V$  into the waveform  $v$  and evaluate the nonlinear devices in the time domain. The response is then converted back into the frequency domain. Assume that the number of frequencies has been truncated to  $K$ ;  $v, u \in AP^N(\Lambda_K; \mathbb{R})$ ; and that a set of time-points  $\{t_0, t_1, \dots, t_{2K-1}\}$  has been chosen so that  $\Gamma^{-1}$  is nonsingular. Then  $V_n = \Gamma v_n$ ,  $I_n(V) = \Gamma i_n(v)$  and  $Q_n(V) = \Gamma q_n(v)$ .

Applying Newton-Raphson to solve (7.26) results in the iteration

$$J_F(V^{(j)})(V^{(j+1)} - V^{(j)}) = -F(V^{(j)}) \quad (7.27)$$

where

$$J_F(V) = \frac{\partial F(V)}{\partial V} = \frac{\partial I(V)}{\partial V} + \Omega \frac{\partial Q(V)}{\partial V} + Y.$$

Or

$$J_F(V) = \left[ J_{F, mn}(V) \right] = \left[ \frac{\partial F_m(V)}{\partial V_n} \right] \quad m, n \in \{1, 2, \dots, N\}$$

where

$$\frac{\partial F_m(V)}{\partial V_n} = \frac{\partial I_m(V)}{\partial V_n} + \Omega_{mn} \frac{\partial Q_m(V)}{\partial V_n} + Y_{mn}.$$

$J_F(V)$  is referred to as the harmonic Jacobian. The matrix  $\partial F_m / \partial V_n$ , known as a *conversion matrix*, is the derivative of the function at node  $m$  with respect to the Fourier

coefficients of the voltage at node  $n$ . The derivation of  $\partial I_m / \partial V_n$  follows with help from the chain rule.

$$I_m(V) = \Gamma i_m(v)$$

$$\frac{\partial I_m(V)}{\partial V_n} = \Gamma \frac{\partial i_m(v)}{\partial v_n} \frac{\partial v_n}{\partial V_n}$$

Since  $i(v)$  is algebraic,  $\partial i_m / \partial v_n$  is a diagonal matrix. Using the fact that  $\Gamma^{-1} V_n = v_n$ ,

$$\frac{\partial I_m(V)}{\partial V_n} = \Gamma \frac{\partial i_m(v)}{\partial v_n} \Gamma^{-1}$$

The derivation of  $\partial Q_m / \partial V_n$  is identical. Now everything needed to evaluate (7.27) is available. If the sequence generated by (7.27) converges, its limit point is the desired solution to (7.26).

The most computationally expensive part of harmonic Newton is the factorization of  $J_F$ , a  $(N \times 2K)$  by  $(N \times 2K)$  sparse matrix. Samanskii's method [ortega70] can be employed to reduce the computation time required by the harmonic Newton algorithm. In this approach the factored Jacobian from the previous iteration is simply reused for several iterations. This algorithm was presented in Chapter 4.

Harmonic Newton, as with any Newton-Raphson-based method, is only guaranteed to converge if the initial guess is close enough to the solution. Thus, finding a good initial guess is a key issue in determining the likelihood of convergence. For many circuits, a good initial guess is generated by linearizing the circuit about the DC operating point, applying the stimulus, and performing a phasor (AC) analysis at each frequency in  $\Lambda_K$ . If the initial guess generated in this manner does not result in convergence, it is necessary to use a variant of Newton-Raphson that is more robust. Currently, the algorithm that appears to be best suited in this situation is arc-length continuation as presented in Chapter

4.

## 7. Error Estimation

There are three dominant sources of error with harmonic balance. The first results from incompletely converging the iteration used to solve the nonlinear harmonic balance equations. Recall that harmonic balance was formulated very simply in (7.5) as

$$F(V) = I(V) + \Omega Q(V) + YV + U = 0. \quad (7.28)$$

Newton-Raphson uses the iteration

$$J_F(V^{(k)})[V^{(k+1)} - V^{(k)}] = -F(V^{(k)}). \quad (7.29)$$

to solve the harmonic balance equation. Roughly, the iteration stops when

$$\|F(V^{(k)})\| < \varepsilon_F \quad (7.30)$$

where  $\varepsilon_F$  is some small positive number. To see how this convergence criteria affects the error in the solution, assume that the true solution is  $\hat{V}$  and that  $\|F(V^{(k)})\| \leq \varepsilon_F$ . By expanding  $F$  about  $V^{(k)}$ , it is easy to show that to first order,

$$J_F(V^{(k)})[\hat{V} - V^{(k)}] \approx -F(V^{(k)}). \quad (7.31)$$

Thus the quantity  $\Delta V^{(k)} = -J_F^{-1}(V^{(k)})F(V^{(k)})$  is a first order estimate to the error in the solution. Notice that this quantity has been previously computed in (7.29). Thus, at very little added cost, the following additional convergence criteria can be added to directly control the error in the solution

$$\|\Delta V^{(k)}\| < \varepsilon_V \quad (7.32)$$

It is best to use both (7.30) and (7.32) as convergence criteria for Newton-Raphson because if only (7.30) is used it is possible to have (7.28) nearly satisfied but still have a large error in the solution (this would occur if  $J_F$  was ill-conditioned). If only (7.32) is used, it is possible to terminate the iteration prematurely when (7.28) is far from being

satisfied because progress toward the solution on one step is slow (and therefore  $\Delta V$  is small).

The second form of error in harmonic balance results from limiting the number of frequencies in the Fourier series that represents the solution. This error has been explored by Huang [huang]. It is difficult to estimate, and so will not be discussed further here.

The last form of error with harmonic balance results from using a finite number of frequencies in the Fourier series representing  $F(V)$ . The error can be split conceptually into two parts, truncation error and aliasing. Consider a circuit whose exact solution is almost periodic over the set of frequencies  $\Lambda$  and consider finding an approximate solution by applying harmonic balance on the truncated set of frequencies  $\Lambda_K \subset \Lambda$ . Thus, given any  $V \in \mathbb{C}^{NK}$ , let  $F : \mathbb{C}^{NK} \rightarrow \mathbb{C}^{NK}$  be the sum of the currents at every node and at  $K$  frequencies as in (7.28). For the purposes of the error analysis, several variants of  $F$  are defined to be the sum of the currents at every node and every frequency. Let  $F_{full} : \mathbb{C}^{N\infty} \rightarrow \mathbb{C}^{N\infty}$  be the result when the circuit equations are evaluated without error at all frequencies in  $\Lambda$ . Let  $F_{trunc} : \mathbb{C}^{N\infty} \rightarrow \mathbb{C}^{N\infty}$  be defined as

$$F_{trunc}(V, k) = \begin{cases} 0 & \text{if } \omega_k \in \Lambda_K \\ F_{full}(V, k) & \text{otherwise.} \end{cases}$$

Thus,  $F_{trunc}$  represents all currents generated by the circuit at frequencies other than those in  $\Lambda_K$ . These currents are not explicitly handled by discrete Fourier transforms (any discrete Fourier transform, including the DFT and APFT) and so these currents are mistaken for currents at frequencies in  $\Lambda_K$ . These error currents, referred to as aliasing, are represented by  $F_{alias} : \mathbb{C}^{N\infty} \rightarrow \mathbb{C}^{N\infty}$ . Finally, let  $F_{approx} : \mathbb{C}^{N\infty} \rightarrow \mathbb{C}^{N\infty}$  be defined as

$$F_{approx}(V, k) = \begin{cases} F(V, k) & \text{if } \omega_k \in \Lambda_K \\ 0 & \text{otherwise.} \end{cases}$$

These four quantities are related by

$$F_{full} = F_{approx} - F_{alias} + F_{trunc}$$

To estimate the effect of truncation and aliasing errors, let  $\hat{V} \in \mathbb{C}^{N_\infty}$  be the exact solution and  $\tilde{V} \in \mathbb{C}^{N_\infty}$  be the solution in the presence of truncation and aliasing errors.

Expand

$$F_{full}(\hat{V}) = 0$$

about the solution to compute  $\Delta V$ , the estimated difference between these two solutions.

$$\begin{aligned} F_{full}(\hat{V}) + \frac{\partial F_{full}(\hat{V})}{\partial V} \Delta V &\approx F_{approx}(\tilde{V}) - F_{trunc}(\hat{V}) + F_{alias}(\hat{V}) \\ 0 + \frac{\partial F_{full}(\hat{V})}{\partial V} \Delta V &\approx 0 - F_{trunc}(\hat{V}) + F_{alias}(\hat{V}) \\ \frac{\partial F_{full}(\hat{V})}{\partial V} \Delta V &\approx F_{alias}(\hat{V}) - F_{trunc}(\hat{V}) \end{aligned}$$

This equation gives an estimate of the error in the solution, but in terms of quantities that are unknown. Assuming  $\Delta V$  is small,  $F_{trunc}(\hat{V})$  and  $F_{alias}(\hat{V})$  are approximated with  $F_{trunc}(\tilde{V})$  and  $F_{alias}(\tilde{V})$ , which will be estimated below. With harmonic Newton,  $\partial F_{full}(\hat{V})/\partial V$  could be approximated by  $J_F(\tilde{V})$ , but since  $J_F(\tilde{V}) \in \mathbb{C}^{NK \times NK}$ , the effect of  $F_{trunc}$  would be lost. This is not a serious problem because  $\|F_{alias}\|$  is generally as large or larger than  $\|F_{trunc}\|$ . Better approximations to  $\partial F_{full}(\hat{V})/\partial V$  can be easily constructed by either treating the circuit as linear at frequencies not in  $\Lambda_K$ , or by exploiting the Toeplitz/Hankel structure of the conversion matrices to extend them to frequencies outside of  $\Lambda_K$ .

One simple approach to estimating the error due to truncation and aliasing is to simply increase the number of frequencies used in the Fourier series representation of  $F(V)$ .

For example, using the same solution, reevaluate all of the nonlinear devices at, say,  $2S$  rather than the normal  $S$  samples, and compute the Fourier series of the resulting waveforms. One note of caution, when using this approach with the APFT, one must be very careful when choosing the new larger set of sample times to assure that error due to aliasing is actually reduced.

It is possible to effectively double the number of frequencies in the Fourier series of the response of a nonlinear device without reevaluating the device at further time-points. Instead, use the previously computed response waveform at the original  $S$  samples and make some further calculations to compute the time derivative of the waveforms at these samples. By using the slope of the waveform at each sample along with the value, twice as much information is available, and so the Fourier series can be computed with twice as many terms. For example, consider a nonlinear resistor with current  $i = i(v(t))$  and conductance  $di(v(t))/dv(t) = g(v(t))$ . The voltage waveform  $v$  is given at  $S$  distinct time-points, and the response waveform is computed by simply evaluating the resistor current equation at these points. The time derivative is computed using the chain rule

$$\frac{di(v(t))}{dt} = \frac{di(v(t))}{dv(t)} \frac{dv(t)}{dt}$$

$$\dot{i}(v(t)) = g(v(t))\dot{v}(t)$$

The conductance  $g$  is available because it was needed for the Newton-Raphson iteration and  $\dot{v}(t)$  is easily computed by transforming  $\Omega V$  into the time domain. With the current (or charge) and its time derivative known at each of the  $S$  sample points, the Fourier series is computed using the ordinate and slope discrete Fourier transform [bracewell78].

The method of estimating the error given above is an inexpensive way of determining whether enough frequencies have been included in the harmonic balance analysis after a

solution has been computed. Huang has developed an apriori estimate of the number of frequencies needed to achieve a prespecified accuracy [huang].

## 8. Oscillators

Recall that oscillators present two problems not found with forced circuits. The period of the oscillation is unknown and must be determined, and the time origin is arbitrary and thus if one solution exists, then an infinite continuum of solutions exists. In other words, if  $v$  is a solution, then so is any time shifted version of  $v$ . The problem is that Newton-Raphson fails if the solution is not isolated. It is necessary to modify either Newton-Raphson to handle nonisolated solutions or the problem formulation to eliminate the non-isolated solutions.

Harmonic balance is modified to handle oscillators by adding the fundamental frequency  $\omega$  to the list of unknowns and an equation to enforce the constraint that solutions be isolated from one another. Perhaps the easiest way to ensure isolated solutions is to chose some signal in the circuit and insist that the imaginary part of its fundamental is zero. This fixes the solution to within a sign change. For this approach to work it is necessary that the fundamental of the signal chosen have nonzero magnitude.

The harmonic balance equations modified for the oscillator problem are

$$F(V, \omega) = I(V) + j\Omega(\omega)Q(V) + Y(\omega)V + U = 0 \quad (7.33)$$

$$\text{Im}\{V_m(1)\} = 0$$

Newton's method is now applied to these two equations,

$$\begin{bmatrix} J_F(V^{(j)}, \omega^{(j)}) & \frac{\partial F(V^{(j)}, \omega^{(j)})}{\partial \omega} \\ e_m(1)^T & 0 \end{bmatrix} \begin{bmatrix} \Delta V^{(j+1)} \\ \Delta \omega^{(j+1)} \end{bmatrix} = - \begin{bmatrix} F(V^{(j)}, \omega^{(j)}) \\ \text{Im}\{V_m(1)\} \end{bmatrix} \quad (7.34)$$

where

$$\frac{\partial F(v, \omega)}{\partial \omega} = \frac{j}{\omega} \Omega(\omega) Q(V) + \frac{\partial Y(\omega)}{\partial \omega} V$$

and  $e_m(1)$  is the unit vector that selects the imaginary part of the first harmonic of the chosen node voltage.

The most difficult part of applying harmonic balance to the oscillator problem is determining a good initial guess for both  $V$  and  $\omega$ . A good initial guess is required not only for the standard reason of assuring convergence, but also to avoid the valid but undesirable solution where all but the DC terms in  $V$  are zero.

# Chapter 8

## Harmonic Balance: Implementation

---

This chapter describes practical algorithms for implementing harmonic balance. Most of these algorithms have been implemented and tested in *Spectre*, a simulation program suitable for analog and microwave circuits. There are two fundamental ideas presented in this chapter. The first is that it is possible to use the DFT with harmonic balance, even when the signals present are not periodic. The benefit of the DFT is the very regular manner in which aliasing occurs, which can be exploited to accelerate the construction and factorization of the conversion matrices. The first portion of this chapter is dedicated to explaining how the DFT can be used in quasiperiodic harmonic balance, and rederiving harmonic Newton with the DFT.

The second idea is that ignoring terms in the Jacobian converts harmonic Newton into a relaxation process. Indeed, the new method that results if any contribution to the harmonic Jacobian due to nonlinear behavior is ignored is identical to harmonic relaxation based on splitting of (7.21). If instead, the off diagonal entries in each conversion matrix were set to zero, the resulting method would be Gauss-Jacobi Newton harmonic relaxation. A new method, referred to as harmonic relaxation-Newton, is developed by ignoring terms in the Jacobian that are sufficiently small. This algorithm can be viewed as either the harmonic Newton algorithm with an approximate Jacobian or as a hybrid of the Gauss-Jacobi Newton harmonic relaxation and harmonic Newton algorithms.

## 1. Accelerating Harmonic Balance

Of the time spent performing harmonic Newton, most is spent constructing and factoring the Jacobian  $J_F(V)$ . Forming  $\Gamma \frac{\partial i_m(v)}{\partial v_n} \Gamma^{-1}$  requires  $O(K^3)$  operations because of the matrix multiplies. There is one such product to form for each of the nonlinear conductors and capacitors. As the number of nonlinear components is typically  $O(N)$ , forming the Jacobian requires  $O(NK^3)$  operations. The computational complexity of LU factoring the block Jacobian matrix is  $O(N^\alpha K^3)$ , where typically  $1.1 < \alpha < 1.5$ .<sup>1</sup> Clearly reducing the computation in both forming and factoring the Jacobian are important to improving the efficiency of harmonic Newton.

The algebraic nature of the nonlinearities can be exploited to reduce the time required to form the Jacobian. Algebraic nonlinearities allow the use of the DFT (or FFT) in lieu of the APFT. This gives three benefits, the actual transform itself is faster (assuming the FFT is used), the construction of the conversion matrices is accelerated because it becomes possible to use an algorithm that requires  $O(K^2)$  operations rather than  $O(K^3)$ , and the factorization of the conversion matrices can be accelerated by techniques given later that increase its sparsity. It is worth noting that in general, only a small fraction of the time required by the harmonic balance algorithm is spent executing the Fourier transform, even when the DFT is used. The benefit of using the FFT is minor (over the DFT or APFT) in comparison to the benefit of using the FFT or DFT (over the APFT) when constructing and factoring the conversion matrices. As an interesting aside, it may be more efficient to use the DFT than the FFT. The reason being that with the FFT the number of frequencies is constrained,

---

<sup>1</sup>This is an approximation. The true operation count for a sparse LU factorization, ignoring the cost of factoring the blocks, is  $c_3 N^3 + c_2 N^2 + c_1 N$ , where  $c_1$ ,  $c_2$ , and  $c_3$  are functions of the sparsity pattern of the matrix. Generally for the sizes and densities found in circuit matrices, the  $c_2$  and  $c_3$  terms are small enough so that the  $N^2$  and  $N^3$  terms are noticeable but do not dominate.

usually to be a power of two and the DFT allows an arbitrary number of frequencies. In general, the number of frequencies needed with the FFT is at least as great as with the DFT. While the extra frequencies can be discarded, the FFT will require the nonlinear devices to be evaluated at a greater number of time-points.

The time required to factor the conversion matrices can be considerably reduced by reducing the density of the conversion matrices by using a hybrid of the harmonic Newton and harmonic relaxation methods. Harmonic Newton can be converted to Gauss-Jacobi-Newton harmonic relaxation by simply setting all off-diagonal terms in the conversion matrices to zero. In the hybrid method, which is referred to as harmonic relaxation-Newton, the bandwidth of selected conversion matrices is reduced. In one limit (when operating on a linear circuit), the bandwidth of all conversion matrices is reduced until they are diagonal, so the method becomes equivalent to the harmonic Gauss-Jacobi-Newton relaxation. In the other limit (when each device in the circuit is behaving very non-linearly), the bandwidth of all conversion matrices is expanded until the whole matrix is included, and the method becomes equivalent to harmonic Newton. The bandwidth of the conversion matrices is chosen to be as small as possible without sacrificing convergence. The bandwidth of each conversion matrix on each iteration can be set independently to achieve this goal. In this way, the method adapts to the problem being solved. The method can be modeled as either a relaxation method or a the Newton-Raphson method with an approximate Jacobian.

### **1.1. Transforms for Quasiperiodic Harmonic Balance**

There are currently five different methods available for transforming signals between time and frequency domains that are suitable for use with harmonic balance. The first three of

these methods are general in nature. Two methods, those of Ushida and Chua [ushida84] and Gilmore and Rosenbaum [gilmore84], were outlined in Chapter 1. They are considered less efficient than the remaining methods and are no longer used. The third method, the APFT, was presented in Chapter 3. This transform has a simple operator notation and so is useful for theoretical manipulation. It is less efficient than the remaining two methods.

The last two methods exploit the fact that in harmonic balance one desires the frequency domain response of a nonlinear device to a frequency domain stimulus and the time-domain waveforms generated along the way are of no interest. These methods transform spectra into waveforms with a distorted time axis. However, they also convert the waveforms with a distorted time axis back into the spectra, and so as long as the nonlinearities being evaluated in the time domain are algebraic, which was a basic assumption with harmonic balance, then the resulting spectra are correct. Of these two remaining methods, the first is based on the multidimensional DFT [bava82, ushida87] and is restricted to the box truncation. The second is based on the one dimensional DFT. It is faster and has fewer restrictions than the multidimensional DFT approach, and is the one presented here.

## 1.2. Harmonic Balance and the Discrete Fourier Transform

There is a trick that allows the use of the DFT — and hence the FFT — with harmonic balance even when the desired solution is quasiperiodic. To use the trick, two conditions must be satisfied.

1. The signals must be quasiperiodic. This is not a limitation for two reasons. First, circuits of practical interest are excited using a finite number of periodic input signals

and so their response is quasiperiodic. Second, any almost-periodic signal when truncated to a finite number of frequencies is quasiperiodic.

2. The time-domain signal must be of no interest. This is true in harmonic balance where going into the time domain is an expedient but not essential way to compute the frequency-domain response of the nonlinear devices to a frequency-domain stimulus.

The trick is best explained with an example. Consider a nonlinear resistor with the constitutive equation

$$i(v) = v^2.$$

Assume that this resistor is being driven with the voltage waveform

$$v(t) = \cos(\alpha t) + \cos(\beta t).$$

The resistor responds with a current waveform of

$$i(v(t)) = 1 + \frac{1}{2}\cos(2\alpha t) + \cos(\alpha t - \beta t) + \cos(\alpha t + \beta t) + \frac{1}{2}\cos(2\beta t).$$

Notice that the coefficients of the cosines (i.e., the spectrum of the response signal) are independent of the frequencies  $\alpha$  and  $\beta$ . This is true, whenever the nonlinearities are algebraic. Thus, for the purposes of evaluating the nonlinear devices, the actual fundamental frequencies are of no importance and can be chosen freely. In particular, the fundamentals can be chosen to be multiples of some arbitrary frequency so that the resulting signals will be periodic. Once the fundamentals are chosen in this manner, the DFT can be used. It is important to realize that these artificially chosen fundamental frequencies are not actually used in the harmonic balance calculations, such as in  $Y$  or  $\Omega$ . Rather, they are used when determining in which order to place the terms in the spectra so that the DFT can be used when evaluating the nonlinear devices.

### 1.2.1. Choosing the Artificial Frequencies

For simplicity, the way in which the artificial frequencies are chosen is illustrated by examples. The actual artificial frequencies, and the scale factors that convert the original fundamental to the artificial frequencies, are of no interest except in determining the correspondence between the quasiperiodic and periodic harmonic indices.

Consider the following set of frequencies.

$$\Lambda_K = \{ \omega \mid \omega = k_1 \lambda_1 + k_2 \lambda_2; 0 \leq k_1 \leq H_1, |k_2| \leq H_2, k_1 \neq 0 \text{ if } k_2 < 0 \}$$

Let  $\alpha_1 = 1$  and  $\alpha_2 = \lambda_1 / [\lambda_2(2H_2 + 1)]$  be the scaling factors of the two fundamentals.

Then the resulting scaled set of frequencies is equally spaced and no two frequencies overlap. This scaling, which is ideal for box truncations, is illustrated in Figure 8.1. The correspondence between original frequencies and artificial frequencies is given by

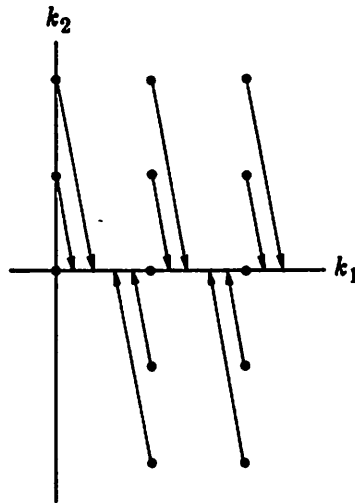


**Figure 8.1** : The mapping of quasiperiodic frequencies into periodic frequencies for box truncations.

---

$$k\lambda_0 = k_1\alpha_1\lambda_1 + k_2\alpha_2\lambda_2 \quad (8.1)$$

where

$$\lambda_0 = \frac{\lambda_1}{2H_2 + 1}$$

and

$$k = (2H_2 + 1)k_1 + k_2$$

Consider another set of frequencies.

$$\Lambda_K = \{\omega \mid \omega = k_1\lambda_1 + k_2\lambda_2; |k_1| + |k_2| \leq H, k_1 + k_2 \geq 0, k_1 \neq k_2 \text{ if } k_2 > 0\}$$

Let  $\alpha_1 = 1$  and  $\alpha_2 = (\lambda_1 + H_2)/[\lambda_2(2H_2 + 1)]$  be the scaling factors of the two fundamentals. Then the resulting scaled set of frequencies is equally spaced and no two frequencies overlap. This scaling, which is ideal for diamond truncations, is illustrated in Figure 8.2.

The correspondence between original frequencies and artificial frequencies is given by

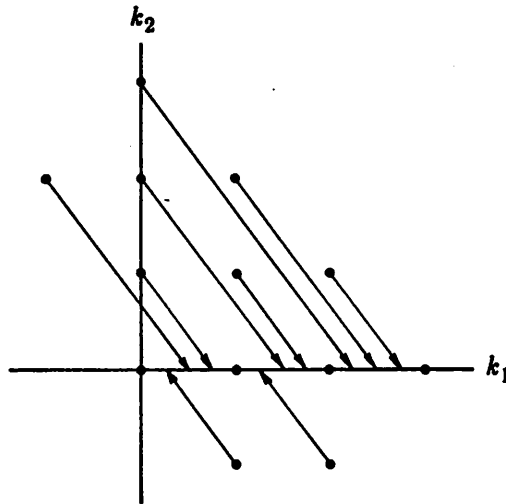


**Figure 8.2 :** The mapping of quasiperiodic frequencies into periodic frequencies for diamond truncations.

---

$$k\lambda_0 = k_1\alpha_1\lambda_1 + k_2\alpha_2\lambda_2 \quad (8.2)$$

where

$$\lambda_0 = \frac{\lambda_1}{H_2 + 1}$$

and

$$k = (H_2 + 1)k_1 + H_2k_2$$

Both approaches can be extended to the case where more than two fundamentals are applied. And while these two methods are ideal for their respective truncations, other truncations can be used, however the resulting set of frequencies may not be densely packed.

## 2. Harmonic Newton

The harmonic Newton algorithm is now rederived using the DFT rather than the APFT. It is assumed that, for the purposes of evaluating the nonlinear devices, the fundamentals have been shifted to make the signals processed by the DFT periodic.

There are two common DFT pairs that can be used in this derivation. Up to this point, the trigonometric or single-sided DFT has been used. This pair is given by

$$x_n(s) = X_n(0) + \sum_{k=1}^{K-1} \begin{bmatrix} \cos(2\pi ks/S) & \sin(2\pi ks/S) \end{bmatrix} \begin{bmatrix} X_n^C(k) \\ X_n^S(k) \end{bmatrix} \quad (8.3)$$

$$X_n(k) = \begin{bmatrix} X_n^C(k) \\ X_n^S(k) \end{bmatrix} = \frac{2 - \delta(k)}{S} \sum_{s=0}^{S-1} \begin{bmatrix} \cos(2\pi ks/S) \\ \sin(2\pi ks/S) \end{bmatrix} x_n(s) \quad (8.4)$$

where  $s$  is the time index,  $S = 2K - 1$ , and  $\delta$  is the Kronecker delta function, which is defined as

$$\delta(k) = \begin{cases} 1 & \text{if } k = 0 \\ 0 & \text{if } k \neq 0 \end{cases}$$

The second common DFT pair is the exponential or double-sided DFT.

$$x_n(s) = \sum_{k=1-K}^{K-1} X_n(k) e^{j2\pi ks/S} \quad (8.5)$$

$$X_n(k) = \frac{1}{S} \sum_{s=0}^{S-1} x_n(s) e^{-j2\pi ks/S} \quad (8.6)$$

where  $X_n(k) = X_n^R(k) + jX_n^I(k)$ . The single- and double-sided coefficients are related by

$$X_n^C(k) = \begin{cases} X_n^R(k) & \text{if } k = 0 \\ 2X_n^R(k) & \text{if } k \neq 0 \end{cases} \quad X_n^S(k) = \begin{cases} -X_n^I(k) & \text{if } k = 0 \\ -2X_n^I(k) & \text{if } k \neq 0 \end{cases}$$

where  $X_n^S(0) = X_n^I(0) = 0$  and the  $C$ ,  $S$ ,  $R$ , and  $I$  superscripts are used to denote the cosine, sine, real, and imaginary coefficients.

In order to simplify the notation used in the following derivation, the trigonometric DFT pair is used with the exponential coefficients. The resulting DFT pair is

$$x_n(s) = X_n^R(0) + 2 \sum_{k=1}^{K-1} \begin{bmatrix} \cos(2\pi ks/S) & -\sin(2\pi ks/S) \end{bmatrix} \begin{bmatrix} X_n^R(k) \\ X_n^I(k) \end{bmatrix} \quad (8.7)$$

$$X_n(k) = \begin{bmatrix} X_n^R(k) \\ X_n^I(k) \end{bmatrix} = \frac{1}{S} \sum_{s=0}^{S-1} \begin{bmatrix} \cos(2\pi ks/S) \\ -\sin(2\pi ks/S) \end{bmatrix} x_n(s) \quad (8.8)$$

The harmonic balance equation (7.5) still holds with  $v$  related to  $V$  by (8.7) and  $I$  and  $Q$  related to  $i$  and  $q$  by (8.8). Applying Newton-Raphson to solve this equation results in the iteration

$$J_F(V^{(j)})(V^{(j+1)} - V^{(j)}) = -F(V^{(j)}) \quad (8.9)$$

where

$$J_F(V) = [J_{F,mn}(V)] = \left[ \frac{\partial F_m(V)}{\partial V_n} \right] \quad m, n \in \{1, 2, \dots, N\}, \quad (8.10)$$

$$J_{F,mn}(V) = [J_{F,mn}(V, k, l)] = \left[ \frac{\partial F_m(V, k)}{\partial V_n(l)} \right] \quad k, l \in \{0, 1, \dots, K-1\}, \quad (8.11)$$

and

$$J_{F,mn}(V, k, l) = \frac{\partial F_m(V, k)}{\partial V_n(l)} = \begin{bmatrix} \frac{\partial F_m^R(V, k)}{\partial V_n^R(l)} & \frac{\partial F_m^R(V, k)}{\partial V_n^I(l)} \\ \frac{\partial F_m^I(V, k)}{\partial V_n^R(l)} & \frac{\partial F_m^I(V, k)}{\partial V_n^I(l)} \end{bmatrix}. \quad (8.12)$$

This derivative consists of the sum of terms

$$\frac{\partial F_m(V, k)}{\partial V_n(l)} = \frac{\partial I_m(V, k)}{\partial V_n(l)} + \begin{bmatrix} 0 & -\omega_k \\ \omega_k & 0 \end{bmatrix} \frac{\partial Q_m(V, k)}{\partial V_n(l)} + Y_{mn}(k, l). \quad (8.13)$$

where

$$Y_{mn}(k, l) = \begin{bmatrix} Y_{mn}^R(k, l) & -Y_{mn}^I(k, l) \\ Y_{mn}^I(k, l) & Y_{mn}^R(k, l) \end{bmatrix}. \quad (8.14)$$

Only  $\frac{\partial I_m(V, k)}{\partial V_n(l)}$  is derived, the derivation of  $\frac{\partial Q_m(V, k)}{\partial V_n(l)}$  is similar.

Compute  $I_m(V, k)$  using (8.8),

$$I_m(V, k) = \frac{1}{S} \sum_{s=0}^{S-1} \begin{bmatrix} \cos(2\pi ks/S) \\ -\sin(2\pi ks/S) \end{bmatrix} i_m(v(s)) \quad (8.15)$$

The waveform  $v$  is considered to be an implicit function of its spectrum  $V$ ; and so the chain rule is employed to compute the derivative.

$$\frac{\partial I_m(V, k)}{\partial V_n(l)} = \frac{1}{S} \sum_{s=0}^{S-1} \begin{bmatrix} \cos(2\pi ks/S) \\ -\sin(2\pi ks/S) \end{bmatrix} \frac{\partial i_m(v(s))}{\partial v_n(s)} \frac{\partial v_n(s)}{\partial V_n(l)} \quad (8.16)$$

Now the derivative of  $v_n(s)$  is calculated using (8.7).

$$v_n(s) = V_n(0) + 2 \sum_{k=1}^{K-1} \begin{bmatrix} \cos(2\pi ks/S) & -\sin(2\pi ks/S) \end{bmatrix} \begin{bmatrix} V_n^R(k) \\ V_n^I(k) \end{bmatrix} \quad (8.17)$$

$$\frac{\partial v_n(s)}{\partial V_n(l)} = \begin{bmatrix} \frac{\partial v_n(s)}{\partial V_n^R(l)} & \frac{\partial v_n(s)}{\partial V_n^I(l)} \end{bmatrix} = (2 - \delta(l)) \begin{bmatrix} \cos(2\pi ls/S) & -\sin(2\pi ls/S) \end{bmatrix} \quad (8.18)$$

This derivative is substituted into (8.16).

$$\frac{\partial I_m(V, k)}{\partial V_n(l)} = \frac{2 - \delta(l)}{S} \sum_{s=0}^{S-1} \begin{bmatrix} \cos(\frac{2\pi ks}{S}) \\ -\sin(\frac{2\pi ks}{S}) \end{bmatrix} \frac{\partial i_m(v(s))}{\partial v_n(s)} \begin{bmatrix} \cos(\frac{2\pi ls}{S}) & -\sin(\frac{2\pi ls}{S}) \end{bmatrix} \quad (8.19)$$

$$= \frac{2 - \delta(l)}{S} \sum_{s=0}^{S-1} \frac{\partial i_m(v(s))}{\partial v_n(s)} \Psi \quad (8.20)$$

where

$$\Psi = \begin{bmatrix} \cos(2\pi ks/S) \cos(2\pi ls/S) & -\cos(2\pi ks/S) \sin(2\pi ls/S) \\ -\sin(2\pi ks/S) \cos(2\pi ls/S) & \sin(2\pi ks/S) \sin(2\pi ls/S) \end{bmatrix}$$

$$\Psi = \frac{1}{2} \begin{bmatrix} \cos(2\pi(k+l)s/S) + \cos(2\pi(k-l)s/S) & -\sin(2\pi(k+l)s/S) + \sin(2\pi(k-l)s/S) \\ -\sin(2\pi(k+l)s/S) - \sin(2\pi(k-l)s/S) & \cos(2\pi(k-l)s/S) - \cos(2\pi(k+l)s/S) \end{bmatrix}$$

Define  $G_{mn}(k) \in \mathbb{C}$  as the  $k^{\text{th}}$  harmonic of  $\frac{\partial i_m(v(s))}{\partial v_n(s)}$ , i.e., let

$$G_{mn}(V, k) = \begin{bmatrix} G_{mn}^R(V, k) \\ G_{mn}^I(V, k) \end{bmatrix} = \frac{1}{S} \sum_{s=0}^{S-1} \frac{\partial i_m(v(s))}{\partial v_n(s)} \begin{bmatrix} \cos(2\pi ks/S) \\ -\sin(2\pi ks/S) \end{bmatrix}. \quad (8.21)$$

Then

$$\frac{\partial I_m(V, k)}{\partial V_n(l)} = \frac{2 - \delta(l)}{2} \begin{bmatrix} G_{mn}^R(k+l) + G_{mn}^R(k-l) & G_{mn}^I(k+l) - G_{mn}^I(k-l) \\ G_{mn}^I(k+l) + G_{mn}^I(k-l) & G_{mn}^R(k-l) - G_{mn}^R(k+l) \end{bmatrix}. \quad (8.22)$$

Equation (8.22) shows that the portion of the conversion matrices due to the nonlinear resistors ( $\partial I_m(V)/\partial V_n$ ) and capacitors ( $\partial Q_m(V)/\partial V_n$ ) can be split into the sum of a Toeplitz and a Hankel matrix<sup>2</sup>. For example

$$\frac{\partial I_m(V)}{\partial V_n} = (T + H)D$$

where

<sup>2</sup>A Toeplitz matrix has the form given by  $a_{ij} = t_{i-j}$  and similarly, the form of a Hankel matrix is given by  $a_{ij} = h_{i+j}$

$$T = \begin{bmatrix} t_0 & t_{-1} & t_{-2} & t_{-3} \\ t_1 & t_0 & t_{-1} & t_{-2} \\ t_2 & t_1 & t_0 & t_{-1} \\ t_3 & t_2 & t_1 & t_0 \end{bmatrix} \quad H = \begin{bmatrix} h_0 & h_1 & h_2 & h_3 \\ h_1 & h_2 & h_3 & h_4 \\ h_2 & h_3 & h_4 & h_5 \\ h_3 & h_4 & h_5 & h_6 \end{bmatrix} \quad D = \begin{bmatrix} 1/2 & & & \\ & 1 & & \\ & & 1 & \\ & & & 1 \end{bmatrix}$$

From (8.22),

$$t_k = \begin{bmatrix} G_{mn}^R(k) & -G_{mn}^I(k) \\ G_{mn}^I(k) & G_{mn}^R(k) \end{bmatrix} \quad h_k = \begin{bmatrix} G_{mn}^R(k) & G_{mn}^I(k) \\ G_{mn}^I(k) & -G_{mn}^R(k) \end{bmatrix}.$$

It is the nature of the DFT that when applied to real waveforms  $G_{nm}(k) = G_{nm}^*(-k)$  when  $k < 0$  and  $G_{nm}(k) = G_{nm}^*(2K-1-k)$  when  $k > K$ , where  $*$  represents the complex conjugate operation in  $\mathbb{C}$  [brigham74]. As a result, the Toeplitz and Hankel portions are rewritten

$$T = \begin{bmatrix} t_0 & t_1^* & t_2^* & t_3^* \\ t_1 & t_0 & t_1^* & t_2^* \\ t_2 & t_1 & t_0 & t_1^* \\ t_3 & t_2 & t_1 & t_0 \end{bmatrix} \quad H = \begin{bmatrix} h_0 & h_1 & h_2 & h_3 \\ h_1 & h_2 & h_3 & h_3^* \\ h_2 & h_3 & h_3^* & h_2^* \\ h_3 & h_3^* & h_2^* & h_1^* \end{bmatrix}$$

This completes the derivation of the harmonic Jacobian  $J_F(V)$ . It is the synthesis of equations (8.10-8.22). This derivation allows the conversion matrices to be constructed with one FFT and  $4K^2$  additions, considerably fewer operations than the  $8K^3$  multiplications and additions needed for the previous derivation.

For a one node circuit at three frequencies the complete harmonic Jacobian would be

$$J_F(V) = \frac{\partial I(V)}{\partial V} + \Omega \frac{\partial Q(V)}{\partial V} + Y$$

where

$$\frac{\partial I(V)}{\partial V} = (T + H)D$$

where

$$T = \begin{bmatrix} G^R(0) & 0 & G^R(1) & G^I(1) & G^R(2) & G^I(2) \\ 0 & G^R(0) & -G^I(1) & G^R(1) & -G^I(2) & G^R(2) \\ G^R(1) & -G^I(1) & G^R(0) & 0 & G^R(1) & G^I(1) \\ G^I(1) & G^R(1) & 0 & G^R(0) & -G^I(1) & G^R(1) \\ G^R(2) & -G^I(2) & G^R(1) & -G^I(1) & G^R(0) & 0 \\ G^I(2) & G^R(2) & G^I(1) & G^R(1) & 0 & G^R(0) \end{bmatrix}$$

$$H = \begin{bmatrix} G^R(0) & 0 & G^R(1) & G^I(1) & G^R(2) & G^I(2) \\ 0 & -G^R(0) & G^I(1) & -G^R(1) & G^I(2) & -G^R(2) \\ G^R(1) & G^I(1) & G^R(2) & G^I(2) & G^R(2) & -G^I(2) \\ G^I(1) & -G^R(1) & G^I(2) & -G^R(2) & -G^I(2) & -G^R(2) \\ G^R(2) & G^I(2) & G^R(2) & -G^I(2) & G^R(1) & -G^I(1) \\ G^I(2) & -G^R(2) & -G^I(2) & -G^R(2) & -G^I(1) & -G^R(1) \end{bmatrix}$$

$$D = \begin{bmatrix} \frac{1}{2} & & & & & \\ & 1 & & & & \\ & & 1 & & & \\ & & & 1 & & \\ & & & & 1 & \\ & & & & & 1 \end{bmatrix}$$

$$\frac{\partial I(V)}{\partial V} = \begin{bmatrix} G^R(0) & 0 & 2G^R(-1) & 2G^I(1) & 2G^R(2) & 2G^I(2) \\ 0 & 0 & 0 & 0 & 0 & 0 \\ G^R(1) & 0 & G^R(0)+G^R(2) & G^I(2) & G^R(1)+G^R(2) & G^I(1)+G^I(2) \\ G^I(1) & 0 & G^I(2) & G^R(0)-G^R(2) & -G^I(1)-G^I(2) & G^R(1)-G^R(2) \\ G^R(2) & 0 & G^R(1)+G^R(2) & -G^I(1)-G^I(2) & G^R(0)+G^R(1) & -G^I(1) \\ G^I(2) & 0 & G^I(1)-G^I(2) & G^R(1)-G^R(2) & -G^I(1) & G^R(0)-G^R(1) \end{bmatrix}$$

$\frac{\partial Q(V)}{\partial V}$  is similar with  $G$  replaced by  $C = \mathbb{F} \frac{\partial q(v(s))}{\partial v(s)}$ .

$$Y = \begin{bmatrix} Y^R(0) & 0 & 0 & 0 & 0 & 0 \\ 0 & 0 & 0 & 0 & 0 & 0 \\ 0 & 0 & Y^R(1) & -Y^I(1) & 0 & 0 \\ 0 & 0 & Y^I(1) & Y^R(1) & 0 & 0 \\ 0 & 0 & 0 & 0 & Y^R(2) & -Y^I(2) \\ 0 & 0 & 0 & 0 & Y^I(2) & Y^R(2) \end{bmatrix}$$

$$\Omega = \begin{bmatrix} 0 & 0 & 0 & 0 & 0 & 0 \\ 0 & 0 & 0 & 0 & 0 & 0 \\ 0 & 0 & 0 & -\omega_o & 0 & 0 \\ 0 & 0 & \omega_o & 0 & 0 & 0 \\ 0 & 0 & 0 & 0 & 0 & -2\omega_o \\ 0 & 0 & 0 & 0 & 2\omega_o & 0 \end{bmatrix}$$

Note that the second row and column of these conversion matrices consist completely of zeros, an artifact that results because phasors at DC must be real. This structural singularity in  $J_F$  can be removed either by deleting the offending row and column or making the diagonal entry nonzero and always setting the DC imaginary term to zero in the right-hand-side vector.

If not all frequencies computed in the transform are used in the harmonic balance calculations, then the resulting conversion matrix should be constructed as if all frequencies were included, except the rows and columns that correspond to the missing frequencies are deleted. This situation occurs if the FFT were used and required more frequencies than the user requested or if quasiperiodic signals were being transformed and the truncation used left some holes in the resulting translated set of frequencies.

## 2.1. Harmonic Relaxation-Newton

The second way to improve the harmonic Newton algorithm is to exploit the structure of the Jacobian to reduce the time required to factor it. Factoring the Jacobian is the most expensive operation required in the harmonic Newton algorithm. The techniques presented in this section are designed to reduce the expense of factoring this matrix. As a side benefit, they also speed its construction and the process of forward and backward substitution.

The Jacobian is organized as a block node admittance matrix that is sparse. Conventional sparse matrix techniques can be used to exploit its sparsity [kundert86a]. Each block is a conversion matrix that is itself a block matrix, consisting of  $2 \times 2$  blocks that result from Fourier coefficients being members of  $\mathbb{C}$ . Conversion matrices are full if they are associated with a node that has a nonlinear device attached, otherwise they are diagonal. In an integrated circuit, nonlinear devices attach to most nodes, so the conversion matrices will in general be full. It often happens, though, that nonlinear devices are either not active or are behaving very linearly. For example, the base-collector junction of a bipolar transistor that is in the forward-active region is reverse biased, and so the junction contributes nothing to its conversion matrices. If there are no other contributions to those conversion matrices, they may be ignored. If there are only contributions from linear components, they are diagonal. During the factorization, it is desirable to keep track of which conversion matrices are full, which are diagonal, and which are zero, and avoid unnecessary operations on known zero conversion matrix elements.

If a circuit contains many linear components, such as is common with hybrid microwave circuits, then much of the matrix will consist of diagonal blocks that are con-

stant from iteration to iteration. It is possible to order the Jacobian during factorization such that the rows and columns associated with nodes that are attached only to linear devices are placed in the upper left corner of the matrix using variability types [norin71] [hachtel72]. These rows and columns are eliminated once before the Newton iteration starts. The elimination proceeds until a full block is encountered. In this way, the harmonic Jacobian is reduced in size by this prefactorization step until the number of rows and columns is equal to, or slightly greater than, the number of nodes with nonlinear devices attached.

A common approach to harmonic balance is to separate the linear devices into their own subcircuit and evaluate them once. A  $y$ -parameter matrix is created that describes the linear subcircuit to the harmonic balance analysis, this matrix becomes  $Y$  in (7.5). In this way,  $N$  is reduced from the number of nodes in the circuit to the number of nodes with nonlinear devices attached. The linear subcircuit approach is similar to using variability types, with one important difference. The variability types approach can be integrated into the normal pivot selection algorithm for the sparse matrix solver. The pivot selection algorithm, now fortified with variability types, can intelligently choose which of the nodes to eliminate and in which order. The order of elimination plays an important role in determining how many operations required for the factorization of a sparse matrix. It is possible to constrain the order in which the rows and columns are eliminated and end up with a reduced matrix that is identical to the one that results from the linear subcircuit approach. However, with variability types, the order is not constrained and it is likely that a better ordering will be found. Thus, using variability types is at least as efficient as using the linear subcircuit approach.

### 2.1.1. Adaptively Pruning the Harmonic Jacobian

Applying traditional sparse matrix techniques is not enough to solve the Newton-Raphson iteration (8.9) efficiently. It is also necessary to reduce the density of the matrix. The Jacobian is only used to generate new iterates; it is not used when confirming convergence, so errors in the Jacobian only affect the rate and region of convergence, not the accuracy of the final solution. Approximations in the Jacobian reduce the asymptotic rate of convergence, but the gain in efficiency can more than make up for this loss. One approximation of this sort is Samanskii's method, presented in Chapter 4, which results in a dramatic speedup for most circuits.

Another approach to approximating the Jacobian and thus speeding the iteration, results from exploiting the natural characteristics of conversion matrices for the nonlinear devices. As mentioned previously, these matrices are the sum of a Toeplitz and a Hankel matrix. Recall that

$$\frac{\partial I_m(V)}{\partial V_n} = (T + H)D$$

where

$$T = \begin{bmatrix} t_0 & t_{-1} & t_{-2} & t_{-3} \\ t_1 & t_0 & t_{-1} & t_{-2} \\ t_2 & t_1 & t_0 & t_{-1} \\ t_3 & t_2 & t_1 & t_0 \end{bmatrix} \quad H = \begin{bmatrix} h_0 & h_1 & h_2 & h_3 \\ h_1 & h_2 & h_3 & h_4 \\ h_2 & h_3 & h_4 & h_5 \\ h_3 & h_4 & h_5 & h_6 \end{bmatrix} \quad D = \begin{bmatrix} 1/2 & & & \\ & 1 & & \\ & & 1 & \\ & & & 1 \end{bmatrix}$$

$$t_k = \begin{bmatrix} G_{mn}^R(k) & -G_{mn}^I(k) \\ G_{mn}^I(k) & G_{mn}^R(k) \end{bmatrix} \quad h_k = \begin{bmatrix} G_{mn}^R(k) & G_{mn}^I(k) \\ G_{mn}^I(k) & -G_{mn}^R(k) \end{bmatrix}$$

where  $G_{mn}$  is the sum of the derivative spectra for nonlinear resistors between node  $m$  and  $n$ , or from  $m$  to ground if  $m = n$ . This spectrum has the characteristic that the more

linear the devices that generate it are behaving, the more the DC component dominates over the harmonics and the faster their magnitude drops off at higher harmonics. As a result, elements in the conversion matrix far from the diagonal will be small compared to those on the diagonal. To reduce the density of the harmonic Jacobian, these small terms far from the diagonal will be ignored.

**Definition:** The *guard harmonic* for a derivative spectrum is the smallest harmonic  $k$  such that

$$|G(l)| < \mu |G(0)| \quad \text{for all } l \geq k$$

where  $\mu$  is a threshold parameter. (Typically  $\mu = 10^{-4}$ .)

When constructing the conversion matrices, (i.e., the blocks in the harmonic Jacobian resulting from nonlinear devices) all harmonics in the derivative spectrum used to form the conversion matrix are considered negligible if they are above the guard harmonic. These harmonics are set to zero, making the conversion matrices banded about the diagonal with the bandwidth an increasing function of how nonlinear the devices contributing to the matrix are behaving. Note that if the bandwidth is restricted to one, so all entries off the main diagonal of a conversion matrix are set to zero, then harmonic Newton collapses to block Gauss-Jacobi-Newton harmonic relaxation.

Ignoring those harmonics of the derivative spectra that fall above the guard harmonics greatly increases the initial sparsity of the harmonic Jacobian, however the Jacobian tends to fill-in while factoring it into L and U. To see this, consider the  $3 \times 3$  banded block matrix in Figure 8.3. The original nonzeros are marked with crosses ( $\times$ ) and the fill-ins are marked with circles ( $\circ$ ). Notice the tendency of the bandwidth to increase in the blocks remaining after a major row and column have been eliminated. Also notice that, of

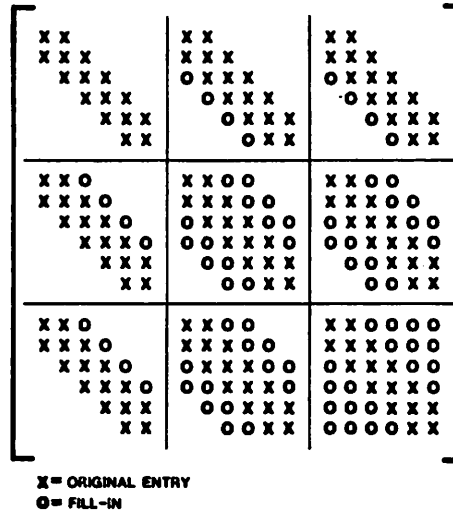


Figure 8.3 : Fill-in pattern of a banded block matrix.

the original nonzeros, those furthest from the diagonal of a block are due to the guard harmonics. These elements are small compared to the diagonal. The fill-ins inside the blocks always involve the guard harmonic, and so these fill-ins are assumed to be negligible. This heuristic does not have a sound theoretical basis, but is usually true if both the blocks and the block matrix are strongly diagonally dominant. Thus the nonlinearities should be resistive and behaving only mildly nonlinear, and each node in the circuit should be connected to ground with an admittance that is large compared to the admittances connecting it to other nodes. These conditions are very restrictive and rarely satisfied in practice, however the heuristic works quite well if  $\mu$  is small and usually results in a considerable speed up.

### 2.1.2. Harmonic Jacobian Data Structure

Implementing a task such as factoring the harmonic Jacobian on a computer not only requires a good algorithm, but also good data structures. The data structure used by

*Spectre* to hold the harmonic Jacobian is a variation on the standard orthogonal-linked list used to hold sparse matrices [kundert86a]. The matrix is written as a block node admittance matrix. Thus, the matrix has  $N$  rows and columns, where  $N$  is the number of nodes in the circuit. Each element in the matrix contains a  $2K \times 2K$  block, where  $K$  is the number of frequencies, and has a pointer to the element below and to the right of itself. The element also carries the bandwidth of the block. The block is allocated as a full  $2K \times 2K$  matrix, but is treated numerically as a banded matrix with the given bandwidth. This approach allows the bandwidth to be set as needed on each iteration, allowing harmonic relaxation-Newton to adapt to the problem being solved.

### 3. Spectre

*Spectre* implements harmonic relaxation-Newton for periodic and quasiperiodic nonautonomous circuits [kundert]. With periodic signals, the FFT is used as the Fourier transform and the number of frequencies used is constrained to be a power of two. With quasiperiodic signals, the APFT is used. A version has been written that also implements the FFT for quasiperiodic circuits and one that implements periodic autonomous circuits. *Spectre* takes as input a file with a SPICE-like description of the circuit, that is a list of components (transistors, resistors, capacitors, transmission lines, etc) with their node connections, and a list of analyses to be performed. Along with harmonic balance, *Spectre* also performs conventional DC, AC, and S-parameter analyses. When a harmonic balance analysis is requested, the desired number of harmonics in the solution must be specified.

### 3.1. Comparisons to Transient Analysis

*Spectre* was used to simulate several circuits to exhibit some of the capabilities of the simulator and to contrast the performance of *Spectre* against the performance of a representative transient analysis simulator such as SPICE [nagel75]. The times for three circuits are presented in this section. The first two circuits are well suited to frequency-domain simulation and poorly suited to time-domain simulation. With the third circuit, the roles are reversed.

The first circuit is the traveling-wave amplifier (TWA) shown in Figure 8.4. It contains four GaAs MESFETs and ten transmission lines of noncommensurate length. While *Spectre* naturally handles lossy and dispersive lines, the lines were constrained to be ideal to be compatible with SPICE. The run times for SPICE2, SPICE3, and *Spectre* are shown in Table 8.1. The long simulation time required by SPICE2 results from the particular break-point algorithm used in this program (see Chapter 2). This algorithm is very inefficient for circuits containing transmission lines. While the problem is not inherent to transient analysis, the wide spread use of SPICE2 has created the misconception that transient analysis is not suitable for microwave circuits. As a partial solution, SPICE3 [quarles89] allows the break-point algorithm to ignore the transmission lines resulting in a shorter simulation time at the expense of increased risk of incorrect answers.

*Spectre* does not yet have automatic error control algorithms, so the user is forced to specify the number of harmonics. This circuit was simulated with 8, 16, and 32 harmonics. On this particular circuit, 8 harmonics resulted in accuracy commensurate with SPICE. Note that doubling the number of harmonics more than doubled the time required to complete the simulation, but the increase is well below the factor of 8 that would be expected

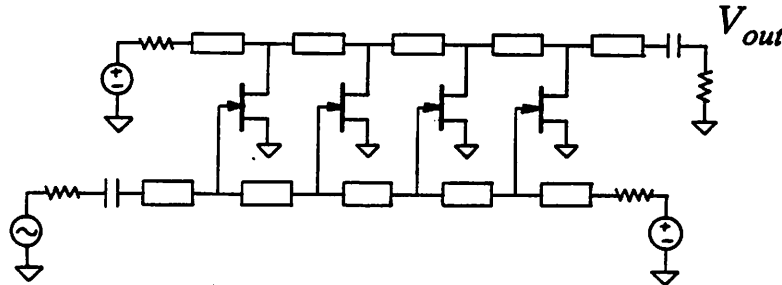


Figure 8.4 : A four-segment traveling-wave amplifier.

from straight harmonic Newton.

TWA Steady State		
SPICE2		62500
SPICE3		240
<i>Spectre</i>	8 harmonics	7
	16 harmonics	22
	32 harmonics	56

Table 8.1 : Time required to simulate the traveling-wave amplifier of Figure 8.4. The simulation interval for SPICE was two periods of the input. The period of the input signal was 10 ns while the electrical lengths of the various transmission lines were 86 ps, 187 ps, and 251 ps. Times were measured on a VAX785.

Figure 8.5 shows the results computed by *Spectre* for the traveling-wave amplifier when the power of the input source was swept from -20 dBm to 20 dBm in 40 steps. Notice that at the highest input power, the amplifier exhibited 10 dB of compression. The time required to perform this analysis is shown in Table 8.2. Swept analyses in harmonic balance exploits the useful characteristic of the Newton-Raphson algorithm that it converges faster and is more likely to converge if primed with an initial guess close to the solution. With a swept analysis, *Spectre* calculates an initial guess by extrapolating from

the solution at the previous step. Thus, a sweep with 40 points is considerable faster than 40 individual analyses. This feature is an advantage harmonic balance has over transient analysis.

TWA Power Sweep		
<i>Spectre</i>	4 harmonics	38
	8 harmonics	130
	16 harmonics	800

**Table 8.2 :** Time required to simulate the traveling-wave amplifier of Figure 8.4 over the input power levels shown in Figure 8.5 in 40 steps. Times were measured on an HP9000/350 with floating point accelerator.

*Spectre* computed the intermodulation distortion of the traveling-wave amplifier by applying two 200 mV signals, one each at 10 GHz and 10.4 GHz. The response is shown,

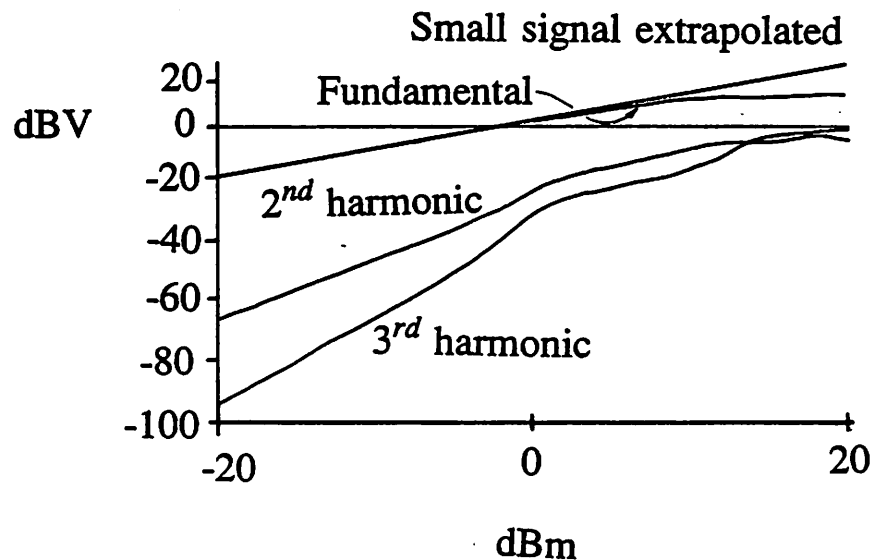


**Figure 8.5 :** The power level of the first three harmonics of the output of the traveling-wave amplifier of Figure 8.4 versus input power.

both in the time and frequency domains, in Figure 8.6. The circuit was simulated with  $H = 5$  using the diamond truncation given in (3.6). The computation time and memory requirements for several values of  $H$  and for both box (3.5) and diamond (3.6) truncation schemes are shown in Table 8.6. There are a few comments that should be made to clarify some of the results in the table. *Spectre's* memory allocator expands array sizes in factors of two, which is why memory requirements sometimes do not change even though  $H$  changes. Each doubling of the array size quadruples the amount of memory required. Most of the approximate factor of two differences between physical and virtual memory requirements can be eliminated by better implementation. Any simulation that needed over 64 frequencies required more memory than the 44 megabytes available from the operating system.

The frequencies of the two tones were chosen so that the various spectral lines in Figure 8.6 could be resolved by eye. The circuit was resimulated with the frequency of the tones set as close as 10 GHz and 10GHz + 1 Hz with no apparent change of accuracy or efficiency. The 1 Hz separation in the two tones results in an intermodulation product at 1 Hz. The combination of 10 GHz and 1 Hz signals make it prohibitively expensive to find the steady-state response of this circuit with a transient analysis simulator such as SPICE.

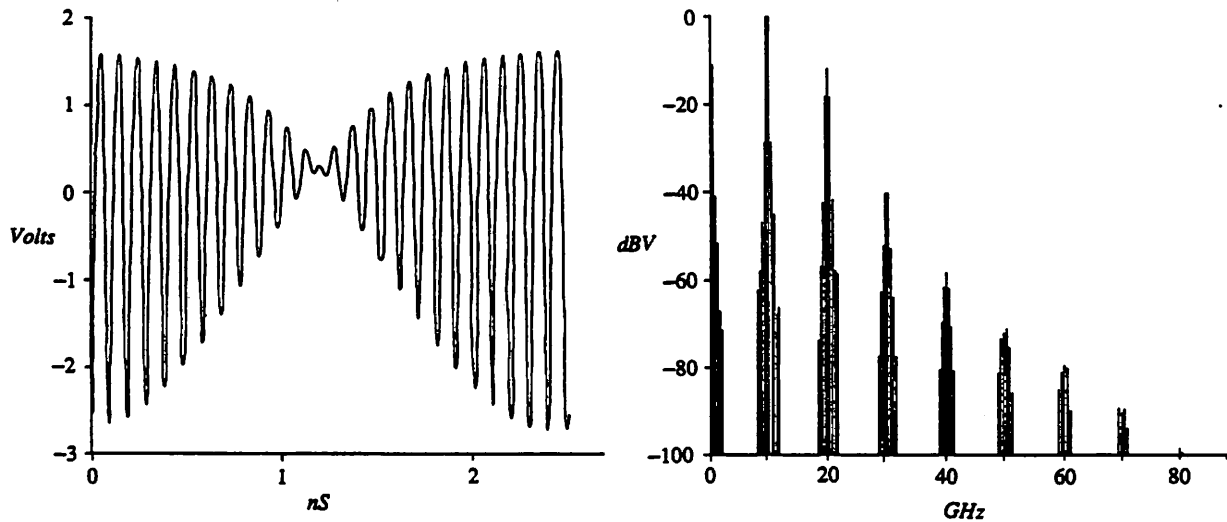


Figure 8.6 : Response of traveling-wave amplifier of Figure 8.4 to two-tone input.

TWA Intermodulation Distortion				
$H$	$K$	time	physical memory	virtual memory
Using $\Lambda_K$ generated by (3.5).				
1	5	0.63 s	0.55 MB	0.78 MB
2	13	4.2 s	0.87 MB	1.5 MB
3	25	24 s	2.2 MB	3.9 MB
4	41	98 s	7.5 MB	14 MB
5	61	320 s	7.6 MB	14 MB
Using $\Lambda_K$ generated by (3.6).				
1	3	0.35 s	0.50 MB	0.80 MB
2	7	1.3 s	0.50 MB	0.80 MB
3	13	4.4 s	0.87 MB	1.5 MB
4	21	15.6 s	2.2 MB	3.9 MB
5	31	43 s	2.3 MB	4.0 MB
6	43	110 s	7.5 MB	14 MB
7	57	245 s	7.6 MB	14 MB

Table 8.3 : Execution times and memory requirements for *Spectre* running an intermodulation distortion test on the traveling-wave amplifier of Figure 8.4. Times were measured on a VAX8800.

Times required to simulate the self-biasing FET tuned amplifier shown in Figure 2.1 is compared in Table 8.4. This circuit is troublesome to transient analysis because of the slow time constant of the input DC blocking capacitor. Normally, time constants due to bias circuits are avoided by using the DC solution as the initial condition. With this circuit, the DC gate voltage is affected by the large input signals. It is very difficult to predict the settling time, and therefore the required simulation time, because of the non-linear effect of the gate diode on the bias circuit time constant. The simulation interval was chosen for this circuit by simulating the circuit several times. Each time the simulation interval was increased and the result compared with the previous simulation until it became clear that the circuit had fully settled. The time reported was that required by SPICE to simulate the circuit over the shortest interval for which the circuit settled to within 0.1% of its steady-state value. *Spectre* found the steady-state solution of this circuit directly without forcing the user to know the circuit's settling time.

Self-Biased Amplifier		
SPICE2		608
<i>Spectre</i>	8 harmonics	1.4
	16 harmonics	5
	32 harmonics	28

**Table 8.4 :** Time required to simulate the self-biased amplifier of Figure 2.1. Times were measured on a VAX785.

The last circuit, shown in Figures 8.7 and 8.8, is a simple noninverting amplifier based on a  $\mu\text{A}$  741 op amp. Results for this circuit are presented in Table 8.5 with various output signal levels and load resistances. The circuit contains no long time constants and so transient analysis can be used to compute the steady-state response efficiently. With large output current, the op amp behaves internally strongly nonlinear, which slows har-

monic balance. Indeed, the output stage goes into class B operation at high output currents. This example shows that harmonic balance is able to handle strongly nonlinear circuits, though it may require more time than traditional transient analysis.

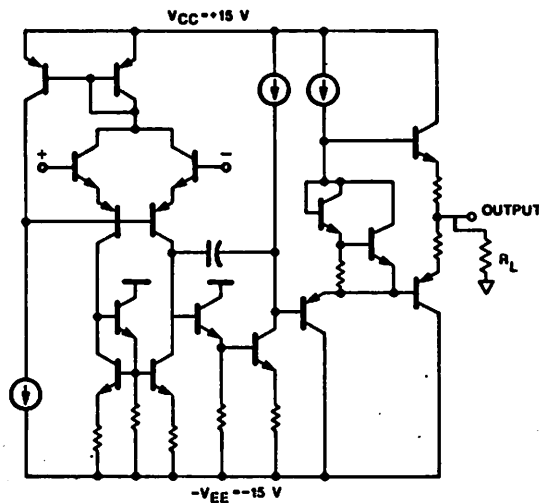


Figure 8.7 : Schematic of  $\mu\text{A}$  741 operational amplifier.

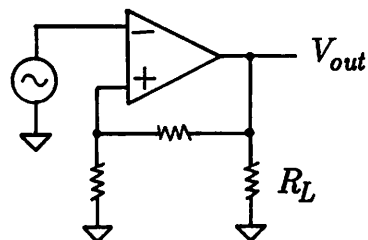


Figure 8.8 : Op amp of Figure 8.7 shown in a noninverting amplifier configuration with gain of 100.

---

Circuit	Conditions	SPICE2	Spectre		
			Harmonics		
			8	16	32
$\mu$ A741	$V_{out} = 1V$ $R_L = \infty$	9	5	11	25
	$V_{out} = 1V$ $R_L = 10K$	13	8	19	40
	$V_{out} = 10V$ $R_L = 10K$	14	32	132	497

Table 8.5 : Time required to simulate the amplifier of Figure 8.8. Times were measured on a VAX785.

### 3.2. Profiles

With transient analysis, the time required to evaluate the nonlinear device equations generally dominates over all other tasks except on very large circuits, where the time required to factor and solve the large system of linear equations dominates. The transition point where the time required of both tasks is equal generally occurs between 1000 and 10,000 nodes, depending on the complexity of the models and the circuit. The situation is completely different with harmonic balance, where the time required for operations involving the system of linear equations completely dominates over all other tasks. For example, consider the circuit shown in Figure 8.9, a seven stage traveling-wave amplifier with 14 GaAsFETs and 24 transmission lines [orr86]. Table 8.6 shows the time required to evaluate device models (eval), convert signals into and out of the frequency domain (Fourier), and construct, factor, and solve the linear system of equations (eqns) for various number of frequencies and power levels. The time required for handling the linear system of equations was further resolved in Table 8.7 where the time required to construct, factor, and solve the factored system of equations is shown.

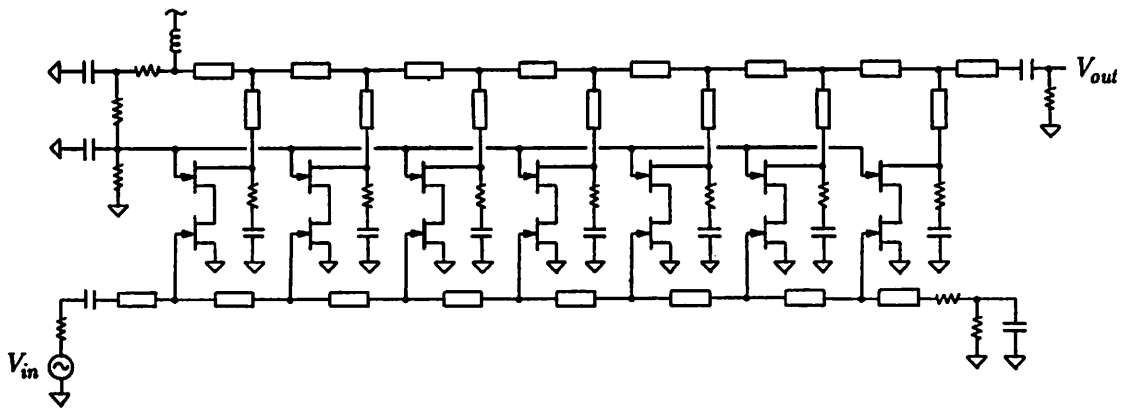


Figure 8.9 : A GaAsFET traveling-wave amplifier [orr86].

Spectre Profiles							
$H_1$	$H_2$	$K$	$P_{in}$	$t_{total}$	Eval	Fourier	Eqns
4	0	4	-10 dBm	6.26 s	1.6%	3.5%	74.5%
4	0	4	0 dBm	6.8 s	2.1%	4.1%	73.2%
4	0	4	10 dBm	16.9 s	4.4%	9.6%	74.1%
8	0	8	-10 dBm	15.5 s	0.5%	3.2%	86.9%
8	0	8	0 dBm	26.38 s	0.7%	1.9%	91.5%
8	0	8	10 dBm	68.32 s	2.3%	4.8%	89.5%
16	0	16	-10 dBm	36.34 s	0.8%	2.4%	87.5%
16	0	16	0 dBm	155.72 s	0.3%	0.6%	97.1%
16	0	16	10 dBm	433.88 s	0.6%	1.4%	96.8%
4	4	13	-10 dBm	186.24 s	0.2%	1.0%	97.2%
4	4	13	0 dBm	267.34 s	0.1%	1.0%	96.6%

Table 8.6 : Time required for various portions of the *Spectre* code for the circuit of Figure 8.9 with various number of frequencies and power levels. Each run required only one full Newton iteration, but the runs at the higher power levels required many Samanskii iterations (where the Jacobian was reused).  $H_i$  represents the number of harmonics for the  $i^{\text{th}}$  fundamental, and  $K$  is the total number of frequencies. Times were measured on an HP9000/350 with floating point accelerator.

Spectre Matrix Profiles							
$K$	$P_{in}$	$t_{total}$	Construct	Factor	Solve	Newton	Saman
4	-10 dBm	6.26 s	10.1%	62.8%	6.7%	1	1
4	0 dBm	6.8 s	11.0%	59.0%	9.4%	1	2
4	10 dBm	16.9 s	25.4%	31.0%	31.8%	1	21
8	-10 dBm	15.5 s	7.0%	77.0%	6.6%	1	1
8	0 dBm	26.38 s	5.4%	82.3%	6.4%	1	2
8	10 dBm	68.32 s	13.4%	55.7%	27.5%	1	22
16	-10 dBm	36.34 s	6.1%	78.7%	5.9%	1	1
16	0 dBm	155.72 s	2.0%	92.9%	3.2%	1	2
16	10 dBm	433.88 s	4.1%	78.7%	16.0%	1	24
13	-10 dBm	186.24 s	4.9%	90.7%	2.8%	1	1
13	0 dBm	267.34 s	4.2%	89.6%	3.9%	1	3

**Table 8.7 :** Time required for various portions of the *Spectre* matrix code for the circuit in Figure 8.9 with various number of frequencies and power levels. The time required to construct the matrix included the time to evaluate the device model equations and convert signals to and from the time domain (Construct). The remaining times are those required to factor and solve the linear system of equations. The number of full (Newton) and Samanskii (Saman) iterations are given. With Samanskii's method the Jacobian from the previous iteration is reused. Times were measured on an HP9000/350 with floating point accelerator.

These results show that the most expensive aspect of harmonic balance is constructing, factoring, and solving the linear system of equations. This is true even with harmonic relaxation-Newton and Samanskii's method being used.

### 3.3. Harmonic Relaxation versus Harmonic Newton

This section explores how reducing the bandwidth of the conversion matrices affects the time required to complete a simulation. In particular, harmonic relaxation, harmonic relaxation-Newton and harmonic Newton are compared versus computation time and number of iterations. It is expected that harmonic relaxation be the fastest but least robust, harmonic Newton be the most robust but slowest, and that harmonic relaxation-Newton should be a robust method that adapts to the problem to provide the speed of harmonic

relaxation when it does not jeopardize convergence. Table 8.8 shows computation time and Table 8.9 shows the number of iterations for *Spectre* simulating the circuit of Figure 8.10 for a periodic solution containing 8 harmonics.

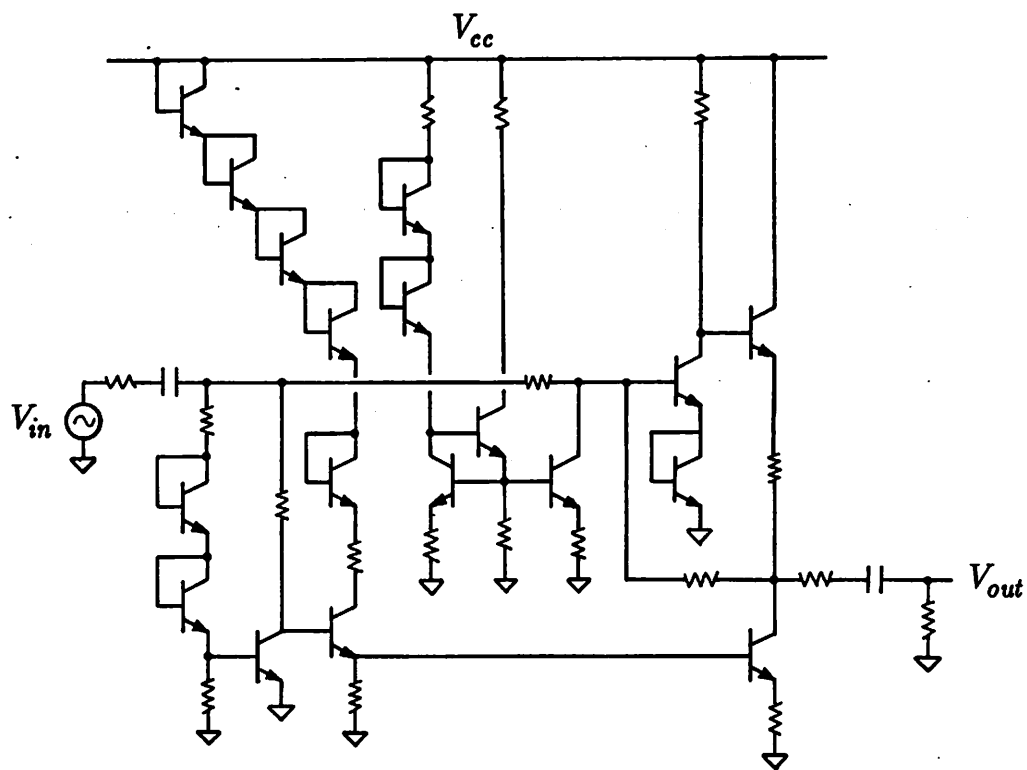


Figure 8.10 : Class AB monolithic power amplifier<sup>3</sup>.

---

<sup>3</sup>R. G. Meyer, private communication.

Spectre Computation Time vs. Method								
$P_{in}$	HR	GJNHR	HRN					HN
			0.3	0.1	0.01	0.001	0.0001	
-20 dBm	$\infty$	22.12	15.9	21.05	29.62	35.68	41.62	85.07
-15 dBm	$\infty$	38.82	25.03	48.23	40.63	49.58	50.60	94.65
-10 dBm	$\infty$	154.58	$\infty$	63.02	77.22	87.87	100.70	135.85
-5 dBm	$\infty$	$\infty$	$\infty$	$\infty$	138.42	139.88	178.68	259.02
0 dBm	$\infty$	$\infty$	$\infty$	$\infty$	$\infty$	412.88	438.72	517.70
5 dBm	$\infty$	$\infty$	$\infty$	$\infty$	$\infty$	694.70	680.30	859.42
10 dBm	$\infty$	$\infty$	$\infty$	$\infty$	$\infty$	1442.82	1417.92	1713.90

**Table 8.8 :** Time required for *Spectre* to simulate the circuit in Figure 8.10 using various harmonic balance methods. Methods include harmonic relaxation, both splitting (HR) and Gauss-Jacobi Newton harmonic relaxation (GJNHR), harmonic relaxation newton (HRN) for various guard harmonic thresholds, and harmonic Newton (HN). Times were measured on an HP9000/350 with floating point accelerator.

Spectre Iteration Count vs. Method								
$P_{in}$	HR	GJNHR	HRN					HN
			0.3	0.1	0.01	0.001	0.0001	
-20 dBm	$\infty$	1/9	1/4	1/4	1/5	1/5	1/5	1/5
-15 dBm	$\infty$	1/18	1/7	2/9	1/8	1/8	1/8	1/8
-10 dBm	$\infty$	3/78	$\infty$	1/21	1/21	1/21	1/21	1/21
-5 dBm	$\infty$	$\infty$	$\infty$	$\infty$	3/19	3/18	3/18	3/18
0 dBm	$\infty$	$\infty$	$\infty$	$\infty$	$\infty$	5/63	5/63	5/63
5 dBm	$\infty$	$\infty$	$\infty$	$\infty$	$\infty$	10/60	10/60	10/60
10 dBm	$\infty$	$\infty$	$\infty$	$\infty$	$\infty$	21/113	22/94	22/94

**Table 8.9 :** Iterations required for *Spectre* to simulate the circuit in Figure 8.10 using various harmonic balance methods. Methods include harmonic relaxation, both splitting (HR) and Gauss-Jacobi Newton harmonic relaxation (GJNHR), harmonic relaxation newton (HRN) for various guard harmonic thresholds, and harmonic Newton (HN). The first number given is the number of full Newton iterations, the second is the number of Samanskii iterations. With a Samanskii iteration, the Jacobian from the previous iteration is reused.

These results show that harmonic relaxation-Newton as implemented in *Spectre* with a fixed guard threshold of typically 0.0001 does not extract as much of the speed of Gauss-Jacobi harmonic relaxation as is possible. Extracting that speed is more complicated

than just changing the guard harmonic threshold, as shown in the following tables. Table 8.10 shows computation time and Table 8.11 shows the number of iterations for *Spectre* simulating the circuit of Figure 8.9 for a periodic solution containing 16 harmonics.

Spectre Computation Time vs. Method								
$P_{in}$	HR	GJNHR	HRN					HN
			0.3	0.1	0.01	0.001	0.0001	
-10 dBm	$\infty$	2.78	2.95	6.49	11.85	14.9	13.77	118.53
-5 dBm	$\infty$	3.18	3.24	6.3	10.97	13.75	16.94	122.65
0 dBm	$\infty$	3.46	86.18	33.45	23.36	36.11	38.95	119.75
5 dBm	$\infty$	4.76	75.85	185.75	117.76	102.46	99.68	135.70
10 dBm	$\infty$	$\infty$	427.79	144.02	152.84	162.01	146.82	184.62

**Table 8.10 :** Time required for *Spectre* to simulate the circuit in Figure 8.9 using various harmonic balance methods with 16 harmonics. Methods include harmonic relaxation, both splitting (HR) and Gauss-Jacobi Newton harmonic relaxation (GJNHR), harmonic relaxation newton (HRN) for various guard harmonic thresholds, and harmonic Newton (HN). Times were measured on an HP9000/350 with floating point accelerator.

Spectre Iteration Count vs. Method								
$P_{in}$	HR	GJNHR	HRN					HN
			0.3	0.1	0.01	0.001	0.0001	
-10 dBm	$\infty$	1/0	1/1	1/1	1/0	1/0	1/0	1/0
-5 dBm	$\infty$	1/2	1/1	1/1	1/1	1/0	1/0	1/0
0 dBm	$\infty$	1/3	4/7	1/1	1/1	1/1	1/1	1/1
5 dBm	$\infty$	1/6	3/9	4/6	2/12	1/2	1/2	1/2
10 dBm	$\infty$	$\infty$	8/30	1/24	1/23	1/23	1/23	1/23

**Table 8.11 :** Iterations required for *Spectre* to simulate the circuit in Figure 8.9 using various harmonic balance methods. Methods include harmonic relaxation, both splitting (HR) and Gauss-Jacobi Newton harmonic relaxation (GJNHR), harmonic relaxation newton (HRN) for various guard harmonic thresholds, and harmonic Newton (HN). The first number given is the number of full Newton iterations, the second is the number of Samanskii iterations. With a Samanskii iteration, the Jacobian from the previous iteration is reused.

With the traveling-wave amplifier, for large thresholds (but less than one), convergence for harmonic relaxation-Newton is worse than for harmonic relaxation. It appears as

if truncating the conversion matrices to be diagonal gives better convergence properties than does truncating the conversion matrices to have a small bandwidth greater than one. This odd behavior has yet to be explained.

### 3.4. APFT versus FFT

In order to explore the advantage of implementing quasiperiodic harmonic balance using the FFT rather than the APFT, a two-tone intermodulation distortion test was performed on the traveling-wave amplifier of Figure 8.9. Two  $-10$  dBm signals were applied to the amplifier at 1 GHz and 1.01 GHz and 3 harmonics of each signal were calculated along with sum and difference frequencies to a total of 13 frequencies. The time required on an HP9000/850 to simulate this circuit was 106 seconds for APFT-based harmonic Newton and 81 seconds for FFT-based harmonic relaxation-Newton<sup>4</sup>. The primary reason that the FFT-based method was faster was because it allowed the use of harmonic relaxation-Newton. When the circuit were resimulated with APFT-based harmonic relaxation-Newton, the time required was 82 seconds. Harmonic relaxation-Newton is not normally used with the APFT because the aliasing pattern of the APFT is incompatible with the guard harmonic heuristic. The speed up achieved on this circuit by using harmonic relaxation-Newton and the FFT is modest, considerably greater speedup can be achieved when much of the circuit is behaving near linearly or when a large number of frequencies are used.

---

<sup>4</sup>The FFT-based measurements were made using the HP85150B Microwave Nonlinear Simulator (MNS). This simulator is a direct descendant of *Spectre*, but has been upgraded to use the FFT rather than the APFT for its transform when performing quasiperiodic harmonic balance.

# Chapter 9

## Comparisons

---

For each of the three classes of steady-state methods presented, finite-difference, shooting, and harmonic balance methods, there are situations where each is best. In this chapter, each method will be summarized and its advantages and disadvantages given. Each of the circuits presented in Chapter 2 are also reviewed and recommendations are given on how to find their steady-state response most efficiently.

### 1. Finite-Difference Methods

Finite-difference methods solve boundary-value problems by discretizing the differential equation for the circuit on a finite set of time-points that cover the simulation interval. This results in a large system of equations which are solved for the node voltages at each time-point simultaneously. The important characteristics of this method are that the equation and solution are formulated in the time domain, it solves boundary-value problems, and it solves for the whole solution simultaneously.

The nonlinear finite-difference equations are usually solved using Newton-Raphson. Since there are large number of equations and unknowns, the Jacobian is quite large. This is a significant drawback. This method cannot be applied to large circuits because of the large amount of memory that is required for the Jacobian. The matrix is sparse, which helps considerably.

When Newton-Raphson is applied to equations generated by the finite-difference method, the intermediate iterates are waveforms that may not satisfy the differential equations, but do satisfy the boundary constraints (assuming that these constraints are linear). For this reason, the finite-difference methods are well suited for finding unstable periodic or quasiperiodic solutions. This may or may not be a feature of the method, depending on whether you wish to find or avoid unstable solutions. The finite-difference methods are like parallel shooting methods in this regard. In fact, a parallel shooting method, when the shooting intervals are taken to be so small that there is one time-step per interval, becomes a finite-difference method. This is easily seen by using the one step approximation  $\phi_k(t_{k-1}) = x_k + \frac{1}{h_k} \dot{x}_k$  in equations (5.31), which becomes a finite-difference method with explicit Euler used to form the difference equations.

Finite-difference methods allow the most freedom when choosing an integration method. The time-steps may be nonuniformly spaced and the spacing may be chosen to increase accuracy by clustering points where waveforms are changing rapidly and increasing efficiency by spreading them out where the waves are quiescent. Furthermore, finite-difference methods allow the integration method to be noncausal. In other words, the value of the solution at future time-points as well as past time-points are used when computing the discretized derivative. Noncausal discretization can be used with finite-difference methods because the solution is calculated for all time at once. No attempt is made to exploit temporal unidirectionality.

Finite-difference methods are able to solve boundary-value problems formulated using the MFT formulation, and so are able to find quasiperiodic solutions with an arbitrary discretization method. They are also able to handle circuits with distributed devices, and

like all steady-state methods, exhibit characteristics that can be exploited on parallel or vector machines.

## 2. Shooting Methods

Shooting methods convert boundary-value problems into a sequence of initial-value problems. They begin with a guess at the solution at the beginning of the shooting interval. The equations are integrated over the interval and the results at each of the boundaries are substituted into the boundary constraint and the initial state is corrected in a manner to better satisfy the boundary constraint. The guess is corrected using either an extrapolation method or a Newton-Raphson method. Unlike finite-difference methods, the intermediate iterates generated by shooting methods satisfy the differential equations, but not the boundary constraint.

Shooting methods exploit the causality inherent in most dynamic systems by evaluating the differential equation as an initial-value problem. They do not compute the solution to the differential equation all at once and only need access to a small piece of it (a few past time-points) at any point in time. As a result, they need considerably less memory.

Shooting methods have limited utility on large circuits however. With Newton-Raphson based shooting methods, a matrix equation involving the Jacobian must be solved at each time-point (solving this equation requires  $N$  forward/backward substitutions of the Jacobian, where  $N$  is the size of the Jacobian). The computational complexity of this step is at best  $O(N^2)$  (for a diagonal Jacobian) and at worst  $O(N^3)$  (for a full Jacobian). The matrix equation is solved when updating the sensitivity matrix. The sensitivity matrix gen-

erally exhibits considerably numerical sparsity<sup>1</sup>, however the sparsity pattern is not known in advance and changes during the course of the computation. How to exploit this sparsity is an open question that, if solved, would result in Newton-Raphson based shooting becoming considerably more efficient on large circuits.

Extrapolation based shooting methods need to evaluate the differential equation over  $p$  shooting intervals, where  $p$  is the number of time constants on the order of, or greater than, the shooting interval. For large circuits,  $p$  could be quite large, but that would be unusual. However, simulating a large circuit over many shooting intervals for each iteration of the shooting method can get quite expensive.

A very important characteristic of shooting methods is that they converge quickly and reliably if the state-transition function is near linear. It is quite often the case (usually by design) that the state-transition function is linear even when the overall circuit behavior is not. The nonlinear behavior is not a problem for the numerical integration used to evaluate  $\phi_T$  because numerical integration is a natural continuation method where time is the continuation parameter. This hiding of the nonlinear behavior gives shooting methods a considerable advantage over the finite-difference methods and harmonic balance on a wide range of problems.

An important disadvantage for shooting methods is that they cannot handle distributed devices. Circuits containing distributed devices could be solved with shooting methods if the distributed devices were replaced with lumped approximations, however the lumped approximation often contains so many internal nodes and significant time constants, that they considerably increase the cost of using shooting methods.

---

<sup>1</sup>The sensitivity matrix numerically sparse in the sense that there are many entries in the matrix that are close to zero. This is not the usual definition of sparsity, where many entries are exactly zero.

Lastly, shooting methods can find the quasiperiodic solution of a circuit if the boundary-value problem is formulated using the MFT method. Shooting methods can be accelerated using parallel and vector machines, and particularly so if parallel shooting methods are used. However, the advantage that shooting methods enjoy by hiding non-linear behavior from the outer loop is often lost with parallel shooting methods.

### 3. Harmonic Balance

Harmonic balance is a frequency-domain method that is unique in two ways. First, the equations are formulated by assuming that the voltages and currents in the circuit are approximated by a Fourier series accurately. Since such signals are almost periodic, the method inherently avoids transient behavior by being incapable of representing it. The complexity of the method is determined by the number of terms needed in the Fourier series to accurately represent the signals, and not by the actual frequencies. The complexity is low and the method efficient if the circuit is behaving near linearly and is driven by signals representable by Fourier series with few terms. In this situation, a truncated Fourier series is often a very good approximation to the true solution, and harmonic balance is very accurate.

The second way that harmonic balance is different from time-domain methods is that it represents signals using the coefficients of the sinusoids rather than a sampled-data representation (i.e., in the frequency domain using the Fourier series rather than in the time domain). Using Fourier coefficients and superposition allows the linear components to be evaluated with phasor analysis. Thus, the large number of distributed device models available in the literature that are formulated using phasors are directly compatible with harmonic balance. Linear component measurements are also made using phasors by network

analyzers and are compatible with harmonic balance.

The harmonic balance equations are formulated by insisting that Kirchoff's laws are satisfied at each frequency being considered. When evaluating nonlinear devices, it is often necessary to transform signals into and out of the time domain, but this is not essential and has no effect on the result, and so harmonic balance is considered a frequency-domain method.

The number of equations and unknowns in a harmonic balance formulation roughly equals two times the number of nodes times the number of frequencies considered. The factor of two results from needing both magnitude and phase in the phasor representation of a signal. When Newton-Raphson is used to solve these equations, the Jacobian gets very large. Thus memory and computation time requirements of harmonic balance can be considerable for large circuits when many frequencies are being considered. The Jacobian is sparse, and this fact must be exploited for harmonic balance to be practical for even moderately sized circuits. It is possible to further exploit sparsity by using the harmonic relaxation-Newton algorithm. Independent of which method is used to solve the nonlinear harmonic balance equations, there is considerable parallelism to exploit.

If harmonic balance were to be converted into a time-domain method, it would be a finite-difference method. By starting from (7.5), harmonic balance is written as a finite-difference method by simply multiplying through by the inverse almost-periodic Fourier transform matrix  $\Gamma^{-1}$ . For node  $n$ ,

$$\Gamma^{-1}I_n(V) + \Gamma^{-1}\Omega_{nn}Q_n(V) + \Gamma^{-1}\sum_{m=1}^N Y_{mn}V_m + \Gamma^{-1}U_n = 0.$$

Knowing that  $V_n = \Gamma v_n$ ,  $I_n(V) = \Gamma i_n(v)$ ,  $Q_n(V) = \Gamma q_n(v)$  and  $U_n = \Gamma u_n$  allows us to simplify this to

$$i_n(v) + \Gamma^{-1}\Omega_{nn}\Gamma q_n(v) + \Gamma^{-1}\sum_{m=1}^N Y_{mn}\Gamma v_n + u_n = 0. \quad (9.1)$$

$\Gamma^{-1}\Omega_{nn}\Gamma$  and  $\Gamma^{-1}Y_{mn}\Gamma$  are constants and so can be precomputed for efficiency. Equation (9.1) shows that harmonic balance can be formulated in the time domain as a finite-difference method. The basic difference between the two approaches is that the frequency-domain version represents the solution using the coefficients of the sinusoids and the finite-difference method represents them in sampled-data form. Though both methods give the same answer, the matrices in the finite-difference method are denser and so that approach will be less efficient.

## 4. Examples

Here we look back at the circuits presented in Chapter 2 as motivation. It is explained how the techniques presented in this dissertation would be applied to these circuits.

### 4.1. Self-Biasing Amplifier

Self-biasing amplifiers, such as the one shown in Figure 2.1, are difficult for transient-based simulators because they exhibit a time constant that is very long compared to the period of a typical input frequency and it is very difficult to predict just how long any turn-on transient will last. Any of the periodic steady-state methods are suitable for use on such circuits. If the circuit contains distributed devices or behaving near-linearly, harmonic balance should be used, otherwise, shooting methods are likely to be more efficient.

### 4.2. Mixers

The wide frequency range and the long time constants present in mixers cause problems for transient analysis. Mixers, by their very nature, generally behave very nonlinearly. The closer the nonlinearities are to acting like ideal switches, the better the conversion

efficiency and noise performance of the mixer. While it is possible to simulate these circuits with harmonic balance, it is expensive because a large number of frequencies will be needed to accurately represent the signals. If the mixer contains distributed devices, which is common at microwave frequencies, then harmonic balance is the only alternative to transient analysis. If the mixer is purely lumped, then quasiperiodic shooting methods based on the MFT algorithm provide an attractive alternative, especially if the circuit is small.

### **4.3. Narrow-band Amplifiers and Filters**

These circuits are difficult for transient analysis because of their long settling times (if they are high- $Q$ ), and because of the widely spaced frequencies present in a two-tone intermodulation distortion test. For lumped filters, either harmonic balance or shooting methods provide an attractive alternative to transient analysis. For a two-tone test, harmonic balance is particularly attractive because the circuit is generally behaving near linearly and so harmonic balance is efficient. For distributed filters, harmonic balance is the only choice.

### **4.4. Switched-Capacitor Filters**

Switched-capacitor filters have a large repetitive clock signal whose period is generally much shorter than the duration of the interval of interest. The high frequencies combined with the long simulation interval result in an expensive transient analysis. Harmonic balance is inappropriate with these filters because of the large number of harmonics in the clock signal, which is always a pulse train. If a sinusoidal input is applied to the filter, the resulting signals are quasiperiodic, and so the only real alternative to transient analysis is MFT-based shooting methods. This is particularly true if two or more sinusoids are applied to the input of the filter, which would be the case if the intermodulation distortion of the filter were being measured.

#### 4.5. Traveling-Wave Amplifiers

The difficulty with traveling-wave amplifiers is that they contain transmission lines. These amplifiers are used up to very high frequencies and so various nonideal effects such as dispersion and loss must be accounted for in the lines. The dispersion and loss present problems for transient analysis and the distributed devices make shooting methods unsuitable. The only appropriate approach is harmonic balance, which usually works well. Traveling-wave amplifiers often exhibit conditional stability (stable for small signals and large signals, but with a range of instability in between). Harmonic balance will have trouble in this situation and so pseudo-arc-length continuation is needed.

#### 4.6. Measured Devices

Measured devices are characterized with S-parameters measured in the frequency domain. As yet, no transient analysis simulator has been able to use such data in a simulation. The only proven simulation technique for nonlinear circuits that contain measured devices is harmonic balance.

#### 4.7. Crystal and Cavity Oscillators

Crystal and cavity oscillators are designed for very high-Q, which implies that these circuits have very long turn-on transients. This makes transient methods inappropriate, but as long as the circuit is lumped, any of the steady-state methods for autonomous systems work fine. With cavity oscillators, the resonator is generally considered to be distributed, and so harmonic balance is the best choice.

# Chapter 10

## Summary

---

This dissertation presented several new algorithms for finding periodic and quasiperiodic responses of analog and microwave circuits in particular and systems of nonlinear ordinary- and integro-differential equations in general. The new algorithms were implemented in two new circuit simulation programs and used to simulate a variety of practical circuits. The main results of the dissertation are summarized below.

Initially a transform suitable for almost-periodic signals that was derived from the matrix form of the DFT was presented. Conceptually, it is easy to extend the matrix form of the DFT for almost-periodic signals, however, a naive implementation is likely to be inaccurate. The concepts of truncation and aliasing were introduced. Truncation is the operation of eliminating all but a finite number of frequencies from consideration. Aliasing refers to the amplification and conversion of those signals at the truncated frequencies into signals at frequencies of interest by the transform. The condition number of the transform matrix was shown to be a measure of the degree to which the aliased terms are amplified. For the transform to be accurate, it is important for the condition number to be as small as possible. A small condition number was shown to be achievable by choosing time-points for the transform so that the rows of the transform matrix are nearly orthogonal. A practical algorithm was given that chooses such a set of time-points. The combination of the almost-periodic transform matrix and the time-step algorithm was referred to as the APFT.

The first application of the APFT was the MFT algorithm. MFT maps the problem of finding the quasiperiodic solution of an ordinary differential equation into a boundary-value problem. In the development of the algorithm, one of the fundamental frequencies of the quasiperiodic signals was chosen to be the clock. All signals were sampled at the beginning of each clock period. MFT's fundamental assumption was that the sampled waveforms, which were also shown to be quasiperiodic, could be accurately represented with a Fourier series with a small number of nonzero Fourier coefficients. Given that  $J$  Fourier coefficients were sufficient, then knowing  $J$  points on the sampled waveforms would be enough to allow the Fourier coefficients to be computed. From the coefficients, all points on the sampled waveforms can be found. In particular, if  $J$  points were known, then their adjacent successors could be computed solely from the assumption that sampled waveforms were accurately approximated with a  $J$  coefficient Fourier series. The relationship of the  $J$  points to their immediate successors through the truncated Fourier series assumption is referred to as the delay operator relation. Another relationship exist between the  $J$  points and their immediate successors through the state-transition function of the differential equation. These two relationships can be combined into one nonlinear system of equations that can be solved for the values of the signals at the  $J$  points. From there, the Fourier coefficients are computed, and then any of the points on the sampled waveform. If the solution is needed at some other time, the state-transition function can be evaluated starting at the closest preceding sample.

The MFT algorithm was implemented in *Nitswit* and was tested on a wide variety of lumped circuits, including switched-capacitor filters and switching mixers. It was shown to be practical on moderately sized circuits.

Harmonic balance was presented as a method that differed from traditional transient analysis in that it approximated the solution to a differential equation as a sum of sinusoids (a Fourier series) rather than a piecewise polynomial. It also used the Fourier coefficients (or phasors) to represent the signals rather than a sampled version of the waveforms. In other words, the circuit simulation problem was formulated by writing Kirchoff's laws in the frequency domain. Using phasors to represent the signals provides important advantages when formulating and evaluating linear device models, particularly when the models are distributed. This is the main reason why harmonic balance is quickly becoming the dominant method for simulating nonlinear circuits at microwave frequencies. In general, nonlinear devices cannot be directly evaluated in the frequency domain, and so signals are converted between the frequency- and time-domains with a discrete Fourier transform. The nonlinear devices are evaluated in the time domain, with the results transformed back into the frequency domain. The DFT and APFT are used for transforming periodic and quasi-periodic signals, respectively. It was also shown that it is possible to avoid the APFT altogether and use the DFT even on quasiperiodic circuits. Doing so results in a noticeable improvement in speed.

Methods for solving the nonlinear system of equations formulated by harmonic balance were grouped into three broad categories, nonlinear programming techniques, nonlinear relaxation techniques, and the Newton-Raphson algorithm. A new method referred to as Gauss-Jacobi harmonic relaxation was shown to be the best of the relaxation methods, by virtue of it being fast and the most likely to converge. A new hybrid adaptive method based on Gauss-Jacobi harmonic relaxation and harmonic Newton was proposed. This method provides the speed of the relaxation method and the large region of convergence of the harmonic Newton method. The hybrid method, referred to as harmonic

relaxation-Newton, was shown to be just as robust as harmonic Newton, but considerably faster. Harmonic relaxation-Newton was further accelerated by employing Samanskii's method.

The Gauss-Jacobi harmonic relaxation, harmonic Newton, and harmonic relaxation-Newton methods were implemented in *Spectre* and the algorithms compared on many practical circuits. The results obtained indicate that the harmonic relaxation-Newton method provides the best tradeoff between speed and region of convergence yet achieved. However, the heuristics used are immature. Considerable improvement in speed could be realized by carefully reworking the block matrix ordering algorithms and the algorithm that sets the block bandwidth.

This dissertation presented several new approaches to finding the periodic and quasi-periodic solutions of nonlinear differential equations, and new ways of improving the efficiency of the standard approaches. These results will eventually provide the designers of analog and microwave circuits useful new capabilities for their circuit simulators, and allow them to explore their designs more fully. However, there is certainly more work that can be done to further improve the efficiency of these approaches, and perhaps a breakthrough or two that remains to be uncovered. Also, efficient methods for determining whether these solutions are stable, and so represent steady-state solutions, are an important research topic that has not been adequately explored. Furthermore, except for standard transient analysis, no method exists today to compute a chaotic steady-state solution. This has become a very important problem with the growing popularity of delta-sigma modulators.

# Appendix A

## Nomenclature

---

- $\mathbb{Z}, \mathbb{R}, \mathbb{C}$  The integer, real, and complex numbers.
- $\mathbb{C} = \mathbb{R}^2$  Throughout most of this dissertation, the trigonometric Fourier series is used rather than the exponential. Thus, a Fourier coefficient is described using the coefficients of sine and cosine. The pair of these two coefficients are said to reside in  $\mathbb{C}$  as opposed to  $\mathbb{C}$ .  $\mathbb{C}$  is related to  $\mathbb{C}$  in that  $[a, b]^T \in \mathbb{C}$  corresponds to  $a + jb \in \mathbb{C}$ .
- $\|\cdot\|_\infty$  The  $l_\infty$  norm. For  $x \in \mathbb{R}^N$ ,  $\|x\|_\infty = \max_i |x_i|$ . For  $A \in \mathbb{R}^{N \times N}$ ,  $\|A\|_\infty = \max_i \sum_{j=1}^N |a_{ij}|$ .
- $\|\cdot\|_2$  The Euclidean or  $l_2$  norm. For  $x \in \mathbb{R}^N$ ,  $\|x\|_2 = \left( \sum_{i=1}^N x_i^2 \right)^{1/2}$ . For vectors in  $\mathbb{R}^N$ , the  $l_2$  and  $l_\infty$  norms are equivalent. That is,  $\frac{1}{\sqrt{N}} \|x\|_2 \leq \|x\|_\infty \leq \|x\|_2$  for all  $x \in \mathbb{R}^N$ .
- $O(\cdot)$   $f(x) = O(g(x))$  when  $x \rightarrow a$  implies that  $|f(x)/g(x)|$  is bounded as  $x \rightarrow a$  ( $a$  can be finite,  $+\infty$ , or  $-\infty$ ).
- $j$  Imaginary operator,  $j = \sqrt{-1}$ .

$\mathbf{0}, \mathbf{1}$	The zero vector or matrix and the identity matrix.
$t, \omega$	Time, radial frequency.
$\lambda$	A fundamental frequency.
$\Lambda, \Lambda_K$	A countable set of frequencies, and a finite set with $K$ elements.
$P(T;E)$	The space of all periodic waveforms of bounded variation with period $T$ with domain $E$ .
$AP(\Lambda;E)$	The space of almost-periodic functions on domain $E$ constructed as a linear combination of sinusoids at frequencies in the set $\Lambda$ .
$QP(\lambda_1, \dots, \lambda_d; E)$	The set of quasiperiodic functions on domain $E$ with fundamental frequencies $\lambda_1, \lambda_2, \dots, \lambda_d$ . Equals $AP(\Lambda;E)$ where $\Lambda$ is the module constructed from the basis of fundamental frequencies.
$\mathbb{F}, \mathbb{F}^{-1}$	Abstract forward and inverse Fourier operators.
$\Gamma, \Gamma^{-1}$	Matrix representation of the forward and inverse Fourier operators.
$x, X$	Arbitrary waveform and its spectrum. $X = \mathbb{F}x$ .
$\longleftrightarrow$	Laplace transform relation.
$f$	Function that maps waveforms to waveforms. Sometime $f$ is an arbitrary differentiable function, other times it is used to represent the sum of currents entering a node or nodes.
$J_f(x_0)$	Jacobian (derivative) of $f$ with respect to $x$ at $x_0$ .
$F$	Function that maps spectra to spectra. Related to $f$ in that if $y = f(x)$ then $Y = F(X)$ .

$H$	The maximum number of harmonics considered.
$K$	The number of frequencies present in the spectra.
$N$	The number of nodes in a circuit.
$S$	The number of time-points present in the sampled waveforms.
$k, l$	Frequency indices. Usually, $k, l \in \{0, 1, \dots, K-1\}$
$m, n$	Node indices. $m, n \in \{1, 2, \dots, N\}$
$r, s$	Time indices. $r, s \in \{0, 1, \dots, S-1\}$
$v, V$	Node voltage waveforms, spectra.
$u, U$	Input current waveforms, spectra.
$i, I$	Function from voltage to current for nonlinear resistors and its frequency-domain equivalent.
$q, Q$	Function from voltage to charge for nonlinear capacitors and its frequency-domain equivalent.
$y$	Matrix-valued impulse response of the circuit with all nonlinear devices removed.
$Y$	Laplace transform of $y$ .
$Y$	Phasor equivalent to $Y$ .
$\Omega$	Matrix used to multiply each particular frequency component in a vector of spectra by the correct $\omega_k$ to perform the frequency-domain equivalent of time differentiation.

# Bibliography

---

- [anobile79] Richard J. Anobile. *Alien*. Avon, 1979. This modification of the *Alien*'s teaser was found on a men's bathroom wall in Cory Hall; U. C. Berkeley.
- [aprille72a] Thomas J. Aprille and Timothy N. Trick. A computer algorithm to determine the steady-state response of nonlinear oscillators. *IEEE Transactions on Circuit Theory*, vol. CT-19, no. 4, July 1972, pp. 354-360.
- [aprille72b] Thomas J. Aprille and Timothy N. Trick. Steady-state analysis of nonlinear circuits with periodic inputs. *Proceedings of the IEEE*, vol. 60, no. 1, January 1972, pp. 108-114.
- [baily69] Everett Minnich Baily. *Steady-state harmonic analysis of nonlinear networks*. Ph. D. dissertation. Stanford University, February 1969.
- [bava82] G. P. Bava, S. Benedetto, E. Biglieri, F. Filicori, V. A. Monaco, C. Naldi, U. Pisani and V. Pozzolo. Modelling and performance simulation techniques of GaAs MESFET's for microwave power amplifiers. In *ESA-ESTEC REPORT*. Noordwijk, Holland, March 1982.
- [bertsekas82] Dimitri P. Bertsekas. *Constrained Optimization and Lagrange Multiplier Methods*. Academic Press, 1982.
- [besicovitch32] A. S. Besicovitch. *Almost Periodic Functions*. Cambridge University Press, 1932. Also published by Dover 1954.
- [bohr47] Harald Bohr. *Almost Periodic Functions*. Chelsea, 1947.
- [bolstad86] John H. Bolstad and Herbert B. Keller. A multigrid continuation method for elliptic problems with folds. *SIAM Journal on Scientific and Statistical Computing*, vol. 7, no. 4, October 1986, pp. 1081-1104.
- [bracewell78] Ronald N. Bracewell. *The Fourier Transform and its Applications*. McGraw-Hill, 1978.
- [brigham74] E. Oran Brigham. *The Fast Fourier Transform*. Prentice-Hall, 1974.
- [chan82] Tony F. Chan. Deflation Techniques and Block-Elimination Algorithms for Solving Bordered Singular Systems. Technical Report #226, Department of Computer Science, Yale University, Yale Station, New Haven, CT 06520, March 10, 1982.
- [childs79] B. Childs, M. Scott, J. W. Daniel, E. Denman and P. Nelson (editors). *Codes for Boundary-Value Problems in Ordinary Differential Equations*. Springer-Verlag, 1979.
- [chua75] Leon O. Chua and Pen-Min Lin. *Computer-Aided Analysis of Electronic Circuits: Algorithms and Computational Techniques*. Prentice-Hall, 1975.

- [chua80] L. O. Chua. Device modeling via basic nonlinear circuit elements. *IEEE Transactions on Circuits and Systems*, vol. CAS-27, no. 11, November 1980, pp. 1014-1044.
- [chua81] L. O. Chua and A. Ushida. Algorithms for computing almost periodic steady-state response of nonlinear systems to multiple input frequencies. *IEEE Transactions on Circuits and Systems*, vol. CAS-28, no. 10, October 1981, pp. 953-971.
- [colon73] Francis R. Colon and Timothy N. Trick. Fast periodic steady-state analysis for large-signal electronic circuits. *IEEE Journal of Solid-State Circuits*, vol. SC-8, no. 4, August 1973, pp. 260-269.
- [corduneanu68] C. Corduneanu. *Almost Periodic Functions*. Interscience, 1968.
- [cunningham58] W. J. Cunningham. *Introduction to Nonlinear Analysis*. McGraw-Hill, 1958.
- [curtice87] Walter R. Curtice. Nonlinear analysis of GaAs MESFET amplifiers, mixers, and distributed amplifiers using the harmonic balance technique. *IEEE Transactions on Microwave Theory and Techniques*, vol. MTT-35, no. 4, April 1987, pp. 441-447.
- [dahlquist74] Germund Dahlquist and Åke Björck. *Numerical Methods*. Prentice-Hall, 1974.
- [dalichow76] Rolf Dalichow and Daniel Harkins. A precision RF source and down-converter for the model 8505a. *Hewlett-Packard Journal*, July 1976.
- [de man80] Hugo J. De Man, Jan Rabaey, Guido Arnout and Joos Vandewalle. Practical implementation of a general computer aided design technique for switched capacitor circuits. *IEEE Journal of Solid-State Circuits*, vol. SC-15, April 1980, pp. 190-200.
- [desoer69] Charles A. Desoer and Ernest S. Kuh. *Basic Circuit Theory*. McGraw-Hill, 1969.
- [director76] Stephen W. Director and K. Wayne Current. Optimization of forced nonlinear periodic circuits. *IEEE Transactions on Circuits and Systems*, vol. CAS-23, no. 6, June 1976, pp. 329-334.
- [djordjevic86] Antonije R. Djordjevic, Tapan K. Sarkar and Roger F. Harrington. Analysis of lossy transmission lines with arbitrary nonlinear terminal networks. *IEEE Transactions on Microwave Theory and Technique*, vol. MTT-34, no. 6, June 1986, pp. 660-666.
- [egami74] Shunichiro Egami. Nonlinear, linear analysis and computer-aided design of resistive mixers. *IEEE Transactions on Microwave Theory and Techniques*, vol. MTT-22, no. 3, March 1974, pp. 270-275.
- [engl82] W. L. Engl, R. Laur and H. K. Dirks. MEDUSA — A simulator for modular circuits. *IEEE Transactions on Computer-Aided Design of Integrated Circuits and Systems*, vol. CAD-1, no. 2, April 1982, pp. 85-93.
- [faber80] Maarek T. Faber and Wojciech K. Gwarek. Nonlinear-linear analysis of microwave mixer with any number of diodes. *IEEE Transactions on*

- Microwave Theory and Techniques*, vol. MTT-28, no. 11, November 1980, pp. 1174-1181.
- [fang83] S. C. Fang and et. al. Switcap: A switched-capacitor network analysis program. *IEEE Circuits and Systems Magazine*, vol. 5, no. 3, September 1983, pp. 4-10, 41-46.
- [filicori79] F. Filicori, V. A. Monaco and C. Naldi. Simulation and design of microwave class-C amplifiers through harmonic analysis. *IEEE Transactions on Microwave Theory and Techniques*, vol. MTT-27, no. 12, December 1979, pp. 1043-1051.
- [filicori88] Fabio Filicori and Vito A. Monaco. Computer-aided design of non-linear microwave circuits. *Alta Frequenza*, vol. LVII, no. 7, September 1988, pp. 355-378.
- [fox57] L. Fox. *The Numerical Solution of Two-Point Boundary Value Problems in Ordinary Differential Equations*. Oxford, 1957.
- [gautschi61] W. Gautschi. Numerical integration of ordinary differential equations based on trigonometric polynomials. *Numerische Mathematik*, vol. 3, 1961, pp. 381-397.
- [gear71] C. William Gear. *Numerical Initial Value Problems in Ordinary Differential Equations*. Prentice-Hall, 1971.
- [gill81] Philip E. Gill, Walter Murray and Margaret H. Wright. *Practical Optimization*. Academic Press, 1981.
- [gilmore84] R. J. Gilmore and F. J. Rosenbaum. Modeling of nonlinear distortion in GaAs MESFETs. *1984 IEEE MTT-S International Microwave Symposium Digest*, May 1984, pp. 430-431.
- [gilmore86] Rowan Gilmore. Nonlinear circuit design using the modified harmonic balance algorithm. *IEEE Transactions on Microwave Theory and Techniques*, vol. MTT-34, no. 12, December 1986, pp. 1294-1307.
- [golub83] Gene H. Golub and Charles F. Van Loan. *Matrix Computations*. The Johns Hopkins University Press, 1983.
- [gopal78] K. Gopal, M. S. Nakhla, K. Singhal and J. Vlach. Distortion analysis of transistor networks. *IEEE Transactions on Circuits and Systems*, vol. CAS-25, no. 2, February 1978, pp. 99-106.
- [grosz82] Francis B. Grosz and Timothy N. Trick. Some modifications to Newton's method for the determination of the steady-state response of nonlinear oscillatory circuits. *IEEE Transactions on Computer-Aided Design of Integrated Circuits and Systems*, vol. CAD-1, no. 3, July 1982, pp. 116-120.
- [gwarek74] Wojciech K. Gwarek. *Nonlinear analysis of microwave mixers*. Masters thesis, Massachusetts Institute of Technology, September 1974.
- [hachtel72] Gary D. Hachtel. Vector and variability types in sparse matrix algorithms. In *Sparse Matrices and Their Applications*, Donald J. Rose and Ralph A. Willoughby (editors). Plenum Press, 1972, pp. 53-64.

- [hale80] Jack K. Hale. *Ordinary Differential Equations*. Krieger, 1980.
- [hall76] G. Hall and J. M. Watt (editors). *Modern Numerical Methods for Ordinary Differential Equations*. Oxford University Press, 1976.
- [harris78] Fredric J. Harris. On the use of windows for harmonic analysis with the discrete Fourier transform. *Proceedings of the IEEE*, vol. 66, no. 1, January 1978, pp. 51-83.
- [hente86] D. Hente and R. H. Jansen. Frequency domain continuation method for the analysis and stability investigation of nonlinear microwave circuits. *IEE Proceedings*, vol. 133, no. 5, October 1986, pp. 351-362.
- [hicks82a] R. G. Hicks and P. J. Khan. Numerical analysis of nonlinear solid-state device excitation in microwave circuits. *IEEE Transactions on Microwave Theory and Techniques*, vol. MTT-30, no. 3, March 1982, pp. 251-259.
- [hicks82b] R. G. Hicks and P. J. Khan. Numerical analysis of subharmonic mixers using accurate and approximate models. *IEEE Transactions on Microwave Theory and Techniques*, vol. MTT-30, no. 12, December 1982, pp. 2113-2120.
- [hirsch70] Morris W. Hirsch and Stephen Smale. *Differential Equations, Dynamical Systems, and Linear Algebra*. Academic Press, 1970.
- [householder75] Alston S. Householder. *The Theory of Matrices in Numerical Analysis*. Dover, 1975.
- [huang] Tammy Huang. *Theoretical Aspects of Relaxation-Based and Nonlinear Frequency-Domain Circuit Simulation*. PhD dissertation, University of California at Berkeley. To appear.
- [kakizaki85] Makiko Kakizaki and Tsutomu Sugawara. A modified Newton method for the steady-state analysis. *IEEE Transactions on Computer-Aided Design of Integrated Circuits and Systems*, vol. CAD-4, no. 4, October 1985, pp. 662-667.
- [keller68] Herbert B. Keller. *Numerical Methods for Two-Point Boundary Value Problems*. Ginn-Blaisdell, Waltham Mass., 1968.
- [keller76] Herbert B. Keller. *Numerical Solution of Two Point Boundary Value Problems*. Society for Industrial and Applied Mathematics, 1976.
- [keller77] Herbert B. Keller. Numerical solution of bifurcation and nonlinear eigenvalue problems. In *Applications of Bifurcation Theory*, Paul H. Rabinowitz (editor), 1977.
- [kerr75] A. R. Kerr. A technique for determining the local oscillator waveforms in a microwave mixer. *IEEE Transactions on Microwave Theory and Techniques*, vol. MTT-23, no. 10, October 1975, pp. 828-831.
- [kundert85] Kenneth S. Kundert and Alberto Sangiovanni-Vincentelli. Nonlinear circuit simulation in the frequency-domain. In *ICCAD-85 Digest of Technical Papers*. IEEE International Conference on Computer-Aided Design, November 1985.

- [kundert86a] Kenneth S. Kundert. Sparse matrix techniques. In *Circuit Analysis, Simulation and Design*, part 1, Albert E. Ruehli (editor). North-Holland, 1986.
- [kundert86b] Kenneth S. Kundert and Alberto Sangiovanni-Vincentelli. Simulation of nonlinear circuits in the frequency domain. *IEEE Transactions on Computer-Aided Design of Integrated Circuits and Systems*, vol. CAD-5, no. 4, October 1986, pp. 521-535.
- [kundert88a] Kenneth S. Kundert, Alberto Sangiovanni-Vincentelli and Tsutomu Sugawara. Techniques for finding the periodic steady-state response of circuits. In *Analog Methods for Circuit Analysis and Diagnosis*, Takao Ozawa (editor). Marcel Dekker, 1988.
- [kundert88b] Kenneth S. Kundert, Gregory B. Sorkin and Alberto Sangiovanni-Vincentelli. Applying harmonic balance to almost-periodic circuits. *IEEE Transactions on Microwave Theory and Techniques*, vol. MTT-36, no. 2, February 1988, pp. 366-378.
- [kundert88c] K. Kundert, J. White and A. Sangiovanni-Vincentelli. An envelope-following method for the efficient transient simulation of switching power and filter circuits. In *ICCAD-88 Digest of Technical Papers*. IEEE International Conference on Computer-Aided Design, November 1988, pp. 446-449.
- [kundert88d] K. Kundert, J. White and A. Sangiovanni-Vincentelli. Mixed frequency-time approach for finding the steady-state solution of clocked analog circuits. *Proceedings of the IEEE 1988 Custom Integrated Circuits Conference*, May 1988, pp. 6.2.1-6.2.4.
- [kundert89] K. Kundert, J. White and A. Sangiovanni-Vincentelli. A mixed frequency-time approach for distortion analysis of switching filter circuits. *IEEE Journal of Solid-State Circuits*, vol. 24, no. 2, April 1989, pp. 443-451.
- [kundert] Kenneth S. Kundert. *Spectre: A Frequency-Domain Simulator for Nonlinear Circuits*. For information write to the EECS Industrial Liaison Program, University of California, Berkeley California, 94720.
- [lewis87] S. H. Lewis and P. R. Gray. A pipelined 5-Msample/s 9-bit analog-to-digital converter. *IEEE Journal of Solid-State Circuits*, vol. SC-22, December 1987, pp. 954-961.
- [lipparini82] Alessandro Lipparini, Ernesto Marazzi and Vittorio Rizzoli. A new approach to the computer-aided design of nonlinear networks and its application to microwave parametric frequency dividers. *IEEE Transactions on Microwave Theory and Techniques*, vol. MTT-30, no. 7, July 1982, pp. 1050-1058.
- [lueberger84] David G. Luenberger. *Linear and Nonlinear Programming*. Addison-Wesley, 1984.
- [maas88] Stephen A. Maas. *Nonlinear Microwave Circuits*. Artech House, 1988.

- [mayaram88] Kartikeya Mayaram and Donald O. Pederson. CODECS: A mixed-level device and circuit simulator. In *ICCAD-88 Digest of Technical Papers*. IEEE International Conference on Computer-Aided Design, November 1988, pp. 112-115.
- [mees81] A. I. Mees. *Dynamics of Feedback Systems*. Wiley, 1981.
- [nagel75] Laurence W. Nagel. *SPICE2: A Computer Program to Simulate Semiconductor Circuits*. PhD dissertation, University of California at Berkeley, May 1975. Available through Electronics Research Laboratory Publications, U. C. B., 94720, Memorandum No. UCB/ERL M520.
- [nakhla76] M. S. Nakhla and J. Vlach. A piecewise harmonic balance technique for determination of the periodic response of nonlinear systems. *IEEE Transactions on Circuits and Systems*, vol. CAS-23, no. 2, February 1976, pp. 85-91.
- [newton83] Arthur Richard Newton and Alberto L. Sangiovanni-Vincentelli. Relaxation-based electrical simulation. *IEEE Transactions on Electron Devices*, vol. ED-30, no. 9, September 1983, pp. 1184-1207. (Also in *SIAM Journal on Scientific and Statistical Computing*, vol. 4, no. 3, September 1983 and *IEEE Transactions on Computer-Aided Design of Integrated Circuits and Systems*, vol. CAD-3, no. 4, October 1984).
- [norin71] Robert S. Norin and Christopher Pottle. Effective ordering of sparse matrices arising from nonlinear electrical networks. *IEEE Transactions on Circuit Theory*, vol. CT-18, no. 1, January 1971, pp. 139-145.
- [orr86] Jerry Orr. A stable 2-26.5 GHz two-stage dual-gate distributed MMIC amplifier. *1986 IEEE MTT-S International Microwave Symposium Digest*, June 1986.
- [ortega70] J. M. Ortega and W. C. Rheinboldt. *Iterative Solution of Nonlinear Equations in Several Variables*. Academic Press, 1970.
- [parker] T. S. Parker and L. O. Chua. *Practical Numerical Algorithms for Chaotic Systems*. Springer-Verlag. To appear.
- [penalosa83] C. Camacho Penalosa. Numerical steady-state analysis of nonlinear microwave circuits with periodic excitation. *IEEE Transactions on Microwave Theory and Techniques*, vol. MTT-31, 1983, pp. 724-730.
- [penalosa87a] C. Camacho Penalosa, L. Mariscal Rico and A. Alonso Pardo. Efficient calculation of partial derivatives in nonlinear conductances driven by periodic input signals. *Electronic Letters*, vol. 23, no. 11, 21 May 1987, pp. 565-566.
- [penalosa87b] Carlos Camacho Penalosa and Colin S. Aitchison. Analysis and design of MESFET gate mixers. *IEEE Transactions on Microwave Theory and Techniques*, vol. MTT-35, no. 7, July 1987, pp. 643-652.
- [petzold81] Linda R. Petzold. An efficient numerical method for highly oscillatory ordinary differential equations. *SIAM Journal on Numerical Analysis*, vol. 18, no. 3, June 1981, pp. 455-479.

- [press86] William H. Press, Brian P. Flannery, Saul A. Teukolsky and William T. Vetterling. *Numerical Recipes: the Art of Scientific Computing*. Cambridge University Press, 1986.
- [quarles89] Thomas Quarles. *Analysis of Performance and Convergence Issues for Circuit Simulation*. PhD dissertation, University of California at Berkeley, May 1989. Available through Electronics Research Laboratory Publications, U. C. B., 94720.
- [rabiner75] Lawrence R. Rabiner and Bernard Gold. *Theory and Application of Digital Signal Processing*. Prentice-Hall, 1975.
- [rabiner78] Lawrence R. Rabiner and Ronald W. Schafer. *Digital Processing of Speech Signals*. Prentice-Hall, 1978.
- [rhyne88] George W. Rhyne, Michael B. Steer and Bevan D. Bates. Frequency-domain nonlinear circuit analysis using generalized power series. *IEEE Transactions on Microwave Theory and Techniques*, vol. MTT-36, no. 2, February 1988, pp. 379-387.
- [rizzoli83] Vittorio Rizzoli, Alessandro Lipparini and Ernesto Marazzi. A general-purpose program for nonlinear microwave circuit design. *IEEE Transactions on Microwave Theory and Techniques*, vol. MTT-31, no. 9, September 1983, pp. 762-770.
- [rizzoli86] V. Rizzoli, A. Lipparini and A. Neri. User-oriented software package for the analysis and optimisation of nonlinear microwave circuits. *IEE Proceedings*, vol. 133, no. 5, October 1986, pp. 385-391.
- [rizzoli87] V. Rizzoli, C. Cecchetti and A. Lipparini. A general-purpose program for the analysis of non-linear microwave circuits under multitone excitation by multidimensional Fourier transform. In *1987 Proceedings of the 17th European Microwave Conference*, September 1987, pp. 635-640.
- [rudin76] Walter Rudin. *Principles of Mathematical Analysis*. McGraw-Hill, 1976.
- [sangiovanni81] Alberto L. Sangiovanni-Vincentelli. Circuit simulation. In *Computer Design Aids for VLSI Circuits*, P. Antognetti, D. O. Pederson and H. De Man (editors). Sijthoff & Noordhoff, 1981, pp. 19-112.
- [schuppert86] Bernd Schuppert. A fast and reliable method for computer analysis of microwave mixers. *IEEE Transactions on Microwave Theory and Techniques*, vol. MTT-34, no. 1, January 1986, pp. 110-119. Also see comments by M. E. Adamski in March 1987 issue of same journal (MTT 35-3, pp. 353).
- [schutt-aine88] Jose E. Schutt-Aine and Raj Mittra. Scattering parameter transient analysis of transmission lines loaded with nonlinear terminations. *IEEE Transactions on Microwave Theory and Technique*, vol. MTT-36, no. 3, March 1988, pp. 529-536.
- [skelboe80] Stig Skelboe. Computation of the periodic steady-state response of nonlinear networks by extrapolation methods. *IEEE Transactions on*

- Circuits and Systems*, vol. CAS-27, no. 3, March 1980, pp. 161-175.
- [skelboe82] Stig Skelboe. Conditions for quadratic convergence of quick periodic steady-state methods. *IEEE Transactions on Circuits and Systems*, vol. CAS-29, no. 4, April 1982, pp. 234-239.
- [sorkin87] Gregory B. Sorkin, Kenneth S. Kundert and Alberto Sangiovanni-Vincentelli. An almost-periodic Fourier transform for use with harmonic balance. In *1987 IEEE MTT-S International Microwave Symposium Digest*, vol. 2, June 1987, pp. 717-720.
- [steer83] Michael B. Steer and Peter J. Khan. An algebraic formula for the output of a system with large-signal, multifrequency excitation. *Proceedings of the IEEE*, vol. 71, no. 1, January 1983, pp. 177-179.
- [stoer80] J. Stoer and R. Bulirsch. *Introduction to Numerical Analysis*. Springer-Verlag, 1980.
- [strang80] Gilbert Strang. *Linear Algebra and Its Applications*. Academic Press, 1980.
- [sugawara] T. Sugawara, M. Okumura and H. Tanimoto. An efficient small signal frequency analysis method for nonlinear circuits with two frequency excitations. *IEEE Transactions on Computer-Aided Design of Integrated Circuits and Systems*, . To appear.
- [trick75] T. N. Trick, F. R. Colon and S. P. Fan. Computation of capacitor voltage and inductor current sensitivities with respect to initial conditions for the steady-state analysis of nonlinear periodic circuits. *IEEE Transactions on Circuits and Systems*, vol. CAS-22, May 1975, pp. 391-396.
- [ushida84] A. Ushida and L. O. Chua. Frequency-domain analysis of nonlinear circuits driven by multi-tone signals. *IEEE Transactions on Circuits and Systems*, vol. CAS-31, no. 9, September 1984, pp. 766-778.
- [ushida87] A. Ushida, L. O. Chua and T. Sugawara. A substitution algorithm for solving nonlinear circuits with multi-frequency components. *International Journal on Circuit Theory and Application*, vol. 15, 1987, pp. 327-355.
- [vidyasagar78] M. Vidyasagar. *Nonlinear Systems Analysis*. Prentice-Hall, 1978.
- [weeks73] W. T. Weeks, A. J. Jimenez, G. W. Mahoney, D. Mehta, H. Qassemzadeh and T. R. Scott. Algorithms for ASTAP — a network analysis program. *IEEE Transactions on Circuit Theory*, vol. CT-20, no. 6, November 1973, pp. 628-634.
- [white86] Jacob K. White and Alberto Sangiovanni-Vincentelli. *Relaxation Techniques for the Simulation of VLSI Circuits*. Kluwer, 1986.
- [yang83] Ping Yang, Berton D. Epler and Pallab K. Chatterjee. An investigation of the charge conservation problem for MOSFET circuit simulation. *IEEE Journal of Solid-State Circuits*, vol. SC-18, no. 1, February 1983, pp. 128-138.

# Epilogue

---

We now return the control of your simulator to you until the next circuit at the same time-step, when the error message will take you to ...

*Time-step too small.*